Noname manuscript No.
(will be inserted by the editor)

Cosmic X-ray surveys of distant active galaxies

The demographics, physics, and ecology of growing supermassive black holes

W.N. Brandt · D.M. Alexander

Received: date / Accepted: date

Abstract We review results from cosmic X-ray surveys of active galactic nuclei (AGNs) over the past ≈ 15 yr that have dramatically improved our understanding of growing supermassive black holes in the distant universe. First, we discuss the utility of such surveys for AGN investigations and the capabilities of the missions making these surveys, emphasizing *Chandra*, *XMM-Newton*, and *NuSTAR*. Second, we briefly describe the main cosmic X-ray surveys, the essential roles of complementary multiwavelength data, and how AGNs are selected from these surveys. We then review key results from these surveys on the AGN population and its evolution ("demographics"), the physical processes operating in AGNs ("physics"), and the interactions between AGNs and their environments ("ecology"). We conclude by describing some significant unresolved questions and prospects for advancing the field.

Keywords surveys · cosmology: observations · galaxies: active · galaxies: nuclei · galaxies: Seyfert · galaxies: quasars · galaxies: evolution · black hole physics

W.N. Brandt
Department of Astronomy and Astrophysics and the Institute for Gravitation and the Cosmos; The Pennsylvania State University; 525 Davey Lab; University Park, PA 16802; USA
Tel.: +1 814 865 3509
E-mail: niel@astro.psu.edu

D.M. Alexander
Department of Physics; Durham University; Durham DH1 3LE; UK
Tel.: +44 191 3343594
E-mail: d.m.alexander@durham.ac.uk

1 Introduction

1.1 General utility of X-ray surveys for studies of active galactic nuclei

Cosmic X-ray surveys have now achieved sufficient sensitivity and sky coverage to allow the study of many distant source populations including active galactic nuclei (AGNs), starburst galaxies, normal galaxies, galaxy clusters, and galaxy groups. Among these, AGNs, representing actively growing supermassive black holes (SMBHs), dominate the source number counts as well as the received integrated X-ray power. This has led to an impressive literature on the demographics, physics, and ecology of distant growing SMBHs found in X-ray surveys.

The intrinsic X-ray emission from AGNs largely originates in the immediate vicinity of the SMBH. The X-ray continuum arises via Compton upscattering in an accretion-disk "corona" over a broad X-ray band, and also perhaps via accretion-disk emission at low X-ray energies (e.g., Mushotzky et al 1993; Reynolds and Nowak 2003; Fabian 2006; Turner and Miller 2009; Done 2010; Gilfanov and Merloni 2014). AGNs hosting powerful jets furthermore often show strong jet-linked X-ray continuum emission (e.g., Worrall 2009; Miller et al 2011). This intrinsic X-ray emission may then interact with matter throughout the nuclear region to produce, via Compton "reflection" and scattering, more distributed X-ray emission. In some cases, when the intrinsic X-rays are obscured, such reflected/scattered emission may dominate the observed luminosity.

Cosmic X-ray surveys of AGNs offer considerable utility for several reasons:

1. X-ray emission appears to be nearly universal from the luminous AGNs that dominate SMBH growth in the Universe. When AGNs have been reliably identified using optical, infrared, and/or radio techniques, they almost always also show X-ray AGN signatures (e.g., see Fig. 1 and Avni and Tananbaum 1986; Brandt et al 2000; Mushotzky 2004; Gibson et al 2008). Thus, the intrinsic X-ray emission from the accretion disk and its corona empirically appears robust, even if its detailed nature is only now becoming clear (e.g., Done 2010; Schnittman and Krolik 2013). This point is discussed further in Section 3.3 and Section 4.2.
2. X-ray emission is penetrating with reduced absorption bias. The high-energy X-ray emission observed from AGNs is capable of directly penetrating through substantial columns with hydrogen column densities of $N_{\rm H} = 10^{21}$–$10^{24.5}$ cm^{-2} (e.g., Wilms et al 2000, and references therein).[1] This is critically important, since the majority of AGNs in the Universe are now known to be absorbed by such column densities (see Section 4.1). X-ray surveys thus aid greatly in identifying the majority AGN populations and, moreover, in allowing their underlying luminosities to be assessed re-

[1] For purposes of basic comparison, the column density through your hand is $N_{\rm H} \sim 10^{23}$ cm^{-2}, while that through your chest is $N_{\rm H} \sim 10^{24}$ cm^{-2} (with significant variation depending upon the amount of bone intercepted).

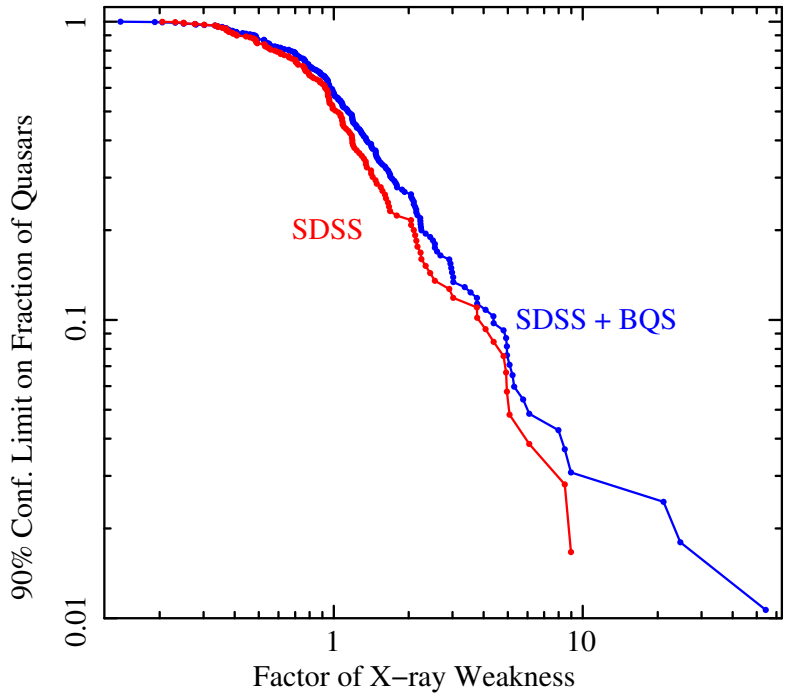

Fig. 1 Upper limit at 90% confidence on the fraction of Sloan Digital Sky Survey (SDSS; red curve) and SDSS+Bright Quasar Survey (BQS; blue curve) radio-quiet quasars that are X-ray weak by a given factor. The factor of X-ray weakness is computed relative to expectations based on optical/UV luminosity (see Section 4.2), where a value of unity represents the average quasar. Broad Absorption Line quasars, which are known often to have heavy X-ray absorption, have been excluded when making this plot. Note that quasars that are X-ray weak by a factor of 10 represent $\lesssim 3\%$ of the population. Adapted from Gibson et al (2008).

liably (in a regime where optical/UV luminosity indicators are generally unreliable). Only in the highly Compton-thick regime ($N_{\rm H} \gg 1/\sigma_{\rm T}$, corresponding to $N_{\rm H} \gg 1.5 \times 10^{24}$ cm^{-2}) does direct transmission become impossible, but here one can still investigate the (much fainter) X-rays that are reflected or scattered around the absorber (e.g., Comastri 2004; Georgantopoulos 2013). An additional relevant advantage of X-ray studies is that, as one studies objects at increasing redshift in a fixed observed-frame band, one gains access to increasingly penetrating rest-frame emission (i.e., higher rest-frame energies are probed); note the opposite generally applies in the optical and UV bandpasses where dust-reddening effects increase toward shorter wavelengths (e.g., Cardelli et al 1989).

3. X-rays have low dilution by host-galaxy starlight (i.e., emission at any wavelength associated with stellar processes). AGNs generally have much higher ratios of $L_{\rm X}/L_{\rm Opt}$ and thus $f_{\rm X}/f_{\rm Opt}$ than stars (e.g., Maccacaro et al 1988). Thus, X-rays provide excellent contrast between SMBH accretion

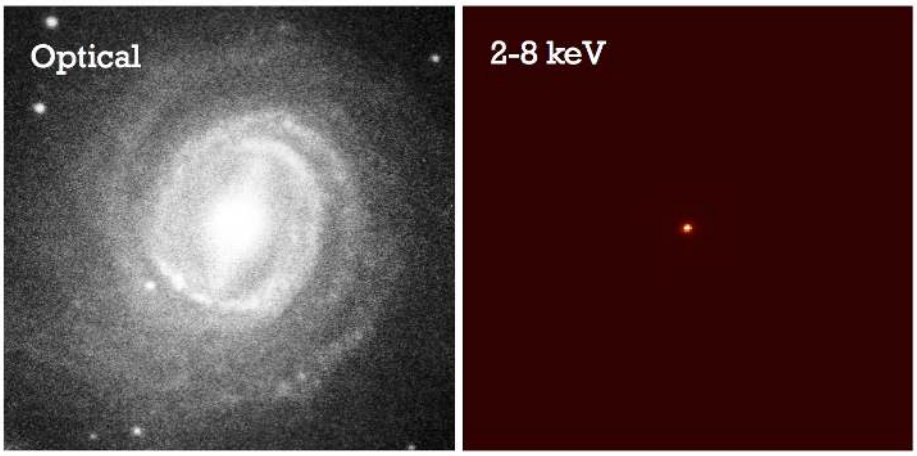

Fig. 2 Optical and *Chandra* 2–8 keV images of a local active galaxy (NGC 3783); each image is 1.5 arcmin on a side. Note the substantial host-galaxy starlight competing with the AGN light in the optical band while, in the X-ray band, only the AGN light is apparent. The large contrast in the X-ray band between AGN light and starlight helps greatly with the identification of distant AGNs.

light and starlight (see Fig. 2), allowing one to construct pure samples of AGNs even down to relatively modest luminosities. This aspect of X-ray surveys is critical, for example, at high redshift where it is often unfeasible, at any wavelength, to resolve spatially the AGN light from host starlight. For weak or highly obscured AGNs, such dilution by host starlight can make AGNs difficult to separate from galaxies in the optical/UV regime (e.g., Moran et al 2002; Hopkins et al 2009).

4. The X-ray spectra of AGNs are rich with diagnostic potential that can be exploited when sufficient source counts are collected. At a basic level, the distinctive X-ray spectral characteristics of AGNs can often aid with their identification, improving still further the purity of AGN samples (see the previous point). Furthermore, measurements of low-energy photoelectric absorption cut-offs, underlying continuum shapes, Compton reflection continua, fluorescent line emission (e.g., from the iron Kα transition), and absorption edges (e.g., the iron K edge) can diagnose system luminosity, obscuration level, nuclear geometry, disk/corona conditions, and Eddington ratio ($L_{\rm Bol}/L_{\rm Edd}$).

While these basic points of utility have led to great success for the enterprise of X-ray surveys, such surveys do have their shortcomings; e.g., in the regime of highly Compton-thick absorption or in cases of intrinsically X-ray weak AGNs (see Section 3.3). Thus, when possible, it is critical to complement X-ray surveys with suitably matched multiwavelength surveys in the area of sky under study. These can help considerably in filling the small chinks in the armor of X-ray surveys, thereby allowing nearly complete identification of all significant SMBH growth.

1.2 The survey capabilities of relevant distant-universe missions: *Chandra*, *XMM-Newton*, and *NuSTAR*

In this review, we will describe some of the main discoveries on AGNs coming from the intensive activity in X-ray (0.5–100 keV) surveys research over the past 15 yr, mainly focusing on missions that can make sensitive "blank-field" surveys of typical AGNs in the distant ($z = 0.1$–5) universe. Our emphasis will thus be on results from the *Chandra X-ray Observatory* (hereafter *Chandra*; e.g., Weisskopf et al 2000), the *X-ray Multi-Mirror Mission* (hereafter *XMM-Newton*; e.g., Jansen et al 2001), and the *Nuclear Spectroscopic Telescope Array* (hereafter *NuSTAR*; e.g., Harrison et al 2013). The new results from these missions rest squarely upon a rich heritage of X-ray survey studies with several superb earlier X-ray missions, as briefly described in, e.g., Section 3.1. We will also introduce more local results from, e.g., the *Swift Gamma-Ray Burst Explorer* (hereafter *Swift*; e.g., Gehrels et al 2004) and the *International Gamma-Ray Astrophysics Laboratory* (hereafter *INTEGRAL*; e.g., Winkler et al 2003) where they connect strongly with results from the distant universe, although these critical local investigations are not our primary focus (and deserve to be the subject of an entirely separate dedicated review).

In terms of basic survey capability, both *Chandra* (launched in 1999 July) and *XMM-Newton* (launched in 1999 December) provide X-ray *spectroscopic imaging* over broad bandpasses (0.3–8 keV and 0.2–10 keV, respectively) and over respectable fields of view (290 arcmin^2 for *Chandra* ACIS-I, and 720 arcmin^2 for *XMM-Newton* EPIC-pn).[2] Their imaging point spread functions are excellent (an on-axis half-power diameter of 0.84 arcsec for *Chandra*) or good (15 arcsec for *XMM-Newton*), though these degrade significantly with increasing off-axis angle. Their most sensitive surveys reach about 80–400 times deeper than those of previous X-ray missions, and excellent source positions (accurate to 0.5–4 arcsec) allow effective multiwavelength follow-up studies even at the faintest X-ray fluxes. Typical survey projects with *Chandra* and *XMM-Newton* generate hundreds-to-thousands of detected AGNs, allowing powerful statistical studies of source populations. Furthermore, systematic public data archiving practices allow effective survey combination, so that source populations spanning wide ranges of luminosity and redshift can be studied together.

NuSTAR is a more recently launched mission (2012 June) that is now transforming surveys of the X-ray universe above 10 keV. It is the first focusing high-energy (3–79 keV) X-ray observatory in orbit; for X-ray surveys of the generally faint sources in the distant universe, *NuSTAR* is most effective up to $\approx$ 24 keV (at higher energies, rising background levels and dropping

[2] Note that many X-ray detectors, including those used on *Chandra* and *XMM-Newton* to perform cosmic surveys, *simultaneously* obtain imaging, spectral, and timing data for the collected photons (e.g., Strüder et al 2001; Turner et al 2001; Garmire et al 2003). Such X-ray observations are qualitatively different from those generally taken in the optical/infrared where, e.g., imaging and spectroscopy are largely distinct.

photon collecting area limit its sensitivity to faint sources). This coverage of high energies equates to reduced absorption bias even relative to *Chandra* and *XMM-Newton*. The reduced bias is particularly key at $z \lesssim 1$ where the rest-frame energies covered by *Chandra* and *XMM-Newton* are still modest. The *NuSTAR* field of view for spectroscopic imaging is 140 arcmin^2, and its imaging point spread function has an on-axis half-power diameter of 58 arcsec but with a sharp core having a full width at half maximum of 18 arcsec (this is about an order of magnitude improvement compared to the imaging capabilities of previous coded-mask instruments in orbit; e.g., Tueller et al 2010). Its sensitivity in probing the hard X-ray sky is about two orders of magnitude better than previous collimated or coded-mask instruments, making it the first genuine surveyor of the distant universe from 10–24 keV. The first publications from the extensive *NuSTAR* survey programs are presently appearing with more in preparation; these have been delivered by the members of the *NuSTAR* survey teams, although the underlying data will be made public for investigations by the whole astronomical community. Many additional *NuSTAR* results are expected in coming years.

1.3 Structure of this review, other relevant reviews, and definitions

As noted above, there is a vast literature on the demographics, physics, and ecology of distant growing SMBHs found in X-ray surveys. Indeed, more than 500 papers on this subject have been published over the past 15 yr based on surveys with *Chandra*, *XMM-Newton*, and *NuSTAR* alone. Our primary aim here is to describe briefly some of the main discoveries coming from these efforts to make them more accessible to interested researchers and students. We note in advance that, owing to the vastness of the literature, it will not be possible to cover all relevant work; our apologies in advance if we could not cover your favorite result or paper.

The structure for the rest of this review will be the following:

- In Section 2, we will review the main X-ray surveys of the distant universe and their supporting observations. We will also describe how AGNs are selected effectively using the X-ray and multiwavelength data.
- Section 3 ("AGN demographics") will cover demographic results for distant X-ray selected AGNs, focusing on AGN evolution over cosmic time. This will also include brief discussions of the population of AGNs missed in cosmic X-ray surveys, the Sołtan and related arguments, and the environmental dependence of AGN evolution.
- Section 4 ("AGN physics") will describe insights on the physical processes operating in AGNs that have come from X-ray surveys.
- Section 5 ("AGN ecology") will describe what X-ray surveys have revealed about interactions between growing SMBHs and their environments (mainly their host galaxies). This section will also discuss the relative radiative output from SMBHs and stars over cosmic time.

– In Section 6, we will outline key outstanding questions. We will also describe prospects for advancing the field both in the near and longer terms using both X-ray and multiwavelength follow-up facilities.

We note that Sections 3, 4, and 5 cover strongly inter-related themes, and that there is inevitably a degree of subjectivity in assigning some results to a single one of these sections. Nevertheless, this structure is useful for basic organizational purposes.

Over the past 15 yr, a number of other relevant in-depth reviews have been prepared that have some overlap with the topics discussed here. These include Hasinger and Zamorani (2000), Gilli (2004), Brandt and Hasinger (2005), Urry and Treister (2007), Hickox (2009), Brandt and Alexander (2010), Alexander and Hickox (2012), Treister and Urry (2012), Kormendy and Ho (2013), Merloni and Heinz (2013), Shankar (2013), and Gilfanov and Merloni (2014). We encourage interested readers to consult these reviews as well, noting that they generally emphasize somewhat different topics than those emphasized here. We also refer interested readers to the chapters in the Astrophysics and Space Science Library volume titled "Supermassive Black Holes in the Distant Universe" (Barger 2004).

Throughout this review we shall adopt J2000 coordinates and a standard cosmology with $H_0 = 70$ km s^{-1} Mpc^{-1}, $\Omega_{\rm M} = 0.3$, and $\Omega_\Lambda = 0.7$. When quoting effective hydrogen column densities estimated from X-ray spectral analyses, we will adopt the cosmic abundances of Anders and Grevesse (1989). When referring to X-ray obscured AGNs, we will be considering systems with $N_{\rm H} \gtrsim 10^{22}$ cm^{-2} unless noted otherwise. This threshold value is commonly adopted though admittedly somewhat arbitrary, being close to the typical maximum absorption expected from a galactic disk. It is also broadly consistent with the division in X-ray absorption level between optically obscured and optically unobscured AGNs. When referring to highly X-ray obscured AGNs, we will generally mean systems with column densities at least a factor of ≈ 50 greater; i.e., $N_{\rm H} \gtrsim 5 \times 10^{23}$ cm^{-2}.

2 The main cosmological X-ray surveys, their supporting observations, and AGN selection

2.1 Description of the current main cosmic X-ray surveys of distant AGNs

The capabilities of *Chandra*, *XMM-Newton*, and *NuSTAR* (see Section 1.2) have led to a substantial number of X-ray surveys being conducted of the distant universe. These include targeted surveys, both deep and wide, where a sky area of particular interest is observed; e.g., a field already having excellent multiwavelength data or a field containing a notable object such as a high-redshift protocluster. Furthermore, these include serendipitous surveys that investigate the serendipitous sources detected in a number of fields observed for other reasons.

Table 1 Selected Extragalactic X-ray Surveys with *Chandra*, *XMM-Newton*, and *NuSTAR*

Survey Name	Rep. Eff. Exp. (ks)	Solid Angle (arcmin^2)	Representative Reference
Chandra (0.3–8 keV)			
Chandra Deep Field-South (CDF-S)	3870	465	Xue et al (2011)
Chandra Deep Field-North (CDF-N)	1950	448	Alexander et al (2003)
AEGIS-X Deep	800	860	Goulding et al (2012)
SSA22 protocluster	392	330	Lehmer et al (2009a)
HRC Lockman Hole	300	900	PI: S.S. Murray
Extended CDF-S (E-CDF-S)	250	1,128	Lehmer et al (2005)
AEGIS-X	200	2,412	Laird et al (2009)
Lynx	185	286	Stern et al (2002)
LALA Cetus	174	297	Wang et al (2007)
LALA Boötes	172	346	Wang et al (2004)
C-COSMOS and COSMOS-Legacy	160	6,120	Elvis et al (2009)
SSA13	101	345	Barger et al (2001b)
Abell 370	94	345	Barger et al (2001a)
3C 295	92	274	D'Elia et al (2004)
ELAIS N1+N2	75	590	Manners et al (2003)
WHDF	72	286	Bielby et al (2012)
CLANS (Lockman Hole)	70	2,160	Trouille et al (2008)
SEXSI[a]	45	7,920	Harrison et al (2003)
CLASXS (Lockman Hole)	40	1,620	Trouille et al (2008)
13 hr Field	40	710	McHardy et al (2003)
ChaMP[a]	25	34,560	Kim et al (2007)
XDEEP2 Shallow	15	9,432	Goulding et al (2012)
Chandra Source Catalog (CSC)[a]	13	1,150,000	Evans et al (2010)
Stripe 82X—*Chandra*[a]	9	22,320	LaMassa et al (2013b)
NDWFS XBoötes	5	33,480	Murray et al (2005)
XMM-Newton (0.2–12 keV)			
Chandra Deep Field-South (CDF-S)	2820	830	Ranalli et al (2013)
Lockman Hole	640	710	Brunner et al (2008)
Chandra Deep Field-North (CDF-N)	180	752	Miyaji et al (2003)
13 hr Field	120	650	Loaring et al (2005)
ELAIS-S1	90	2,160	Puccetti et al (2006)
Groth-Westphal	81	730	Miyaji et al (2004)
COSMOS	68	7,670	Cappelluti et al (2009)
Subaru *XMM-Newton* Deep Survey (SXDS)	40	4,100	Ueda et al (2008)
Marano Field	30	2,120	Lamer et al (2003)
HELLAS2XMM[a]	25	10,440	Baldi et al (2002)
XMM-LSS XMDS	23	3,600	Chiappetti et al (2005)
3XMM[a]	15	2,300,000	Watson (2012)
Stripe 82X—*XMM-Newton*[a]	15	37,800	LaMassa et al (2013a)
XMM-LSS	10	39,960	Chiappetti et al (2013)
XMM-XXL	10	180,000	Pierre (2012)
Stripe 82X—*XMM-Newton* Targeted	8	129,600	PI: C.M. Urry
XMM-Newton Slew Survey (XMMSL1)[a]	0.006	8×10^7	Warwick et al (2012)
NuSTAR (3–24 keV)			
Extended CDF-S (E-CDF-S)	200	1,100	Mullaney et al, in prep
AEGIS-X	270	860	Aird et al, in prep
COSMOS	65	6,120	Civano et al, in prep
Serendipitous Survey[a]	22	19,000	Alexander et al (2013)

[a]Serendipitious survey; see Section 2.1 for brief discussion regarding such surveys.

Some selected extragalactic surveys conducted with *Chandra*, *XMM-Newton*, and *NuSTAR* are listed in Table 1. A number of aspects of this table deserve note:

1. These surveys often have wide ranges of sensitivity across their associated solid angles due to, e.g., differing satellite pointing strategies and instrumental effects. The serendipitous surveys (e.g., ChaMP, SEXSI, CSC, HELLAS2XMM, 3XMM) particularly stand out in this regard, often being made up of observations differing by an order of magnitude or more in exposure time.
2. The solid angles quoted generally represent the total sky coverage at bright X-ray flux limits.
3. When listing *XMM-Newton* exposure times, we have attempted to remove time intervals affected by strong background flaring; such intervals are generally not useful for surveys of faint cosmic sources.
4. The listed exposure times are for a single X-ray telescope and focal plane module (FPM). Note that *XMM-Newton* and *NuSTAR* have three and two simultaneously operating telescopes/FPMs, respectively.
5. Some of the surveys have overlap of their solid angles of coverage (e.g., CDF-S vs. E-CDF-S; AEGIS-X Deep vs. AEGIS-X; XDEEP2 Shallow vs. Stripe 82X—*Chandra*; SXDS vs. XMM-LSS XMDS vs. XMM-LSS vs. XMM-XXL).
6. Some of these surveys are still increasing in solid angle and/or depth. For example, many of the serendipitous surveys continue to grow as more X-ray observations are performed, and the *Chandra* CDF-S survey is presently being raised to a 7 Ms exposure.
7. Some of the listed surveys have been conducted in multiple epochs spanning up to ≈ 15 yr, allowing assessments of long-timescale X-ray variability for the detected sources (e.g., Paolillo et al 2004; Papadakis et al 2008; Young et al 2012b; Lanzuisi et al 2014).

Interested readers should consult the cited papers in Table 1 for survey-specific details. Plots of solid angle of sky coverage vs. sensitivity in both the 0.5–2 keV and 2–10 keV bands for *Chandra* and *XMM-Newton* surveys are given in Figure 3.

Together, all these surveys cover a broad part of the practically accessible sensitivity vs. solid-angle "discovery space" via the standard "wedding-cake" design, providing a quite complete understanding of AGN populations in the distant universe (though, as discussed in Section 6.2, there is still room for important improvements). One persistent limitation of X-ray surveys in general, however, has been the lack of sensitive and thoroughly followed-up surveys over hundreds-to-thousands of deg^2; the widest sensitive surveys presently are 3XMM and XMM-XXL. This limitation has hindered X-ray constraints upon rare objects, such as the most luminous AGNs in the Universe, although targeted X-ray follow-up studies of such objects selected at other wavelengths have mitigated this issue to some degree (e.g., Vignali et al 2005; Just et al 2007; Stern et al 2014). *eROSITA* (e.g., Merloni et al 2012) is expected to im-

prove this situation significantly in the near future, and dedicated wide-field X-ray telescopes (e.g., Murray et al 2013; Rau et al 2013) could make major additional strides (see Section 6.4 for more detailed discussion).

Surveys with *Chandra* and *XMM-Newton* have resolved ≈ 75–80% of the cosmic X-ray background (CXRB) from 0.5–10 keV into point sources (e.g., see Section 1.3 of Brandt and Hasinger 2005 for further discussion). Up-to-date measurements of the resolved fraction of the CXRB below 10 keV in discrete energy bands may be found in, e.g., Hickox and Markevitch (2006), Lehmer et al (2012), Xue et al (2012), and Ranalli et al, in prep; Fig. 4 shows results from one such analysis. These measurements provide useful integral constraints upon remaining undetected X-ray source populations, although they still lie significantly below the peak of the CXRB at 20–40 keV. The deepest surveys with *NuSTAR* are expected to resolve 30–40% of the 8–24 keV CXRB (e.g., Ballantyne et al 2011; J.A. Aird 2014, private communication), reaching closer to its peak. This is a large improvement over pre-*NuSTAR* results, where only a few percent of the 10–100 keV CXRB was resolved (e.g., Krivonos et al 2005; Treister et al 2009b).

2.2 Supporting multiwavelength observations and spectroscopic follow-up

Characterization of the detected X-ray sources using both multiwavelength photometric data and spectroscopic observations is crucial for investigating their nature. At the most basic level, a detected X-ray source must be matched reliably to a multiwavelength photometric counterpart so that, e.g., the feasibility of spectroscopic observations can be determined; such matching is done most effectively using a likelihood-ratio technique (e.g., Sutherland and Saunders 1992; Rutledge et al 2000; Ciliegi et al 2003; Naylor et al 2013). Counterpart matching is straightforward for the majority of sources in *Chandra* surveys owing to the excellent angular resolution of *Chandra* (generally providing 0.5–1.5″ positions; e.g., Evans et al 2010), although there are genuine matching challenges for the faintest optical, near-infrared (NIR; about 1–5 μm), and/or mid-infrared (MIR; about 5–30 μm) counterparts. For *XMM-Newton* surveys the counterpart matching is more challenging (generally 2–4″ positions; e.g., Watson et al 2009), although the majority of sources in *XMM-Newton* surveys can also be matched to optical/NIR/MIR counterparts. In current *NuSTAR* surveys (generally 10–20″ positions; e.g., Harrison et al 2013), the detected sources are typically first matched to *Chandra*/*XMM-Newton* (or other X-ray) sources which then are matched to optical/NIR/MIR counterparts. The X-ray sources found in the surveys listed in Table 1 span an extremely broad range of optical/NIR/MIR flux; e.g., the I-band magnitudes for AGNs range from brighter than 15th to fainter than 28th magnitude (e.g., Barger et al 2003b; Szokoly et al 2004; Laird et al 2009; Brusa et al 2010; Luo et al 2010; Pineau et al 2011; Rovilos et al 2011; Xue et al 2011; Civano et al 2012; Trichas et al 2012).

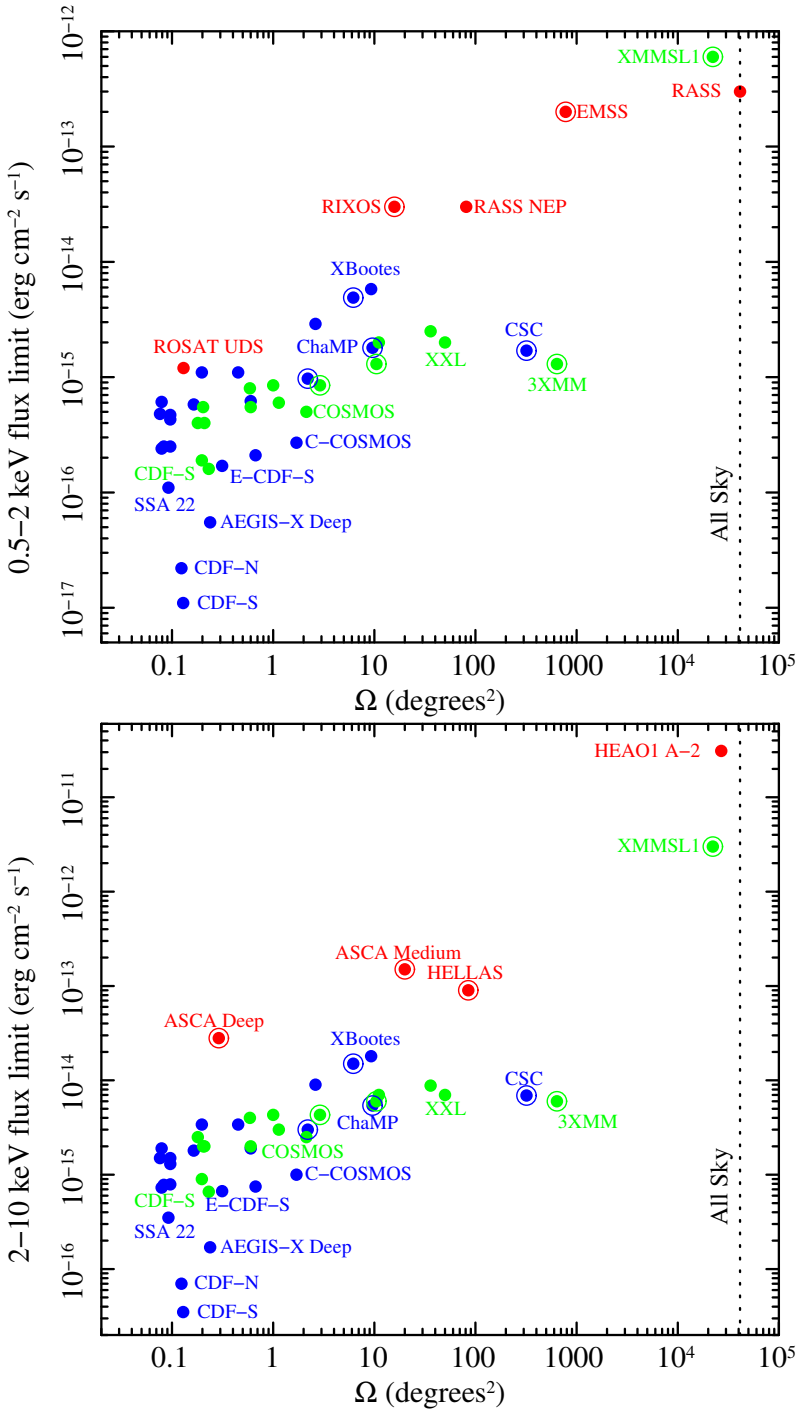

Fig. 3 Solid angle of sky coverage vs. sensitivity in both the 0.5–2 keV and 2–10 keV bands for the surveys in Table 1 from *Chandra* (blue) and *XMM-Newton* (green). For comparison purposes, a few surveys from previous X-ray missions are shown in red. The circles around some of the points indicate serendipitous surveys as also denoted in Table 1. Some of the surveys are labeled by name (sometimes abbreviated) in regions where symbol crowding is not too strong. The vertical dotted line shows the solid angle for the whole sky. Each of the surveys has a range of sensitivity across its solid angle, and different authors use somewhat different methodologies for computing and quoting sensitivity; this leads to small uncertainties in the precise relative locations of the data points.

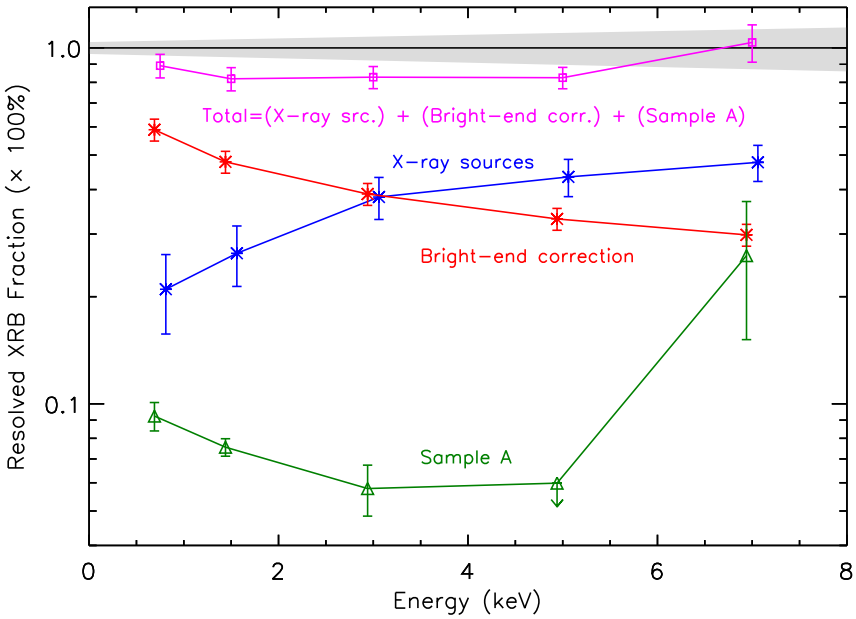

Fig. 4 The resolved fraction of the CXRB in the 4 Ms CDF-S observation as a function of energy from 0.5–8 keV. Shown are the resolved fraction from the 4 Ms CDF-S sources (blue), the "bright-end correction" that accounts for bright sources too rare to be found within the studied CDF-S field of view (red), and results from stacking X-ray photons coincident with z-band identified galaxies that are not individually X-ray detected (green, titled "Sample A"). The summation of these three components is also shown (magenta). The total CXRB intensity is taken from Hickox and Markevitch (2006) with (non-negligible) uncertainty indicated by the gray area. The unresolved CXRB below ≈ 5 keV, even after inclusion of the stacked emission coincident with galaxies, is likely associated with groups/clusters of galaxies. Adapted from Xue et al (2012).

The X-ray data from current surveys generally do not allow direct redshift determination, although there are occasional cases where redshifts can be measured based on the strong iron Kα line and/or iron K edge in X-ray spectra (e.g., Iwasawa et al 2012; Del Moro et al 2014). Thus, spectroscopic and/or photometric determination of redshifts, usually in the optical/infrared, is essential for, e.g., calculation of source luminosity, the most meaningful X-ray spectral modeling, and studies of source cosmic evolution. In line with the broad range of optical/NIR/MIR flux for the counterparts, a wide variety of facilities have been used productively for spectroscopic redshift determination, including the largest telescopes on Earth (e.g., Keck, the Very Large Telescope, and Subaru) for the faintest sources in deep surveys. Enormous progress has been made with spectroscopic redshift determination for X-ray survey sources, particularly when multi-object spectrographs can be utilized to target efficiently large numbers of X-ray sources simultaneously; the field

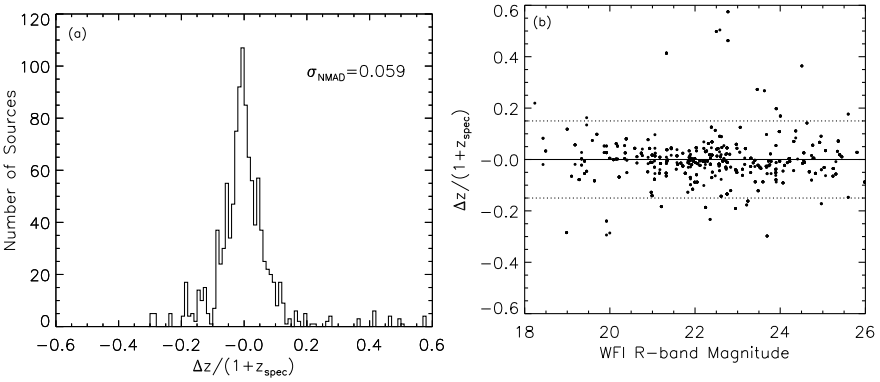

Fig. 5 (a) Distribution of the photometric redshift (photo-z, or $z_{\rm photo}$) accuracy, $\Delta z/(1+z_{\rm spec})$, derived from an unbiased blind-test sample of X-ray AGNs in the CDF-S ($z_{\rm spec}$ values are spectroscopic redshifts). The typical photo-z accuracy for the sample is evaluated with a robust estimator, the normalized median absolute deviation ($\sigma_{\rm NMAD}$): $\sigma_{\rm NMAD} = 1.48 \times {\rm median}[(|\Delta z - {\rm median}(\Delta z)|)/(1+z_{\rm spec})]$. (b) Photo-$z$ accuracy, $\Delta z/(1+z_{\rm spec})$, vs. R-band magnitude for the blind-test sample. The solid line indicates $z_{\rm photo} = z_{\rm spec}$, and the dotted lines represent relations of $z_{\rm photo} = z_{\rm spec} \pm 0.15(1+z_{\rm spec})$. The photo-$z$ accuracy declines toward faint R-band magnitudes, particularly when considering the frequency of catastrophically incorrect photo-z values. Adapted from Luo et al (2010).

sizes of these spectrographs often match the sizes of the X-ray survey fields well. Large samples of X-ray sources with reasonably complete spectroscopic identification down to $I = 22$–24 are now available for statistical studies (e.g., Barger et al 2003b; Fiore et al 2003; Szokoly et al 2004; Eckart et al 2006; Della Ceca et al 2008; Trouille et al 2008; Trump et al 2009; Silverman et al 2010; Kochanek et al 2012; Trichas et al 2012). This being said, much work is still needed to improve the spectroscopic completeness for some key fields, in some cases by systematically publishing spectra already acquired. At fainter fluxes of $I = 24$–28 where many X-ray sources are found, particularly in the deepest X-ray surveys, the spectroscopic completeness drops rapidly (e.g., even in the intensively studied CDF-S, only $\approx 65\%$ of the X-ray sources overall have spectroscopic redshifts). This bottleneck remains one persistent driver for the construction of future Extremely Large Telescopes in the optical/NIR (see Section 6.3).

It is often possible to derive photometric redshifts of reasonable quality for X-ray AGNs when spectroscopic redshifts are unavailable, although these are generally of lower quality than those for comparable non-AGN galaxies (e.g., see Fig. 5). Photometric redshifts also provide a useful cross-check even when spectroscopic redshifts are available; e.g., if only one emission line is clearly detected then there can be significant uncertainty in the correct spectroscopic redshift determination. In the best cases, photometric redshifts are derived from $\gtrsim 20$ bands of MIR-to-UV photometric data, utilize dedicated templates suitable for X-ray sources such as AGN/galaxy hybrids, utilize dedicated sets of medium-band filters, and/or allow for AGN optical/NIR/MIR variability

effects between different filters observed non-simultaneously (e.g., Salvato et al 2009; Cardamone et al 2010; Luo et al 2010; Xue et al 2012; Hsu et al 2014). Photometric redshift derivations for X-ray sources can reach much fainter optical magnitudes than can be reached spectroscopically (e.g., to $I \approx 28$). When compared with relatively bright optical sources having spectroscopic redshifts, they have a (magnitude-dependent) typical accuracy in $\Delta z/(1+z)$ of 1–10% (using $\sigma_{\rm NMAD}$, see Fig. 5) with an outlier fraction of catastrophically incorrect redshifts of 3–20%. Further improvements in statistical redshift estimation for optically faint X-ray sources should be possible in the near future using clustering-based techniques (e.g., Matthews and Newman 2010; Ménard et al 2014).

In addition to counterpart identification and redshift determination, multiwavelength observations play many further key roles in the effective investigation of sources from cosmic X-ray surveys. These include basic characterization of the nature of the detected sources (see Section 2.3), measurements of broad-band AGN spectral energy distributions (SEDs) to determine more reliable bolometric luminosities and investigate accretion processes, and measurements of AGN host-galaxy properties [e.g., stellar mass, star-formation rate (SFR), morphology, interaction status, and large-scale environment; see Section 5]. Furthermore, these multiwavelength data have been used to identify AGNs and AGN candidates missed by the X-ray selection technique (e.g., Compton-thick and/or intrinsically X-ray weak AGNs; see Section 3.3).

2.3 AGN selection from the general X-ray source population

The main classes of extragalactic X-ray sources detected in cosmic surveys include AGNs, starburst galaxies, normal galaxies, galaxy clusters, and galaxy groups. We will not review the non-AGN classes here and instead refer readers to the other reviews cited in Section 1.3 for relevant details (e.g., see Section 2.2 of Brandt and Hasinger 2005). Instead, consistent with our focus in this review, we will describe how AGNs are selected from the general X-ray source population.

Multiple methods can be used to derive a highly reliable sample of AGNs, including obscured and low-luminosity systems, from a sample of X-ray survey point sources. Those relying upon direct use of the X-ray data include the following:

1. *X-ray luminosity.* Sources with 0.5–10 keV luminosities above 3×10^{42} erg s^{-1} are predominantly AGNs. Only rare extreme starburst galaxies in the distant universe, such as luminous submillimeter galaxies, can exceed this threshold without an AGN being present; caution is needed in applying the luminosity threshold when such sources are under study.
2. *X-ray luminosity vs. SFR.* Many researchers have established relations between X-ray luminosity and SFR for starburst/normal galaxies that lack AGNs (e.g., Bauer et al 2002; Ranalli et al 2003; Persic and Rephaeli 2007; Lehmer et al 2010; Mineo et al 2014). X-ray sources lying well above

(typically, $\gtrsim 5$ times is used) such relations are found to be AGNs. When quality data capable of constraining host-galaxy SFR are available (e.g., in the radio, infrared, and/or UV), this method is both more reliable and more complete than the straight X-ray luminosity cut of method 1 above. If host-galaxy stellar mass is also available, then the expected X-ray luminosity can be estimated as a function of both SFR and stellar mass.

3. *X-ray-to-optical/NIR flux ratio.* Consistent with the low dilution of X-ray emission by host-galaxy starlight noted in Section 1.1, AGNs tend to have higher X-ray-to-optical/NIR flux ratios than starburst/normal galaxies. Typically thresholds of $\log(f_{0.5-10\,\mathrm{keV}}/f_R) > -1$ using the observed-frame R band or $\log(f_{0.5-10\,\mathrm{keV}}/f_{3.6\mu\mathrm{m}}) > -1$ using the observed-frame 3.6 μm band from *Spitzer* (e.g., Werner et al 2004) serve to select samples that are 90–95% AGNs (other bands can also be used in a similar fashion, although the requisite threshold will vary). Ideally these ratios would be derived using rest-frame rather than observed-frame bands, since the X-ray and optical/NIR fluxes have significantly different k-corrections. However, this is often not practical or possible, and when using observed-frame bands it is generally best to use the reddest optical/NIR band available (e.g., to at least minimize the effects of dust extinction in high-redshift sources).
4. *X-ray spectral shape.* X-ray sources with flat effective power-law photon indices in the 0.5–10 keV band of $\Gamma_{\mathrm{eff}} < 1.0$ are generally obscured AGNs (obscured AGNs can also have larger Γ_{eff} values, but use of a larger Γ_{eff} threshold can lead to uncertain AGN identifications). The effective photon index from a simple power-law fit is a useful first-order indicator of spectral shape even when the observed spectrum does not precisely have a power-law form. It can be estimated based upon direct X-ray spectral fitting or, in cases of limited counts, based upon a hardness/band ratio. In $\Gamma_{\mathrm{eff}} < 1.0$ cases, the effective photon index is generally flat owing to X-ray absorption and/or Compton reflection. The X-ray binary populations that dominate the emission from starburst/normal galaxies are empirically found to produce steeper X-ray spectra with $\Gamma_{\mathrm{eff}} \gtrsim 1.5$.
5. *X-ray variability.* Rapid X-ray variability by large amplitudes is commonly seen among those AGNs where the direct continuum produced close to the SMBH is observable. This variability is generally stronger than that seen from collections of X-ray binaries in starburst/normal galaxies (e.g., Young et al 2012b). Furthermore, as noted above, some of the X-ray surveys in Table 1 allow variability studies over much longer timescales. Significantly variable sources that also have X-ray luminosities larger than $\approx 10^{41}$ erg s^{-1} are likely to be AGNs, although there are rare notable exceptions (e.g., Kaaret et al 2001; Webb et al 2010).
6. *X-ray position.* The X-ray positions of AGNs are generally coincident with the apparent nuclei of their host galaxies (as opposed to, e.g., X-ray binaries, which can be identified across the extent of the host galaxy often as off-nuclear sources). This positional coincidence can be checked for relatively low-redshift objects ($z \lesssim 0.5$) when high-resolution X-ray (e.g., *Chan-*

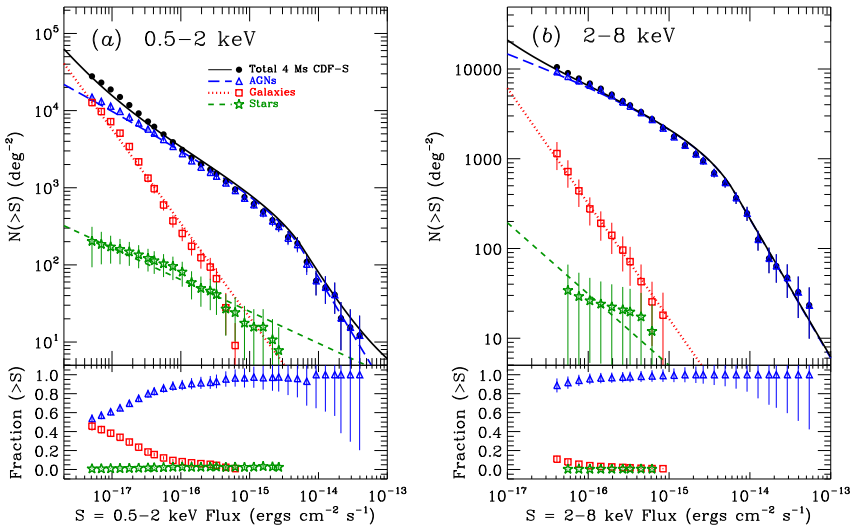

Fig. 6 Cumulative number counts for the 4 Ms CDF-S in the (a) 0.5–2 keV and (b) 2–8 keV bands. The total number counts (black) have been apportioned by source class, as labeled, into AGNs (blue), galaxies (red), and stars (green). The bottom portions of each panel show the fractional contributions of each source class to the cumulative number counts. Note that AGNs remain the numerically dominant source population down to faint fluxes, although at still-fainter 0.5–2 keV fluxes galaxies will become numerically dominant. The AGN number counts reach $\approx 14,900$ deg^{-2} at the faintest 0.5–2 keV fluxes, and this is the highest sky density of reliably identified AGNs found at any wavelength. Taken from Lehmer et al (2012).

dra) and optical/NIR (e.g., *HST*) imaging are available (e.g., Lehmer et al 2006).

Some of these methods have a long history (e.g., Maccacaro et al 1988 for method 3) while others have been developed/refined more recently. A few in-depth applications of these methods include Alexander et al (2005a), Brusa et al (2010), Laird et al (2010), Xue et al (2011), Lehmer et al (2012), Civano et al (2012), and Wang et al (2013). Note that some of these methods rely upon having fairly precise redshift information available while others depend much less upon redshift; AGN samples can often be selected reasonably well using methods 3–6 together prior to redshift determination. AGNs are generally found to make up 75–95% of the sources by number in current X-ray surveys, with their percentage contribution dropping with survey depth as many starburst/normal galaxies are detected at faint fluxes (primarily at low X-ray energies). The precise fractional contribution from AGNs as a function of survey depth has been quantified in number counts apportioned by source type (see Fig. 6; e.g., Bauer et al 2004; Civano et al 2012; Lehmer et al 2012).

In addition to the approaches above relying upon the direct use of X-ray data, approaches relying upon independent multiwavelength data can also be

used for AGN selection/confirmation from a sample of X-ray sources. These include the detection of broad and/or high-ionization emission lines in optical/NIR spectra, high surface brightness radio core emission or extended radio jets/lobes, strong infrared emission from hot dust heated by an AGN continuum, and distinctive optical variability. In well-studied X-ray and multiwavelength survey fields, multiple independent methods have been applied to cross-validate AGN candidates, leading to the most reliable and pure samples of distant AGNs available.

3 AGN demographics

3.1 The status of AGN evolution studies before *Chandra* and *XMM-Newton*

The number-density evolution of the AGN population over cosmic time has been a topic of intense interest since the 1960's (e.g., Schmidt 1968). Early work focused on the evolution of luminous quasars and radio galaxies detected in wide-field optical/radio surveys (see, e.g., Hartwick and Schade 1990; Hewett and Foltz 1994; Boyle 2001; Osmer 2004; Merloni and Heinz 2013 for reviews), and such wide-field studies have continued to advance until the present (e.g., Wall et al 2005; Richards et al 2006b; Massardi et al 2010; Ross et al 2013). Wide-field optical surveys remain largely constrained to the relatively rare systems where the AGN significantly outshines the host galaxy, owing to the selection techniques employed (typically based upon source colors measured in photometric data).

Prior to the launches of *Chandra* and *XMM-Newton*, the population of luminous quasars had been well established to evolve strongly over cosmic time, peaking in number density at $z \approx 2$–3. Most analyses up to the year ≈ 2000 found that the form of the evolution at $z \lesssim 2.5$ could be fit acceptably with pure luminosity evolution models, although there were reports of more complex evolution at bright magnitudes (e.g., Hartwick and Schade 1990; Boyle et al 2000). Many researchers reasonably expected that the basic evolutionary behavior derived for luminous quasars would also apply at lower luminosities.

The German-USA-UK *ROSAT* mission was the most effective surveyor of the distant X-ray (0.1–2.4 keV) universe prior to *Chandra*/*XMM-Newton*, contributing to a number of fundamental results on AGN demographics. The *ROSAT* Deep Survey in the Lockman Hole, resolving 70–80% of the 0.5–2 keV CXRB, directly showed that AGNs produce most of the background in this band (e.g., Hasinger et al 1998; Schmidt et al 1998). The responsible AGNs showed a range of optical spectral types, including broad-line and narrow-line spectra, and X-ray-to-optical flux ratios $[-1 \lesssim \log(f_{0.5-2\,\mathrm{keV}}/f_R) \lesssim 1]$. Results on the X-ray luminosity function (XLF) derived from *ROSAT* surveys spanning a range of depths indicated that luminosity-dependent density evolution (LDDE) described the data better than pure luminosity evolution or pure density evolution (e.g., Miyaji et al 2000, 2001; but see also Page et al 1997), importantly indicating a luminosity dependence of AGN evolution. At

higher energies, the Japanese-USA *ASCA* and Dutch-Italian *BeppoSAX* missions were able to resolve $\approx 30\%$ of the 2–10 keV CXRB, and follow-up studies indicated that the majority of the sources in this band were also AGNs (e.g., Ueda et al 1998; Fiore et al 1999). Many of these sources had hard X-ray spectra with effective power-law photon indices of $\Gamma_{\rm Eff} = 1.3$–1.7, consistent with longstanding expectations that obscured AGNs make much of the CXRB which has $\Gamma_{\rm Eff} = 1.4$ from 2–10 keV (e.g., Setti and Woltjer 1989; Comastri et al 1995).

The demographics of high-redshift AGNs at $z = 3$–6 were highly uncertain when *Chandra* and *XMM-Newton* began operation. Optical and radio surveys of luminous quasars both indicated a consistent strong decline in number density above $z \approx 3$ (e.g., Schmidt et al 1995; Shaver et al 1999). However, X-ray surveys of somewhat less luminous quasars suggested a lack of any strong decline (e.g., Miyaji et al 2000) and were consistent with a constant number density at $z > 2$. Theoretical considerations offered few further constraints, allowing extremely high quasar space densities in principle (e.g., Haiman and Loeb 1999). Given the available constraints, it was feasible that the Universe was reionized at $z \approx 5$–7 by AGNs.

3.2 X-ray luminosity functions and the luminosity dependence of AGN evolution

Owing to the advantages of X-ray surveys detailed in Section 1.1, *Chandra* and *XMM-Newton* have allowed the effective selection of distant AGNs, including obscured systems, that are up to ≈ 100 times less bolometrically luminous than those found in wide-field quasar surveys such as the SDSS (e.g., Ross et al 2012; the vast majority of SDSS broad-line quasars are straightforwardly detected in moderate-depth X-ray surveys). Objects similar to local moderate-luminosity Seyfert galaxies can be identified out to $z \approx 5$. The sky density of X-ray selected AGNs in the deepest *Chandra* surveys has now reached $\approx 14,900$ deg^{-2} (see Fig. 6; Lehmer et al 2012), making them ≈ 500 times more numerous on the sky than SDSS quasars. As another comparison, the deepest optical photometric AGN surveys reaching $B \approx 24.5$ have delivered AGN sky densities of ≈ 400 deg^{-2} (e.g., Wolf et al 2004; Beck-Winchatz and Anderson 2007; also see Palanque-Delabrouille et al 2013). Furthermore, the $\approx 14,900$ deg^{-2} sky density is ≈ 15 times larger than that from the *ROSAT* Deep Survey (970 deg^{-2}; Hasinger et al 1998), the deepest X-ray survey conducted prior to *Chandra* and *XMM-Newton*. *NuSTAR* is now further broadening the parameter space of discovery, allowing improved identification of highly obscured AGNs at relatively bright flux levels (e.g., Del Moro et al 2014).

AGN samples from *Chandra* and *XMM-Newton* are now thought to be sufficiently complete over a broad part of the luminosity-redshift plane to allow many fundamental issues regarding AGN evolution to be addressed (though further improvements are still critical; e.g., see Section 3.3). A key finding, first reported by Cowie et al (2003) and now a subject of many studies, is

a notable "anti-hierarchical" luminosity dependence of AGN evolution, such that the number density of lower-luminosity AGNs peaks later in cosmic time than that of powerful quasars (see Fig. 7; e.g., Barger et al 2005; Hasinger et al 2005; La Franca et al 2005; Silverman et al 2008a; Ebrero et al 2009; Yencho et al 2009; Aird et al 2010; Ueda et al 2014). This qualitative behavior is also broadly seen in star-forming galaxies (e.g., Cowie et al 1996) and is often referred to as "cosmic downsizing", although this term has developed a number of usages with respect to galaxies (e.g., Bundy et al 2006; Cimatti et al 2006; Faber et al 2007; Fontanot et al 2009). AGN downsizing was not widely anticipated prior to its observational discovery; AGN population synthesis models for the CXRB at the time generally adopted the basic evolutionary behavior of luminous quasars for AGNs of all luminosities. The most X-ray luminous AGNs with $L_X = 10^{45}$–10^{47} erg s^{-1} peak in number density at $z \approx 2$–3, consistent with the behavior of optically selected quasars, while more common AGNs with $L_X = 10^{43}$–10^{44} erg s^{-1} peak at $z \approx 0.8$–1.5. Fig. 7 shows that the luminosity dependence of AGN evolution appears sufficiently important to shift the overall peak of cosmic SMBH power production to lower redshifts ($z \approx 1.5$–2) than would be expected solely from the study of luminous quasars ($z \approx 2$–3). Roughly, at $z < 1$, $z = 1$–2, and $z > 2$ the integrated fractions of SMBH growth (i.e., the total accreted mass onto SMBHs) are broadly comparable at 25–35%, 37–47%, and 23–33%, respectively. AGNs with $L_X = 10^{44}$–10^{45} erg s^{-1} dominate SMBH power production at $z = 1.5$–4, while those with $L_X = 10^{43}$–10^{44} erg s^{-1} dominate at lower redshifts (at very low redshifts of $z \lesssim 0.5$, AGNs with $L_X = 10^{41}$–10^{43} erg s^{-1} also make large fractional contributions). Ongoing *NuSTAR* surveys at higher X-ray energies up to ≈ 24 keV, while providing valuable insights, do not suggest any qualitative revisions to this basic picture (e.g., Alexander et al 2013; Del Moro et al 2014; Civano et al, in prep; Mullaney et al, in prep); e.g., the vast majority of the *NuSTAR* survey sources were previously detected by *Chandra* and/or *XMM-Newton*. The downsizing behavior of AGNs has also now been found in optically selected (e.g., Bongiorno et al 2007; Croom et al 2009; Shen and Kelly 2012; Ross et al 2013) and radio-selected (e.g., Massardi et al 2010; Rigby et al 2011) samples, confirming the generality of this phenomenon, although X-ray selected samples remain the most effective at constraining the downsizing behavior.

Measurement of the quantitative details of the downsizing behavior for X-ray AGNs depends upon many challenging issues, including initial detection completeness (and corrections for missed AGNs), multiwavelength counterpart identification, completeness in redshift determination, X-ray spectral modeling (e.g., X-ray absorption corrections to luminosity estimates), and statistical methodology in XLF calculation. Thus, while the basic downsizing phenomenon appears securely established, there is still some remaining debate over the precise form of the XLF and its evolution. The most recent in-depth studies have proposed either LDDE (e.g., Ueda et al 2014) or luminosity and density evolution (LADE; e.g., Aird et al 2010); in the latter the shape of the XLF is constant with redshift, but it undergoes strong luminos-

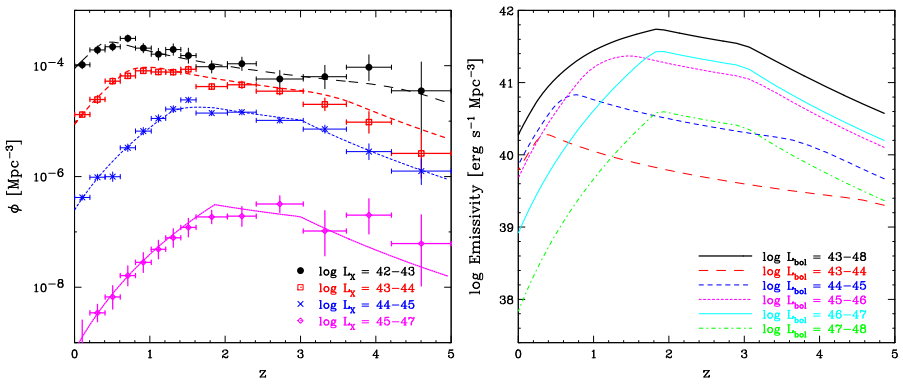

Fig. 7 (a) Comoving number density vs. redshift for AGNs, selected from multiple X-ray surveys, in four rest-frame 2–10 keV luminosity classes [as labeled; in units of log(erg s^{-1})]. Note that the number density of moderate-luminosity AGNs peaks later in cosmic time than that of powerful quasars (i.e., AGN cosmic downsizing). (b) Comoving bolometric luminosity density vs. redshift for the same AGN sample in six bolometric luminosity classes [as labeled; in units of log(erg s^{-1})]. Note the peak luminosity density at $z \approx 1.8$ for AGNs over the broad range of $L_{\rm Bol} = 10^{43}$–10^{48} erg s^{-1}. Taken from Ueda et al (2014).

ity evolution at $z \lesssim 1$, and overall negative density evolution toward increasing redshift. Especially at high redshifts of $z \gtrsim 3$, the LDDE and LADE models predict quite different numbers of AGNs. The latest high-redshift constraints appear to favor the LDDE model, but further testing is needed.

The observed AGN downsizing behavior seen via the measured XLF could arise due to changes in the mass of the typical active SMBH and/or changes in the typical accretion rate. A variety of modeling efforts have been made to understand the physical nature of AGN downsizing, including analytic models, semi-analytic models, and large-scale numerical simulations (e.g., Hopkins et al 2008; Degraf et al 2010; Fanidakis et al 2012; Hirschmann et al 2012, 2014; Menci et al 2013); these efforts sometimes also attempt to model simultaneously the growth of AGN host galaxies and their downsizing behavior. The numerical simulations continue to advance rapidly and include many of the mechanisms relevant to SMBH fueling and growth, including galaxy interactions, disk instabilities, and gas cooling. They have had genuine success in plausibly reproducing the apparent basic anti-hierarchical behavior of SMBH growth within the context of the hierarchical paradigm for cosmic structure formation. This being said, even the most intensive simulations to date lack the spatial/mass resolution to model in detail the still uncertain but essential accretion and feedback processes operating on small scales, and approximate "sub-grid" approaches are often adopted for these processes.

Given the immense modeling challenges, it is understandable that the model predictions for XLF evolution and the nature of downsizing end up differing in detail. Broadly, and as would initially be expected from the XLF results, the models generally indicate that more massive SMBHs grew earlier in cosmic time. Some furthermore quantitatively predict a decline in average

Eddington ratio with redshift (e.g., Fanidakis et al 2012; Hirschmann et al 2012, 2014). The strong early drop in number density of the luminous AGN population is predicted to result from the exhaustion of cold gas in massive halos due to strong early star formation and feedback, as well as a decline over time in merging activity. Less-luminous AGNs evolve more mildly and can remain numerous later in cosmic time, however, as the gas content of their generally lower mass halos evolves more mildly. A significant fraction of the less-luminous AGNs are also remnants of formerly luminous AGNs that have faded; i.e., objects with low Eddington ratios, perhaps intermittently triggered, whose massive SMBHs are no longer rapidly growing (in a fractional sense) but can still appear as AGNs. Additional observational evidence consistent with this basic picture includes estimates of SMBH masses and Eddington ratios for distant AGNs in X-ray surveys (see Section 5.4) and observations of the mass-dependent growth timescales of local SMBHs (e.g., Heckman et al 2004).

Chandra and *XMM-Newton* have also greatly clarified the demographics of AGNs at $z = 3$–6, although there is still scope for significant improvements. In contrast to the earlier suggestions from *ROSAT* surveys (see Section 3.1), the X-ray data now clearly support an exponential decline in the number density of luminous AGNs above $z \approx 3$ (e.g., Barger et al 2003a; Cristiani et al 2004; Fontanot et al 2007; Silverman et al 2008a; Brusa et al 2009a; Civano et al 2011; Fiore et al 2012a; Hiroi et al 2012; Vito et al 2013, 2014a; Kalfountzou et al 2014; Ueda et al 2014), ruling out some of the more exotic early predictions (e.g., Haiman and Loeb 1999) by ≈ 2 orders of magnitude. Furthermore, quantitative comparisons of space densities for optically selected quasars (e.g., McGreer et al 2013) and X-ray selected quasars indicate statistical agreement to within factors of 2–3. At lower AGN luminosities, the situation is significantly less clear, largely owing to the small solid angles with sufficiently sensitive X-ray data as well as substantial challenges with spectroscopic/photometric follow-up studies. The current data generally suggest a decline in space density for moderate-luminosity AGNs at $z > 3$ (e.g., Fiore et al 2012a; Vito et al 2013, 2014a; Kalfountzou et al 2014; Ueda et al 2014). Some recent work has found this decline may be less pronounced at the lowest luminosities, and if this trend holds then "cosmic upsizing" would apply in this regime, perhaps consistent with expectations for hierarchical structure formation in the early universe (i.e., given the young age of the Universe, most SMBHs would not yet have sufficient masses to generate high luminosities). Improved measurements are required for clarification, especially for the most highly obscured AGNs at high redshift (e.g., Gilli et al 2011). The available space-density estimates indicate that, in the absence of dramatic changes in the XLF at very low luminosities, SMBHs probably did not produce sufficient power to reionize the Universe at $z \approx 5$–7; they likely have secondary effects upon reionization (e.g., Grissom et al 2014; but see Giallongo et al 2012). Stacking analyses of high-redshift galaxies have also set upper limits on the accreted mass density in black holes out to $z \approx 8$, providing useful inputs into models of early SMBH formation (e.g., Cowie et al 2012; Fiore et al 2012b; Basu-Zych et al 2013; Treister et al 2013).

3.3 AGNs missed in cosmic X-ray surveys and their importance

As noted in Section 1.1, X-ray surveys do have (small) shortcomings, and thus it is essential to utilize well-matched multiwavelength surveys to find AGNs missed by the X-ray technique (as well as to characterize more reliably the underlying bolometric luminosities of X-ray detected AGNs; see Section 2.2). Particularly important are missed AGNs that still have sufficiently large bolometric luminosities to contribute materially to cosmic SMBH growth. The primary way that luminous AGNs can be missed in X-ray surveys involves heavy obscuration, and that will be the focus of this section below. Additionally, however, there is growing evidence that a small fraction of the luminous AGN population is intrinsically X-ray weak (e.g., Leighly et al 2007; Wu et al 2011; Luo et al 2014; Teng et al 2014), thereby mildly challenging the rule of universal luminous X-ray emission from AGNs (see point 1 of Section 1.1). Even in the absence of obscuration, such AGNs will often be difficult to detect, but thankfully current assessments indicate that intrinsically X-ray weak AGNs are sufficiently rare that they should not substantially impact demographic studies (e.g., Gibson et al 2008; Wu et al 2011; Luo et al 2014).

Heavy obscuration with $N_{\rm H} = (5\text{–}50) \times 10^{23}$ cm^{-2} or more, as is commonly seen in the local universe, can diminish the measurable X-ray emission from an AGN to below the limits of detectability, even for intrinsically luminous AGNs in deep X-ray surveys. The factor of diminution depends upon the sampled rest-frame energy band, the absorption column density, and the absorption geometry (the latter setting the level of flux that is Compton reflected/scattered around the absorber); the factor can be 10–100 or more in the 0.5–10 keV band for large column densities (e.g., Comastri 2004; Burlon et al 2011). Furthermore, owing to the largely energy independent nature of Compton scattering below a couple hundred keV, observations at tens of keV offer only limited improvements for sources with highly Compton-thick absorption column densities.

Multiple methods have been applied to identify AGN candidates that are undetected in the X-ray band, and tens of papers have now been written on this subject. Arguably the most successful methods have utilized infrared observations, largely from *Spitzer*, that home in on AGN "waste heat" (i.e., AGN-heated dust emission) and have reduced extinction bias. Such infrared selection techniques include the following:

1. *Color-color selection from MIR photometric data* (e.g., Lacy et al 2004; Stern et al 2005; Polletta et al 2006; Hickox et al 2007; Cardamone et al 2008; Donley et al 2008, 2012; Mateos et al 2013). See Fig. 8.
2. *Power-law selection from MIR photometric and/or MIR spectroscopic data* (e.g., Alonso-Herrero et al 2006; Donley et al 2007; Alexander et al 2008; Donley et al 2008; Park et al 2010). See Fig. 8.
3. *Excess MIR emission relative to SFR expectations* (e.g., Daddi et al 2007a; Donley et al 2008; Treister et al 2009b; Alexander et al 2011; Luo et al 2011).

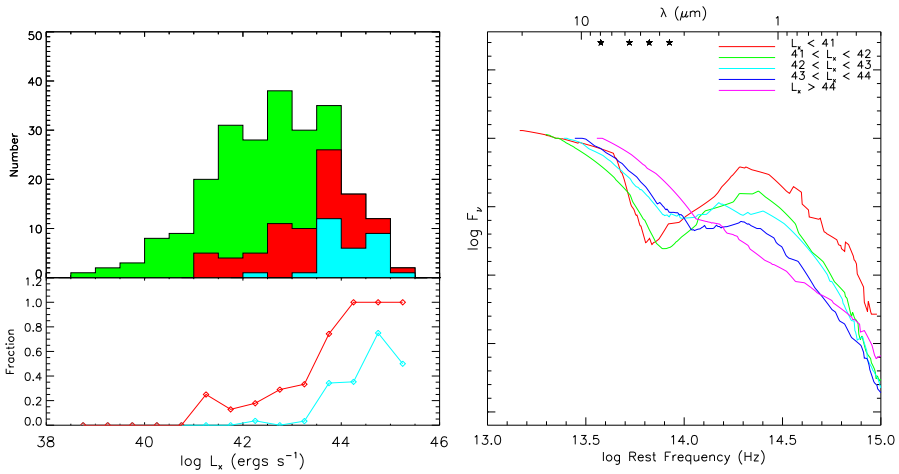

Fig. 8 (a) Distributions of X-ray luminosity for X-ray detected *Spitzer* IRAC sources in the CDF-N (green histogram), AGNs selected by the Lacy et al (2004) MIR color-color criteria (red histogram), and MIR power-law galaxies (cyan histogram). The bottom panel shows the fraction of X-ray sources meeting the Lacy et al. (red) or power-law (cyan) criteria. These MIR criteria are the most effective at selecting luminous AGNs and do not perform as well for moderate-to-low luminosity AGNs. (b) Median best-fit optical-to-MIR SEDs of the X-ray detected *Spitzer* IRAC sources separated into groups by X-ray luminosity [as labeled; in units of log(erg s^{-1})]. At high X-ray luminosities the SEDs show a distinctive power-law shape, while moving toward lower luminosities the stellar bump increasingly dominates. The observed-frame wavelengths of the four IRAC bands are shown near the top of this panel as stars. Adapted from Donley et al (2007).

4. *High 24 μm-to-optical flux ratios and red optical/NIR colors* (e.g., Fiore et al 2008, 2009; Treister et al 2009a).
5. *MIR spectroscopic selection based on deep 9.7 μm Si features* (e.g., Georgantopoulos et al 2011).

Optical, radio, and other techniques have also been utilized to identify AGN candidates, including the following:

1. *Optical spectroscopic selection based on high-ionization emission lines* (e.g., Steidel et al 2002; Hunt et al 2004; Alexander et al 2008; Trump et al 2011b; Juneau et al 2013, 2014; Vignali et al 2014).
2. *Optical variability in multi-epoch photometric data* (e.g., Boutsia et al 2009; Villforth et al 2010, 2012; Sarajedini et al 2011).
3. *Excess radio emission relative to SFR expectations* (e.g., Donley et al 2005; Del Moro et al 2013).
4. *Radio morphology with jet/lobe structure and/or radio spectral properties* (e.g., Muxlow et al 2005; Barger et al 2007).
5. *Selected populations in the color-mass diagram* (e.g., Xue et al 2012).

All of these methods have their strengths and weaknesses, in terms of completeness and reliability (e.g., see Fig. 8), and they are best utilized together

to enable cross-checking of candidates. X-ray stacking analyses using samples of AGN candidates derived with the methods above often show hard average X-ray spectral shapes, indicating that at least some highly obscured AGNs are indeed present. However, large uncertainties remain about the fraction of candidates that are bona-fide AGNs and the corresponding AGN luminosities, particularly among the infrared-selected samples, and much further candidate characterization is required; e.g., with deeper or harder X-ray observations and high-quality optical/NIR/MIR spectroscopy. Furthermore, many of these methods, on their own, are not effective at distinguishing between highly obscured and moderately obscured AGNs.

The X-ray undetected obscured AGNs presumably produce the $\approx 25\%$ of the 6–8 keV CXRB that remains unresolved (see Section 2.1), and this provides one integral limit upon their overall importance to cosmic SMBH growth (e.g., Xue et al 2012; Ueda et al 2014); also see Section 3.4. If they have low intrinsic luminosities, as some analyses suggest, they might increase the current AGN number counts ($\approx 14,900$ deg^{-2}; Lehmer et al 2012) by 50% or more.

3.4 The Sołtan argument for X-ray selected AGNs

The established relations between the bulge properties of local galaxies and the masses of the SMBHs at their centers (e.g., Kormendy and Ho 2013; Shankar 2013; and references therein) allow estimation of the total local mass density of SMBHs ($\rho_{\bullet,\rm loc}$, in M$_\odot$ Mpc^{-3}). Following Sołtan (1982), this quantity then serves as an integral constraint upon the allowed amount of total cosmic SMBH growth. Multiple authors have performed this local SMBH mass-density estimation; e.g., Marconi et al (2004) estimate $\rho_{\bullet,\rm loc} = (4.6^{+1.9}_{-1.4}) \times 10^5$ M$_\odot$ Mpc^{-3}, Vika et al (2009) estimate $\rho_{\bullet,\rm loc} = (4.8 \pm 0.7) \times 10^5$ M$_\odot$ Mpc^{-3}, and Li et al (2011) estimate $\rho_{\bullet,\rm loc} = (5.8 \pm 1.2) \times 10^5$ M$_\odot$ Mpc^{-3}. The $\rho_{\bullet,\rm loc}$ values derived over about the past decade have generally been in acceptable, though not perfect, agreement. However, Kormendy and Ho (2013) have recently argued that some past SMBH mass estimates need to be revised upward by a factor of about 2–4, owing to improvements in data, improvements in modeling, and the identification of downward biases in emission-line based SMBH masses (see their Section 6.6). This leads to an increase in $\rho_{\bullet,\rm loc}$ by a factor of ≈ 2 (L.C. Ho 2014, private communication). Given that this change would be well in excess of the error bars of past $\rho_{\bullet,\rm loc}$ estimates, it is clear that one must presently tread cautiously when using the Sołtan argument! The size of the required upward revision of $\rho_{\bullet,\rm loc}$ is still a matter of debate (A. Marconi 2014, private communication).

X-ray AGN demographers have integrated AGN bolometric luminosity functions, derived from XLFs via bolometric corrections, to estimate the total amount of cosmic SMBH growth, $\rho_{\bullet,\rm XLF}$, for comparison to $\rho_{\bullet,\rm loc}$ (e.g., Marconi et al 2004; Shankar 2013; Ueda et al 2014; also see Delvecchio et al 2014 for a recent infrared-based perspective). Acceptable agreement can be achieved, broadly supporting the idea that radiatively efficient gas accre-

tion (i.e., AGN phases) has driven much of cosmic SMBH growth (significant SMBH merging is allowed, provided the merging progenitors grew via radiatively efficient accretion). For example, Ueda et al (2014) find $\rho_{\bullet,\mathrm{XLF}} = (3.9 \pm 0.6) \times 10^5 \eta_{0.1}^{-1}\ \mathrm{M}_\odot\ \mathrm{Mpc}^{-3}$, where $\eta_{0.1}$ is the average mass-to-energy conversion efficiency of accretion divided by 0.1. $\eta_{0.1} \approx 0.8$ would give consistency with $\rho_{\bullet,\mathrm{loc}}$ estimates from 2000–2012, while $\eta_{0.1} \approx 0.4$ would be required if the recent upward revision of Kormendy and Ho (2013) is adopted. For comparison, accretion onto a Schwarzschild SMBH would give $\eta_{0.1} \approx 0.57$ or higher (with the exact $\eta_{0.1}$ depending upon the role of magnetic stress at the innermost stable circular orbit around the SMBH), while (prograde) accretion onto a Kerr SMBH would give $\eta_{0.1}$ as high as ≈ 3.6 (e.g., Agol and Krolik 2000; Noble et al 2009, 2011; J.H. Krolik 2014, private communication). The $\rho_{\bullet,\mathrm{XLF}}$ vs. $\rho_{\bullet,\mathrm{loc}}$ agreement is thus fair, though the implied accretion efficiency would appear low for upward revisions of $\rho_{\bullet,\mathrm{loc}}$ as suggested by Kormendy and Ho (2013). This could be remedied if XLFs still suffer from incompleteness due to, e.g., highly obscured and/or intrinsically X-ray weak AGNs (see Section 3.3).[3] Such objects are very difficult to detect in X-ray surveys, making this hypothesis challenging to assess. Detailed considerations also indicate that η may depend significantly upon SMBH mass and redshift (e.g., Li et al 2012; Shankar 2013; Ueda et al 2014).

The Sołtan argument can be utilized in a differential, rather than an integral, manner to investigate the evolution of the mass function of SMBHs (e.g., Marconi et al 2004; Shankar 2013; Ueda et al 2014). The most robust conclusion arising from such work is that more massive SMBHs generally grew earlier in cosmic time (also see Section 3.2). Unfortunately, present uncertainties in bolometric corrections, η, $\rho_{\bullet,\mathrm{loc}}$, and XLFs limit the precision of Sołtan-argument constraints for, e.g., constraining the amount of SMBH growth missed by X-ray surveys (see Section 3.3). Sołtan-argument constraints are currently a good first-order "sanity check" but should not be over-interpreted.

3.5 The environmental dependence of AGN evolution

Theoretical models of structure formation predict that galaxy growth is environmentally dependent (i.e., it is accelerated in high-density regions; e.g., Kauffmann 1996; De Lucia et al 2006). Observational support for this hypothesis comes from the finding that the most evolved and massive spheroids reside in galaxy clusters (high-density regions) by the present day (e.g., Baldry et al 2004; Smith et al 2009). How is the growth of SMBHs influenced by the large-scale environment? A powerful way to address this question is to compare the fraction of galaxies hosting AGNs in galaxy clusters (and their high-redshift

[3] Additional (likely smaller) relevant factors to consider include (1) XLF incompleteness due to uncertainties in the masses and growth processes of the high-redshift "seeds" of SMBHs (see Section 3.2), and (2) the ejection of SMBHs from galactic nuclei due to gravitational-wave production in SMBH merger events. Volonteri et al (2013) and Gilfanov and Merloni (2014) provide further discussion of these factors.

progenitors, protoclusters) to that in the field, as measured from blank-field X-ray surveys.

To first order, the fraction of galaxies in clusters hosting X-ray luminous AGNs ($L_{\rm X} \gtrsim 10^{43}$ erg s^{-1}) is found to evolve strongly with redshift out to $z \approx 1$, qualitatively similar to what is seen for the field-galaxy population. However, the cluster AGN fraction is lower than that in the field by about an order of magnitude at low redshift, and it appears to rise more rapidly with redshift (e.g., Eastman et al 2007; Martini et al 2009, 2013). This evolution of the AGN fraction with redshift also broadly tracks that seen for the star-forming galaxy population in galaxy clusters. There is evidence that the relative suppression of AGNs in galaxy clusters is dependent on the richness of the cluster, the cluster-centric radius explored, and the adopted luminosity threshold for AGN activity (e.g., Kocevski et al 2009; Klesman and Sarajedini 2012, 2014; Ehlert et al 2014b,a; Koulouridis et al 2014), complicating comparisons between different studies. In less extreme large-scale environments, such as galaxy groups, there is no clear evidence for a decrease in the AGN fraction when compared to the field out to at least $z \approx 1$ (e.g., Georgakakis et al 2008; Silverman et al 2009a; Pentericci et al 2013; Oh et al 2014).

The source statistics are more limited at $z \gtrsim 1$, but, on the basis of current results, the AGN fraction in galaxy clusters at $z = 1.0$–1.5 appears broadly similar to that in the field (e.g., Martini et al 2013). At yet higher redshifts there is a deficit of galaxy cluster systems, although studies of AGNs in protoclusters (large-scale overdense regions at $z \gtrsim 2$) have found an order of magnitude *increase* in the AGN fraction when compared to the field (e.g., Lehmer et al 2009b, 2013; Digby-North et al 2010), an apparent reversal of what is seen at $z < 1$. There is also tentative evidence that the AGN fraction in protoclusters increases in regions of higher galaxy density (e.g., Lehmer et al 2009b, 2013), potentially the opposite to what is seen in massive lower-redshift galaxy clusters (e.g., Ehlert et al 2014b). Overall, the current results suggest that the large-scale environment has an effect on the growth of SMBHs, which is presumably driven by the availability of a cold-gas supply in the vicinity of the SMBH and may be sparse in massive, evolved (i.e., virialized) galaxy clusters but is prevalent in less-evolved galaxy clusters and protoclusters (e.g., van Breukelen et al 2009). However, there are potentially conflicting results between the suite of published studies, which may be driven by a number of effects, including the analyses employed to measure AGN activity, the approach adopted when comparing to non AGNs (e.g., luminosity and mass thresholds when calculating the AGN fraction), and the selection of the galaxy clusters and protoclusters.

The large-scale environment can also be quantified with the two-point correlation function, which measures the clustering strength of selected populations and provides an estimate of the dark-matter halo mass. Clustering-strength measurements for X-ray selected AGNs over the broad redshift range of $z \approx 0$–3 imply a characteristic halo mass of $\approx 10^{12}$–10^{13} $M_{\odot}$ (e.g., Coil et al 2009; Hickox et al 2009; Cappelluti et al 2010; Koutoulidis et al 2013), with no highly significant trends with obscuration or luminosity (e.g., Gandhi

et al 2006; Plionis et al 2008; Coil et al 2009; Gilli et al 2009; Allevato et al 2011; Krumpe et al 2012; Koutoulidis et al 2013). This range in halo mass is in agreement with that found for luminous star-forming galaxies, optically selected quasars, and massive galaxies, but it is lower than that found for radio-selected AGNs (e.g., Coil et al 2009; Hickox et al 2009, 2011, 2012; Georgakakis et al 2014a; see Fig. 5 of Alexander and Hickox 2012). On the basis of dark-matter halo models, $\approx 10^{13}\ M_{\odot}$ broadly corresponds to the maximum mass where a halo can support a large cold-gas supply—the gas in halos significantly more massive than this is mostly in a hot form, which is less easily accreted onto the SMBH (e.g., Cattaneo et al 2006; Croton 2009; Kereš et al 2009). The dark-matter halo may, therefore, have a strong controlling influence on the fuelling of AGNs (e.g., Booth and Schaye 2010; Volonteri et al 2011).

Further useful constraints can be placed by measuring how X-ray AGNs are distributed in dark-matter halos using the halo occupation distribution (HoD; e.g., Berlind and Weinberg 2002; Zheng et al 2005) formalism. The main parameters of the HoD are the fraction of central and satellite galaxies hosting AGN activity as a function of the halo mass. Current constraints suggest a preference for X-ray AGNs to reside in central galaxies, with $< 5\%$ identified with satellites (e.g., Starikova et al 2011; Richardson et al 2013); however, models with X-ray AGNs solely hosted in satellite galaxies can also fit the observed clustering in some cases (e.g., Miyaji et al 2011).

4 AGN physics

The large and relatively complete samples of AGNs detected in X-ray surveys can provide unique insights, usually of a statistical character, into the physical processes that shape their emission (i.e., "AGN physics"). These physical processes span scales from the immediate vicinity of the SMBH (light minutes to light hours) to that of the obscuring material (light days to light years). Such survey-based physical investigations critically complement the in-depth targeted X-ray studies of individual and small samples of AGNs that are another major thrust of X-ray astronomy (e.g., Mushotzky et al 1993; Reynolds and Nowak 2003; Fabian 2006; Turner and Miller 2009; Done 2010; Gilfanov and Merloni 2014). In this section, we will briefly review results on AGN physics coming from three key areas of survey-based investigation: the basic properties, luminosity dependence, and redshift dependence of AGN X-ray obscuration (Section 4.1), X-ray-to-optical/UV SEDs (Section 4.2), and the X-ray continuum shape and its connection to Eddington ratio (Section 4.3).

4.1 AGN X-ray obscuration: Basic properties, luminosity dependence, and redshift dependence

Understanding of the nature of the obscuring material in AGNs, often referred to generally as the obscuring "torus" of orientation-based unification models

(e.g., Antonucci 1993), continues to improve rapidly. In recent years, for example, it has become possible to obtain direct estimates of the (luminosity dependent) extent of the torus (e.g., Burtscher et al 2013; Koshida et al 2014) and to ascertain its apparently clumpy nature (e.g., Elitzur and Shlosman 2006; Mor et al 2009). Studies based on X-ray surveys have advanced understanding of AGN obscuration in several regards. First, X-ray surveys provide arguably the clearest evidence that the majority of the AGNs in the Universe are obscured. Basic X-ray spectral analyses of the detected AGNs in deep X-ray surveys find that the majority show evidence for obscuration (e.g., Dwelly and Page 2006; Tozzi et al 2006; Merloni et al 2014), even before accounting for biases against detecting heavily obscured objects (see Section 3.3). The inferred column-density distribution of the underlying obscured population, before separation into luminosity and redshift bins, appears to peak roughly around $N_{\rm H} \approx 10^{23}$ cm^{-2} with an approximately log-normal shape having a logarithmic $\sigma \approx 1$. This result implies that a substantial fraction of AGNs will be highly obscured and even Compton-thick. Additionally, there is a significant minority of low-obscuration systems with $N_{\rm H}$ values consistent with zero, in agreement with expectations from unification models.

Another key advance, where recent X-ray surveys covering a broad part of the luminosity-redshift plane have contributed substantially, has been in clarifying the long-suspected (e.g., Lawrence and Elvis 1982; Lawrence 1991) luminosity dependence of the fraction of obscured AGNs (e.g., Treister and Urry 2006; Hasinger 2008; Burlon et al 2011; Brightman et al 2014; Merloni et al 2014; Ueda et al 2014). The fraction of AGNs showing X-ray obscuration drops strongly with rising X-ray luminosity, from $\approx 70\%$ at $L_{2-10\ {\rm keV}} = 10^{43}$ erg s^{-1} to $\approx 20\%$ at $L_{2-10\ {\rm keV}} = 10^{45}$ erg s^{-1} (for $z < 1$). Results from recent infrared (e.g., Ballantyne et al 2006; Treister et al 2008; Assef et al 2013; Lusso et al 2013; Toba et al 2014) and optical (e.g., Simpson 2005) surveys broadly confirm this basic revision of orientation-based unification models (but see Lawrence and Elvis 2010). AGNs of higher luminosities may be able to evacuate or destroy, via radiative feedback, circumnuclear gas and dust more effectively, leading to a so-called "receding torus" with larger opening angle (e.g., Menci et al 2008; Nenkova et al 2008). Alternatively, luminosity-dependent changes in the underlying X-ray-to-optical/UV SED (see Section 4.2) may drive changes in the absorption properties; e.g., if the obscuring material is often in the form of a radiatively driven wind. The precise numerical values for obscured fractions differ between different authors and have remaining systematic uncertainties owing to, e.g., selection biases against highly obscured AGNs and limited photon statistics in absorption spectral modeling; at faint X-ray fluxes currently only crude hardness-ratio based absorption estimates can be effectively used, and these cannot appropriately characterize complex X-ray absorption (e.g., Mayo and Lawrence 2013; Buchner et al 2014). Moreover, wide-field infrared surveys suggest, somewhat surprisingly, that the fraction of highly obscured AGNs may rise upward substantially again at the highest luminosities ($L_{\rm Bol} \sim 10^{47}$ erg s^{-1}) reaching $\approx 50\%$ (e.g., Assef et al 2014; Stern et al 2014). At the highest AGN luminosities, the nature of the material

typically providing the obscuration may change from the standard small-scale torus to something else, perhaps more distributed gas and dust that has been perturbed by galaxy major mergers leading to high Eddington-ratio AGNs (e.g., Draper and Ballantyne 2010).

The fraction of AGNs showing X-ray obscuration, after allowing for luminosity effects, also appears to rise with redshift (e.g., Treister and Urry 2006; Hasinger 2008; Hiroi et al 2012; Iwasawa et al 2012; Vito et al 2013, 2014a; Brightman et al 2014; Merloni et al 2014; Ueda et al 2014). Recent studies find this rise can be parameterized as proportional to $(1+z)^{0.4-0.6}$ at least up to $z \approx 2$, beyond which the uncertainties become substantial. Such evolution of the obscured fraction might arise due to the generally greater availability of nuclear gas and dust in galaxies at earlier cosmic times. There remains debate regarding whether this redshift evolution applies for all AGNs or primarily for the most-luminous ones (e.g., Iwasawa et al 2012; Vito et al 2013; Merloni et al 2014; Ueda et al 2014); a luminosity dependence of the evolution might arise if low-to-moderate luminosity AGNs and high-luminosity AGNs have different fueling mechanisms (see Section 5.3). This evolution of AGNs on the physical scale of the absorbing medium is notably not accompanied by apparent small-scale evolution of the accretion disk and its corona (see Section 4.2).

Finally, we note briefly that this section has primarily focused on X-ray obscuration. The relations between X-ray obscuration and that at other wavelengths (e.g., optical/UV reddening, blocking of line emission from the Broad Line Region, UV absorption lines) remain an extremely complex issue requiring much further work, and understanding such relations thoroughly will elucidate the structure and kinematics of the obscuring material (e.g., Mainieri et al 2007; Trouille et al 2009; Lawrence and Elvis 2010; Luo et al 2010; Merloni et al 2014 and references therein).

4.2 Basic X-ray-to-optical/UV spectral energy distribution properties

One of the most effective ways to investigate the accretion physics of the SMBHs in AGNs is to study their overall broad-band SEDs. The part of the AGN SED spanning from the X-ray to the optical/UV (hereafter, the "X-ray-to-optical/UV SED") is the spectral region where direct accretion emission dominates for relatively unobscured systems (after subtraction/removal of the light from the AGN host galaxy; see Section 5.1). Studies of X-ray-to-optical/UV SEDs have a long history (e.g., Avni and Tananbaum 1986), and they continue to deliver fundamental insights as improved data, analysis techniques, and theoretical modeling become available. In addition to providing constraints upon accretion physics, these studies also are critically important, e.g., when

1. Assessing the universality of AGN X-ray emission and selecting remarkable AGNs that deviate from the typical X-ray-to-optical/UV SED (see Section 1.1 and 3.3).
2. Making bolometric corrections in the Sołtan argument (see Section 3.4).

3. Modeling the winds responsible for many of the absorption-line properties of AGNs and likely feedback; the UV and extreme-UV (EUV) continuum largely drives these winds, which must also be protected from overionization by the underlying X-ray emission (e.g., Murray et al 1995; Proga et al 2000; Luo et al 2014).

While the X-ray-to-optical/UV portion of the AGN SED is complex (e.g., Vasudevan and Fabian 2009; Trump et al 2011a; Elvis et al 2012; Jin et al 2012a; Scott and Stewart 2014), its first-order properties can be described in large samples with the use of simple parameters. The most common such parameter is $\alpha_{\rm ox}$, defined to be the slope of a nominal power law connecting the rest-frame 2500 Å and 2 keV monochromatic luminosities; i.e., $\alpha_{\rm ox} = 0.3838 \log(L_{2\ {\rm keV}}/L_{2500\ {\rm \AA}})$. For systems where the direct accretion emission is dominant, $\alpha_{\rm ox}$ compares the relative amounts of power coming from the optically thick accretion disk (at rest-frame 2500 Å) and the accretion-disk corona (at rest-frame 2 keV).

X-ray surveys have now provided sensitive and often relatively uniform coverage for substantial numbers of unobscured or mildly obscured AGNs that span a broad part of the AGN luminosity-redshift plane. These have been used, often in conjunction with other AGN samples, to extend studies of X-ray-to-optical/UV SEDs using $\alpha_{\rm ox}$ (e.g., Steffen et al 2006; Just et al 2007; Kelly et al 2007; Green et al 2009; Lusso et al 2010; Young et al 2010); importantly, sensitive X-ray surveys have allowed the majority population of moderate-luminosity AGNs at high redshift to be included in such analyses. $\alpha_{\rm ox}$ shows a clear correlation with optical/UV luminosity ($L_{2500\ {\rm \AA}}$) at all investigated redshifts ($z = 0$–6), such that AGNs with higher $L_{2500\ {\rm \AA}}$ produce less X-ray emission per unit optical/UV emission (see Fig. 9). This finding is qualitatively in agreement with earlier studies (e.g., Avni and Tananbaum 1986; Anderson and Margon 1987; Wilkes et al 1994), and the correlation with $L_{2500\ {\rm \AA}}$ appears stronger and tighter than that with estimates of $L_{\rm Bol}/L_{\rm Edd}$. The correlation is now well established over at least five orders of magnitude in $L_{2500\ {\rm \AA}}$, and the observed range of $\alpha_{\rm ox}$ corresponds to a substantial range of ≈ 20 in X-ray vs. optical/UV luminosity. There is considerable object-to-object scatter, corresponding to a factor of ≈ 3 in X-ray vs. optical/UV luminosity in either direction around the $\alpha_{\rm ox}$-$\log(L_{2500\ {\rm \AA}})$ relation. Some of this scatter simply arises from (generally) non-simultaneous observations of AGNs that vary both in the X-ray and optical/UV, but the majority appears to be genuine intrinsic scatter (e.g., Gibson and Brandt 2012; Vagnetti et al 2013). Additional physical parameters beyond $L_{2500\ {\rm \AA}}$, such as $L_{\rm Bol}/L_{\rm Edd}$, likely can explain much of this scatter (e.g., Kelly et al 2008; Shemmer et al 2008; Lusso et al 2010; Young et al 2010; Jin et al 2012a). The $\alpha_{\rm ox}$-$\log(L_{2500\ {\rm \AA}})$ relation is also likely nonlinear (e.g., Steffen et al 2006; Maoz 2007; Green et al 2009; Vagnetti et al 2013), appearing flatter at low luminosities and steeper at high luminosities, but detailed constraints on the form of the nonlinearity remain limited.

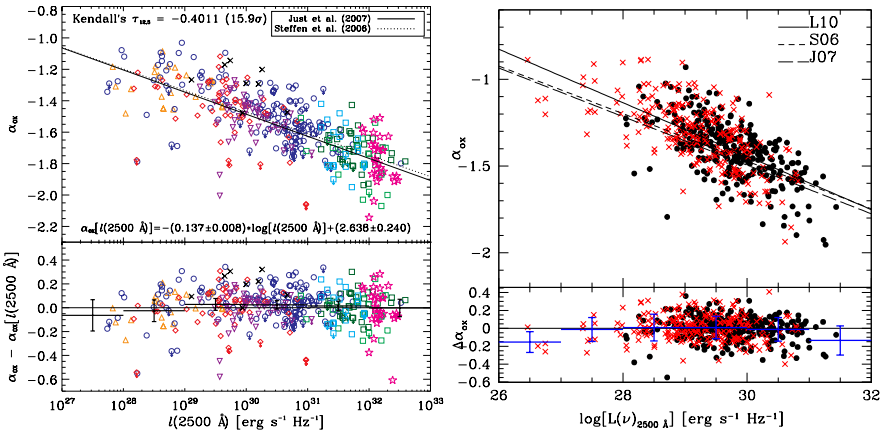

Fig. 9 The α_{ox} parameter vs. 2500 Å monochromatic luminosity for (a) optically selected AGNs from Steffen et al (2006) and Just et al (2007), and (b) X-ray selected AGNs from Lusso et al (2010). Larger negative values of α_{ox} correspond to weaker X-ray emission relative to optical/UV emission. The bottom portions of each panel show the residuals relative to the best-fit relation. In panel (a), the Kendall's τ coefficient and its significance are presented, along with the functional form of the best-fit relation. In panel (b), the abbreviated references for the plotted fits refer to Steffen et al (2006), Just et al (2007), and Lusso et al (2010). The symbol colors/types in each panel denote the AGN samples utilized; see the cited papers for details. AGNs become relatively X-ray weaker with increasing optical/UV luminosity, over a very wide range of this luminosity. Taken from Just et al (2007) and Lusso et al (2010).

The functional form and parameters of the α_{ox}-log($L_{2500\ \text{Å}}$) relation provide fundamental constraints that any successful model of the SMBH disk-corona system must be able to reproduce. For example, as large-scale numerical magnetohydrodynamic simulations of black-hole accretion flows continue their rapid advances (e.g., Schnittman and Krolik 2013), it is expected that researchers will soon be able to determine which physical parameters (L_{Bol}/L_{Edd}, SMBH mass, SMBH spin, magnetic-field structure) set the disk-to-corona power balance and the observed X-ray-to-optical/UV SED. Given this importance for accretion models, it is of concern that the recent improved studies of the α_{ox}-log($L_{2500\ \text{Å}}$) relation, while agreeing on its existence, sometimes disagree about its slope/intercept and functional form; e.g., fitted parameters disagree by more than is allowed by their statistical uncertainties. Until such systematic uncertainties in the observational results are resolved, it will be difficult to use them to inform physical disk-corona models with high fidelity. Furthermore, α_{ox} was defined at rest-frame 2500 Å and 2 keV largely for observational convenience, rather than for fundamental reasons, and it is not obvious that these are the optimal wavelength/energy choices to consider for characterization of X-ray-to-optical/UV SEDs. In this vein, Young et al (2010) have considered the effects of varying these choices. The slope of the α_{ox}-log(L_{Opt}) relation does depend significantly upon chosen X-ray energy, generally becoming steeper/flatter as the definition is moved to lower/higher

energies. On the other hand, the slope does not appear to depend strongly upon the chosen optical/UV wavelength.

Most recent studies of X-ray-to-optical/UV SEDs using $\alpha_{\rm ox}$ find no significant evolution with redshift (e.g., Steffen et al 2006; Just et al 2007; Green et al 2009; Lusso et al 2010); the tightest limits require the X-ray-to-optical/UV luminosity ratio to change by $\lesssim$30% out to $z = 5$–6. However, there are counterclaims finding evidence for redshift evolution (e.g., Kelly et al 2007), and the issue requires further scrutiny with even further improved samples. The current consensus is that, in spite of the dramatic evolution of AGN number densities over cosmic time (see Section 3.2), the inner accretion properties of the individual AGN unit are notably stable.

4.3 X-ray continuum shape as an estimator of Eddington ratio

As the primary indicator of SMBH growth rate, the Eddington ratio is of critical importance in studies of SMBH demographics (see Section 3.2), physics (see Section 4.2), and ecology (see Section 5.4). $L_{\rm Bol}/L_{\rm Edd}$ is typically derived by estimating the mass of a SMBH (and thus its Eddington limit) and also its bolometric luminosity. Unfortunately, mass estimates and bolometric corrections for SMBHs in the distant universe generally have substantial uncertainties (e.g., see Shen 2013 and Peterson 2014 for discussion of virial SMBH mass estimators and Hao et al 2014 for discussion of bolometric corrections; also see Section 5.4). Thus, it is important to have as many methods as possible for $L_{\rm Bol}/L_{\rm Edd}$ estimation, so that different approaches can be cross checked.

It has long been suspected that the intrinsic hard X-ray (rest-frame 2–10 keV) power-law photon index (Γ) of a radio-quiet AGN can be used as an estimator of $L_{\rm Bol}/L_{\rm Edd}$ (e.g., Pounds et al 1995; Brandt et al 1997). Higher $L_{\rm Bol}/L_{\rm Edd}$ is expected to lead to increased Compton cooling of the accretion-disk corona, and thus steeper 2–10 keV power-law spectra (i.e., larger values of Γ; higher $L_{\rm Bol}/L_{\rm Edd}$ also often leads to the production of a strong "soft X-ray excess" affecting the spectrum below rest-frame 2 keV). The early suspicions have now been confirmed via both targeted (e.g., Shemmer et al 2006, 2008) and X-ray survey-based (e.g., Risaliti et al 2009; Jin et al 2012a; Brightman et al 2013; Fanali et al 2013) studies, which find clear $\Gamma - L_{\rm Bol}/L_{\rm Edd}$ correlations across a broad range of luminosity and redshift (and no apparent redshift dependence); see Fig. 10. The $\Gamma - L_{\rm Bol}/L_{\rm Edd}$ correlation does have significant object-to-object scatter (a factor of ≈ 3, when high-quality Γ measurements are available; e.g., Shemmer et al 2008) and thus, as with other methods of $L_{\rm Bol}/L_{\rm Edd}$ estimation, it is best used in a statistical sense to characterize the average Eddington ratio of a sample of objects. The $\Gamma - L_{\rm Bol}/L_{\rm Edd}$ technique, of course, requires a reliable measurement of the *intrinsic* power-law photon index; i.e., corrected for X-ray absorption and Compton-reflection effects. The penetrating nature of 2–10 keV X-rays naturally mitigates absorption effects, and this technique should be effective for moderate column densities up to

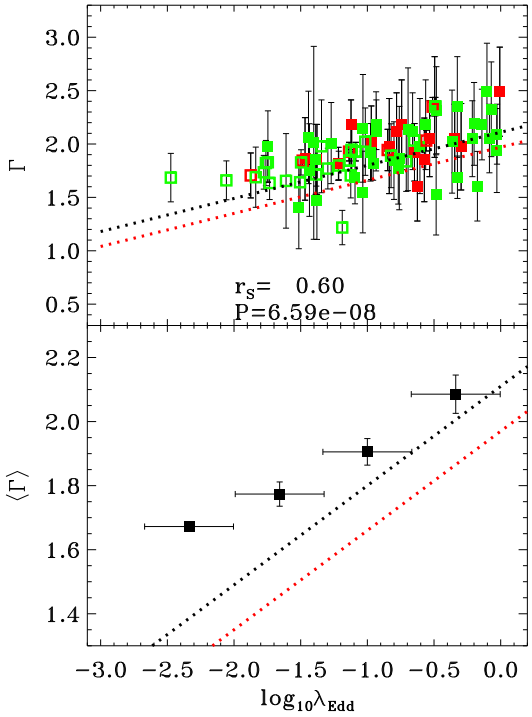

Fig. 10 Hard X-ray power-law photon index vs. Eddington ratio ($\lambda_{\rm Edd} = L_{\rm Bol}/L_{\rm Edd}$) for a sample of AGNs from COSMOS and E-CDF-S. The top panel shows results for the individual AGNs, where red and green points indicate $L_{\rm Bol}/L_{\rm Edd}$ measurements based upon Hα and Mg II virial estimators, respectively. A correlation is clearly present (the Spearman-test correlation coefficient and probability are listed), albeit with significant object-to-object scatter. The bottom panel shows binned average values for groups of individual AGNs from the top panel. The black and red dotted lines show earlier $\Gamma - L_{\rm Bol}/L_{\rm Edd}$ correlations from Shemmer et al (2008) and Risaliti et al (2009), respectively. The apparent systematic offsets of the three correlations may be due to differences in SMBH mass estimation and spectral fitting methodology. Taken from Brightman et al (2013).

$N_{\rm H} \approx 10^{22.5}$ cm^{-2} where some other techniques fail (e.g., due to reddening of optical line emission from the Broad Line Region). It may be possible, with broad-band X-ray coverage and in-depth modeling, to recover the intrinsic photon index for even larger values of $N_{\rm H}$ (e.g., Arévalo et al 2014; Puccetti et al 2014). Finally, the $\Gamma - L_{\rm Bol}/L_{\rm Edd}$ technique, once calibrated, is a *direct* $L_{\rm Bol}/L_{\rm Edd}$ estimator that does not require intermediate estimation of SMBH mass. In fact, it can be utilized to serve as another SMBH mass-estimation technique via the dependence of $L_{\rm Edd}$ on SMBH mass (e.g., Shemmer et al 2008).

5 AGN ecology

Ecology refers to the relationship between "organisms" and their physical surroundings. From the point of view of this review, the ecology of AGNs refers to the relationship between the AGN and the host-galaxy environment.[4] Until comparatively recently AGNs were considered an exotic phenomenon with no close connection to their host galaxies. However, over the past 20 years, the identification of tight relationships between the mass of the SMBH and various host-galaxy properties for nearby galaxies (e.g., the bulge luminosity, mass, and velocity dispersion; Kormendy and Richstone 1995; Magorrian et al 1998; Gebhardt et al 2000; Kormendy and Ho 2013) has comprehensively dismissed this view by implying that (1) most (if not all) massive galaxies have hosted AGN activity at some time over the past ≈ 13 Gyr of cosmic evolution and (2) the growth of SMBHs and galaxies is connected, potentially via a link between AGN activity and star formation (the two primary processes whereby SMBHs and galaxies are grown). Since the majority of the growth of SMBHs has occurred at $z \gtrsim 0.2$ (see Section 3.2 and Fig. 7), X-ray surveys of distant AGNs provide key insight into when, where, and how these SMBHs grew, and can shed light on any connections between AGN activity and star formation (when combined with other multiwavelength observations).

In this section we review research on the host galaxies of distant X-ray AGNs and explore if anything "special" is happening in the AGN-hosting galaxies by making comparisons to galaxies that lack AGN activity. We start with a brief overview of the broad-band emission from galaxies and AGNs to illustrate how the properties of an AGN host galaxy can be measured without significant contamination from the AGN itself. To provide the broadest redshift baseline to search for trends in the host-galaxy properties of distant AGNs we often include comparisons to the host-galaxy properties of AGNs in the nearby universe, principally those detected by the *Swift*-BAT survey (e.g., Tueller et al 2010; Baumgartner et al 2013).

5.1 The broad-band emission from galaxies and AGNs

The bulk of the emission from galaxies is produced at UV–submillimeter wavelengths ($\approx$ 0.1–1000 μm; e.g., Kennicutt and Evans 2012) and is primarily due to the radiation produced by populations of stars as well as AGN activity, when present. The intrinsic emission from these stellar populations peaks at UV–NIR wavelengths and corresponds to the (approximate) black-body radiation from stars over a range of masses and ages (Kurucz 1979). This intrinsic emission is typically modified by the presence of dust, particularly in regions of young and forming stars, which are generally optically thick to short-wavelength UV–NIR radiation. Consequently, the emission from young and forming stars is

[4] In this review we use the term host-galaxy environment to describe the properties of the host galaxy (e.g., mass, color, morphology, SFR) rather than the large-scale environment in which the galaxy resides.

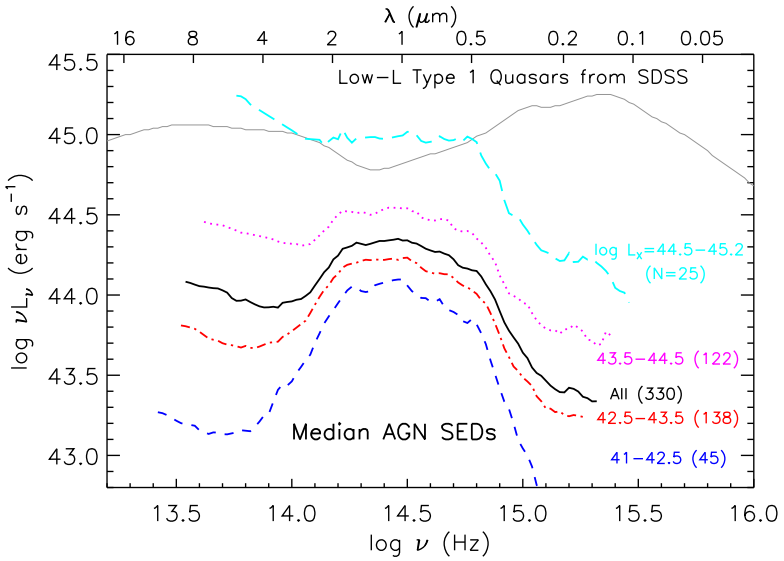

Fig. 11 The median rest-frame UV–MIR SEDs of X-ray AGNs at $z \approx 0$–4. The range in X-ray luminosity [in units of log(erg s^{-1})] for subsets of the X-ray AGNs are shown in addition to the number of X-ray AGNs used to produce the median SEDs. These SEDs are compared to the mean SED of the low-luminosity quasars from the SDSS, with the host-galaxy contribution removed to indicate the expected SED from a "pure AGN" (gray curve; Richards et al 2006a). The emission at rest-frame ≈ 0.2–4 μm from the X-ray AGNs is predominantly due to starlight from the host galaxy since the majority of the AGNs are obscured or intrinsically weak at optical wavelengths. Taken from Luo et al (2010).

often most efficiently measured using infrared observations since the starlight will heat the dust and thermally reradiate the emission at FIR wavelengths ($\lambda \approx 30$–300 μm; typical temperatures of $T \approx 10$–100 K). The majority of the emission from galaxies undergoing intense star formation is, therefore, produced at FIR wavelengths, while the majority of the emission from quiescent galaxies (i.e., those with little on-going star formation) is produced at UV–NIR wavelengths.

A significant fraction of the AGNs detected in X-ray surveys are obscured or intrinsically weak at UV–NIR wavelengths; see Section 1.1 and 4.1. While this makes it challenging to determine the properties of the AGN over that band pass, it allows for convenient measurements of the host-galaxy properties without significant contamination from the AGN (e.g., Simmons and Urry 2008; Silverman et al 2009b; Pierce et al 2010a; Xue et al 2010; Lusso et al 2011). See Fig. 11 for the SEDs of distant X-ray AGNs, showing the host-galaxy emission peaking at ≈ 0.2–4 μm. Reliable host-galaxy measurements for the population of luminous and unobscured AGNs are also possible provided the AGN emission can be accurately constrained (and therefore removed) at UV–NIR wavelengths (e.g., Assef et al 2010; Merloni et al 2010; Bongiorno et al 2012; Santini et al 2012). The most basic host-galaxy properties that we

can measure at UV–NIR wavelengths are luminosity, color, and morphology. The host-galaxy color provides a basic characterization of the galaxy integrated stellar populations and, when combined with the luminosity, a reliable estimate of the mass of the host galaxy (e.g., Bell and de Jong 2001; Zibetti et al 2009; Conroy 2013). The morphology can provide clues to the formation and evolution of galaxies and, when spatially resolved color information is available, basic constraints on the stellar populations across the galaxy. We explore the host-galaxy masses, colors, and morphologies of X-ray AGNs in Section 5.2 and 5.3.

AGNs are often luminous at infrared wavelengths due to the thermal emission from dust in the vicinity of the accretion disk (e.g., the putative obscuring torus; Antonucci 1993), potentially contaminating infrared-based SFR estimates. However, since the accretion disk is hotter than young stars, the dust is typically heated to higher temperatures ($\approx$ 100–1000 K) and, therefore, the majority of the infrared emission from the AGN is shifted to shorter NIR–MIR wavelengths than that from star formation ($\approx$ 3–30 μm; e.g., Netzer et al 2007; Mullaney et al 2011). Consequently, for many AGN studies, the FIR emission is taken as a measurement of the SFR; however, to provide the most accurate SFR constraints it is necessary to decompose the infrared emission into the AGN and star-formation components, which is essential for reliable SFR measurements from intrinsically luminous AGNs (e.g., Netzer et al 2007; Symeonidis et al 2010; Mullaney et al 2011; Kirkpatrick et al 2012; Del Moro et al 2013; Delvecchio et al 2014). We explore the SFRs of X-ray AGNs in Section 5.5.

5.2 Host-galaxy masses and colors

The large numbers of optically obscured and intrinsically weak AGNs detected in *Chandra* and *XMM-Newton* surveys provided the first detailed measurements of the host-galaxy properties of distant AGNs without significant contamination from AGN activity at UV–NIR wavelengths. Initial studies noted that the AGN host galaxies were typically luminous ($\gtrsim L_*$; i.e., the knee of the galaxy luminosity function; Schechter 1976) and have red optical colors, suggesting massive early type systems (Hubble types Sa–E; e.g., Alexander et al 2001, 2002; Barger et al 2001b, 2002; Cowie et al 2001; Severgnini et al 2003; Gandhi et al 2004). More recent studies estimated the host-galaxy stellar masses by fitting the UV–NIR emission with stellar-population models and applied appropriate mass-to-light conversions to the host-galaxy luminosities. These analyses were significantly helped by the launch of *Spitzer* in 2004, which provided the first extensive rest-frame NIR data for distant sources using the IRAC instrument (3.6–8 μm; Fazio et al 2004). As expected, given the results from the initial studies, the majority of the distant X-ray AGNs were found to be hosted by massive galaxies ($> 3 \times 10^{10}$ $M_\odot$; e.g., Akiyama 2005; Papovich et al 2006; Alonso-Herrero et al 2008; Bundy et al 2008; Brusa et al 2009b; Xue et al 2010; Mainieri et al 2011; Lusso et al 2011), with the average stellar

mass comparable to that of M_* ($\approx 10^{11}$ $M_\odot$; i.e., the knee of the stellar-mass function; Cole et al 2001; Marchesini et al 2009; Ilbert et al 2010). Distant AGNs are also identified in lower-mass host galaxies (down to $\approx 10^7$–10^9 $M_\odot$) and are most prevalent in the deepest *Chandra* surveys (e.g., Shi et al 2008; Brusa et al 2009b; Xue et al 2010, 2012; Schramm et al 2013) but they always comprise a minority of the AGN population in X-ray surveys. As discussed in Section 5.4 this is more due to challenges in detecting these sources rather than their intrinsic rarity. No strong trend for an increase or decrease in the average stellar mass of X-ray AGNs with redshift is found down to $z \approx 0.2$. However, by contrast, the average stellar mass of *Swift*-BAT selected AGNs at $z < 0.05$ is found to be substantially lower than the distant X-ray AGNs ($\approx 2 \times 10^{10}$ $M_\odot$; e.g., Koss et al 2011). This lower average stellar mass is not obviously due to selection effects since the majority of the sources have X-ray luminosities comparable to the distant AGNs (14–195 keV luminosities of $\approx 10^{43}$–10^{44} erg s^{-1}; Tueller et al 2010; Koss et al 2011). Therefore, the differences in the average stellar masses of distant and nearby X-ray AGNs appear to be due to either a genuine decrease in the host-galaxy masses over the narrow redshift range of $z \approx 0.05$–0.2 or different approaches in the estimation of the host-galaxy masses.

A common diagnostic to characterize the properties of galaxies is the color-magnitude diagram (CMD), which plots rest-frame optical colors vs. absolute magnitude and provides insight into the integrated stellar populations (e.g., Strateva et al 2001; Baldry et al 2004). The CMD for galaxies is found to be bimodal out to at least $z \approx 1$–2 (e.g., Bell et al 2004; Brammer et al 2009; Xue et al 2010), with the majority of galaxies either falling on the "red sequence" or the "blue cloud", which are believed to correspond broadly to quiescent and star-forming galaxies, respectively. Intense star-forming galaxies can also lie on the red sequence due to the presence of dust-obscured star formation rather than quiescent stellar populations (e.g., Cardamone et al 2010; Bongiorno et al 2012; Rosario et al 2013b; Wang et al 2013). Consequently, the CMD is not, in isolation, a reliable indicator of the degree of on-going star formation and other analyses are often required to determine which red-sequence galaxies are quiescent and which are intensely forming stars (e.g., Rosario et al 2013b); see Section 5.1. A modest fraction of the galaxy population lies in a narrow "green valley" between these two dominant regions, which is likely to comprise galaxies with a mix of red and blue stellar populations (e.g., a galaxy with both significant ongoing star-formation and a significant old stellar population) in addition to galaxies transiting from the blue cloud to the red sequence due to the (potentially rapid) shut down of star formation in the host galaxy (e.g., Faber et al 2007; Martin et al 2007; Hasinger 2008; Schawinski et al 2009, 2014; Cimatti et al 2013; Goulding et al 2014; Pan et al 2014).

The first CMD analyses of distant X-ray AGNs showed that many lie in the green valley (e.g., Nandra et al 2007; Silverman et al 2008b; Hickox et al 2009), where only a minority of the optically selected galaxy population is found. The distinct difference between the locations of the AGNs and the optically selected galaxy populations in the CMD implies that distant AGNs are

found in a subset of the galaxy population and, tentatively, suggests that they are the catalysts for the transition of galaxies from the blue cloud to the red sequence (e.g., through the suppression of star formation via energetic winds, outflows, and jets; see Veilleux et al 2005; Alexander and Hickox 2012; Fabian 2012 for reviews). However, later studies showed that clear distinctions between the host-galaxy colors of the AGN and the galaxy populations mostly disappear when the galaxy sample is matched in mass to the AGN sample (e.g., Silverman et al 2009b; Xue et al 2010; Pierce et al 2010b; Rosario et al 2013b), with broadly similar fractions of coeval galaxies and AGNs found in the red sequence, green valley, and blue cloud out to at least $z \approx 3$.[5] The lack of significant differences in the host-galaxy colors appears to suggest that, in general, distant X-ray AGNs are not found in "special" host-galaxy environments (at least in terms of the color-mass plane). This general conclusion is in contrast to that found for X-ray AGNs in the nearby universe, where the hosts of *Swift*-BAT AGNs at $z \lesssim 0.05$ are found to have bluer colors than the coeval galaxy population (when matched in mass to the AGN sample; e.g., Koss et al 2011), suggesting a connection between the presence of young stars and AGN activity. These apparent disagreements are not necessarily in contradiction since there is evidence that the host galaxies of X-ray AGNs out to $z \approx 1$ have experienced more recent star formation than the coeval galaxy population (e.g., from the resolved host-galaxy colors and the depth of the 4000 Å break; e.g., Ammons et al 2009; Silverman et al 2009b; Pierce et al 2010b; Ammons et al 2011; Rosario et al 2013a; Hernán-Caballero et al 2014); see Section 5.5 for a more detailed discussion of the star-formation properties of distant AGNs.

5.3 Host-galaxy morphologies

Many of the cosmic X-ray survey fields have extensive coverage at UV–NIR wavelengths from *Hubble Space Telescope (HST)* observations. The excellent spatial resolution of *HST* ($\approx 0.1''$) allows moderately detailed characterization of the rest-frame optical host-galaxy properties of distant AGNs through kpc-scale measurements of the host-galaxy morphology and the identification of potential triggers of AGN activity (e.g., galaxy merger and galaxy interaction signatures). A number of different approaches for measuring host-galaxy morphologies have been developed (e.g., automated classifications based on the distribution of light in the galaxy, two-dimensional fits to the surface brightness profiles to provide disk/bulge decompositions, and human "eyeball" classification), which appear to give broadly similar results (e.g., Huertas-Company et al 2014). The contribution of the AGN to the optical emission can significantly bias morphological measurements (e.g., Simmons and Urry 2008; Pierce et al 2010b) and, therefore, the majority of the studies focus on optically obscured or intrinsically weak AGNs.

[5] Given the evident mass dependence on the colors of galaxies, color-*mass* diagrams are now often used in preference to color-magnitude diagrams for host-galaxy analyses.

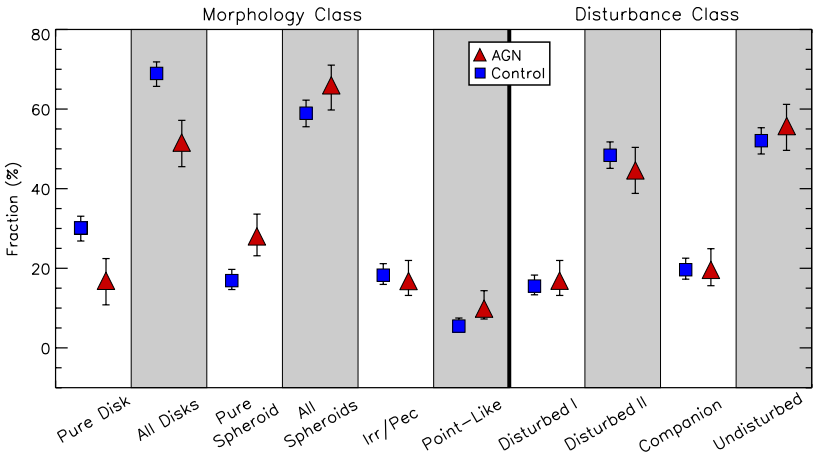

Fig. 12 Fraction of AGN host galaxies (AGN: red triangles) and non-AGN host galaxies (control: blue squares) at $1.5 < z < 2.5$ in a given morphological and disturbance class. The non-AGN sample is matched in mass to the AGN host-galaxy sample. In terms of both morphology and disturbance classifications the AGN and the non-AGN sample appear very similar. Taken from Kocevski et al (2012).

Distant X-ray AGNs are found to reside in a broad range of host-galaxy types out to at least $z \approx 3$, from disk-dominated to bulge-dominated systems (e.g., Grogin et al 2005; Pierce et al 2007, 2010b; Gabor et al 2009; Georgakakis et al 2009; Cisternas et al 2011, 2014; Kocevski et al 2012; Böhm et al 2013; Fan et al 2014). See Fig. 12 for a comparison of the morphologies of AGNs and mass-matched galaxies at $1.5 < z < 2.5$. The first studies found that AGNs typically reside in more bulge-dominated systems than the coeval galaxy population (e.g., Grogin et al 2005; Pierce et al 2007). However, as with the CMD analyses, clear differences mostly disappeared when the galaxy sample was matched in mass to the AGN sample (e.g., Kocevski et al 2012; Böhm et al 2013; Fan et al 2014; Villforth et al 2014); we note that recent evidence from a systematic morphological analysis of AGNs and mass-matched galaxies over the broad redshift range of $z = 0.5$–2.5 has found evidence that AGNs at $z \approx 1$ are preferentially hosted in disk-dominated galaxies when compared to the galaxy population, although the differences are comparatively subtle (Rosario et al 2014). More significant morphological differences are found by the present day, with *Swift*-BAT AGNs ≈ 2 times more likely to reside in spiral (disk dominated) galaxies than comparably massive inactive galaxies (e.g., Koss et al 2011), suggesting that not all host-galaxy environments are capable of hosting significant AGN activity by $z \approx 0$.

How is the AGN activity triggered? Prior to the launches of *Chandra* and *XMM-Newton*, it was widely predicted that distant AGNs are triggered by gas-rich major mergers, violent events where two similar-mass galaxies interact and merge, torquing the gas and driving it toward the central SMBH, where it can be accreted (e.g., Sanders et al 1988; Barnes and Hernquist 1992; Mihos and Hernquist 1996; Hopkins et al 2008). Contrary to these expectations, only

a minority ($\lesssim$20%) of the AGN population over the broad redshift range of $z \approx 0.2$–2.5 were found to have the clear signatures expected for major mergers (disturbed host-galaxy morphologies and tidal tails; Silverman et al 2011; Cisternas et al 2011; Kocevski et al 2012; Böhm et al 2013; Villforth et al 2014). The fraction of *Swift*-BAT AGNs at $z < 0.05$ with major-merger signatures is also $\approx$ 20%, consistent with that found for the distant AGNs (Koss et al 2010; Cotini et al 2013). These results, therefore, suggest that other processes such as galaxy interactions, minor mergers, and secular processes (e.g., galaxy bars, disk instabilities, and clumpy cloud accretion) may be responsible for triggering the majority of AGN activity (e.g., Silverman et al 2011; Cisternas et al 2011, 2014; Bournaud et al 2012; Kocevski et al 2012; Böhm et al 2013; Cheung et al 2014; Trump et al 2014; Villforth et al 2014). However, we note that there is evidence that the most luminous AGNs are preferentially triggered by major mergers, as also found for the most powerful star-forming galaxies (e.g., Treister et al 2012; Kartaltepe et al 2012), which could indicate that major mergers are required to drive sufficient quantities of gas into the central regions of galaxies to power the most luminous systems.

In general, the fraction of the coeval galaxy population with major merger signatures is comparable to that found for the (majority of) distant AGNs, when the galaxy sample is matched in mass to the AGN sample; however, see Rosario et al (2014) for tentative evidence of a factor ≈ 2 decrease in the fraction of $z = 0.5$–1.0 galaxies with major-merger signatures when compared to the coeval AGN population. More significant differences are found by the present day, with a ≈ 5 times lower fraction of the galaxy population hosted in major mergers when compared to *Swift*-BAT selected AGNs ($\approx$ 4% vs. $\approx$ 20%; Cotini et al 2013). The emerging picture, therefore, suggests that, while the absolute fraction of moderate-luminosity AGNs with major merger signatures is comparatively constant at $\approx$ 20% over the broad redshift range of $z \approx 0$–3, there are significant differences between the major-merger fraction of the AGN and coeval galaxy populations by $z \approx 0$. As we discuss in Section 5.5, these differences may be related to the greater availability of a cold-gas supply in the distant universe when compared to the local universe (i.e., the ubiquity of gas-rich galaxies may be a key factor).

5.4 AGN fraction and Eddington-ratio distribution

On the basis of the suite of studies explored in the previous sections, there are few significant differences between the host-galaxy properties of distant X-ray AGNs and the coeval galaxy population, when the samples are matched in mass. More significant differences are evident by $z \approx 0$ and some differences may already be in place by $z \approx 1$. However, to first order, these results suggest that any galaxy with similar properties to the AGN host galaxies is also capable of hosting an AGN and, therefore, the fraction of galaxies with AGN activity provides a basic measurement of the AGN duty cycle (i.e., how often mass accretion onto the SMBH switches on and off).

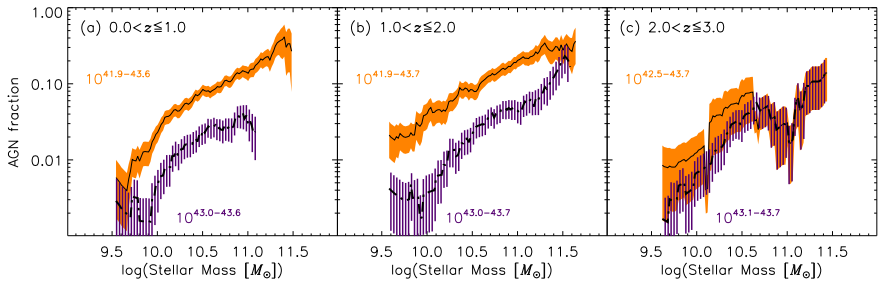

Fig. 13 The fraction of galaxies hosting an AGN as a function of stellar mass for different redshift and X-ray luminosity ranges [as labeled; luminosity ranges in $\log(\mathrm{erg\ s^{-1}})$]. A strong stellar-mass dependence on the AGN fraction is found for all redshifts. Adapted from Xue et al (2010).

As revealed from a large number of studies to date, the fraction of galaxies hosting AGN activity above a fixed X-ray luminosity threshold rises steeply with host-galaxy mass out to at least $z \approx 2$–3 (e.g., Bundy et al 2008; Brusa et al 2009b; Xue et al 2010; Georgakakis et al 2011; Bluck et al 2011; Aird et al 2012; Bongiorno et al 2012; Mullaney et al 2012b). See Fig. 13 for the AGN fraction as a function of stellar mass across different redshift and X-ray luminosity ranges. For example, the fraction of $z \approx 1$ galaxies hosting AGN activity with $L_{\rm X} > 10^{43}$ erg s^{-1} increases from $\approx 0.3\%$ at a stellar mass of $\approx 10^{10}\ M_\odot$ to $\approx 3\%$ at a stellar mass of $\approx 10^{11}\ M_\odot$; the AGN fraction globally increases by a further factor of ≈ 5 for a lower luminosity threshold of $L_{\rm X} > 10^{42}$ erg s^{-1}. The AGN fraction does not appear to have a strong dependence on host-galaxy color (e.g., Xue et al 2010; Georgakakis et al 2011), although it is a strong function of SFR; see Section 5.5. There are no comparably detailed analyses for X-ray AGNs in the nearby universe; however, on the basis of optically selected AGNs from the SDSS (e.g., Kauffmann et al 2003; Best et al 2005), the AGN fraction is found to rise with increasing stellar mass but then flattens out at masses of $\gtrsim 10^{11}\ M_\odot$. No statistically significant evidence for a flattening in the X-ray AGN fraction at high stellar masses is found for distant AGNs, leaving some uncertainty over whether this result is specific to optically selected AGNs or whether a significant decrease in the duty cycle of X-ray AGN activity has occurred in the most massive galaxies at $z < 0.2$ that is not seen at $z > 0.2$. It is also possible that the observational signature for a decrease in the duty cycle of X-ray AGN activity at high stellar masses is too subtle to identify in the current studies.

Overall these results suggest that AGNs are more common in massive galaxies than less massive galaxies, suggesting that the SMBHs in massive galaxies are growing more rapidly than the SMBHs in less massive galaxies. However, we must be careful in our physical interpretation of this result as there are strong biases against detecting AGNs *at a fixed luminosity threshold* in lower-mass galaxies than higher-mass galaxies since a lower-mass SMBH would need to be accreting at a higher Eddington ratio than a higher-mass

SMBH to be detected.[6] To directly explore whether there is a mass dependence to the growth rates of SMBHs requires measuring the Eddington ratios of SMBHs across a broad range in mass.

The calculation of an Eddington ratio (referred to here as $\lambda_{\rm Edd}$) relies on knowing a number of uncertain quantities, including the SMBH mass and the bolometric AGN luminosity, which typically has to be indirectly estimated from a single-wavelength measurement of the AGN luminosity (e.g., from the X-ray band, which represents only a few percent of the bolometric luminosity; Elvis et al 1994; Marconi et al 2004; Hopkins et al 2007; Hao et al 2014).[7] Consequently, it is challenging to derive accurate Eddington ratios, particularly for large numbers of distant AGNs where the majority of the sources lack direct SMBH mass measurements and indirect methods are required to provide mass constraints (e.g., a proxy for the SMBH mass such as the host-galaxy mass, luminosity, velocity dispersion, or bulge luminosity). To remove the uncertainty on the SMBH mass, an approach adopted by some researchers is to calculate the "specific accretion rate", where the SMBH mass is replaced with the stellar mass, which is a more directly measured quantity (e.g., Brusa et al 2009b; Aird et al 2012; Bongiorno et al 2012). In this review we will refer to Eddington ratios but we caution that this is not a directly measured quantity and any Eddington-ratio measurements are subject to considerable (factor of a few) systematic uncertainties.

The Eddington ratios estimated for distant X-ray AGNs cover a broad range: $\lambda_{\rm Edd} \approx 10^{-5}$–1 for implied SMBH masses of $\approx 10^{6}$–10^{9} $M_{\odot}$, with the majority at $\lambda_{\rm Edd} \approx 10^{-4}$–$10^{-1}$ (e.g., Babić et al 2007; Ballo et al 2007; Rovilos and Georgantopoulos 2007; Alonso-Herrero et al 2008; Hickox et al 2009; Raimundo et al 2010; Simmons et al 2011; Trump et al 2011a; Lusso et al 2012; Nobuta et al 2012; Matsuoka et al 2013). The distribution of Eddington ratios implied from these studies is, at least partially, dictated by limitations in the data (i.e., incompleteness effects such as the X-ray sensitivity limits and the X-ray luminosity threshold adopted to identify AGN activity in these studies) and, consequently, does not provide a reliable measurement of the intrinsic Eddington-ratio distribution. The first studies to correct for these limitations and construct an intrinsic Eddington-ratio distribution revealed striking results: the Eddington-ratio distribution can be characterized by a power law with a slope that is independent of *both* host-galaxy mass and redshift out to $z \approx 2$–3 (Aird et al 2012, 2013a; Bongiorno et al 2012); however, we note that the current data would also be consistent with a broad log-normal distribu-

[6] Here it is assumed that higher-mass galaxies have more massive SMBHs than lower-mass galaxies, which is reasonable since (1) there is a broad relationship between host-galaxy mass and SMBH mass and (2) any evolution in the stellar–SMBH mass relationship with redshift appears to be modest (e.g., Jahnke et al 2009; Bennert et al 2011; Schramm and Silverman 2013).

[7] Ideally the bolometric luminosity would be directly measured from the primary AGN continuum over the optical–X-ray waveband. However, it is expected to peak at far-UV wavelengths, which is unobservable due to absorption from the Galaxy. See, for example, Vasudevan and Fabian (2009) and Jin et al (2012b) for some observational approaches to estimating the primary AGN continuum of nearby AGNs.

tion, if the peak of the distribution lies below current sensitivity limits. The slope of the power law is steep and corresponds to a $\approx$ 5–10 increase in the probability to detect an SMBH that is accreting at a $\approx$ 10 times lower Eddington ratio. See Fig. 14 for the derived Eddington-ratio distribution for a range of stellar masses at $0.2 < z < 1.0$. A power-law Eddington-ratio distribution is qualitatively consistent with the latest constraints for distant optically selected quasars (e.g., Schulze and Wisotzki 2010; Shen and Kelly 2012; Kelly and Shen 2013); however, more quantitative comparisons are limited by the different approaches adopted in estimating SMBH masses between the X-ray studies (scaled from the stellar mass) and the optical quasar studies (virial SMBH mass) and the different AGN selection approaches. No comparably detailed measurements of the Eddington-ratio distribution have been produced for X-ray AGNs in the nearby universe. Nevertheless, on the basis of optically selected AGNs from the SDSS, Kauffmann and Heckman (2009) have argued that there are two regimes of growth in nearby AGNs: for systems with significant star formation the Eddington-ratio distribution is characterized by a broad log-normal distribution while for quiescent systems with little or no star formation the Eddington-ratio distribution is characterized by a power-law distribution. Further work is required to understand the differences between these results and those found for the distant X-ray AGNs.

The fraction of galaxies hosting AGN activity at a given Eddington ratio is found to increase with redshift out to at least $z \approx$ 2–3 (e.g., Aird et al 2012; Bongiorno et al 2012); i.e., the normalization of the Eddington-ratio distribution increases with redshift. The current constraints suggest that this redshift dependence is strong [$\approx (1+z)^{3.5-4.0}$; Aird et al 2012; Bongiorno et al 2012], indicating that AGN activity was about an order of magnitude more common in galaxies at $z \approx 1$ for a fixed Eddington ratio than at $z \approx 0$; however, it is not clear whether this evolution is independent of mass across all redshifts. This strong redshift evolution is consistent with the evolution in SFR found for star-forming galaxies (see Section 5.5).

What insight do these results provide on "AGN downsizing" (see Section 3.2)? The strong increase in the AGN fraction with redshift can be explained by either (1) an increase in the duty cycle of AGN activity at a given Eddington ratio or (2) an increase in the characteristic Eddington ratio with redshift. The majority of the theoretical models predict the second scenario as being a major driver of AGN downsizing (see Section 3.2); however, since the observed Eddington-ratio distribution is a power law it is not possible to distinguish between these different scenarios with the current data (i.e., there are no distinctive features to measure a shift in the characteristic Eddington ratio). Many of the theoretical models also predict a redshift dependence in the characteristic mass of accreting SMBHs, which is not clearly observed but may be due to limitations in the current data (see Section 6.1.1).

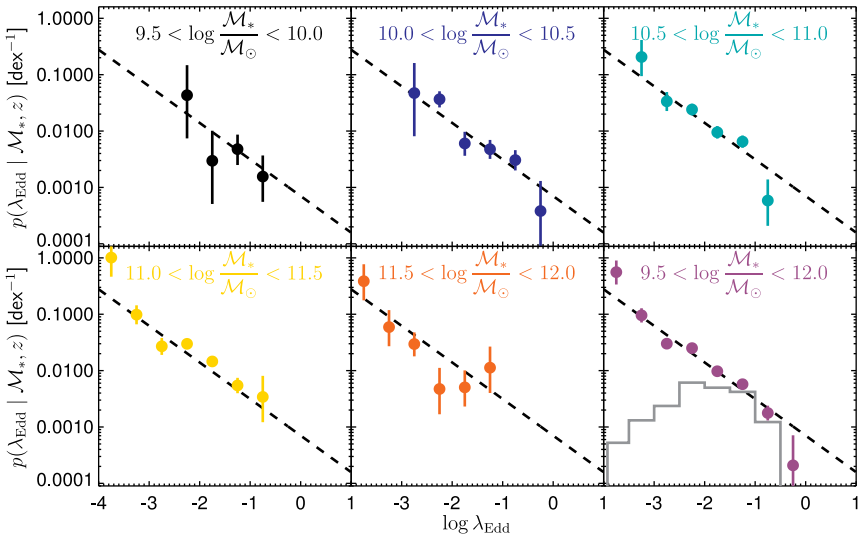

Fig. 14 Eddington-ratio distribution (i.e., the probability that a galaxy will host an AGN at a given Eddington ratio) for different ranges in stellar mass for galaxies at $0.2 < z < 1.0$. The data have been corrected for X-ray sensitivity incompleteness effects to provide an accurate measurement of the intrinsic Eddington-ratio distribution. The final panel compares the observed Eddington-ratio distribution (gray histogram) to the intrinsic Eddington-ratio distribution measured across the full range in mass and demonstrates the need to account for the effects of incompleteness in the X-ray data. The dashed line is a best-fit power-law model to the Eddington-ratio distribution, evaluated at $z = 0.6$. The Eddington-ratio distribution is consistent with being independent of stellar mass over $9.5 < log(M_*/M_\odot) < 12.0$ at $0.2 < z < 1.0$. Taken from Aird et al (2012).

5.5 Star formation and specific star formation rates

The suite of studies explored in this review have revealed when, where, and how SMBHs have grown in the distant universe. However, we have not yet investigated how the growth of the SMBH relates to the growth of the host galaxy; i.e., the connection between AGN activity and star formation. We would expect at least a broad connection between AGN activity and star formation since (1) the volume averaged star formation and SMBH mass accretion rates track each other (with a 3–4 orders of magnitude offset) out to at least $z \approx 2$ (e.g., Heckman et al 2004; Merloni et al 2004; Silverman et al 2008a; Aird et al 2010; Mullaney et al 2012a) and (2) there is a tight relationship between the SMBH mass and spheroid mass for galaxies in the nearby universe (e.g., Kormendy and Richstone 1995; Magorrian et al 1998; Gebhardt et al 2000; Kormendy and Ho 2013), which provides "archaeological" evidence for past joint SMBH–galaxy growth. However, these results only afford broad integrated constraints on the overall SMBH–galaxy growth and do not provide clear clues on how the SMBH and galaxy have grown in individual systems, which requires more direct SFR measurements.

The first studies to constrain the SFRs of distant X-ray AGNs used a broad variety of star-formation indicators, including optical spectroscopy, MIR data, and submillimeter (submm) observations (e.g., Alexander et al 2005b; Polletta et al 2007; Silverman et al 2009b; Trichas et al 2009; Mullaney et al 2010; Lutz et al 2010; Xue et al 2010; Rafferty et al 2011). These initial studies showed that AGNs of a fixed X-ray luminosity can have a broad range of SFRs (up to ≈ 5 orders of magnitude variation between individual sources; see Fig. 14 in Rafferty et al 2011) and provided evidence that the average SFRs of AGNs increase with redshift. However, significant uncertainties remained in the SFR measurements, such as (1) potential contamination from AGN activity to the SFR estimates, (2) potential underestimation of the SFR due to obscuration by dust, and (3) uncertain extrapolation from the observed wavelength to the total SFR. These issues are best addressed by FIR observations, which trace the peak of the star-formation emission with less contamination from AGN activity; see Section 5.1. Consequently, the launch of the *Herschel* observatory in 2009, the first observatory with high sensitivity at FIR wavelengths (six photometric bands over ≈ 70–500 μm; Pilbratt et al 2010), offered the potential to make the first accurate SFR measurements of distant AGNs (see Lutz 2014 for a recent review of *Herschel* survey results).

On the basis of a large number of studies using *Herschel* data, it is now abundantly clear that the average SFRs of X-ray AGNs increase strongly with redshift out to at least $z \approx 3$ (e.g., Shao et al 2010; Harrison et al 2012; Mullaney et al 2012b; Rosario et al 2012, 2013b; Rovilos et al 2012; Santini et al 2012), confirming the trend found from the first SFR studies. See Fig. 15a for an example of the average SFR as a function of redshift and AGN luminosity. The majority of the studies used stacking analyses to provide average FIR constraints since only a modest fraction of the X-ray AGNs are detected by *Herschel*; however, these results are also broadly reproduced using more detailed SED fitting analyses taking account of photometric upper limits and calculating average constraints using survival analysis techniques (F. Stanley et al. in preparation).[8] In general, most studies showed no clear evidence for any luminosity dependence on the average SFR for moderate-luminosity AGNs ($L_{\rm X} = 10^{42}$–10^{44} erg s^{-1}) and the average SFR was found to be broadly constant over this luminosity range, at any given redshift; however, we note that some X-ray luminosity dependence on the average SFR is often seen at $z \lesssim 1$ and is most prominent at $z \approx 0$ (see Fig. 15).

By contrast, a broad range of results have been found for high-luminosity AGNs ($L_{\rm X} \gtrsim 10^{44}$ erg s^{-1}) at $z \gtrsim 1$, with researchers arguing that either the average SFR increases with both redshift and X-ray luminosity, increases only with redshift (following the trend seen for the moderate-luminosity AGNs), or decreases with X-ray luminosity (e.g., Harrison et al 2012; Page et al 2012;

[8] In stacking analyses, the images of a selected source population are combined (i.e., stacked) and the flux is measured from the combined image, providing a constraint on the average flux of the source population. An advantage of stacking is that individually undetected sources can be included in the analysis and average constraints can even be placed on the fluxes of source populations when none of the sources are individually detected.

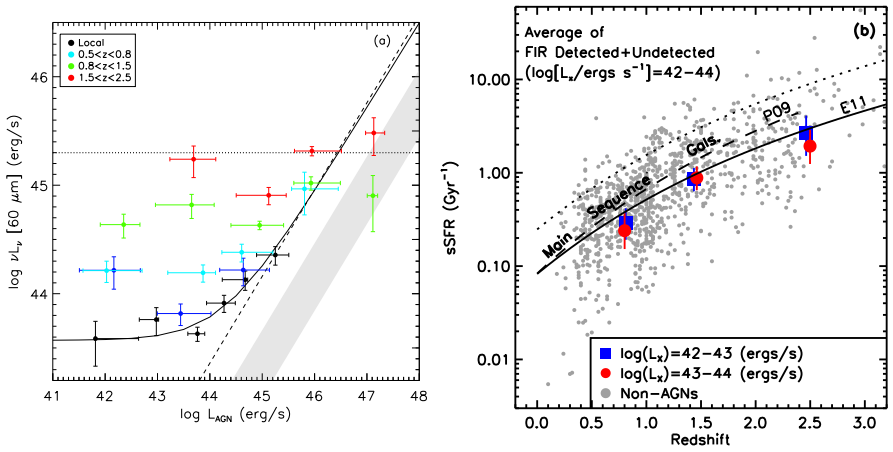

Fig. 15 (a) Median 60 μm (FIR) luminosity vs. AGN luminosity for X-ray AGNs over $z \approx 0$–2.5 (as labeled), showing the observed relationship between AGN activity and star formation. The solid curve shows the two-component functional fit to the local AGN data from *Swift*-BAT, the dotted line is the expected FIR luminosity for typical star-forming galaxies at $z = 2$ (see also panel b), the dashed line is the AGN–star formation luminosity relationship for AGN-dominated systems from Netzer (2009), and the shaded region corresponds to the estimated 1 σ range for an AGN SED (see Section 3.1 of Rosario et al 2012). $L_{\rm AGN}$ corresponds to the bolometric AGN luminosity: $L_{2-10{\rm keV}} = 10^{42}$ erg s^{-1} and $L_{2-10{\rm keV}} = 10^{44}$ erg s^{-1} correspond to $L_{\rm AGN} = 5.7 \times 10^{42}$ erg s^{-1} and $L_{\rm AGN} = 3.4 \times 10^{45}$ erg s^{-1}, respectively; (b) Average sSFR vs. redshift for X-ray AGNs with $L_{\rm X} = 10^{42}$–10^{44} erg s^{-1} (as labeled) over $z = 0.5$–3. The AGNs are compared to FIR-detected star-forming galaxies not hosting AGN activity (non AGNs) and the tracks trace the evolution in sSFR found for star-forming galaxies with redshift, as defined by Pannella et al (2009) and Elbaz et al (2011). Overall, the X-ray AGNs broadly trace the evolution in SFR and sSFR found for the star-forming galaxy population. However, the observed relationship between the AGN and star-formation luminosity is complex and is probably, at least partially, driven by the different timescales of stability between star formation and AGN activity; see Section 5.5. Adapted from Mullaney et al (2012b) and Rosario et al (2012).

Rosario et al 2012, 2013b; Rovilos et al 2012; Santini et al 2012). Some of the variation between the different results for high-luminosity AGNs is due to two practical factors: (1) the SFRs of luminous AGNs are more difficult to measure reliably since the AGN can contribute significantly to the FIR emission and (2) luminous AGNs are less common than moderate-luminosity AGNs, limiting the statistical power of studies restricted to small-area fields. Indeed, the studies performed in large-area fields with good source statistics all find that the average SFR of luminous AGNs is either constant with X-ray luminosity (extending the trend seen for the moderate-luminosity AGNs) or rises with X-ray luminosity, with the change from a rising trend to a flat trend found to be a function of redshift (e.g., Harrison et al 2012; Rosario et al 2012, 2013b, F. Stanley et al. in preparation); see Fig. 15.

The strong increase in the average SFR for the X-ray AGNs with redshift tracks the increase seen in the overall star-forming galaxy population [$\approx (1+z)^4$; e.g., Daddi et al 2007b; Noeske et al 2007; Rodighiero et al 2010;

Elbaz et al 2011]. The increase in SFR with redshift for star-forming galaxies is found to be independent of galaxy mass, such that the specific star formation rate (sSFR; the ratio of stellar mass to SFR) evolves strongly with redshift across all stellar masses, and is thought to be driven by the availability of a cold-gas supply (i.e., the distant galaxies are more gas rich than the nearby galaxies; e.g., Daddi et al 2010; Genzel et al 2010; Tacconi et al 2013). The tightness of the sSFR at any given redshift and the lack of a strong mass dependence is often referred to as the "main sequence" of star formation. The average SFRs and sSFRs of the X-ray AGNs are in good quantitative agreement with those found for the star-forming galaxy population (e.g., Xue et al 2010; Mainieri et al 2011; Mullaney et al 2012b; Rosario et al 2012, 2013b), suggesting that the same factors that drive star formation also drive AGN activity. See Fig. 15b for a comparison of sSFR between X-ray AGNs and star-forming galaxies over $z = 0.5$–3. This connection between AGN activity and star formation is further strengthened by the following additional results:

1. The average SFRs of distant X-ray AGNs are systematically higher than the *overall* galaxy population, which includes quiescent galaxies in addition to star-forming galaxies (e.g., Santini et al 2012; Symeonidis et al 2013; Vito et al 2014b), demonstrating that AGN activity is more closely connected to star-forming galaxies than the general galaxy population. We note that AGNs are also detected in quiescent galaxies but they appear to comprise a minority of the population (e.g., Azadi et al 2014; Georgakakis et al 2014b).
2. The fraction of galaxies hosting X-ray AGN activity at a fixed luminosity threshold increases strongly with SFR (e.g., Kartaltepe et al 2010; Symeonidis et al 2010; Xue et al 2010; Rafferty et al 2011; Juneau et al 2013).
3. The SFR is found to correlate tightly with AGN luminosity when averaged over all galaxies in a cosmological volume, irrespective of whether an AGN is detected or not (e.g., when calculated as a function of galaxy mass or SFR; e.g., Rafferty et al 2011; Mullaney et al 2012a; Chen et al 2013).
4. The host galaxies of X-ray AGNs at $z \lesssim 1$ appear to, preferentially, have younger stellar populations than the coeval galaxy population (e.g., Silverman et al 2009b; Pierce et al 2010b; Rosario et al 2013a; Hernán-Caballero et al 2014); see Section 5.2.
5. The strong increase in the fraction of galaxies hosting AGN activity at a fixed Eddington ratio is consistent with the increase in the average SFR with redshift [$\approx (1+z)^4$; e.g., Aird et al 2012; Bongiorno et al 2012; see Section 5.4], suggesting that the duty cycle of AGN activity increases in accordance with the cosmological increase in SFR.

These results imply a general connection between AGN activity and star formation. However, the observed relationship between AGN and star-formation luminosity does not clearly indicate a *correlation*, particularly at moderate AGN luminosities where the average SFR is flat across at least 2 orders of magnitude in AGN luminosity; see Fig. 15a. As shown by several models (e.g., Gabor and Bournaud 2013; Hickox et al 2014; Neistein and Netzer 2014; Thacker et al 2014), these apparently uncorrelated data can be explained by

differences in the timescales of stability between star formation and AGN activity: star formation is assumed to be relatively stable over long periods (of order $\approx$ 100 Myr) while AGNs are assumed to vary significantly on short timescales ($\lesssim$ Myrs). As an example, the Hickox et al (2014) model assumes that the long-term average of AGN activity and star formation is constant (i.e., when averaged over many duty cycles of mass accretion) but allows the *observed* X-ray luminosity to vary by orders of magnitude on short timescales on the basis of an assumed Eddington-ratio distribution. This model, and the other models referenced above, reproduce the broad trends seen between X-ray luminosity and average SFR and demonstrate how short-term variations can significantly disguise an underlying correlation over longer timescales. It, therefore, seems likely that the general hypothesis that AGN activity varies significantly on short timescales while the star formation is comparatively stable is broadly correct. However, it is not yet clear which model provides the best physical description of the observed trends between X-ray luminosity and average SFR, and further observational diagnostics beyond a simple average SFR (e.g., the distribution of SFRs as a function of X-ray luminosity, the fraction of quiescent galaxies hosting AGNs as a function of X-ray luminosity, the stellar-mass dependence) are required to provide greater diagnostic power.

We finally conclude our discussion of the connection between AGN activity and star formation by considering whether AGNs have significant impact on the star formation in the host galaxy (e.g., by driving energetic winds, outflows, and jets, commonly referred to as "AGN feedback"; see Veilleux et al 2005; Alexander and Hickox 2012; Fabian 2012 for reviews). On the basis of many AGN-feedback models we would expect a decrease (i.e., a suppression) in the SFR of X-ray AGNs when compared to the overall galaxy population, particularly at the highest X-ray luminosities. However, depending on how quickly the star formation is suppressed, the signatures of suppressed star formation could be comparatively subtle, particularly when averaged over AGN populations (e.g., as a function of X-ray luminosity; see Section 4 of Harrison et al 2012 for a further discussion of some potential limitations). More sensitive SFR constraints for individual systems, in addition to the measurement of sensitive SFR distributions as a function of, e.g., X-ray luminosity and redshift, are required to provide more sensitive tests of the impact of AGN activity on star formation.

5.6 The cosmic balance of power: SMBH mass accretion vs. stellar radiation

How much does SMBH mass accretion contribute to the balance of power in the cosmos? As mentioned in Section 2.1 and 3.3, AGNs dominate the CXRB. However, the CXRB only comprises a minority of the overall cosmic background radiation, which has broadly equal contributions from the cosmic UV–optical background and the cosmic infrared background (CIRB; Hauser and Dwek 2001), when the strongly dominant cosmic microwave background is

excluded (i.e., the relic emission from the Big Bang; e.g., Penzias and Wilson 1965).

The cosmic UV–optical background is dominated by stellar emission (e.g., Madau 1992; Totani et al 2001; Finke et al 2010) but, prior to the launch of *Chandra* and *XMM-Newton*, it was predicted that AGNs may contribute several tens of percent of the CIRB (e.g., Almaini et al 1999; Fabian and Iwasawa 1999; Gunn and Shanks 1999). These models typically assumed that powerful obscured quasars would contribute significantly to the CIRB through the re-radiation of the dust-obscured AGN emission at infrared wavelengths. However, direct observational measurements from the AGNs detected in the *Chandra* and *XMM-Newton* surveys showed that the contribution to the CIRB from AGNs is much more modest at $\approx$ 5–10% (even before subtracting contributions from star formation to the infrared emission from the X-ray AGN host galaxies), with the majority of the CIRB produced by star formation (e.g., Elbaz et al 2002; Fadda et al 2002; Silva et al 2004; Treister and Urry 2006; Ballantyne and Papovich 2007). Therefore, the cosmic background emission since the formation of galaxies is dominated by stellar radiation processes rather than mass accretion onto SMBHs. Part of the origin for the discrepancy between the original predictions and the observations is the assumed AGN evolution (i.e., the original models did not anticipate the "AGN downsizing" results; see Section 3.2) and the assumed contribution from Compton-thick AGNs to the CIRB, a component that is still relatively poorly constrained but is unlikely to fundamentally change these broad conclusions.

6 Future prospects

In this review we have highlighted how cosmic X-ray surveys of distant AGNs have provided key insight into the demographics, physics, and ecology of growing SMBHs. Thanks to the revolutionary X-ray facilities of *Chandra*, *XMM-Newton*, and *NuSTAR*, we now have a dramatically improved picture of how SMBHs grew through cosmic time, their accretion and obscuration physics, and the connection between SMBHs, their host galaxies and the larger scale environment. However, despite these great advances, many fundamental questions remain unanswered. In this final section we focus on some of the key remaining big questions and discuss how current and future facilities can be used to address them over the coming decades.

6.1 Remaining big questions

6.1.1 What drives AGN downsizing?

Excellent progress has been made over the past decade in measuring the space density and luminosity density evolution of X-ray AGNs, and it is now clear that lower-luminosity AGNs peaked at lower redshifts than higher-luminosity

AGNs, often referred to as "AGN downsizing"; see Section 3.2 and Fig. 7. However, what is not yet clear from the observational data are the factors that drive this luminosity dependence. Theoretical models broadly predict that this behavior is driven by a decrease in the characteristic Eddington ratio and/or a decrease in the characteristic active SMBH mass with decreasing redshift. The current observational constraints (e.g., Aird et al 2012; Bongiorno et al 2012) suggest a decrease in the characteristic Eddington ratio with decreasing redshift but they do not find any clear SMBH mass dependences (modulo that the stellar mass is often used as a proxy for the SMBH mass in these studies); see Section 5.4. However, on the basis of optical studies, at $z \lesssim 0.2$ there is clear evidence for a strong mass dependence on the volume-average growth rates of SMBHs, where the growth times of the most massive SMBHs are orders of magnitude longer than those of lower-mass SMBHs, indicating that the most massive SMBHs must have been growing more rapidly in the past (e.g., Heckman et al 2004). Testing this result with X-rays is important to verify that the mass dependence of SMBH growth is not specific to optical studies and will require sensitive X-ray data and good source statistics at both $z \lesssim 0.2$ and $z \gtrsim 0.2$. Connecting our picture of SMBH growth at $z \lesssim 0.2$ to the emerging picture of SMBH growth at $z \gtrsim 0.2$ will be key to a greater understanding of AGN downsizing and the cosmological growth of SMBHs.

6.1.2 How did the first SMBHs form and grow?

There are several theoretical models for the formation of the first SMBHs (remnants of population III stars; direct collapse of primordial gas clouds; BH merging in dense stellar clusters; e.g., see Volonteri 2010 for a recent review), which predict different initial SMBH masses (typically referred to as "seed" SMBHs) of $\approx$ 100–100,000 $M_{\odot}$. Since the mass of a SMBH dictates the maximum luminosity that can be produced through accretion (i.e., the Eddington luminosity), high-redshift XLFs can help distinguish between these different formation scenarios and, from the evolution of the XLFs, constrain the growth of the first SMBHs. The small bias against absorption makes X-rays a powerful probe of accretion in the early growth of SMBHs (e.g., rest-frame 14–70 keV at $z > 6$ for observed-frame 2–10 keV), particularly since the early SMBH growth phases were likely to be heavily absorbed [as may be expected given the gas-rich environment and small physical sizes of the first SMBHs (M. Volonteri et al. in preparation) and implied by the redshift-dependence of X-ray absorption; see Section 4.1]. One clear observational signature of early SMBH growth is "cosmic upsizing" (e.g., Ueda et al 2014), which would be revealed by a change in the relative ratio between the number density of high-luminosity and lower-luminosity AGNs (i.e., a change in the shape of the XLF) at $z \gtrsim$ 3–4; see Section 3.2. To model accurately the early growth of SMBHs it will be necessary to construct XLFs in several redshift bins down to moderate luminosities over $z \approx$ 4–8, requiring excellent high-redshift source statistics. The current XLF constraints are weak at $z \gtrsim 4$, which is due to the intrinsic rarity of such AGNs as well as source identification challenges (see Section 6.2).

Constraining the evolution of the highest-redshift AGNs is a primary goal of several future X-ray observatories (see Section 6.4), although deep *Chandra* surveys over large areas, in combination with ambitious targeted follow-up programs (see Section 6.3), can better constrain the faint end of the $z \gtrsim 4$ XLF.

6.1.3 How many obscured AGNs are missed in the current X-ray surveys?

X-ray surveys arguably provide the most efficient selection of obscured AGNs, particularly at high energies and at high redshifts where the rest-frame energies allow for penetration of large absorbing column densities (up to $N_{\rm H} \approx 10^{24}$ cm^{-2}). However, many of the most highly obscured AGNs will be missed in the current X-ray surveys, restricting our census of the overall AGN population; see Section 3.3. The identification of the most highly obscured AGNs could be more than just a "book keeping" exercise since they may reside in qualitatively different environments than less obscured AGNs (e.g., in galaxy major mergers and the most intense starbursts, where there is potentially more gas to obscure the AGN) and, therefore, may evolve differently, possibly modifying results on the fraction of obscured AGNs with redshift and luminosity; see Section 4.1. The majority of the current studies are based around *Chandra* and *XMM-Newton* surveys, but significant progress will be made using *NuSTAR*, where the higher-energy sensitivity provides a "cleaner" selection of AGNs with less absorption bias, particularly at $z \lesssim 1$ where the rest-frame energies probed by *Chandra* and *XMM-Newton* are modest. On longer timescales *Athena* will also provide greatly improved identification and characterization of heavily obscured AGNs from X-ray spectral fitting (i.e., accurate $N_{\rm H}$ and reflection measurements; see Section 6.4). Multiwavelength observations will also allow for the identification of X-ray undetected AGNs that produce luminous emission at other wavelengths (e.g., at infrared, radio, and optical wavelengths, when the contaminating emission from the host galaxy is reliably accounted for using SED decomposition and/or spectroscopy) and will become very powerful when the *James Webb Space Telescope (JWST)*, the successor to *HST*, is launched (see Section 6.3).

6.1.4 What causes the dependence of $\alpha_{\rm ox}$ on optical/UV luminosity, and why are there intrinsically X-ray weak outliers?

Although the basic dependence of $\alpha_{\rm ox}$ upon optical/UV luminosity has been known for about three decades, recent studies have substantially improved measurements of the form of this relation (see Section 4.2). This being said, further improvement is still needed since the quantitative results of some recent studies disagree by considerably more than their statistical uncertainties. Future work must aim to reduce and realistically assess the inevitable systematic errors that enter such analyses (e.g., AGN variability effects, detection-fraction effects, absorption effects, host-galaxy light contamination, and AGN misclassification). The effects of additional physical parameters, particularly Edding-

ton ratio, also need better investigation. Furthermore, the few outstanding claims for a significant dependence of $\alpha_{\rm ox}$ upon redshift need checking given the general consensus against a measurable redshift dependence (e.g., via reanalysis of the original data used to claim redshift dependence). At the same time as the observational situation is advanced, improved numerical simulations of the SMBH disk-corona system are required so that expectations for the behavior of the X-ray-to-optical/UV SED, including the basic cause of the $\alpha_{\rm ox}$-log($L_{2500\ \text{Å}}$) relation, can be derived from first-principles physics.

Additionally, outliers from the $\alpha_{\rm ox}$-log($L_{2500\ \text{Å}}$) relation that appear to be intrinsically X-ray weak need further investigation (see Section 3.3). While these objects seem sufficiently rare that they should not affect AGN demographic studies materially, they may nevertheless provide novel insights (cf. Eddington 1922) into the SMBH disk-corona system and emission-line regions. For example, some X-ray weak outliers may be systems with extremely high Eddington ratios where radiation-trapping effects largely prevent X-ray emission from escaping the accretion flow. Alternatively, perhaps these outliers are not truly intrinsically X-ray weak, and we have simply been tricked by a complex absorption scenario that is not yet properly understood or appreciated.

6.1.5 What host-galaxy environments are conducive to AGN activity?

A somewhat surprising result is how inconspicuous the host galaxies of distant X-ray AGNs are when compared to galaxies not hosting AGN activity. There are no clear differences in the host-galaxy colors and morphologies (broad-scale galactic structure and galaxy merger/interaction signatures) of X-ray AGNs and galaxies when matched in stellar mass (see Sections 5.2 and 5.3), at least at $z \gtrsim 1$ (there is evidence for some differences at $z \lesssim 1$). The star-formation properties of distant X-ray AGNs also appear to be broadly similar to those of distant star-forming galaxies and elevated when compared to the overall galaxy population (see Section 5.5), suggesting a general connection between AGN activity and star formation. Clearer differences between the host galaxies of X-ray AGNs and galaxies are more evident by the present day, when it appears that X-ray AGNs reside in a subset of the overall galaxy population. However, it is not yet clear when and how these differences arose, primarily because no study has yet uniformly measured the host-galaxy properties of both nearby and distant systems, as required to remove any potential differences between the methods used in the broad suite of studies published to date. From the point of view of the star-formation properties, deeper infrared–mm data are required to provide more powerful tests than a comparison of average SFRs (see Section 6.3.2); for example, a comparison of the SFR distributions between AGNs and galaxies and improved measurements on the fraction of AGNs in quiescent galaxies.

6.1.6 How does large-scale environment affect AGN activity?

Large-scale environment appears to have a significant affect on AGN activity, as demonstrated, for example, from the increased fraction (decreased fraction) of galaxies hosting AGN activity in protoclusters (rich galaxy clusters) versus the field; see Section 3.5. The availability of a cold-gas supply in the $\lesssim$ pc vicinity of the SMBH is presumably the essential requirement for mass accretion but these results suggest that the gas availability may be controlled by the large-scale environment. For example, there is no lack of gas in the most massive galaxy clusters, but it is mostly in a hot form rather than in the cold form that can be easily accreted by SMBHs. Protoclusters and rich galaxy clusters represent the most extreme high-density environments but to provide a fully coherent picture of the role of large-scale environment on the growth of SMBHs requires measurements of AGN activity across all environments as a function of redshift (e.g., voids; field; groups; poor clusters; rich clusters; protoclusters). To achieve this aim requires X-ray observations covering a large enough cosmic volume to detect significant numbers of X-ray sources across the full range of large-scale environments down to X-ray sensitivity limits sufficient to detect the majority of the SMBH growth. With sufficient data it would then be possible to construct XLFs and explore the host-galaxy properties as a function of environment and redshift. Improved measurements of the clustering of AGNs as a function of physical parameters (e.g., AGN type, AGN luminosity, redshift) will further reveal how the dark-matter halo affects the growth of SMBHs, particularly for HoD analyses, which require excellent source statistics to more accurately constrain the fractions of X-ray AGNs in the satellite and central galaxies within halos (see Section 3.5). Good progress can be made with current facilities (see Section 6.2) while the large FOVs of future planned and proposed X-ray observatories will make them ideally suited to addressing this key question (see Section 6.4).

6.2 Additional targeted X-ray surveys with operating missions

The *Chandra*, *XMM-Newton*, and *NuSTAR* observatories are performing well and, subject to funding considerations, have the capability to undertake productive observations of the cosmos for at least the next ≈ 5 yr. Having operated successfully over the last ≈ 15 yr, *Chandra* and *XMM-Newton* have already covered much of the accessible flux–solid angle plane, from deep pencil-beam surveys to shallow wide-area surveys; see Fig. 3. Considering all of the *Chandra* and *XMM-Newton* surveys listed in Table 1, there are an estimated $\approx 500{,}000$ unique X-ray sources detected over $\approx 1{,}000$ deg^2 of the sky. However, the source statistics and areal coverage are strongly dominated by the serendipitous surveys, which are non contiguous and typically have limited spectroscopic coverage; see Section 6.3 for future large-area/all sky multiwavelength survey plans. The blank-field surveys comprise of order $\approx 45{,}000$ unique X-ray

sources detected over ≈ 80 deg^2, of which about half are from the on-going, and currently unpublished, *XMM-Newton* XXL survey.

The current suite of *Chandra* and *XMM-Newton* surveys with good spectroscopic completeness have covered a broad swathe of the $L_{\rm X}$–z plane (e.g., see Fig. 3 of Ueda et al 2014). The majority of the detected sources lie at $z \approx 0.3$–4 and have $L_{\rm X} \approx 10^{43}$–$10^{45}$ erg s^{-1}. The excellent source statistics over this redshift range allow for the accurate construction of XLFs in discrete redshift ranges and reliable inferences about the overall source properties in discrete bins across the $L_{\rm X}$–z plane. However, only a modest number of AGNs are detected at $z < 0.3$ and $z > 4$ in the current *Chandra* and *XMM-Newton* surveys ($\lesssim 50$; e.g., Kalfountzou et al 2014; Vito et al 2014a), which is at least partially due to the small cosmological volumes probed at these redshifts; for example, the predicted yield of $z < 0.3$ ($z > 4$) AGNs with 2–10 keV luminosities of $\gtrsim 10^{43}$ erg s^{-1} ($\gtrsim 10^{44}$ erg s^{-1}) is $\approx$ 2–3 deg^{-2} ($\approx$ 10–65 deg^{-2}, depending on whether there is a high-redshift space-density decline) down to 2–10 keV fluxes of $\approx 10^{-14}$ erg cm^{-2} s^{-1} ($\approx 10^{-15}$ erg cm^{-2} s^{-1}).[9] The modest number of AGNs at $z < 0.3$ from the *Chandra* and *XMM-Newton* surveys is partially mitigated by the *ASCA* medium sensitivity survey (e.g., Akiyama et al 2003) and the high-energy all-sky X-ray surveys, such as *Swift*-BAT (e.g., Tueller et al 2010; Baumgartner et al 2013) and will be greatly bolstered by the *XMM-Newton* XXL survey, in addition to the *Chandra* and *XMM-Newton* serendipitous surveys and *eROSITA* (see Section 6.4). At $z > 4$, a major challenge in addition to the relative rarity of high-redshift AGNs, is obtaining a reliable redshift constraint, particularly for moderate-luminosity AGNs where the majority are likely to be optically faint (i.e., $R \gtrsim 25$ mag). However, improving the source statistics of $z > 4$ and $z < 0.3$ AGNs is a worthwhile endeavor since $z > 4$ corresponds to < 1.5 Gyr after the Big Bang and the era of the first growth and formation of SMBHs (see Section 6.1.2) while the $z = 0.0$–0.3 redshift range corresponds to 1/4 of cosmic history and an epoch that connects the evolution of AGNs from higher redshifts to the present day.

Despite the effective exploration of parameter space from the current *Chandra* and *XMM-Newton* surveys, an area of inquiry that is still relatively unexplored is the role of environment in the growth of SMBHs; see Sections 3.5 and 6.1.6. Current results suggest that the large-scale environment has a significant effect on the growth of SMBHs. However, the current *Chandra* and *XMM-Newton* surveys have not yet had the combination of both area and sensitivity sufficient to detect the majority of the growth of SMBHs (i.e., a factor of ≈ 10 below the knee of the XLF, L_*) across the full range of large-scale structure environments; based on cosmological simulations, regions of $\gtrsim 4$ deg^2 are required to map out the largest structures (e.g., Springel et al 2005). The *XMM-Newton* XXL survey covers sufficient survey volume (≈ 50 deg^2 in two fields) but is only sensitive to the most-luminous AGNs, close to the knee of the XLF, while the *Chandra* and *XMM-Newton* observations of COSMOS

[9] The X-ray source density predictions are based on the Gilli et al (2007) model for AGNs with $N_{\rm H} = 10^{20}$–10^{24} cm^{-2}; see http://www.bo.astro.it/∼gilli/counts.html

have sufficient sensitivity but only cover ≈ 2 deg^2 and, therefore, have a comparatively poor sampling of all large-scale structure environments. The richest galaxy clusters will typically be too rare to be included in a blank-field survey of ≈ 4 deg^2 but analyses of the pointed observations of galaxy clusters (e.g., Martini et al 2009, 2013) could be included to trace the most extreme large-scale structure environments. To map out the large-scale structures requires large contiguous fields and, therefore, this is not a scientific project that could be undertaken by the serendipitous surveys.

NuSTAR has only been operating for ≈ 2 yr and, with a comparatively small FOV, has covered a more limited swathe of the flux–solid angle plane than *Chandra* and *XMM-Newton*. The current source statistics from the combination of all of the *NuSTAR* surveys (see Table 1) are good at intermediate X-ray fluxes [$\gtrsim 100$ sources with 8–24 keV fluxes of $(5{-}50){\times}10^{-14}$ erg cm^{-2} s^{-1}], allowing for statistically significant inferences about the source populations in this flux range. However, < 10 sources are detected at both faint and bright X-ray fluxes (8–24 keV fluxes of $< 5 \times 10^{-14}$ erg cm^{-2} s^{-1} and $> 5 \times 10^{-13}$ erg cm^{-2} s^{-1}), restricting the reliability of any inferences about the properties of these source populations. Further *NuSTAR* surveys with comparable exposure times to the deepest current surveys in addition to a shallow *NuSTAR* survey will improve the source statistics at both the faint and bright X-ray flux ends, and also bridge the (approximate) order of magnitude difference in flux between the brightest *NuSTAR* survey sources and the faintest *Swift*-BAT survey sources.

6.3 Multiwavelength follow-up observations of X-ray surveys

The heart of an X-ray survey is of course the X-ray data. But the backbones are the supporting multiwavelength observations, which provide the necessary data to measure the key properties and environments of the detected sources and to construct XLFs. The majority of the extragalactic X-ray surveys listed in Table 1 are in well-established survey fields with extensive multiwavelength data. The available multiwavelength data are more limited for the serendipitous surveys, which cover non-contiguous areas across the sky and often have to rely on shallow all-sky survey data. Here we review current and future plans for multiwavelength follow-up observations of X-ray surveys, focusing on both all-sky and large-area survey plans in addition to deeper targeted multiwavelength follow-up facilities. As a demonstration of the sensitivity of several selected future observatories, see Fig. 16.

6.3.1 Optical–MIR wavelengths

At optical wavelengths, often the band pass of choice for initial counterpart identification and spectroscopic observations of X-ray sources, the entire sky has been observed in three bands down to an R-band magnitude of $R \approx 21$–22 (the SuperCOSMOS Sky Survey; e.g., Hambly et al 2001). Recently completed

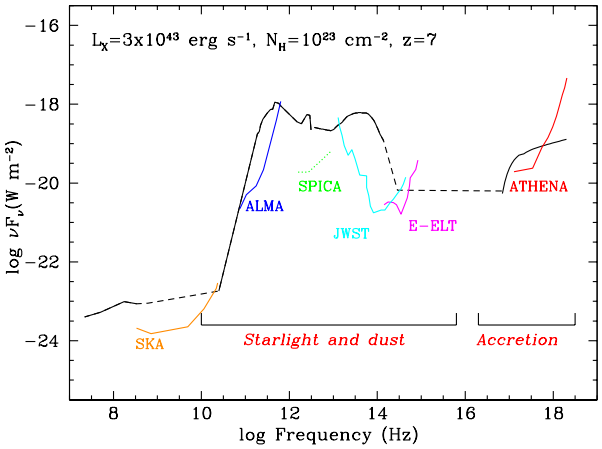

Fig. 16 Multiwavelength SED of a $z = 7$ obscured AGN with $L_{\rm X} = 3 \times 10^{43}$ erg s^{-1} and $N_{\rm H} = 10^{23}$ cm^{-2}, based on the template SED constructed by Lusso et al (2011). The relative sensitivities of selected future observatories are shown to illustrate their potential for characterizing a high-redshift AGN; ALMA has started operations but has not yet reached its full potential. The 3 σ sensitivity limits for a $\approx$ 40 ks exposure are plotted for all of the observatories except for *Athena*, where a 300 ks exposure was assumed. Adapted from Aird et al (2013b).

and on-going optical large-area surveys will extend the coverage down to optical magnitudes of 23–24 in five optical bands over practically the entire sky: for example, the SDSS (e.g., York et al 2000; Aihara et al 2011), VST ATLAS (e.g., Shanks et al 2013), PanSTARRS (e.g., Kaiser et al 2010; Magnier et al 2013), and DES (e.g., Flaugher 2005). From 2022–2032, LSST will increase the optical coverage over $\approx$ 18,000–30,000 deg^2 in six bands down to $r \approx 27.5$ with a 10 yr survey on a dedicated 8.4 m telescope (e.g., Ivezic et al 2008), sufficient to identify optical counterparts for almost all X-ray detected sources, including the $z \gtrsim 4$ AGNs required to constrain the early phases of SMBH growth in the universe.

Broader wavelength coverage over optical–MIR wavelengths is required to extend simple counterpart identification to the measurement of accurate photometric redshifts and host-galaxy masses of the X-ray sources. In the NIR–MIR band pass, 2MASS (Skrutskie et al 2006) and *WISE* (Wright et al 2010) have provided shallow to moderate-depth data across the entire sky. While providing a good general resource, the 1.1–2.3 μm 2MASS survey is too shallow ($K \approx 14$ mag) to detect many of the sources found in X-ray surveys; however, the *WISE* 3.4–22 μm survey is an excellent complement to wide-field or shallow X-ray surveys, particularly for the *NuSTAR* surveys where the majority of the sources are bright at MIR wavelengths (e.g., Alexander et al 2013; Lansbury et al 2014). The on-going VISTA surveys are observing $\approx$ 20,000 deg^2 of the Southern hemisphere at NIR wavelengths to $\gtrsim$ 4 mags deeper than 2MASS (principally the VHS survey; e.g., McMahon et al 2013; Sutherland et al 2014)

and the UKIDSS surveys have observed $\approx$ 4,000 deg^2 of, predominantly, the Northern hemisphere to $\gtrsim$ 4 mags deeper than 2MASS (principally the LAS survey; Lawrence et al 2007), with substantially deeper data in smaller regions (e.g., in the VST ATLAS survey; e.g., Arnaboldi et al 2007). These surveys are particularly useful for characterizing the properties of the X-ray sources detected in large-area and serendipitious X-ray surveys (e.g., providing photometric redshifts and host-galaxy masses), where the existing NIR coverage is comparatively shallow. As described below, deeper optical–MIR coverage over smaller areas of the sky will be possible over the coming decade with, for example, the *Wide-Field Infrared Survey Telescope (WFIRST)*, *JWST*, and the operation of the first Extremely Large Telescopes (ELTs; telescopes with $\gtrsim$ 30 m diameter mirrors).

The deployment of highly multiplexing optical–NIR spectrographs on large telescopes over the next $\approx$ 5 yr (e.g., Blanco-DESpec; *Euclid*; Mayall-DESI; SDSS IV-eBOSS; Subaru-PFS; VISTA-4MOST; VLT-MOONS; e.g., Laureijs et al 2011; Abdalla et al 2012; de Jong et al 2012; Levi et al 2013; Sugai et al 2014; Takada et al 2014; Cirasuolo et al 2014) will provide the spectroscopic complement to large-area and serendipitious X-ray surveys by yielding redshifts for hundreds to thousands of X-ray sources in an individual observation over large FOVs (typically $\approx$ 1–5 deg^2) down to optical magnitudes of $\approx$ 24. In addition to providing accurate source redshifts, the spectroscopic observations allow for characterization of the emission-line properties of the X-ray sources (e.g., identification of broad emission lines; measuring the emission-line gas conditions from emission-line ratios; e.g., Veilleux and Osterbrock 1987; Kewley et al 2013) and the identification of the large-scale structure environment in which they reside (e.g., identifying "filaments" of galaxies and AGNs in narrow redshift ranges). These analyses are particularly powerful when using spectrographs with sensitivity out to NIR wavelengths since they allow for the identification of rest-frame optical emission lines of distant AGNs at $z \gtrsim 1$ (e.g., *Euclid*; Subaru-PSF; VLT-MOONS). Many ambitious observing programs are already planned using these instruments to obtain spectroscopic redshifts for millions of galaxies and AGNs (e.g., SDSS IV-eBOSS and 4MOST follow up of *eROSITA* sources). On slightly longer timescales (mid 2020's), *WFIRST* is expected to launch and observe $>$ 1,000 deg^2 of the sky down to faint NIR depths at *HST* resolution and obtain NIR spectroscopic-grism redshifts for millions of distant galaxies and AGNs out to $z \gtrsim 8$ (e.g., Spergel et al 2013; Gehrels and Spergel 2014).

A non-negligible fraction ($\lesssim$ 3%) of the sources detected in the deepest X-ray surveys remain undetected at optical–MIR wavelengths even with the most sensitive current observatories (e.g., *HST*; 8–10 m class telescopes; *Spitzer*), and a larger fraction ($\lesssim$ 40%) lack spectroscopic redshifts (e.g., Luo et al 2010; Xue et al 2011; Hsu et al 2014). Revolutionary advances in ultra-faint imaging and spectroscopy will be made over the next 5–10 yr with the launch of *JWST* and the first ELTs. *JWST* (Gardner et al 2006) is a NASA–ESA–Canadian Space Agency satellite hosting a 6.5 m telescope with high sensitivity at 0.6–28 μm and diffraction-limited spatial resolution ($\approx$ 0.1–1 arcsec).

JWST is planned to be launched in the next ≈ 5 yr and will provide NIR–MIR imaging and spectroscopy a factor $\gtrsim 10$ times below current facilities, providing the potential to achieve (near) complete spectroscopic redshifts for the X-ray sources.[10] Several ELTs are planned over the next decade, including the European ELT (E-ELT), the Giant Magellan Telescope, and the Thirty Meter Telescope. The ELTs will complement *JWST* in an analogous manner to how the current 8–10 m telescopes complement *HST*, with innovative instruments and ultra-deep imaging and spectroscopy over large FOVs.[11]

6.3.2 Infrared–radio wavelengths

Long-wavelength data at MIR–submm wavelengths are required to measure the energetics for the dust-obscured star formation and AGN components of the X-ray sources. *Spitzer* and *Herschel* have provided an excellent resource at MIR–FIR wavelengths over the past decade for the majority of the X-ray survey fields. However, they have only covered a comparatively small fraction of the overall sky ($\approx$ 1,000 deg^2; see Lutz 2014), which often restricts MIR–FIR studies of the X-ray sources detected in the serendipitious surveys to the all-sky MIR–FIR coverage. *WISE* has provided moderate-depth MIR imaging across the whole sky (see above), although the available all-sky survey data at FIR wavelengths ($\approx$ 30–200 μm) is limited to the shallow *IRAS* and *AKARI* surveys, which typically only provide useful FIR measurements for $z \lesssim 0.1$ sources, severely restricting SFR constraints for serendipitous X-ray sources that lack *Herschel* coverage. The only currently operating FIR telescope is SOFIA (e.g., Young et al 2012a; the effective operational lifetimes of *Spitzer* and *Herschel* at MIR–FIR wavelengths were limited by their helium cryogen supply), an airborne observatory with moderate sensitivity over the broad $\approx$ 0.3–1600 μm band pass. While providing good FIR constraints for nearby AGNs, only the brightest distant AGNs will be detected by SOFIA and it, therefore, does not provide significant improvements over existing SFR constraints for the X-ray sources detected in the serendipitious surveys.

On longer timescales ($\approx$ 2025–2030), the *Space Infrared Telescope for Cosmology and Astrophysics (SPICA)* is currently the leading concept for a next-generation MIR–FIR observatory, although it is not yet fully funded. The primary aim of *SPICA* (e.g., Nakagawa et al 2014; Roelfsema et al 2014) is faint medium-resolution spectroscopy over the broad 20–210 μm band pass, which will allow for the first extensive studies of the MIR–FIR emission lines of distant systems to provide accurate measurements of the star-formation properties and the interstellar medium of distant X-ray AGNs; however, *SPICA* will also provide deep broadband MIR–FIR photometry to sensitivity levels slightly below those of *Spitzer* and *Herschel*, allowing for deep MIR–FIR observations beyond the X-ray survey regions with existing *Spitzer–Herschel* coverage. Future MIR–FIR space-borne observatories such as *SPICA* are key

[10] For further details of *JWST*, see http://www.jwst.nasa.gov.

[11] For further details of the ELTs, see http://www.eso.org/public/teles-instr/e-elt/, http://www.gmto.org/, and http://www.tmt.org/.

to drive forward our understanding of the role that distant AGNs play in the formation and evolution of galaxies.

The terrestrial atmosphere is mostly opaque at MIR–FIR wavelengths and the majority of the MIR–FIR telescopes described above are mounted inside space-borne observatories (SOFIA is the exception but it is still operated from an aircraft). However, there are discrete band passes at $\approx$ 0.3–3 mm, in the submm–mm wave band, where the atmosphere is sufficiently transparent to allow for sensitive ground-based observations (see Fig. 4 of Casey et al 2014). The negative K-correction for typical AGN and galaxy SEDs at these wavelengths means that a distant AGN or galaxy with a given SFR has a comparable submm–mm flux across the broad redshift range of $z \approx 0.5$–6 (e.g., Blain et al 2002; Casey et al 2014). Over the past two decades there have been several ground-based observatories sensitive at submm–mm wavelengths (e.g., APEX; ASTE; CARMA; IRAM; JCMT; SMA; see Casey et al 2014 for a recent review), which have provided the first clear views of the submm emission from distant AGNs and galaxies. The most recent submm–mm observatories, which have either started operations or are planned to start in the next $\approx$ 5 yr are the Atacama Large Millimeter/Submillimeter Array (ALMA; Wootten and Thompson 2009), the Large Millimeter Telescope (LMT; e.g., Hughes et al 2010), and CCAT (e.g., Woody et al 2012). ALMA is an interferometer and provides high-resolution imaging and spectroscopy down to sensitivities over an order of magnitude deeper than previous submm–mm facilities with sub-arcsec resolution. ALMA has the potential to provide unprecedented insight into the star-formation properties of distant X-ray AGNs (e.g., SFR constraints down to those of quiescent galaxies and potentially resolving the extent of star formation in some sources); see Fig. 16. Both the LMT and CCAT aim to reach a broadly similar submm–mm sensitivity limit as ALMA but at a lower spatial resolution over larger FOVs (e.g., up to 1 deg^2 for CCAT) and will provide deep submm–mm measurements of the star-formation properties for large samples of distant X-ray AGN, particularly when combined with sensitive MIR–FIR data.

Radio observations provide independent constraints on the amount of star formation and (radio bright) AGN activity in distant X-ray sources, allowing for a more complete census of AGN activity and the exploration of the connection between AGN activity and star formation. Over the past two decades, large area X-ray surveys and serendipitous X-ray surveys have largely relied on the NRAO VLA Sky Survey (NVSS; Condon et al 1998) and the VLA FIRST survey (Becker et al 1995), which cover $\approx$ 10,000–33,000 deg^2 down to mJy levels at 1.4 GHz. These data are sufficient to detect radio-bright X-ray sources, although the majority of the X-ray source population is $\approx$ 1–2 orders of magnitude fainter than the sensitivity of NVSS and FIRST. However, substantially deeper radio surveys are now being undertaken over $\gtrsim$ 1,000 deg^2 and many aim to cover the majority of the visible sky (e.g., at low $\lesssim$ 200 MHz frequencies: GMRT-TGSS; LOFAR; MWA; at mid $\approx$ 1 GHz frequencies: Apertif-WODAN; ASKAP-EMU; MeerKAT-MIGHTEE; VLA-VLASS; see Norris et al 2011, 2013; Lazio et al 2014 for a recent summary). Many of these surveys are pre-

cursors and pathfinders to the Square Kilometer Array (SKA; e.g., Dewdney et al 2009; Carilli 2014), an international project to build the world's largest radio telescope, planned to start operations over the next $\approx$ 10–20 yr. The SKA is designed to operate over a very broad range of frequencies ($\approx$ 50 MHz to 20 GHz) down to sub-μJy levels at sub-arcsec resolution, sufficient to detect essentially all of the X-ray sources at radio frequencies and provide an independent method of AGN selection (i.e., radio bright AGNs undetected at X-ray energies) in addition to sensitive SFR constraints; see Fig. 16. Due to the high sensitivity and large FOV, SKA will be able to undertake a near all-sky survey (3 π steradians) to sensitivities equivalent to the deepest current radio surveys ($\approx$ 1–2 μJy rms at 1.4 GHz; R. P. Norris, 2014, private communication), sufficient to detect the majority of the X-ray sources in the current serendipitious and all-sky X-ray surveys.

6.4 New X-ray survey missions

Several new X-ray observatories are planned in the near (< 5 yr) and long (> 10 yr) term that will extend the great progress that *Chandra*, *XMM-Newton*, and *NuSTAR* have made toward our understanding of the demographics, physics, and ecology of distant SMBHs.

In the near term, both *eROSITA* and *ASTRO-H* are expected to become operational, with launch dates of 2015–2016. *eROSITA* (Merloni et al 2012) is a joint Russian–German mission and will provide imaging and spectroscopy over $\approx$ 0.5–10 keV. The primary objective of *eROSITA* is to perform a moderate-depth survey of the entire sky within the first 4 yr of launch at relatively low spatial resolution (effective half-energy width of $\approx$ 28–40 arcsec, depending on energy), detecting $\approx$ 3 million AGNs out to $z \approx 6$. The expected sensitivities of the all-sky survey are $\approx 1 \times 10^{-14}$ erg cm^{-2} s^{-1} (0.5–2 keV) and $\approx 2 \times 10^{-13}$ erg cm^{-2} s^{-1} (2–10 keV) and will be $\approx$ 4 times more sensitive in the deepest regions at the ecliptic poles; the all-sky sensitivity limits are $\approx$ 20 times deeper than *ROSAT* at 0.5–2 keV (Voges et al 1999) and $\approx$ 200 times deeper than HEAO 1 A-2 at 2–10 keV (Piccinotti et al 1982). *ASTRO-H* (Takahashi et al 2012) is a joint JAXA-NASA mission and will provide imaging and spectroscopy of cosmic X-ray sources over the broad energy range of $\approx$ 0.3–80 keV. *ASTRO-H* should have a comparable angular resolution and sensitivity limit as *NuSTAR* at $\gtrsim$ 3 keV but over a broader energy range. *ASTRO-H* also has a wide-field imaging spectrometer and a high-resolution micro-calorimeter that will provide spectroscopy of cosmic X-ray sources over 0.3–12 keV at a higher spectral resolution than *Chandra*, *XMM-Newton*, and *NuSTAR* ($\Delta E < 7$ eV). The relatively small FOV of *ASTRO-H* for imaging at hard X-ray energies ($\approx 9 \times 9$ arcmin; see Table 2 of Takahashi et al 2012) means that it is potentially better suited to observing the well-established survey fields than undertaking new wide-area surveys at hard X-ray energies.

In the longer term, many exciting X-ray observatory concepts have been proposed that will provide revolutionary advances in our understanding of the

properties and evolution of the sources detected in cosmic X-ray surveys.[12] We do not have the space in this review to discuss all of these concepts and, to date, only one has been selected for long-term financial support (*Athena*; Nandra et al 2013). However, to provide some flavor of the X-ray facilities that may be available in the next $\approx$ 10–30 yr, we briefly describe four different proposed concepts: *Athena*, *HEX-P*, *SMART-X*, and *WFXT*.

Athena is an ESA-led mission that is scheduled for launch in 2028. With a large collecting area ($\approx$ 2.0–2.5 m^2 at 1 keV), large FOV ($\approx 40 \times 40$ arcmin), and good spatial resolution ($\approx$ 3–5 arcsec half-energy width), *Athena* will be an excellent general-purpose X-ray observatory and a devastatingly effective survey machine, achieving a given flux–solid angle limit $\approx$ 2 orders of magnitude more quickly than *Chandra* and *XMM-Newton*. The large effective area and good angular resolution combination is achieved from innovative Siliconpore optic technology. The ultimate sensitivity limit of *Athena* is dictated by the confusion limit and will be comparable to that of a $\approx$ 2 Ms *Chandra* observation [0.5–2 keV fluxes of $\approx$ (2–3) $\times 10^{-17}$ erg cm^{-2} s^{-1}; e.g., Alexander et al 2003; Luo et al 2008]. However, *Athena* will be able to achieve that sensitivity limit in $\approx$ 200–400 ks and, therefore, a 2 Ms *Athena* survey would cover $\approx$ 1 deg^2 to this depth, as compared to *Chandra* which only reaches this sensitivity limit over the central region. The large collecting area of *Athena* will also provide high signal-to-noise X-ray spectroscopy of distant X-ray AGNs at $\approx$ 100 eV resolution, allowing for direct redshift measurements from the identification of iron Kα emission lines, and accurate measurements of their spectral properties (i.e., $N_{\rm H}$, Γ, reflection, intrinsic X-ray luminosity); a high spectral resolution microcalorimeter (called the X-IFU) will provide $\approx$ 2.5 eV resolution but over a smaller $\approx 5 \times 5$ arcmin FOV. With these capabilities, *Athena* will (among other things) efficiently identify moderate-luminosity AGNs at $z \gtrsim 6$ (see Fig. 16), potentially constraining the seeds of SMBHs (see Section 6.1.2), and perform a near-complete census of AGNs out to at least $z \approx 3$, even identifying many Compton-thick systems from the detection of strong iron Kα emission (e.g., Aird et al 2013b).

HEX-P (PI: F. Harrison) is a natural successor to *NuSTAR* and combines an optimized optics design at high energies (half-power diameter resolution of $\approx$ 10–15 arcsec) with a broader energy bandpass of $\approx$ 0.1–200 keV and a larger effective area than *NuSTAR* and *XMM-Newton*. *HEX-P* aims to be $\approx$ 40 times more sensitive than *NuSTAR*, sufficient to resolve $\approx$ 90% of the CXRB at its $\approx$ 20–40 keV peak and to detect AGNs almost independent of the presence of absorption out to $z \approx 6$. *SMART-X* (PI: A. Vikhlinin) is a natural successor to *Chandra* and aims to use adaptive optics to achieve excellent $\approx$ 0.5 arcsec resolution (half-power diameter) at 0.2–10 keV with $\approx$ 30 times the effective area of *Chandra*. *SMART-X* is predicted to reach the depth of the 4 Ms CDF-S survey over 5 deg^2 in 4 Ms of exposure or $\approx 3 \times 10^{-19}$ erg cm^{-2} s^{-1} at 0.5–2 keV in a single pointing of 4 Ms, sufficient

[12] For example, see the list of proposed X-ray observatory concepts solicited by NASA in 2012: http://pcos.gsfc.nasa.gov/studies/xray/x-ray-mission-rfis.php.

to detect the first growing SMBHs at $z \approx 10$–20 [$L_{\rm X} = (0.4$–$2) \times 10^{42}$ erg s^{-1}; e.g., Vikhlinin and SMARTX Collaboration 2013]. *WFXT* (PI: S. Murray) is a natural successor to *eROSITA* and combines a large ≈ 1 deg^2 FOV with good angular resolution of ≈ 5 arcsec (half-energy width) to provide mapping of large areas of the sky to faint flux limits at ≈ 0.5–7 keV. *WFXT* is predicted to achieve a sensitivity limit comparable to that of a 2 Ms *Chandra* observation and with a dedicated 3 yr program would be able to survey ≈ 100 deg^2 and $\approx 3{,}000$ deg^2 to 0.5–2 keV flux limits of $\approx 4 \times 10^{-17}$ erg cm^{-2} s^{-1} and $\approx 5 \times 10^{-16}$ erg cm^{-2} s^{-1}, respectively, sufficient to detect ≈ 5 million AGNs overall and tens of AGNs even at $z = 8$–10 (e.g., Murray et al 2013). With high X-ray sensitivity, large FOV (with good spatial resolution across the full FOV), and good positional accuracy, *WFXT* provides a great complement to the next-generation optical imaging surveys undertaken by, for example, LSST (see Section 6.3.1).

Ever since the first rocket flights of the 1960's, cosmic X-ray surveys have been an essential tool for elucidating the processes of mass accretion onto SMBHs. With orders of magnitude improvements in sensitivity over previous generation X-ray missions, the *Chandra*, *XMM-Newton*, and, most recently, *NuSTAR* observatories have (arguably) provided greater leaps forward in our understanding of the demographics, physics, and ecology of distant growing SMBHs than any other facility over the past two decades. This is a subject area strongly driven by technological advances in telescope and instrument design, and the revolutionary developments in X-ray and multiwavelength facilities over the coming decades promise yet greater advances in our understanding of when, where, and how SMBHs have grown in the distant universe.

Acknowledgements We thank J.A. Aird, F.E. Bauer, P.N. Best, J.N. Bregman, M. Brightman, M. Brusa, A. Comastri, J.L. Donley, P. Gandhi, R. Gilli, C.M. Harrison, R.C. Hickox, L.C. Ho, D.D. Kocevski, J.H. Krolik, B.D. Lehmer, B. Luo, E. Lusso, A. Merloni, J.R. Mullaney, R.P. Norris, D.J. Rosario, A.E. Scott, O. Shemmer, Y. Shen, F. Stanley, M. Sun, E. Treister, J.R. Trump, Y. Ueda, C. Vignali, M. Volonteri, and Y.Q. Xue for feedback, helpful discussions, and sharing information. We gratefully acknowledge financial support from NASA ADP grant NNX10AC99G (WNB), Chandra X-ray Center grants AR3-14015X and G04-15130A (WNB), the Leverhulme Trust (DMA), and the Science and Technology Facilities Council (ST/I001573/1; DMA).

References

Abdalla F, Annis J, Bacon D, Bridle S, Castander F, Colless M, DePoy D, Diehl HT, Eriksen M, Flaugher B, Frieman J, Gaztanaga E, Hogan C, Jouvel S, Kent S, Kirk D, Kron R, Kuhlmann S, Lahav O, Lawrence J, Lin H, Marriner J, Marshall J, Mohr J, Nichol RC, Sako M, Saunders W, Soares-Santos M, Thomas D, Wechsler R, West A, Wu H (2012) The Dark Energy Spectrometer (DESpec): A Multi-Fiber Spectroscopic Upgrade of the Dark

Energy Camera and Survey for the Blanco Telescope. ArXiv e-prints 1209.2451

Agol E, Krolik JH (2000) Magnetic Stress at the Marginally Stable Orbit: Altered Disk Structure, Radiation, and Black Hole Spin Evolution. Astrophys J 528:161–170, astro-ph/9908049

Aihara H, Allende Prieto C, An D, Anderson SF, Aubourg É, Balbinot E, Beers TC, Berlind AA, Bickerton SJ, Bizyaev D, Blanton MR, Bochanski JJ, Bolton AS, Bovy J, Brandt WN, Brinkmann J, Brown PJ, Brownstein JR, Busca NG, Campbell H, Carr MA, Chen Y, Chiappini C, Comparat J, Connolly N, Cortes M, Croft RAC, Cuesta AJ, da Costa LN, Davenport JRA, Dawson K, Dhital S, Ealet A, Ebelke GL, Edmondson EM, Eisenstein DJ, Escoffier S, Esposito M, Evans ML, Fan X, Femenía Castellá B, Font-Ribera A, Frinchaboy PM, Ge J, Gillespie BA, Gilmore G, González Hernández JI, Gott JR, Gould A, Grebel EK, Gunn JE, Hamilton JC, Harding P, Harris DW, Hawley SL, Hearty FR, Ho S, Hogg DW, Holtzman JA, Honscheid K, Inada N, Ivans II, Jiang L, Johnson JA, Jordan C, Jordan WP, Kazin EA, Kirkby D, Klaene MA, Knapp GR, Kneib JP, Kochanek CS, Koesterke L, Kollmeier JA, Kron RG, Lampeitl H, Lang D, Le Goff JM, Lee YS, Lin YT, Long DC, Loomis CP, Lucatello S, Lundgren B, Lupton RH, Ma Z, MacDonald N, Mahadevan S, Maia MAG, Makler M, Malanushenko E, Malanushenko V, Mandelbaum R, Maraston C, Margala D, Masters KL, McBride CK, McGehee PM, McGreer ID, Ménard B, Miralda-Escudé J, Morrison HL, Mullally F, Muna D, Munn JA, Murayama H, Myers AD, Naugle T, Neto AF, Nguyen DC, Nichol RC, O'Connell RW, Ogando RLC, Olmstead MD, Oravetz DJ, Padmanabhan N, Palanque-Delabrouille N, Pan K, Pandey P, Pâris I, Percival WJ, Petitjean P, Pfaffenberger R, Pforr J, Phleps S, Pichon C, Pieri MM, Prada F, Price-Whelan AM, Raddick MJ, Ramos BHF, Reylé C, Rich J, Richards GT, Rix HW, Robin AC, Rocha-Pinto HJ, Rockosi CM, Roe NA, Rollinde E, Ross AJ, Ross NP, Rossetto BM, Sánchez AG, Sayres C, Schlegel DJ, Schlesinger KJ, Schmidt SJ, Schneider DP, Sheldon E, Shu Y, Simmerer J, Simmons AE, Sivarani T, Snedden SA, Sobeck JS, Steinmetz M, Strauss MA, Szalay AS, Tanaka M, Thakar AR, Thomas D, Tinker JL, Tofflemire BM, Tojeiro R, Tremonti CA, Vandenberg J, Vargas Magaña M, Verde L, Vogt NP, Wake DA, Wang J, Weaver BA, Weinberg DH, White M, White SDM, Yanny B, Yasuda N, Yeche C, Zehavi I (2011) The Eighth Data Release of the Sloan Digital Sky Survey: First Data from SDSS-III. Astrophys J Supp 193:29, DOI 10.1088/0067-0049/193/2/29, 1101.1559

Aird J, Nandra K, Laird ES, Georgakakis A, Ashby MLN, Barmby P, Coil AL, Huang JS, Koekemoer AM, Steidel CC, Willmer CNA (2010) The evolution of the hard X-ray luminosity function of AGN. MNRAS 401:2531–2551, 0910.1141

Aird J, Coil AL, Moustakas J, Blanton MR, Burles SM, Cool RJ, Eisenstein DJ, Smith MSM, Wong KC, Zhu G (2012) PRIMUS: The Dependence of AGN Accretion on Host Stellar Mass and Color. Astrophys J 746:90, DOI 10.1088/0004-637X/746/1/90, 1107.4368

Aird J, Coil AL, Moustakas J, Diamond-Stanic AM, Blanton MR, Cool RJ, Eisenstein DJ, Wong KC, Zhu G (2013a) PRIMUS: An Observationally Motivated Model to Connect the Evolution of the Active Galactic Nucleus and Galaxy Populations out to z ˜ 1. Astrophys J 775:41, DOI 10.1088/0004-637X/775/1/41, 1301.1689

Aird J, Comastri A, Brusa M, Cappelluti N, Moretti A, Vanzella E, Volonteri M, Alexander D, Afonso JM, Fiore F, Georgantopoulos I, Iwasawa K, Merloni A, Nandra K, Salvaterra R, Salvato M, Severgnini P, Schawinski K, Shankar F, Vignali C, Vito F (2013b) The Hot and Energetic Universe: The formation and growth of the earliest supermassive black holes. ArXiv e-prints 1306.2325

Akiyama M (2005) Host Galaxies of High-Redshift Active Galactic Nuclei in the Great Observatories Origins Deep Surveys Fields. Astrophys J 629:72–87, DOI 10.1086/431291, arXiv:astro-ph/0505315

Akiyama M, Ueda Y, Ohta K, Takahashi T, Yamada T (2003) Optical Identification of the ASCA Medium Sensitivity Survey in the Northern Sky: Nature of Hard X-Ray-Selected Luminous Active Galactic Nuclei. Astrophys J Supp 148:275–315, DOI 10.1086/376441, astro-ph/0307164

Alexander DM, Hickox RC (2012) What drives the growth of black holes? New Astron Rev 56:93–121, 1112.1949

Alexander DM, Brandt WN, Hornschemeier AE, Garmire GP, Schneider DP, Bauer FE, Griffiths RE (2001) The Chandra Deep Field North Survey. VI. The Nature of the Optically Faint X-Ray Source Population. Astron J 122:2156–2176, DOI 10.1086/323540, astro-ph/0107450

Alexander DM, Vignali C, Bauer FE, Brandt WN, Hornschemeier AE, Garmire GP, Schneider DP (2002) The Chandra Deep Field North Survey. X. X-Ray Emission from Very Red Objects. Astron J 123:1149–1162, DOI 10.1086/338852, astro-ph/0111397

Alexander DM, Bauer FE, Brandt WN, Schneider DP, Hornschemeier AE, Vignali C, Barger AJ, Broos PS, Cowie LL, Garmire GP, Townsley LK, Bautz MW, Chartas G, Sargent WLW (2003) The Chandra Deep Field North Survey. XIII. 2 Ms Point-Source Catalogs. Astron J 126:539–574, astro-ph/0304392

Alexander DM, Bauer FE, Chapman SC, Smail I, Blain AW, Brandt WN, Ivison RJ (2005a) The X-Ray Spectral Properties of SCUBA Galaxies. Astrophys J 632:736–750, astro-ph/0506608

Alexander DM, Smail I, Bauer FE, Chapman SC, Blain AW, Brandt WN, Ivison RJ (2005b) Rapid growth of black holes in massive star-forming galaxies. Nature 434:738–740, DOI 10.1038/nature03473, astro-ph/0503453

Alexander DM, Chary RR, Pope A, Bauer FE, Brandt WN, Daddi E, Dickinson M, Elbaz D, Reddy NA (2008) Reliable Identification of Compton-thick Quasars at $z \sim 2$: Spitzer Mid-Infrared Spectroscopy of HDF-oMD49. Astrophys J 687:835–847, 0803.0636

Alexander DM, Bauer FE, Brandt WN, Daddi E, Hickox RC, Lehmer BD, Luo B, Xue YQ, Young M, Comastri A, Del Moro A, Fabian AC, Gilli R, Goulding AD, Mainieri V, Mullaney JR, Paolillo M, Rafferty DA, Schneider DP,

Shemmer O, Vignali C (2011) X-Ray Spectral Constraints for $z \approx 2$ Massive Galaxies: The Identification of Reflection-dominated Active Galactic Nuclei. Astrophys J 738:44, 1106.1443

Alexander DM, Stern D, Del Moro A, Lansbury GB, Assef RJ, Aird J, Ajello M, Ballantyne DR, Bauer FE, Boggs SE, Brandt WN, Christensen FE, Civano F, Comastri A, Craig WW, Elvis M, Grefenstette BW, Hailey CJ, Harrison FA, Hickox RC, Luo B, Madsen KK, Mullaney JR, Perri M, Puccetti S, Saez C, Treister E, Urry CM, Zhang WW, Bridge CR, Eisenhardt PRM, Gonzalez AH, Miller SH, Tsai CW (2013) The NuSTAR Extragalactic Survey: A First Sensitive Look at the High-energy Cosmic X-Ray Background Population. Astrophys J 773:125, 1307.1733

Allevato V, Finoguenov A, Cappelluti N, Miyaji T, Hasinger G, Salvato M, Brusa M, Gilli R, Zamorani G, Shankar F, James JB, McCracken HJ, Bongiorno A, Merloni A, Peacock JA, Silverman J, Comastri A (2011) The XMM-Newton Wide Field Survey in the COSMOS Field: Redshift Evolution of AGN Bias and Subdominant Role of Mergers in Triggering Moderate-luminosity AGNs at Redshifts up to 2.2. Astrophys J 736:99, 1105.0520

Almaini O, Lawrence A, Boyle BJ (1999) The AGN contribution to deep submillimetre surveys and the far-infrared background. MNRAS 305:L59–L63, astro-ph/9903178

Alonso-Herrero A, Pérez-González PG, Alexander DM, Rieke GH, Rigopoulou D, Le Floc'h E, Barmby P, Papovich C, Rigby JR, Bauer FE, Brandt WN, Egami E, Willner SP, Dole H, Huang JS (2006) Infrared Power-Law Galaxies in the Chandra Deep Field-South: Active Galactic Nuclei and Ultraluminous Infrared Galaxies. Astrophys J 640:167–184, astro-ph/0511507

Alonso-Herrero A, Pérez-González PG, Rieke GH, Alexander DM, Rigby JR, Papovich C, Donley JL, Rigopoulou D (2008) The Host Galaxies and Black Holes of Typical $z \approx 0.5$–1.4 AGNs. Astrophys J 677:127–136, 0712.3121

Ammons SM, Melbourne J, Max CE, Koo DC, Rosario DJV (2009) Spatially Resolved Stellar Populations of Eight Goods-South Active Galactic Nuclei at z ˜ 1. Astron J 137:470–497, DOI 10.1088/0004-6256/137/1/470, 0810.3945

Ammons SM, Rosario DJV, Koo DC, Dutton AA, Melbourne J, Max CE, Mozena M, Kocevski DD, McGrath EJ, Bouwens RJ, Magee DK (2011) AGN Unification at z ˜ 1: u - R Colors and Gradients in X-Ray AGN Hosts. Astrophys J 740:3, DOI 10.1088/0004-637X/740/1/3, 1107.2147

Anders E, Grevesse N (1989) Abundances of the elements - Meteoritic and solar. Geochimica et Cosmochimica Acta 53:197–214

Anderson SF, Margon B (1987) The X-ray properties of high-redshift quasi-stellar objects. Astrophys J 314:111–128

Antonucci R (1993) Unified models for active galactic nuclei and quasars. Ann Rev Astron Astrophys 31:473–521

Arévalo P, Bauer FE, Puccetti S, Walton DJ, Koss M, Boggs SE, Brandt WN, Brightman M, Christensen FE, Comastri A, Craig WW, Fuerst F, Gandhi P, Grefenstette BW, Hailey CJ, Harrison FA, Luo B, Madejski G, Madsen KK, Marinucci A, Matt G, Saez C, Stern D, Stuhlinger M, Treister E, Urry CM, Zhang WW (2014) The 2-79 keV X-Ray Spectrum of the Circinus Galaxy

with NuSTAR, XMM-Newton, and Chandra: A Fully Compton-thick Active Galactic Nucleus. Astrophys J 791:81, 1406.3345

Arnaboldi M, Neeser MJ, Parker LC, Rosati P, Lombardi M, Dietrich JP, Hummel W (2007) ESO Public Surveys with the VST and VISTA. The Messenger 127:28

Assef RJ, Kochanek CS, Brodwin M, Cool R, Forman W, Gonzalez AH, Hickox RC, Jones C, Le Floc'h E, Moustakas J, Murray SS, Stern D (2010) Low-Resolution Spectral Templates for Active Galactic Nuclei and Galaxies from 0.03 to 30 μm. Astrophys J 713:970–985, DOI 10.1088/0004-637X/713/2/970, 0909.3849

Assef RJ, Stern D, Kochanek CS, Blain AW, Brodwin M, Brown MJI, Donoso E, Eisenhardt PRM, Jannuzi BT, Jarrett TH, Stanford SA, Tsai CW, Wu J, Yan L (2013) Mid-infrared Selection of Active Galactic Nuclei with the Wide-field Infrared Survey Explorer. II. Properties of WISE-selected Active Galactic Nuclei in the NDWFS Boötes Field. Astrophys J 772:26, 1209.6055

Assef RJ, Eisenhardt PRM, Stern D, Tsai CW, Wu J, Wylezalek D, Blain AW, Bridge CR, Donoso E, Gonzales A, Griffith RL, Jarrett TH (2014) Half of the Most Luminous Quasars May Be Obscured: Investigating the Nature of WISE-Selected Hot, Dust-Obscured Galaxies. ArXiv e-prints 1408.1092

Avni Y, Tananbaum H (1986) X-ray properties of optically selected QSOs. Astrophys J 305:83–99

Azadi M, Aird J, Coil A, Moustakas J, Mendez A, Blanton M, Cool R, Eisenstein D, Wong K, Zhu G (2014) PRIMUS: The relationship between Star formation and AGN accretion. ArXiv e-prints 1407.1975

Babić A, Miller L, Jarvis MJ, Turner TJ, Alexander DM, Croom SM (2007) Low accretion rates at the AGN cosmic downsizing epoch. Astron Astrophys 474:755–762, 0709.0786

Baldi A, Molendi S, Comastri A, Fiore F, Matt G, Vignali C (2002) The HELLAS2XMM Survey. I. The X-Ray Data and the logN-logS Relation. Astrophys J 564:190–195, astro-ph/0108514

Baldry IK, Glazebrook K, Brinkmann J, Ivezić Ž, Lupton RH, Nichol RC, Szalay AS (2004) Quantifying the Bimodal Color-Magnitude Distribution of Galaxies. Astrophys J 600:681–694, DOI 10.1086/380092, astro-ph/0309710

Ballantyne DR, Papovich C (2007) On the Contribution of Active Galactic Nuclei to the Cosmic Background Radiation. Astrophys J 660:988–994, DOI 10.1086/513183, astro-ph/0701775

Ballantyne DR, Shi Y, Rieke GH, Donley JL, Papovich C, Rigby JR (2006) Does the AGN Unified Model Evolve with Redshift? Using the X-Ray Background to Predict the Mid-Infrared Emission of AGNs. Astrophys J 653:1070–1088, astro-ph/0609002

Ballantyne DR, Draper AR, Madsen KK, Rigby JR, Treister E (2011) Lifting the Veil on Obscured Accretion: Active Galactic Nuclei Number Counts and Survey Strategies for Imaging Hard X-Ray Missions. Astrophys J 736:56, 1105.0965

Ballo L, Cristiani S, Fasano G, Fontanot F, Monaco P, Nonino M, Pignatelli

E, Tozzi P, Vanzella E, Fontana A, Giallongo E, Grazian A, Danese L (2007) Black Hole Masses and Eddington Ratios of AGNs at $z < 1$: Evidence of Retriggering for a Representative Sample of X-Ray-selected AGNs. Astrophys J 667:97–116

Barger AJ (ed) (2004) Supermassive Black Holes in the Distant Universe, Astrophysics and Space Science Library, vol 308

Barger AJ, Cowie LL, Bautz MW, Brandt WN, Garmire GP, Hornschemeier AE, Ivison RJ, Owen FN (2001a) Supermassive Black Hole Accretion History Inferred from a Large Sample of Chandra Hard X-Ray Sources. Astron J 122:2177–2189, astro-ph/0106219

Barger AJ, Cowie LL, Mushotzky RF, Richards EA (2001b) The Nature of the Hard X-Ray Background Sources: Optical, Near-Infrared, Submillimeter, and Radio Properties. Astron J 121:662–682, astro-ph/0007175

Barger AJ, Cowie LL, Brandt WN, Capak P, Garmire GP, Hornschemeier AE, Steffen AT, Wehner EH (2002) X-Ray, Optical, and Infrared Imaging and Spectral Properties of the 1 Ms Chandra Deep Field North Sources. Astron J 124:1839–1885, DOI 10.1086/342448, astro-ph/0206370

Barger AJ, Cowie LL, Capak P, Alexander DM, Bauer FE, Brandt WN, Garmire GP, Hornschemeier AE (2003a) Very High Redshift X-Ray-selected Active Galactic Nuclei in the Chandra Deep Field-North. Astrophys J Let 584:L61–L64, astro-ph/0301232

Barger AJ, Cowie LL, Capak P, Alexander DM, Bauer FE, Fernandez E, Brandt WN, Garmire GP, Hornschemeier AE (2003b) Optical and Infrared Properties of the 2 Ms Chandra Deep Field North X-Ray Sources. Astron J 126:632–665, astro-ph/0306212

Barger AJ, Cowie LL, Mushotzky RF, Yang Y, Wang WH, Steffen AT, Capak P (2005) The Cosmic Evolution of Hard X-Ray-selected Active Galactic Nuclei. Astron J 129:578–609, astro-ph/0410527

Barger AJ, Cowie LL, Wang WH (2007) The Microjansky Radio Galaxy Population. Astrophys J 654:764–781, astro-ph/0609374

Barnes JE, Hernquist L (1992) Dynamics of interacting galaxies. Ann Rev Astron Astrophys 30:705–742, DOI 10.1146/annurev.aa.30.090192.003421

Basu-Zych AR, Lehmer BD, Hornschemeier AE, Bouwens RJ, Fragos T, Oesch PA, Belczynski K, Brandt WN, Kalogera V, Luo B, Miller N, Mullaney JR, Tzanavaris P, Xue Y, Zezas A (2013) The X-Ray Star Formation Story as Told by Lyman Break Galaxies in the 4 Ms CDF-S. Astrophys J 762:45, 1210.3357

Bauer FE, Alexander DM, Brandt WN, Hornschemeier AE, Vignali C, Garmire GP, Schneider DP (2002) The Chandra Deep Field North Survey. XII. The Link between Faint X-Ray and Radio Source Populations. Astron J 124:2351–2363, astro-ph/0207433

Bauer FE, Alexander DM, Brandt WN, Schneider DP, Treister E, Hornschemeier AE, Garmire GP (2004) The Fall of Active Galactic Nuclei and the Rise of Star-forming Galaxies: A Close Look at the Chandra Deep Field X-Ray Number Counts. Astron J 128:2048–2065, astro-ph/0408001

Baumgartner WH, Tueller J, Markwardt CB, Skinner GK, Barthelmy S,

Mushotzky RF, Evans PA, Gehrels N (2013) The 70 Month Swift-BAT All-sky Hard X-Ray Survey. Astrophys J Supp 207:19, DOI 10.1088/0067-0049/207/2/19, 1212.3336

Beck-Winchatz B, Anderson SF (2007) Faint quasar candidates from Hubble Space Telescope imaging: number counts from 31 new high-latitude fields. MNRAS 374:1506–1514

Becker RH, White RL, Helfand DJ (1995) The FIRST Survey: Faint Images of the Radio Sky at Twenty Centimeters. Astrophys J 450:559, DOI 10.1086/176166

Bell EF, de Jong RS (2001) Stellar Mass-to-Light Ratios and the Tully-Fisher Relation. Astrophys J 550:212–229, DOI 10.1086/319728, astro-ph/0011493

Bell EF, Wolf C, Meisenheimer K, Rix HW, Borch A, Dye S, Kleinheinrich M, Wisotzki L, McIntosh DH (2004) Nearly 5000 Distant Early-Type Galaxies in COMBO-17: A Red Sequence and Its Evolution since z˜1. Astrophys J 608:752–767, DOI 10.1086/420778, astro-ph/0303394

Bennert VN, Auger MW, Treu T, Woo JH, Malkan MA (2011) The Relation between Black Hole Mass and Host Spheroid Stellar Mass Out to z ˜ 2. Astrophys J 742:107, DOI 10.1088/0004-637X/742/2/107, 1102.1975

Berlind AA, Weinberg DH (2002) The Halo Occupation Distribution: Toward an Empirical Determination of the Relation between Galaxies and Mass. Astrophys J 575:587–616, DOI 10.1086/341469, astro-ph/0109001

Best PN, Kauffmann G, Heckman TM, Brinchmann J, Charlot S, Ivezić Ž, White SDM (2005) The host galaxies of radio-loud active galactic nuclei: mass dependences, gas cooling and active galactic nuclei feedback. MNRAS 362:25–40, DOI 10.1111/j.1365-2966.2005.09192.x, astro-ph/0506269

Bielby RM, Hill MD, Metcalfe N, Shanks T (2012) Submillimetre observations of X-ray active galactic nuclei in the William Herschel Deep Field. MNRAS 419:1315–1323, 1108.3934

Blain AW, Smail I, Ivison RJ, Kneib JP, Frayer DT (2002) Submillimeter galaxies. Phys Rep 369:111–176, DOI 10.1016/S0370-1573(02)00134-5, astro-ph/0202228

Bluck AFL, Conselice CJ, Almaini O, Laird ES, Nandra K, Grützbauch R (2011) On the co-evolution of supermassive black holes and their host galaxies since z= 3. MNRAS 410:1174–1196, DOI 10.1111/j.1365-2966.2010.17521.x, 1008.2162

Böhm A, Wisotzki L, Bell EF, Jahnke K, Wolf C, Bacon D, Barden M, Gray ME, Hoeppe G, Jogee S, McIntosh DH, Peng CY, Robaina AR, Balogh M, Barazza FD, Caldwell JAR, Heymans C, Häußler B, van Kampen E, Lane K, Meisenheimer K, Sánchez SF, Taylor AN, Zheng X (2013) AGN host galaxies at redshift $z \approx 0.7$: peculiar or not? Astron Astrophys 549:A46, DOI 10.1051/0004-6361/201015444, 1210.6214

Bongiorno A, Zamorani G, Gavignaud I, Marano B, Paltani S, Mathez G, Møller P, Picat JP, Cirasuolo M, Lamareille F, Bottini D, Garilli B, Le Brun V, Le Fèvre O, Maccagni D, Scaramella R, Scodeggio M, Tresse L, Vettolani G, Zanichelli A, Adami C, Arnouts S, Bardelli S, Bolzonella M, Cappi A,

Charlot S, Ciliegi P, Contini T, Foucaud S, Franzetti P, Guzzo L, Ilbert O, Iovino A, McCracken HJ, Marinoni C, Mazure A, Meneux B, Merighi R, Pellò R, Pollo A, Pozzetti L, Radovich M, Zucca E, Hatziminaoglou E, Polletta M, Bondi M, Brinchmann J, Cucciati O, de la Torre S, Gregorini L, Mellier Y, Merluzzi P, Temporin S, Vergani D, Walcher CJ (2007) The VVDS type-1 AGN sample: the faint end of the luminosity function. Astron Astrophys 472:443–454, 0704.1660

Bongiorno A, Merloni A, Brusa M, Magnelli B, Salvato M, Mignoli M, Zamorani G, Fiore F, Rosario D, Mainieri V, Hao H, Comastri A, Vignali C, Balestra I, Bardelli S, Berta S, Civano F, Kampczyk P, Le Floc'h E, Lusso E, Lutz D, Pozzetti L, Pozzi F, Riguccini L, Shankar F, Silverman J (2012) Accreting supermassive black holes in the COSMOS field and the connection to their host galaxies. MNRAS 427:3103–3133, DOI 10.1111/j.1365-2966.2012.22089.x, 1209.1640

Booth CM, Schaye J (2010) Dark matter haloes determine the masses of supermassive black holes. MNRAS 405:L1–L5, DOI 10.1111/j.1745-3933.2010.00832.x, 0911.0935

Bournaud F, Juneau S, Le Floc'h E, Mullaney J, Daddi E, Dekel A, Duc PA, Elbaz D, Salmi F, Dickinson M (2012) An Observed Link between Active Galactic Nuclei and Violent Disk Instabilities in High-redshift Galaxies. Astrophys J 757:81, DOI 10.1088/0004-637X/757/1/81, 1111.0987

Boutsia K, Leibundgut B, Trevese D, Vagnetti F (2009) Spectroscopic follow-up of variability-selected active galactic nuclei in the Chandra Deep Field South. Astron Astrophys 497:81–95, 0902.0933

Boyle BJ (2001) The Evolution of QSOs. In: Aretxaga I, Kunth D, Mújica R (eds) Advanced Lectures on the Starburst-AGN, p 325

Boyle BJ, Shanks T, Croom SM, Smith RJ, Miller L, Loaring N, Heymans C (2000) The 2dF QSO Redshift Survey - I. The optical luminosity function of quasi-stellar objects. MNRAS 317:1014–1022, astro-ph/0005368

Brammer GB, Whitaker KE, van Dokkum PG, Marchesini D, Labbé I, Franx M, Kriek M, Quadri RF, Illingworth G, Lee KS, Muzzin A, Rudnick G (2009) The Dead Sequence: A Clear Bimodality in Galaxy Colors from z = 0 to z = 2.5. Astrophys J Let 706:L173–L177, DOI 10.1088/0004-637X/706/1/L173, 0910.2227

Brandt WN, Alexander DM (2010) Supermassive black-hole growth over cosmic time: Active galaxy demography, physics, and ecology from Chandra surveys. Proceedings of the National Academy of Science 107:7184–7189, 1001.5054

Brandt WN, Hasinger G (2005) Deep Extragalactic X-Ray Surveys. Ann Rev Astron Astrophys 43:827–859, astro-ph/0501058

Brandt WN, Mathur S, Elvis M (1997) A comparison of the hard ASCA spectral slopes of broad- and narrow-line Seyfert 1 galaxies. MNRAS 285:L25–L30, astro-ph/9703100

Brandt WN, Laor A, Wills BJ (2000) On the Nature of Soft X-Ray Weak Quasi-stellar Objects. Astrophys J 528:637–649, astro-ph/9908016

Brightman M, Silverman JD, Mainieri V, Ueda Y, Schramm M, Matsuoka K,

Nagao T, Steinhardt C, Kartaltepe J, Sanders DB, Treister E, Shemmer O, Brandt WN, Brusa M, Comastri A, Ho LC, Lanzuisi G, Lusso E, Nandra K, Salvato M, Zamorani G, Akiyama M, Alexander DM, Bongiorno A, Capak P, Civano F, Del Moro A, Doi A, Elvis M, Hasinger G, Laird ES, Masters D, Mignoli M, Ohta K, Schawinski K, Taniguchi Y (2013) A statistical relation between the X-ray spectral index and Eddington ratio of active galactic nuclei in deep surveys. MNRAS 433:2485–2496, 1305.3917

Brightman M, Nandra K, Salvato M, Hsu LT, Aird J, Rangel C (2014) Compton thick active galactic nuclei in Chandra surveys. MNRAS 443:1999–2017, 1406.4502

Brunner H, Cappelluti N, Hasinger G, Barcons X, Fabian AC, Mainieri V, Szokoly G (2008) XMM-Newton observations of the Lockman Hole: X-ray source catalogue and number counts. Astron Astrophys 479:283–300, 0711.4822

Brusa M, Comastri A, Gilli R, Hasinger G, Iwasawa K, Mainieri V, Mignoli M, Salvato M, Zamorani G, Bongiorno A, Cappelluti N, Civano F, Fiore F, Merloni A, Silverman J, Trump J, Vignali C, Capak P, Elvis M, Ilbert O, Impey C, Lilly S (2009a) High-Redshift Quasars in the COSMOS Survey: The Space Density of $z > 3$ X-Ray Selected QSOs. Astrophys J 693:8–22, 0809.2513

Brusa M, Fiore F, Santini P, Grazian A, Comastri A, Zamorani G, Hasinger G, Merloni A, Civano F, Fontana A, Mainieri V (2009b) Black hole growth and starburst activity at z = 0.6-4 in the Chandra Deep Field South. Host galaxies properties of obscured AGN. Astron Astrophys 507:1277–1289, DOI 10.1051/0004-6361/200912261, 0910.1007

Brusa M, Civano F, Comastri A, Miyaji T, Salvato M, Zamorani G, Cappelluti N, Fiore F, Hasinger G, Mainieri V, Merloni A, Bongiorno A, Capak P, Elvis M, Gilli R, Hao H, Jahnke K, Koekemoer AM, Ilbert O, Le Floc'h E, Lusso E, Mignoli M, Schinnerer E, Silverman JD, Treister E, Trump JD, Vignali C, Zamojski M, Aldcroft T, Aussel H, Bardelli S, Bolzonella M, Cappi A, Caputi K, Contini T, Finoguenov A, Fruscione A, Garilli B, Impey CD, Iovino A, Iwasawa K, Kampczyk P, Kartaltepe J, Kneib JP, Knobel C, Kovac K, Lamareille F, Leborgne JF, Le Brun V, Le Fevre O, Lilly SJ, Maier C, McCracken HJ, Pello R, Peng YJ, Perez-Montero E, de Ravel L, Sanders D, Scodeggio M, Scoville NZ, Tanaka M, Taniguchi Y, Tasca L, de la Torre S, Tresse L, Vergani D, Zucca E (2010) The XMM-Newton Wide-field Survey in the Cosmos Field (XMM-COSMOS): Demography and Multiwavelength Properties of Obscured and Unobscured Luminous Active Galactic Nuclei. Astrophys J 716:348–369, 1004.2790

Buchner J, Georgakakis A, Nandra K, Hsu L, Rangel C, Brightman M, Merloni A, Salvato M, Donley J, Kocevski D (2014) X-ray spectral modelling of the AGN obscuring region in the CDFS: Bayesian model selection and catalogue. Astron Astrophys 564:A125, 1402.0004

Bundy K, Ellis RS, Conselice CJ, Taylor JE, Cooper MC, Willmer CNA, Weiner BJ, Coil AL, Noeske KG, Eisenhardt PRM (2006) The Mass Assembly History of Field Galaxies: Detection of an Evolving Mass Limit for

Star-Forming Galaxies. Astrophys J 651:120–141, astro-ph/0512465
Bundy K, Georgakakis A, Nandra K, Ellis RS, Conselice CJ, Laird E, Coil A, Cooper MC, Faber SM, Newman JA, Pierce CM, Primack JR, Yan R (2008) AEGIS: New Evidence Linking Active Galactic Nuclei to the Quenching of Star Formation. Astrophys J 681:931–943, DOI 10.1086/588719, arXiv:0710.2105
Burlon D, Ajello M, Greiner J, Comastri A, Merloni A, Gehrels N (2011) Three-year Swift-BAT Survey of Active Galactic Nuclei: Reconciling Theory and Observations? Astrophys J 728:58, 1012.0302
Burtscher L, Meisenheimer K, Tristram KRW, Jaffe W, Hönig SF, Davies RI, Kishimoto M, Pott JU, Röttgering H, Schartmann M, Weigelt G, Wolf S (2013) A diversity of dusty AGN tori. Data release for the VLTI/MIDI AGN Large Program and first results for 23 galaxies. Astron Astrophys 558:A149, 1307.2068
Cappelluti N, Brusa M, Hasinger G, Comastri A, Zamorani G, Finoguenov A, Gilli R, Puccetti S, Miyaji T, Salvato M, Vignali C, Aldcroft T, Böhringer H, Brunner H, Civano F, Elvis M, Fiore F, Fruscione A, Griffiths RE, Guzzo L, Iovino A, Koekemoer AM, Mainieri V, Scoville NZ, Shopbell P, Silverman J, Urry CM (2009) The XMM-Newton wide-field survey in the COSMOS field. The point-like X-ray source catalogue. Astron Astrophys 497:635–648, 0901.2347
Cappelluti N, Ajello M, Burlon D, Krumpe M, Miyaji T, Bonoli S, Greiner J (2010) Active Galactic Nuclei Clustering in the Local Universe: An Unbiased Picture from Swift-BAT. Astrophys J Let 716:L209–L213, DOI 10.1088/2041-8205/716/2/L209, 1005.4968
Cardamone CN, Urry CM, Damen M, van Dokkum P, Treister E, Labbé I, Virani SN, Lira P, Gawiser E (2008) Mid-Infrared Properties and Color Selection for X-Ray-Detected Active Galactic Nuclei in the MUSYC Extended Chandra Deep Field-South. Astrophys J 680:130–142, 0803.0251
Cardamone CN, van Dokkum PG, Urry CM, Taniguchi Y, Gawiser E, Brammer G, Taylor E, Damen M, Treister E, Cobb BE, Bond N, Schawinski K, Lira P, Murayama T, Saito T, Sumikawa K (2010) The Multiwavelength Survey by Yale-Chile (MUSYC): Deep Medium-band Optical Imaging and High-quality 32-band Photometric Redshifts in the ECDF-S. Astrophys J Supp 189:270–285, 1008.2974
Cardelli JA, Clayton GC, Mathis JS (1989) The relationship between infrared, optical, and ultraviolet extinction. Astrophys J 345:245–256
Carilli CL (2014) Square Kilometre Array key science: a progressive retrospective. ArXiv e-prints 1408.5317
Casey CM, Narayanan D, Cooray A (2014) Dusty star-forming galaxies at high redshift. Phys Rep 541:45–161, DOI 10.1016/j.physrep.2014.02.009, 1402.1456
Cattaneo A, Dekel A, Devriendt J, Guiderdoni B, Blaizot J (2006) Modelling the galaxy bimodality: shutdown above a critical halo mass. MNRAS 370:1651–1665, DOI 10.1111/j.1365-2966.2006.10608.x, astro-ph/0601295
Chen CTJ, Hickox RC, Alberts S, Brodwin M, Jones C, Murray SS, Alexan-

der DM, Assef RJ, Brown MJI, Dey A, Forman WR, Gorjian V, Goulding AD, Le Floc'h E, Jannuzi BT, Mullaney JR, Pope A (2013) A Correlation between Star Formation Rate and Average Black Hole Accretion in Star-forming Galaxies. Astrophys J 773:3, DOI 10.1088/0004-637X/773/1/3, 1306.1227

Cheung E, Trump JR, Athanassoula E, Bamford SP, Bell EF, Bosma A, Cardamone CN, Casteels KRV, Faber SM, Fang JJ, Fortson LF, Kocevski DD, Koo DC, Laine S, Lintott C, Masters KL, Melvin T, Nichol RC, Schawinski K, Simmons B, Smethurst R, Willett KW (2014) Galaxy Zoo: Are Bars Responsible for the Feeding of Active Galactic Nuclei at $0.2 < z < 1.0$? ArXiv e-prints 1409.5434

Chiappetti L, Tajer M, Trinchieri G, Maccagni D, Maraschi L, Paioro L, Pierre M, Surdej J, Garcet O, Gosset E, Le Fèvre O, Bertin E, McCracken HJ, Mellier Y, Foucaud S, Radovich M, Ripepi V, Arnaboldi M (2005) The XMM-LSS survey. The XMDS/VVDS 4σ catalogue. Astron Astrophys 439:413–425, astro-ph/0505117

Chiappetti L, Clerc N, Pacaud F, Pierre M, Guéguen A, Paioro L, Polletta M, Melnyk O, Elyiv A, Surdej J, Faccioli L (2013) The XMM-Large Scale Structure catalogue - II. X-ray sources and associated multiwavelength data. MNRAS 429:1652–1673

Ciliegi P, Zamorani G, Hasinger G, Lehmann I, Szokoly G, Wilson G (2003) A deep VLA survey at 6 cm in the Lockman Hole. Astron Astrophys 398:901–918, astro-ph/0211625

Cimatti A, Daddi E, Renzini A (2006) Mass downsizing and "top-down" assembly of early-type galaxies. Astron Astrophys 453:L29–L33, astro-ph/0605353

Cimatti A, Brusa M, Talia M, Mignoli M, Rodighiero G, Kurk J, Cassata P, Halliday C, Renzini A, Daddi E (2013) Active Galactic Nucleus Feedback at z ˜ 2 and the Mutual Evolution of Active and Inactive Galaxies. Astrophys J Let 779:L13, 1311.4401

Cirasuolo M, Afonso J, Carollo M, Flores H, Maiolino R, Oliva E, Paltani S, Vanzi L, Evans C, Abreu M, Atkinson D, Babusiaux C, Beard S, Bauer F, Bellazzini M, Bender R, Best P, Bezawada N, Bonifacio P, Bragaglia A, Bryson I, Busher D, Cabral A, Caputi K, Centrone M, Chemla F, Cimatti A, Cioni MR, Clementini G, Coelho J, Crnojevic D, Daddi E, Dunlop J, Eales S, Feltzing S, Ferguson A, Fisher M, Fontana A, Fynbo J, Garilli B, Gilmore G, Glauser A, Guinouard I, Hammer F, Hastings P, Hess A, Ivison R, Jagourel P, Jarvis M, Kaper L, Kauffman G, Kitching AT, Lawrence A, Lee D, Lemasle B, Licausi G, Lilly S, Lorenzetti D, Lunney D, Maiolino R, Mannucci F, McLure R, Minniti D, Montgomery D, Muschielok B, Nandra K, Navarro R, Norberg P, Oliver S, Origlia L, Padilla N, Peacock J, Pedichini F, Peng J, Pentericci L, Pragt J, Puech M, Randich S, Rees P, Renzini A, Ryde N, Rodrigues M, Roseboom I, Royer F, Saglia R, Sanchez A, Schiavon R, Schnetler H, Sobral D, Speziali R, Sun D, Stuik R, Taylor A, Taylor W, Todd S, Tolstoy E, Torres M, Tosi M, Vanzella E, Venema L, Vitali F, Wegner M, Wells M, Wild V, Wright G, Zamorani G, Zoccali M (2014)

MOONS: the Multi-Object Optical and Near-infrared Spectrograph for the VLT. In: Society of Photo-Optical Instrumentation Engineers (SPIE) Conference Series, Society of Photo-Optical Instrumentation Engineers (SPIE) Conference Series, vol 9147, p 0, DOI 10.1117/12.2056012

Cisternas M, Jahnke K, Inskip KJ, Kartaltepe J, Koekemoer AM, Lisker T, Robaina AR, Scodeggio M, Sheth K, Trump JR, Andrae R, Miyaji T, Lusso E, Brusa M, Capak P, Cappelluti N, Civano F, Ilbert O, Impey CD, Leauthaud A, Lilly SJ, Salvato M, Scoville NZ, Taniguchi Y (2011) The Bulk of the Black Hole Growth Since z ˜ 1 Occurs in a Secular Universe: No Major Merger-AGN Connection. Astrophys J 726:57–+, DOI 10.1088/0004-637X/726/2/57, 1009.3265

Cisternas M, Sheth K, Salvato M, Knapen JH, Civano F, Santini P (2014) The role of bars in AGN fueling in disk galaxies over the last seven billion years. ArXiv e-prints 1409.2871

Civano F, Brusa M, Comastri A, Elvis M, Salvato M, Zamorani G, Capak P, Fiore F, Gilli R, Hao H, Ikeda H, Kakazu Y, Kartaltepe JS, Masters D, Miyaji T, Mignoli M, Puccetti S, Shankar F, Silverman J, Vignali C, Zezas A, Koekemoer AM (2011) The Population of High-redshift Active Galactic Nuclei in the Chandra-COSMOS Survey. Astrophys J 741:91, 1103.2570

Civano F, Elvis M, Brusa M, Comastri A, Salvato M, Zamorani G, Aldcroft T, Bongiorno A, Capak P, Cappelluti N, Cisternas M, Fiore F, Fruscione A, Hao H, Kartaltepe J, Koekemoer A, Gilli R, Impey CD, Lanzuisi G, Lusso E, Mainieri V, Miyaji T, Lilly S, Masters D, Puccetti S, Schawinski K, Scoville NZ, Silverman J, Trump J, Urry M, Vignali C, Wright NJ (2012) The Chandra COSMOS Survey. III. Optical and Infrared Identification of X-Ray Point Sources. Astrophys J Supp 201:30, 1205.5030

Coil AL, Georgakakis A, Newman JA, Cooper MC, Croton D, Davis M, Koo DC, Laird ES, Nandra K, Weiner BJ, Willmer CNA, Yan R (2009) AEGIS: The Clustering of X-Ray Active Galactic Nucleus Relative to Galaxies at z ˜ 1. Astrophys J 701:1484–1499, DOI 10.1088/0004-637X/701/2/1484, 0902.0363

Cole S, Norberg P, Baugh CM, Frenk CS, Bland-Hawthorn J, Bridges T, Cannon R, Colless M, Collins C, Couch W, Cross N, Dalton G, De Propris R, Driver SP, Efstathiou G, Ellis RS, Glazebrook K, Jackson C, Lahav O, Lewis I, Lumsden S, Maddox S, Madgwick D, Peacock JA, Peterson BA, Sutherland W, Taylor K (2001) The 2dF galaxy redshift survey: near-infrared galaxy luminosity functions. MNRAS 326:255–273, DOI 10.1046/j.1365-8711.2001.04591.x, astro-ph/0012429

Comastri A (2004) Compton-Thick AGN: The Dark Side of the X-Ray Background. In: Barger AJ (ed) Supermassive Black Holes in the Distant Universe, Astrophysics and Space Science Library, vol 308, p 245, astro-ph/0403693

Comastri A, Setti G, Zamorani G, Hasinger G (1995) The contribution of AGNs to the X-ray background. Astron Astrophys 296:1, astro-ph/9409067

Condon JJ, Cotton WD, Greisen EW, Yin QF, Perley RA, Taylor GB, Brod-

erick JJ (1998) The NRAO VLA Sky Survey. Astron J 115:1693–1716, DOI 10.1086/300337

Conroy C (2013) Modeling the Panchromatic Spectral Energy Distributions of Galaxies. Ann Rev Astron Astrophys 51:393–455, DOI 10.1146/annurev-astro-082812-141017, 1301.7095

Cotini S, Ripamonti E, Caccianiga A, Colpi M, Della Ceca R, Mapelli M, Severgnini P, Segreto A (2013) The merger fraction of active and inactive galaxies in the local Universe through an improved non-parametric classification. MNRAS 431:2661–2672, DOI 10.1093/mnras/stt358, 1303.0036

Cowie LL, Songaila A, Hu EM, Cohen JG (1996) New Insight on Galaxy Formation and Evolution From Keck Spectroscopy of the Hawaii Deep Fields. Astron J 112:839, astro-ph/9606079

Cowie LL, Barger AJ, Bautz MW, Capak P, Crawford CS, Fabian AC, Hu EM, Iwamuro F, Kneib JP, Maihara T, Motohara K (2001) Detecting High-Redshift Evolved Galaxies as the Hosts of Optically Faint Hard X-Ray Sources. Astrophys J Let 551:L9–L12, DOI 10.1086/319839, astro-ph/0102306

Cowie LL, Barger AJ, Bautz MW, Brandt WN, Garmire GP (2003) The Redshift Evolution of the 2-8 keV X-Ray Luminosity Function. Astrophys J Let 584:L57–L60, astro-ph/0301231

Cowie LL, Barger AJ, Hasinger G (2012) The Faintest X-Ray Sources from z = 0 TO 8. Astrophys J 748:50, 1110.3326

Cristiani S, Alexander DM, Bauer F, Brandt WN, Chatzichristou ET, Fontanot F, Grazian A, Koekemoer A, Lucas RA, Monaco P, Nonino M, Padovani P, Stern D, Tozzi P, Treister E, Urry CM, Vanzella E (2004) The Space Density of High-redshift QSOs in the Great Observatories Origins Deep Survey. Astrophys J Let 600:L119–L122, astro-ph/0309049

Croom SM, Richards GT, Shanks T, Boyle BJ, Strauss MA, Myers AD, Nichol RC, Pimbblet KA, Ross NP, Schneider DP, Sharp RG, Wake DA (2009) The 2dF-SDSS LRG and QSO survey: the QSO luminosity function at $0.4 < z < 2.6$. MNRAS 399:1755–1772, 0907.2727

Croton DJ (2009) A simple model to link the properties of quasars to the properties of dark matter haloes out to high redshift. MNRAS 394:1109–1119, DOI 10.1111/j.1365-2966.2009.14429.x, 0901.4104

Daddi E, Alexander DM, Dickinson M, Gilli R, Renzini A, Elbaz D, Cimatti A, Chary R, Frayer D, Bauer FE, Brandt WN, Giavalisco M, Grogin NA, Huynh M, Kurk J, Mignoli M, Morrison G, Pope A, Ravindranath S (2007a) Multiwavelength Study of Massive Galaxies at z˜2. II. Widespread Compton-thick Active Galactic Nuclei and the Concurrent Growth of Black Holes and Bulges. Astrophys J 670:173–189, 0705.2832

Daddi E, Dickinson M, Morrison G, Chary R, Cimatti A, Elbaz D, Frayer D, Renzini A, Pope A, Alexander DM, Bauer FE, Giavalisco M, Huynh M, Kurk J, Mignoli M (2007b) Multiwavelength Study of Massive Galaxies at z˜2. I. Star Formation and Galaxy Growth. Astrophys J 670:156–172, DOI 10.1086/521818, 0705.2831

Daddi E, Bournaud F, Walter F, Dannerbauer H, Carilli CL, Dickinson M,

Elbaz D, Morrison GE, Riechers D, Onodera M, Salmi F, Krips M, Stern D (2010) Very High Gas Fractions and Extended Gas Reservoirs in z = 1.5 Disk Galaxies. Astrophys J 713:686–707, DOI 10.1088/0004-637X/713/1/686, 0911.2776

de Jong RS, Bellido-Tirado O, Chiappini C, Depagne É, Haynes R, Johl D, Schnurr O, Schwope A, Walcher J, Dionies F, Haynes D, Kelz A, Kitaura FS, Lamer G, Minchev I, Müller V, Nuza SE, Olaya JC, Piffl T, Popow E, Steinmetz M, Ural U, Williams M, Winkler R, Wisotzki L, Ansorge WR, Banerji M, Gonzalez Solares E, Irwin M, Kennicutt RC, King D, McMahon RG, Koposov S, Parry IR, Sun D, Walton NA, Finger G, Iwert O, Krumpe M, Lizon JL, Vincenzo M, Amans JP, Bonifacio P, Cohen M, Francois P, Jagourel P, Mignot SB, Royer F, Sartoretti P, Bender R, Grupp F, Hess HJ, Lang-Bardl F, Muschielok B, Böhringer H, Boller T, Bongiorno A, Brusa M, Dwelly T, Merloni A, Nandra K, Salvato M, Pragt JH, Navarro R, Gerlofsma G, Roelfsema R, Dalton GB, Middleton KF, Tosh IA, Boeche C, Caffau E, Christlieb N, Grebel EK, Hansen C, Koch A, Ludwig HG, Quirrenbach A, Sbordone L, Seifert W, Thimm G, Trifonov T, Helmi A, Trager SC, Feltzing S, Korn A, Boland W (2012) 4MOST: 4-metre multi-object spectroscopic telescope. In: Society of Photo-Optical Instrumentation Engineers (SPIE) Conference Series, Society of Photo-Optical Instrumentation Engineers (SPIE) Conference Series, vol 8446, DOI 10.1117/12.926239, 1206.6885

De Lucia G, Springel V, White SDM, Croton D, Kauffmann G (2006) The formation history of elliptical galaxies. MNRAS 366:499–509, DOI 10.1111/j.1365-2966.2005.09879.x, astro-ph/0509725

Degraf C, Di Matteo T, Springel V (2010) Faint-end quasar luminosity functions from cosmological hydrodynamic simulations. MNRAS 402:1927–1936, 0910.1843

Del Moro A, Alexander DM, Mullaney JR, Daddi E, Pannella M, Bauer FE, Pope A, Dickinson M, Elbaz D, Barthel PD, Garrett MA, Brandt WN, Charmandaris V, Chary RR, Dasyra K, Gilli R, Hickox RC, Hwang HS, Ivison RJ, Juneau S, Le Floc'h E, Luo B, Morrison GE, Rovilos E, Sargent MT, Xue YQ (2013) GOODS-Herschel: radio-excess signature of hidden AGN activity in distant star-forming galaxies. Astron Astrophys 549:A59, 1210.2521

Del Moro A, Mullaney JR, Alexander DM, Comastri A, Bauer FE, Treister E, Stern D, Civano F, Ranalli P, Vignali C, Aird JA, Ballantyne DR, Baloković M, Boggs SE, Brandt WN, Christensen FE, Craig WW, Gandhi P, Gilli R, Hailey CJ, Harrison FA, Hickox RC, LaMassa SM, Lansbury GB, Luo B, Puccetti S, Urry M, Zhang WW (2014) NuSTAR J033202-2746.8: Direct Constraints on the Compton Reflection in a Heavily Obscured Quasar at $z \approx 2$. Astrophys J 786:16, 1403.2491

D'Elia V, Fiore F, Elvis M, Cappi M, Mathur S, Mazzotta P, Falco E, Cocchia F (2004) The faint X-ray source population near 3C 295. Astron Astrophys 422:11–21, astro-ph/0403401

Della Ceca R, Caccianiga A, Severgnini P, Maccacaro T, Brunner H, Carrera

FJ, Cocchia F, Mateos S, Page MJ, Tedds JA (2008) The cosmological properties of AGN in the XMM-Newton Hard Bright Survey. Astron Astrophys 487:119–130, 0805.1919

Delvecchio I, Gruppioni C, Pozzi F, Berta S, Zamorani G, Cimatti A, Lutz D, Scott D, Vignali C, Cresci G, Feltre A, Cooray A, Vaccari M, Fritz J, Le Floc'h E, Magnelli B, Popesso P, Oliver S, Bock J, Carollo M, Contini T, Le Févre O, Lilly S, Mainieri V, Renzini A, Scodeggio M (2014) Tracing the cosmic growth of supermassive black holes to $z \sim 3$ with Herschel. MNRAS 439:2736–2754, DOI 10.1093/mnras/stu130, 1401.4503

Dewdney PE, Hall PJ, Schilizzi RT, Lazio TJLW (2009) The Square Kilometre Array. IEEE Proceedings 97:1482–1496, DOI 10.1109/JPROC.2009.2021005

Digby-North JA, Nandra K, Laird ES, Steidel CC, Georgakakis A, Bogosavljević M, Erb DK, Shapley AE, Reddy NA, Aird J (2010) Excess AGN activity in the z = 2.30 Protocluster in HS 1700+64. MNRAS 407:846–853, DOI 10.1111/j.1365-2966.2010.16977.x, 1005.1833

Done C (2010) Observational characteristics of accretion onto black holes. ArXiv e-prints 1008.2287

Donley JL, Rieke GH, Rigby JR, Pérez-González PG (2005) Unveiling a Population of AGNs Not Detected in X-Rays. Astrophys J 634:169–182, astro-ph/0507676

Donley JL, Rieke GH, Pérez-González PG, Rigby JR, Alonso-Herrero A (2007) Spitzer Power-Law Active Galactic Nucleus Candidates in the Chandra Deep Field-North. Astrophys J 660:167–190, astro-ph/0701698

Donley JL, Rieke GH, Pérez-González PG, Barro G (2008) Spitzer's Contribution to the AGN Population. Astrophys J 687:111–132, 0806.4610

Donley JL, Koekemoer AM, Brusa M, Capak P, Cardamone CN, Civano F, Ilbert O, Impey CD, Kartaltepe JS, Miyaji T, Salvato M, Sanders DB, Trump JR, Zamorani G (2012) Identifying Luminous Active Galactic Nuclei in Deep Surveys: Revised IRAC Selection Criteria. Astrophys J 748:142, 1201.3899

Draper AR, Ballantyne DR (2010) The Evolution and Eddington Ratio Distribution of Compton Thick Active Galactic Nuclei. Astrophys J Let 715:L99–L103, 1004.0690

Dwelly T, Page MJ (2006) The distribution of absorption in AGN detected in the XMM-Newton observations of the CDFS. MNRAS 372:1755–1775, astro-ph/0608479

Eastman J, Martini P, Sivakoff G, Kelson DD, Mulchaey JS, Tran KV (2007) First Measurement of a Rapid Increase in the AGN Fraction in High-Redshift Clusters of Galaxies. Astrophys J Let 664:L9–L12, DOI 10.1086/520577, 0706.0209

Ebrero J, Carrera FJ, Page MJ, Silverman JD, Barcons X, Ceballos MT, Corral A, Della Ceca R, Watson MG (2009) The XMM-Newton serendipitous survey. VI. The X-ray luminosity function. Astron Astrophys 493:55–69, 0811.1450

Eckart ME, Stern D, Helfand DJ, Harrison FA, Mao PH, Yost SA (2006) The Serendipitous Extragalactic X-Ray Source Identification (SEXSI) Program.

III. Optical Spectroscopy. Astrophys J Supp 165:19–56, astro-ph/0603556
Eddington AS (1922) Society Business: Introductory address delivered on the occasion of the Society's centenary celebration. MNRAS 82:432
Ehlert S, Allen SW, Brandt WN, Canning REA, Luo B, Mantz A, Morris RG, von der Linden A, Xue YQ (2014a) X-ray bright active galactic nuclei in massive galaxy clusters III: New insights into the triggering mechanisms of cluster AGN. ArXiv e-prints 1407.8181
Ehlert S, von der Linden A, Allen SW, Brandt WN, Xue YQ, Luo B, Mantz A, Morris RG, Applegate D, Kelly P (2014b) X-ray bright active galactic nuclei in massive galaxy clusters - II. The fraction of galaxies hosting active nuclei. MNRAS 437:1942–1949, DOI 10.1093/mnras/stt2025, 1310.5711
Elbaz D, Cesarsky CJ, Chanial P, Aussel H, Franceschini A, Fadda D, Chary RR (2002) The bulk of the cosmic infrared background resolved by ISO-CAM. Astron Astrophys 384:848–865, DOI 10.1051/0004-6361:20020106, astro-ph/0201328
Elbaz D, Dickinson M, Hwang HS, Díaz-Santos T, Magdis G, Magnelli B, Le Borgne D, Galliano F, Pannella M, Chanial P, Armus L, Charmandaris V, Daddi E, Aussel H, Popesso P, Kartaltepe J, Altieri B, Valtchanov I, Coia D, Dannerbauer H, Dasyra K, Leiton R, Mazzarella J, Alexander DM, Buat V, Burgarella D, Chary RR, Gilli R, Ivison RJ, Juneau S, Le Floc'h E, Lutz D, Morrison GE, Mullaney JR, Murphy E, Pope A, Scott D, Brodwin M, Calzetti D, Cesarsky C, Charlot S, Dole H, Eisenhardt P, Ferguson HC, Förster Schreiber N, Frayer D, Giavalisco M, Huynh M, Koekemoer AM, Papovich C, Reddy N, Surace C, Teplitz H, Yun MS, Wilson G (2011) GOODS-Herschel: an infrared main sequence for star-forming galaxies. Astron Astrophys 533:A119, DOI 10.1051/0004-6361/201117239, 1105.2537
Elitzur M, Shlosman I (2006) The AGN-obscuring Torus: The End of the "Doughnut" Paradigm? Astrophys J Let 648:L101–L104, astro-ph/0605686
Elvis M, Wilkes BJ, McDowell JC, Green RF, Bechtold J, Willner SP, Oey MS, Polomski E, Cutri R (1994) Atlas of quasar energy distributions. Astrophys J Supp 95:1–68, DOI 10.1086/192093
Elvis M, Civano F, Vignali C, Puccetti S, Fiore F, Cappelluti N, Aldcroft TL, Fruscione A, Zamorani G, Comastri A, Brusa M, Gilli R, Miyaji T, Damiani F, Koekemoer AM, Finoguenov A, Brunner H, Urry CM, Silverman J, Mainieri V, Hasinger G, Griffiths R, Carollo CM, Hao H, Guzzo L, Blain A, Calzetti D, Carilli C, Capak P, Ettori S, Fabbiano G, Impey C, Lilly S, Mobasher B, Rich M, Salvato M, Sanders DB, Schinnerer E, Scoville N, Shopbell P, Taylor JE, Taniguchi Y, Volonteri M (2009) The Chandra COSMOS Survey. I. Overview and Point Source Catalog. Astrophys J Supp 184:158–171, 0903.2062
Elvis M, Hao H, Civano F, Brusa M, Salvato M, Bongiorno A, Capak P, Zamorani G, Comastri A, Jahnke K, Lusso E, Mainieri V, Trump JR, Ho LC, Aussel H, Cappelluti N, Cisternas M, Frayer D, Gilli R, Hasinger G, Huchra JP, Impey CD, Koekemoer AM, Lanzuisi G, Le Floc'h E, Lilly SJ, Liu Y, McCarthy P, McCracken HJ, Merloni A, Roeser HJ, Sanders DB,

Sargent M, Scoville N, Schinnerer E, Schiminovich D, Silverman J, Taniguchi Y, Vignali C, Urry CM, Zamojski MA, Zatloukal M (2012) Spectral Energy Distributions of Type 1 Active Galactic Nuclei in the COSMOS Survey. I. The XMM-COSMOS Sample. Astrophys J 759:6, 1209.1478

Evans IN, Primini FA, Glotfelty KJ, Anderson CS, Bonaventura NR, Chen JC, Davis JE, Doe SM, Evans JD, Fabbiano G, Galle EC, Gibbs DG II, Grier JD, Hain RM, Hall DM, Harbo PN, (Helen He X, Houck JC, Karovska M, Kashyap VL, Lauer J, McCollough ML, McDowell JC, Miller JB, Mitschang AW, Morgan DL, Mossman AE, Nichols JS, Nowak MA, Plummer DA, Refsdal BL, Rots AH, Siemiginowska A, Sundheim BA, Tibbetts MS, Van Stone DW, Winkelman SL, Zografou P (2010) The Chandra Source Catalog. Astrophys J Supp 189:37, 1005.4665

Faber SM, Willmer CNA, Wolf C, Koo DC, Weiner BJ, Newman JA, Im M, Coil AL, Conroy C, Cooper MC, Davis M, Finkbeiner DP, Gerke BF, Gebhardt K, Groth EJ, Guhathakurta P, Harker J, Kaiser N, Kassin S, Kleinheinrich M, Konidaris NP, Kron RG, Lin L, Luppino G, Madgwick DS, Meisenheimer K, Noeske KG, Phillips AC, Sarajedini VL, Schiavon RP, Simard L, Szalay AS, Vogt NP, Yan R (2007) Galaxy Luminosity Functions to z˜1 from DEEP2 and COMBO-17: Implications for Red Galaxy Formation. Astrophys J 665:265–294, astro-ph/0506044

Fabian AC (2006) A short introduction to broad and variable iron lines around black holes. Astronomische Nachrichten 327:943

Fabian AC (2012) Observational Evidence of Active Galactic Nuclei Feedback. Ann Rev Astron Astrophys 50:455–489, DOI 10.1146/annurev-astro-081811-125521, 1204.4114

Fabian AC, Iwasawa K (1999) The mass density in black holes inferred from the X-ray background. MNRAS 303:L34–L36, DOI 10.1046/j.1365-8711.1999.02404.x, astro-ph/9901121

Fadda D, Flores H, Hasinger G, Franceschini A, Altieri B, Cesarsky CJ, Elbaz D, Ferrando P (2002) The AGN contribution to mid-infrared surveys. X-ray counterparts of the mid-IR sources in the Lockman Hole and HDF-N. Astron Astrophys 383:838–853, DOI 10.1051/0004-6361:20011842

Fan L, Fang G, Chen Y, Li J, Lv X, Knudsen KK, Kong X (2014) Structure and Morphology of X-Ray-selected Active Galactic Nucleus Hosts at $1 < z < 3$ in the CANDELS-COSMOS Field. Astrophys J Let 784:L9, DOI 10.1088/2041-8205/784/1/L9, 1402.6470

Fanali R, Caccianiga A, Severgnini P, Della Ceca R, Marchese E, Carrera FJ, Corral A, Mateos S (2013) Studying the relationship between X-ray emission and accretion in AGN using the XMM-Newton Bright Serendipitous Survey. MNRAS 433:648–658, 1305.0564

Fanidakis N, Baugh CM, Benson AJ, Bower RG, Cole S, Done C, Frenk CS, Hickox RC, Lacey C, Del P Lagos C (2012) The evolution of active galactic nuclei across cosmic time: what is downsizing? MNRAS 419:2797–2820, 1011.5222

Fazio GG, Hora JL, Allen LE, Ashby MLN, Barmby P, Deutsch LK, Huang JS, Kleiner S, Marengo M, Megeath ST, Melnick GJ, Pahre MA, Patten

BM, Polizotti J, Smith HA, Taylor RS, Wang Z, Willner SP, Hoffmann WF, Pipher JL, Forrest WJ, McMurty CW, McCreight CR, McKelvey ME, McMurray RE, Koch DG, Moseley SH, Arendt RG, Mentzell JE, Marx CT, Losch P, Mayman P, Eichhorn W, Krebs D, Jhabvala M, Gezari DY, Fixsen DJ, Flores J, Shakoorzadeh K, Jungo R, Hakun C, Workman L, Karpati G, Kichak R, Whitley R, Mann S, Tollestrup EV, Eisenhardt P, Stern D, Gorjian V, Bhattacharya B, Carey S, Nelson BO, Glaccum WJ, Lacy M, Lowrance PJ, Laine S, Reach WT, Stauffer JA, Surace JA, Wilson G, Wright EL, Hoffman A, Domingo G, Cohen M (2004) The Infrared Array Camera (IRAC) for the Spitzer Space Telescope. Astrophys J Supp 154:10–17, DOI 10.1086/422843, astro-ph/0405616

Finke JD, Razzaque S, Dermer CD (2010) Modeling the Extragalactic Background Light from Stars and Dust. Astrophys J 712:238–249, DOI 10.1088/0004-637X/712/1/238, 0905.1115

Fiore F, La Franca F, Giommi P, Elvis M, Matt G, Comastri A, Molendi S, Gioia I (1999) The contribution of faint active galactic nuclei to the hard X-ray background. MNRAS 306:L55–L60, astro-ph/9903447

Fiore F, Brusa M, Cocchia F, Baldi A, Carangelo N, Ciliegi P, Comastri A, La Franca F, Maiolino R, Matt G, Molendi S, Mignoli M, Perola GC, Severgnini P, Vignali C (2003) The HELLAS2XMM survey. IV. Optical identifications and the evolution of the accretion luminosity in the Universe. Astron Astrophys 409:79–90, astro-ph/0306556

Fiore F, Grazian A, Santini P, Puccetti S, Brusa M, Feruglio C, Fontana A, Giallongo E, Comastri A, Gruppioni C, Pozzi F, Zamorani G, Vignali C (2008) Unveiling Obscured Accretion in the Chandra Deep Field-South. Astrophys J 672:94–101, 0705.2864

Fiore F, Puccetti S, Brusa M, Salvato M, Zamorani G, Aldcroft T, Aussel H, Brunner H, Capak P, Cappelluti N, Civano F, Comastri A, Elvis M, Feruglio C, Finoguenov A, Fruscione A, Gilli R, Hasinger G, Koekemoer A, Kartaltepe J, Ilbert O, Impey C, Le Floc'h E, Lilly S, Mainieri V, Martinez-Sansigre A, McCracken HJ, Menci N, Merloni A, Miyaji T, Sanders DB, Sargent M, Schinnerer E, Scoville N, Silverman J, Smolcic V, Steffen A, Santini P, Taniguchi Y, Thompson D, Trump JR, Vignali C, Urry M, Yan L (2009) Chasing Highly Obscured QSOs in the COSMOS Field. Astrophys J 693:447–462, 0810.0720

Fiore F, Puccetti S, Grazian A, Menci N, Shankar F, Santini P, Piconcelli E, Koekemoer AM, Fontana A, Boutsia K, Castellano M, Lamastra A, Malacaria C, Feruglio C, Mathur S, Miller N, Pannella M (2012a) Faint high-redshift AGN in the Chandra deep field south: the evolution of the AGN luminosity function and black hole demography. Astron Astrophys 537:A16, 1109.2888

Fiore F, Puccetti S, Mathur S (2012b) Demography of High-Redshift AGN. Advances in Astronomy 2012:271502, 1109.4586

Flaugher B (2005) The Dark Energy Survey. International Journal of Modern Physics A 20:3121–3123, DOI 10.1142/S0217751X05025917

Fontanot F, Cristiani S, Monaco P, Nonino M, Vanzella E, Brandt WN,

Grazian A, Mao J (2007) The luminosity function of high-redshift quasi-stellar objects. A combined analysis of GOODS and SDSS. Astron Astrophys 461:39–48, astro-ph/0608664

Fontanot F, De Lucia G, Monaco P, Somerville RS, Santini P (2009) The many manifestations of downsizing: hierarchical galaxy formation models confront observations. MNRAS 397:1776–1790, 0901.1130

Gabor JM, Bournaud F (2013) Simulations of supermassive black hole growth in high-redshift disc galaxies. MNRAS 434:606–620, DOI 10.1093/mnras/stt1046, 1306.2954

Gabor JM, Impey CD, Jahnke K, Simmons BD, Trump JR, Koekemoer AM, Brusa M, Cappelluti N, Schinnerer E, Smolčić V, Salvato M, Rhodes JD, Mobasher B, Capak P, Massey R, Leauthaud A, Scoville N (2009) Active Galactic Nucleus Host Galaxy Morphologies in COSMOS. Astrophys J 691:705–722, DOI 10.1088/0004-637X/691/1/705, 0809.0309

Gandhi P, Crawford CS, Fabian AC, Johnstone RM (2004) Powerful, obscured active galactic nuclei among X-ray hard, optically dim serendipitous Chandra sources. MNRAS 348:529–550, DOI 10.1111/j.1365-2966.2004.07341.x, astro-ph/0310772

Gandhi P, Garcet O, Disseau L, Pacaud F, Pierre M, Gueguen A, Alloin D, Chiappetti L, Gosset E, Maccagni D, Surdej J, Valtchanov I (2006) The XMM large scale structure survey: properties and two-point angular correlations of point-like sources. Astron Astrophys 457:393–404, DOI 10.1051/0004-6361:20065284, astro-ph/0607135

Gardner JP, Mather JC, Clampin M, Doyon R, Greenhouse MA, Hammel HB, Hutchings JB, Jakobsen P, Lilly SJ, Long KS, Lunine JI, McCaughrean MJ, Mountain M, Nella J, Rieke GH, Rieke MJ, Rix HW, Smith EP, Sonneborn G, Stiavelli M, Stockman HS, Windhorst RA, Wright GS (2006) The James Webb Space Telescope. Space Sci. Rev. 123:485–606, DOI 10.1007/s11214-006-8315-7, astro-ph/0606175

Garmire GP, Bautz MW, Ford PG, Nousek JA, Ricker GR Jr (2003) Advanced CCD imaging spectrometer (ACIS) instrument on the Chandra X-ray Observatory. In: Truemper JE, Tananbaum HD (eds) X-Ray and Gamma-Ray Telescopes and Instruments for Astronomy., Society of Photo-Optical Instrumentation Engineers (SPIE) Conference Series, vol 4851, pp 28–44

Gebhardt K, Bender R, Bower G, Dressler A, Faber SM, Filippenko AV, Green R, Grillmair C, Ho LC, Kormendy J, Lauer TR, Magorrian J, Pinkney J, Richstone D, Tremaine S (2000) A Relationship between Nuclear Black Hole Mass and Galaxy Velocity Dispersion. Astrophys J Let 539:L13–L16

Gehrels N, Spergel DN (2014) Wide-Field InfraRed Survey Telescope (WFIRST) Mission and Synergies with LISA and LIGO-Virgo. ArXiv e-prints 1411.0313

Gehrels N, Chincarini G, Giommi P, Mason KO, Nousek JA, Wells AA, White NE, Barthelmy SD, Burrows DN, Cominsky LR, Hurley KC, Marshall FE, Mészáros P, Roming PWA, Angelini L, Barbier LM, Belloni T, Campana S, Caraveo PA, Chester MM, Citterio O, Cline TL, Cropper MS, Cummings JR, Dean AJ, Feigelson ED, Fenimore EE, Frail DA, Fruchter AS, Garmire

GP, Gendreau K, Ghisellini G, Greiner J, Hill JE, Hunsberger SD, Krimm HA, Kulkarni SR, Kumar P, Lebrun F, Lloyd-Ronning NM, Markwardt CB, Mattson BJ, Mushotzky RF, Norris JP, Osborne J, Paczynski B, Palmer DM, Park HS, Parsons AM, Paul J, Rees MJ, Reynolds CS, Rhoads JE, Sasseen TP, Schaefer BE, Short AT, Smale AP, Smith IA, Stella L, Tagliaferri G, Takahashi T, Tashiro M, Townsley LK, Tueller J, Turner MJL, Vietri M, Voges W, Ward MJ, Willingale R, Zerbi FM, Zhang WW (2004) The Swift Gamma-Ray Burst Mission. Astrophys J 611:1005–1020

Genzel R, Tacconi LJ, Gracia-Carpio J, Sternberg A, Cooper MC, Shapiro K, Bolatto A, Bouché N, Bournaud F, Burkert A, Combes F, Comerford J, Cox P, Davis M, Schreiber NMF, Garcia-Burillo S, Lutz D, Naab T, Neri R, Omont A, Shapley A, Weiner B (2010) A study of the gas-star formation relation over cosmic time. MNRAS 407:2091–2108, DOI 10.1111/j.1365-2966.2010.16969.x, 1003.5180

Georgakakis A, Gerke BF, Nandra K, Laird ES, Coil AL, Cooper MC, Newman JA (2008) X-ray selected AGN in groups at redshifts z ˜ 1. MNRAS 391:183–189, DOI 10.1111/j.1365-2966.2008.13649.x, 0807.2240

Georgakakis A, Coil AL, Laird ES, Griffith RL, Nandra K, Lotz JM, Pierce CM, Cooper MC, Newman JA, Koekemoer AM (2009) Host galaxy morphologies of X-ray selected AGN: assessing the significance of different black hole fuelling mechanisms to the accretion density of the Universe at z ˜ 1. MNRAS 397:623–633, DOI 10.1111/j.1365-2966.2009.14951.x, 0904.3747

Georgakakis A, Coil AL, Willmer CNA, Nandra K, Kocevski DD, Cooper MC, Rosario DJ, Koo DC, Trump JR, Juneau S (2011) Observational constraints on the physics behind the evolution of active galactic nuclei since $z \sim 1$. MNRAS 418:2590–2603, DOI 10.1111/j.1365-2966.2011.19650.x, 1109.0287

Georgakakis A, Mountrichas G, Salvato M, Rosario D, Pérez-González PG, Lutz D, Nandra K, Coil A, Cooper MC, Newman JA, Berta S, Magnelli B, Popesso P, Pozzi F (2014a) Large-scale clustering measurements with photometric redshifts: comparing the dark matter haloes of X-ray AGN, star-forming and passive galaxies at z ≈ 1. MNRAS 443:3327–3340, DOI 10.1093/mnras/stu1326, 1407.1863

Georgakakis A, Pérez-González PG, Fanidakis N, Salvato M, Aird J, Messias H, Lotz JM, Barro G, Hsu LT, Nandra K, Rosario D, Cooper MC, Kocevski DD, Newman JA (2014b) Investigating evidence for different black hole accretion modes since redshift $z \leq 1$. MNRAS 440:339–352, DOI 10.1093/mnras/stu236, 1402.2277

Georgantopoulos I (2013) Recent Developments in the Search for Compton-Thick AGN. International Journal of Modern Physics Conference Series 23:1–10, 1204.2173

Georgantopoulos I, Dasyra KM, Rovilos E, Pope A, Wu Y, Dickinson M, Comastri A, Gilli R, Elbaz D, Armus L, Akylas A (2011) X-ray observations of highly obscured $\tau_{9.7m} > 1$ sources: an efficient method for selecting Compton-thick AGN? Astron Astrophys 531:A116, 1105.1441

Giallongo E, Menci N, Fiore F, Castellano M, Fontana A, Grazian A, Pentericci L (2012) Active Galactic Nuclei as Main Contributors to the Ultraviolet

Ionizing Emissivity at High Redshifts: Predictions from a Λ-CDM Model with Linked AGN/Galaxy Evolution. Astrophys J 755:124, 1206.2950

Gibson RR, Brandt WN (2012) The X-Ray Variability of a Large, Serendipitous Sample of Spectroscopic Quasars. Astrophys J 746:54, 1110.5341

Gibson RR, Brandt WN, Schneider DP (2008) Are Optically Selected Quasars Universally X-Ray Luminous? X-Ray-UV Relations in Sloan Digital Sky Survey Quasars. Astrophys J 685:773–786, 0808.2603

Gilfanov M, Merloni A (2014) Observational Appearance of Black Holes in X-Ray Binaries and AGN. Space Sci. Rev. 183:121–148

Gilli R (2004) The X-ray background and the deep X-ray surveys. Advances in Space Research 34:2470–2477, astro-ph/0303115

Gilli R, Comastri A, Hasinger G (2007) The synthesis of the cosmic X-ray background in the Chandra and XMM-Newton era. Astron Astrophys 463:79–96, DOI 10.1051/0004-6361:20066334, astro-ph/0610939

Gilli R, Zamorani G, Miyaji T, Silverman J, Brusa M, Mainieri V, Cappelluti N, Daddi E, Porciani C, Pozzetti L, Civano F, Comastri A, Finoguenov A, Fiore F, Salvato M, Vignali C, Hasinger G, Lilly S, Impey C, Trump J, Capak P, McCracken H, Scoville N, Taniguchi Y, Carollo CM, Contini T, Kneib JP, Le Fevre O, Renzini A, Scodeggio M, Bardelli S, Bolzonella M, Bongiorno A, Caputi K, Cimatti A, Coppa G, Cucciati O, de La Torre S, de Ravel L, Franzetti P, Garilli B, Iovino A, Kampczyk P, Knobel C, Kovač K, Lamareille F, Le Borgne JF, Le Brun V, Maier C, Mignoli M, Pellò R, Peng Y, Perez Montero E, Ricciardelli E, Tanaka M, Tasca L, Tresse L, Vergani D, Zucca E, Abbas U, Bottini D, Cappi A, Cassata P, Fumana M, Guzzo L, Leauthaud A, Maccagni D, Marinoni C, Memeo P, Meneux B, Oesch P, Scaramella R, Walcher J (2009) The spatial clustering of X-ray selected AGN in the XMM-COSMOS field. Astron Astrophys 494:33–48, DOI 10.1051/0004-6361:200810821, 0810.4769

Gilli R, Su J, Norman C, Vignali C, Comastri A, Tozzi P, Rosati P, Stiavelli M, Brandt WN, Xue YQ, Luo B, Castellano M, Fontana A, Fiore F, Mainieri V, Ptak A (2011) A Compton-thick Active Galactic Nucleus at z ˜ 5 in the 4 Ms Chandra Deep Field South. Astrophys J Let 730:L28, 1102.4714

Goulding AD, Forman WR, Hickox RC, Jones C, Kraft R, Murray SS, Vikhlinin A, Coil AL, Cooper MC, Davis M, Newman JA (2012) The Chandra X-Ray Point-source Catalog in the DEEP2 Galaxy Redshift Survey Fields. Astrophys J Supp 202:6, 1206.6884

Goulding AD, Forman WR, Hickox RC, Jones C, Murray SS, Paggi A, Ashby MLN, Coil AL, Cooper MC, Huang JS, Kraft R, Newman JA, Weiner BJ, Willner SP (2014) Tracing the Evolution of Active Galactic Nuclei Host Galaxies over the Last 9 Gyr of Cosmic Time. Astrophys J 783:40, DOI 10.1088/0004-637X/783/1/40, 1310.8298

Green PJ, Aldcroft TL, Richards GT, Barkhouse WA, Constantin A, Haggard D, Karovska M, Kim DW, Kim M, Vikhlinin A, Anderson SF, Mossman A, Kashyap V, Myers AC, Silverman JD, Wilkes BJ, Tananbaum H (2009) A Full Year's Chandra Exposure on Sloan Digital Sky Survey Quasars from the Chandra Multiwavelength Project. Astrophys J 690:644–669, 0809.1058

Grissom RL, Ballantyne DR, Wise JH (2014) On the contribution of active galactic nuclei to reionization. Astron Astrophys 561:A90, 1312.1358

Grogin NA, Conselice CJ, Chatzichristou E, Alexander DM, Bauer FE, Hornschemeier AE, Jogee S, Koekemoer AM, Laidler VG, Livio M, Lucas RA, Paolillo M, Ravindranath S, Schreier EJ, Simmons BD, Urry CM (2005) AGN Host Galaxies at z˜0.4-1.3: Bulge-dominated and Lacking Merger-AGN Connection. Astrophys J Let 627:L97–L100, DOI 10.1086/432256, arXiv:astro-ph/0507091

Gunn KF, Shanks T (1999) Implications of an Obscured AGN Model for the X-ray Background at Sub-mm and Far Infra-Red Wavelengths. ArXiv Astrophysics e-prints astro-ph/9909089

Haiman Z, Loeb A (1999) X-Ray Emission from the First Quasars. Astrophys J Let 521:L9–L12, astro-ph/9904340

Hambly NC, MacGillivray HT, Read MA, Tritton SB, Thomson EB, Kelly BD, Morgan DH, Smith RE, Driver SP, Williamson J, Parker QA, Hawkins MRS, Williams PM, Lawrence A (2001) The SuperCOSMOS Sky Survey - I. Introduction and description. MNRAS 326:1279–1294, DOI 10.1111/j.1365-8711.2001.04660.x, astro-ph/0108286

Hao H, Elvis M, Civano F, Zamorani G, Ho LC, Comastri A, Brusa M, Bongiorno A, Merloni A, Trump JR, Salvato M, Impey CD, Koekemoer AM, Lanzuisi G, Celotti A, Jahnke K, Vignali C, Silverman JD, Urry CM, Schawinski K, Capak P (2014) Spectral energy distributions of type 1 AGN in XMM-COSMOS - II. Shape evolution. MNRAS 438:1288–1304, 1210.3033

Harrison CM, Alexander DM, Mullaney JR, Altieri B, Coia D, Charmandaris V, Daddi E, Dannerbauer H, Dasyra K, Del Moro A, Dickinson M, Hickox RC, Ivison RJ, Kartaltepe J, Le Floc'h E, Leiton R, Magnelli B, Popesso P, Rovilos E, Rosario D, Swinbank AM (2012) No Clear Submillimeter Signature of Suppressed Star Formation among X-Ray Luminous Active Galactic Nuclei. Astrophys J Let 760:L15, DOI 10.1088/2041-8205/760/1/L15, 1209.3016

Harrison FA, Eckart ME, Mao PH, Helfand DJ, Stern D (2003) The Serendipitous Extragalactic X-Ray Source Identification Program. I. Characteristics of the Hard X-Ray Sample. Astrophys J 596:944–956, astro-ph/0306610

Harrison FA, Craig WW, Christensen FE, Hailey CJ, Zhang WW, Boggs SE, Stern D, Cook WR, Forster K, Giommi P, Grefenstette BW, Kim Y, Kitaguchi T, Koglin JE, Madsen KK, Mao PH, Miyasaka H, Mori K, Perri M, Pivovaroff MJ, Puccetti S, Rana VR, Westergaard NJ, Willis J, Zoglauer A, An H, Bachetti M, Barrière NM, Bellm EC, Bhalerao V, Brejnholt NF, Fuerst F, Liebe CC, Markwardt CB, Nynka M, Vogel JK, Walton DJ, Wik DR, Alexander DM, Cominsky LR, Hornschemeier AE, Hornstrup A, Kaspi VM, Madejski GM, Matt G, Molendi S, Smith DM, Tomsick JA, Ajello M, Ballantyne DR, Baloković M, Barret D, Bauer FE, Blandford RD, Brandt WN, Brenneman LW, Chiang J, Chakrabarty D, Chenevez J, Comastri A, Dufour F, Elvis M, Fabian AC, Farrah D, Fryer CL, Gotthelf EV, Grindlay JE, Helfand DJ, Krivonos R, Meier DL, Miller JM, Natalucci L, Ogle P, Ofek EO, Ptak A, Reynolds SP, Rigby JR, Tagliaferri G, Thorsett SE, Treister

E, Urry CM (2013) The Nuclear Spectroscopic Telescope Array (NuSTAR) High-energy X-Ray Mission. Astrophys J 770:103, 1301.7307
Hartwick FDA, Schade D (1990) The space distribution of quasars. Ann Rev Astron Astrophys 28:437–489
Hasinger G (2008) Absorption properties and evolution of active galactic nuclei. Astron Astrophys 490:905–922, 0808.0260
Hasinger G, Zamorani G (2000) The X-Ray Background and the ROSAT Deep Surveys. In: Gursky H, Ruffini R, Stella L (eds) Exploring the Universe, pp 119–138
Hasinger G, Burg R, Giacconi R, Schmidt M, Trumper J, Zamorani G (1998) The ROSAT Deep Survey. I. X-ray sources in the Lockman Field. Astron Astrophys 329:482–494, astro-ph/9709142
Hasinger G, Miyaji T, Schmidt M (2005) Luminosity-dependent evolution of soft X-ray selected AGN. New Chandra and XMM-Newton surveys. Astron Astrophys 441:417–434, astro-ph/0506118
Hauser MG, Dwek E (2001) The Cosmic Infrared Background: Measurements and Implications. Ann Rev Astron Astrophys 39:249–307, DOI 10.1146/annurev.astro.39.1.249, astro-ph/0105539
Heckman TM, Kauffmann G, Brinchmann J, Charlot S, Tremonti C, White SDM (2004) Present-Day Growth of Black Holes and Bulges: The Sloan Digital Sky Survey Perspective. Astrophys J 613:109–118, astro-ph/0406218
Hernán-Caballero A, Alonso-Herrero A, Pérez-González PG, Barro G, Aird J, Ferreras I, Cava A, Cardiel N, Esquej P, Gallego J, Nandra K, Rodríguez-Zaurín J (2014) Higher prevalence of X-ray selected AGN in intermediate-age galaxies up to $z \sim 1$. MNRAS 443:3538–3549, DOI 10.1093/mnras/stu1413, 1404.2056
Hewett PC, Foltz CB (1994) Quasar surveys. PASP 106:113–130
Hickox RC (2009) Black Holes through Cosmic Time. Chandra News 16:3
Hickox RC, Markevitch M (2006) Absolute Measurement of the Unresolved Cosmic X-Ray Background in the 0.5-8 keV Band with Chandra. Astrophys J 645:95–114, astro-ph/0512542
Hickox RC, Jones C, Forman WR, Murray SS, Brodwin M, Brown MJI, Eisenhardt PR, Stern D, Kochanek CS, Eisenstein D, Cool RJ, Jannuzi BT, Dey A, Brand K, Gorjian V, Caldwell N (2007) A Large Population of Mid-Infrared-selected, Obscured Active Galaxies in the Boötes Field. Astrophys J 671:1365–1387, 0708.3678
Hickox RC, Jones C, Forman WR, Murray SS, Kochanek CS, Eisenstein D, Jannuzi BT, Dey A, Brown MJI, Stern D, Eisenhardt PR, Gorjian V, Brodwin M, Narayan R, Cool RJ, Kenter A, Caldwell N, Anderson ME (2009) Host Galaxies, Clustering, Eddington Ratios, and Evolution of Radio, X-Ray, and Infrared-Selected AGNs. Astrophys J 696:891–919, 0901.4121
Hickox RC, Myers AD, Brodwin M, Alexander DM, Forman WR, Jones C, Murray SS, Brown MJI, Cool RJ, Kochanek CS, Dey A, Jannuzi BT, Eisenstein D, Assef RJ, Eisenhardt PR, Gorjian V, Stern D, Le Floc'h E, Caldwell N, Goulding AD, Mullaney JR (2011) Clustering of Obscured and Unobscured Quasars in the Boötes Field: Placing Rapidly Growing Black Holes in

the Cosmic Web. Astrophys J 731:117, DOI 10.1088/0004-637X/731/2/117, 1102.4850

Hickox RC, Wardlow JL, Smail I, Myers AD, Alexander DM, Swinbank AM, Danielson ALR, Stott JP, Chapman SC, Coppin KEK, Dunlop JS, Gawiser E, Lutz D, van der Werf P, Weiß A (2012) The LABOCA survey of the Extended Chandra Deep Field-South: clustering of submillimetre galaxies. MNRAS 421:284–295, DOI 10.1111/j.1365-2966.2011.20303.x, 1112.0321

Hickox RC, Mullaney JR, Alexander DM, Chen CTJ, Civano FM, Goulding AD, Hainline KN (2014) Black Hole Variability and the Star Formation-Active Galactic Nucleus Connection: Do All Star-forming Galaxies Host an Active Galactic Nucleus? Astrophys J 782:9, DOI 10.1088/0004-637X/782/1/9, 1306.3218

Hiroi K, Ueda Y, Akiyama M, Watson MG (2012) Comoving Space Density and Obscured Fraction of High-redshift Active Galactic Nuclei in the Subaru/XMM-Newton Deep Survey. Astrophys J 758:49, 1208.5050

Hirschmann M, Somerville RS, Naab T, Burkert A (2012) Origin of the anti-hierarchical growth of black holes. MNRAS 426:237–257, 1206.6112

Hirschmann M, Dolag K, Saro A, Bachmann L, Borgani S, Burkert A (2014) Cosmological simulations of black hole growth: AGN luminosities and downsizing. MNRAS 442:2304–2324, 1308.0333

Hopkins PF, Richards GT, Hernquist L (2007) An Observational Determination of the Bolometric Quasar Luminosity Function. Astrophys J 654:731–753, DOI 10.1086/509629, arXiv:astro-ph/0605678

Hopkins PF, Hernquist L, Cox TJ, Kereš D (2008) A Cosmological Framework for the Co-Evolution of Quasars, Supermassive Black Holes, and Elliptical Galaxies. I. Galaxy Mergers and Quasar Activity. Astrophys J Supp 175:356–389, 0706.1243

Hopkins PF, Hickox R, Quataert E, Hernquist L (2009) Are most low-luminosity active galactic nuclei really obscured? MNRAS 398:333–349, 0901.2936

Hsu LT, Salvato M, Nandra K, Brusa M, Bender R, Buchner J, Donley JL, Kocevski DD, Guo Y, Hathi NP, Rangel C, Willner SP, Brightman M, Georgakakis A, Budavári T, Szalay AS, Ashby MLN, Barro G, Dahlen T, Faber SM, Ferguson HC, Galametz A, Grazian A, Grogin NA, Huang KH, Koekemoer AM, Lucas RA, McGrath E, Mobasher B, Peth M, Rosario DJ, Trump JR (2014) CANDELS/GOODS-S, CDFS, ECDFS: Photometric Redshifts For Normal and for X-Ray-Detected Galaxies. ArXiv e-prints 1409.7119

Huertas-Company M, Kaviraj S, Mei S, O'Connell RW, Windhorst R, Cohen SH, Hathi P, Koekemoer AM, Licitra R, Raichoor A, Rutkowski MJ (2014) Measuring galaxy morphology at $z > 1$. I - calibration of automated proxies. ArXiv e-prints 1406.1175

Hughes DH, Jáuregui Correa JC, Schloerb FP, Erickson N, Romero JG, Heyer M, Reynoso DH, Narayanan G, Perez-Grovas AS, Souccar K, Wilson G, Yun M (2010) The Large Millimeter Telescope. In: Society of Photo-Optical Instrumentation Engineers (SPIE) Conference Series, Society of Photo-Optical Instrumentation Engineers (SPIE) Conference Series, vol 7733, p 12, DOI

10.1117/12.857974

Hunt MP, Steidel CC, Adelberger KL, Shapley AE (2004) The Faint End of the QSO Luminosity Function at z=3. Astrophys J 605:625–630, astro-ph/0312041

Ilbert O, Salvato M, Le Floc'h E, Aussel H, Capak P, McCracken HJ, Mobasher B, Kartaltepe J, Scoville N, Sanders DB, Arnouts S, Bundy K, Cassata P, Kneib JP, Koekemoer A, Le Fèvre O, Lilly S, Surace J, Taniguchi Y, Tasca L, Thompson D, Tresse L, Zamojski M, Zamorani G, Zucca E (2010) Galaxy Stellar Mass Assembly Between $0.2 < z < 2$ from the S-COSMOS Survey. Astrophys J 709:644–663, DOI 10.1088/0004-637X/709/2/644, 0903.0102

Ivezic Z, Tyson JA, Abel B, Acosta E, Allsman R, AlSayyad Y, Anderson SF, Andrew J, Angel R, Angeli G, Ansari R, Antilogus P, Arndt KT, Astier P, Aubourg E, Axelrod T, Bard DJ, Barr JD, Barrau A, Bartlett JG, Bauman BJ, Beaumont S, Becker AC, Becla J, Beldica C, Bellavia S, Blanc G, Blandford RD, Bloom JS, Bogart J, Borne K, Bosch JF, Boutigny D, Brandt WN, Brown ME, Bullock JS, Burchat P, Burke DL, Cagnoli G, Calabrese D, Chandrasekharan S, Chesley S, Cheu EC, Chiang J, Claver CF, Connolly AJ, Cook KH, Cooray A, Covey KR, Cribbs C, Cui W, Cutri R, Daubard G, Daues G, Delgado F, Digel S, Doherty P, Dubois R, Dubois-Felsmann GP, Durech J, Eracleous M, Ferguson H, Frank J, Freemon M, Gangler E, Gawiser E, Geary JC, Gee P, Geha M, Gibson RR, Gilmore DK, Glanzman T, Goodenow I, Gressler WJ, Gris P, Guyonnet A, Hascall PA, Haupt J, Hernandez F, Hogan C, Huang D, Huffer ME, Innes WR, Jacoby SH, Jain B, Jee J, Jernigan JG, Jevremovic D, Johns K, Jones RL, Juramy-Gilles C, Juric M, Kahn SM, Kalirai JS, Kallivayalil N, Kalmbach B, Kantor JP, Kasliwal MM, Kessler R, Kirkby D, Knox L, Kotov I, Krabbendam VL, Krughoff S, Kubanek P, Kuczewski J, Kulkarni S, Lambert R, Le Guillou L, Levine D, Liang M, Lim K, Lintott C, Lupton RH, Mahabal A, Marshall P, Marshall S, May M, McKercher R, Migliore M, Miller M, Mills DJ, Monet DG, Moniez M, Neill DR, Nief J, Nomerotski A, Nordby M, O'Connor P, Oliver J, Olivier SS, Olsen K, Ortiz S, Owen RE, Pain R, Peterson JR, Petry CE, Pierfederici F, Pietrowicz S, Pike R, Pinto PA, Plante R, Plate S, Price PA, Prouza M, Radeka V, Rajagopal J, Rasmussen A, Regnault N, Ridgway ST, Ritz S, Rosing W, Roucelle C, Rumore MR, Russo S, Saha A, Sassolas B, Schalk TL, Schindler RH, Schneider DP, Schumacher G, Sebag J, Sembroski GH, Seppala LG, Shipsey I, Silvestri N, Smith JA, Smith RC, Strauss MA, Stubbs CW, Sweeney D, Szalay A, Takacs P, Thaler JJ, Van Berg R, Vanden Berk D, Vetter K, Virieux F, Xin B, Walkowicz L, Walter CW, Wang DL, Warner M, Willman B, Wittman D, Wolff SC, Wood-Vasey WM, Yoachim P, Zhan H, for the LSST Collaboration (2008) LSST: from Science Drivers to Reference Design and Anticipated Data Products. ArXiv e-prints 0805.2366

Iwasawa K, Gilli R, Vignali C, Comastri A, Brandt WN, Ranalli P, Vito F, Cappelluti N, Carrera FJ, Falocco S, Georgantopoulos I, Mainieri V, Paolillo M (2012) The XMM deep survey in the CDF-S. II. A 9-20 keV selection of heavily obscured active galaxies at $z > 1.7$. Astron Astrophys 546:A84,

1209.0916

Jahnke K, Bongiorno A, Brusa M, Capak P, Cappelluti N, Cisternas M, Civano F, Colbert J, Comastri A, Elvis M, Hasinger G, Ilbert O, Impey C, Inskip K, Koekemoer AM, Lilly S, Maier C, Merloni A, Riechers D, Salvato M, Schinnerer E, Scoville NZ, Silverman J, Taniguchi Y, Trump JR, Yan L (2009) Massive Galaxies in COSMOS: Evolution of Black Hole Versus Bulge Mass but not Versus Total Stellar Mass Over the Last 9 Gyr? Astrophys J Let 706:L215–L220, DOI 10.1088/0004-637X/706/2/L215, 0907.5199

Jansen F, Lumb D, Altieri B, Clavel J, Ehle M, Erd C, Gabriel C, Guainazzi M, Gondoin P, Much R, Munoz R, Santos M, Schartel N, Texier D, Vacanti G (2001) XMM-Newton observatory. I. The spacecraft and operations. Astron Astrophys 365:L1–L6

Jin C, Ward M, Done C (2012a) A combined optical and X-ray study of unobscured type 1 active galactic nuclei - III. Broad-band SED properties. MNRAS 425:907–929, 1109.2069

Jin C, Ward M, Done C, Gelbord J (2012b) A combined optical and X-ray study of unobscured type 1 active galactic nuclei - I. Optical spectra and spectral energy distribution modelling. MNRAS 420:1825–1847, DOI 10.1111/j.1365-2966.2011.19805.x

Juneau S, Dickinson M, Bournaud F, Alexander DM, Daddi E, Mullaney JR, Magnelli B, Kartaltepe JS, Hwang HS, Willner SP, Coil AL, Rosario DJ, Trump JR, Weiner BJ, Willmer CNA, Cooper MC, Elbaz D, Faber SM, Frayer DT, Kocevski DD, Laird ES, Monkiewicz JA, Nandra K, Newman JA, Salim S, Symeonidis M (2013) Widespread and Hidden Active Galactic Nuclei in Star-forming Galaxies at Redshift > 0.3. Astrophys J 764:176, 1211.6436

Juneau S, Bournaud F, Charlot S, Daddi E, Elbaz D, Trump JR, Brinchmann J, Dickinson M, Duc PA, Gobat R, Jean-Baptiste I, Le Floc'h É, Lehnert MD, Pacifici C, Pannella M, Schreiber C (2014) Active Galactic Nuclei Emission Line Diagnostics and the Mass-Metallicity Relation up to Redshift $z \sim 2$: The Impact of Selection Effects and Evolution. Astrophys J 788:88, 1403.6832

Just DW, Brandt WN, Shemmer O, Steffen AT, Schneider DP, Chartas G, Garmire GP (2007) The X-Ray Properties of the Most Luminous Quasars from the Sloan Digital Sky Survey. Astrophys J 665:1004–1022, 0705.3059

Kaaret P, Prestwich AH, Zezas A, Murray SS, Kim DW, Kilgard RE, Schlegel EM, Ward MJ (2001) Chandra High-Resolution Camera observations of the luminous X-ray source in the starburst galaxy M82. MNRAS 321:L29–L32, astro-ph/0009211

Kaiser N, Burgett W, Chambers K, Denneau L, Heasley J, Jedicke R, Magnier E, Morgan J, Onaka P, Tonry J (2010) The Pan-STARRS wide-field optical/NIR imaging survey. In: Society of Photo-Optical Instrumentation Engineers (SPIE) Conference Series, Society of Photo-Optical Instrumentation Engineers (SPIE) Conference Series, vol 7733, DOI 10.1117/12.859188

Kalfountzou E, Civano F, Elvis M, Trichas M, Green P (2014) The Largest X-ray Selected Sample of $z > 3$ AGNs: C-COSMOS and ChaMP. ArXiv

e-prints 1408.6280

Kartaltepe JS, Sanders DB, Le Floc'h E, Frayer DT, Aussel H, Arnouts S, Ilbert O, Salvato M, Scoville NZ, Surace J, Yan L, Brusa M, Capak P, Caputi K, Carollo CM, Civano F, Elvis M, Faure C, Hasinger G, Koekemoer AM, Lee N, Lilly S, Liu CT, McCracken HJ, Schinnerer E, Smolčić V, Taniguchi Y, Thompson DJ, Trump J (2010) A Multiwavelength Study of a Sample of 70 μm Selected Galaxies in the COSMOS Field. I. Spectral Energy Distributions and Luminosities. Astrophys J 709:572–596, DOI 10.1088/0004-637X/709/2/572, 0911.4515

Kartaltepe JS, Dickinson M, Alexander DM, Bell EF, Dahlen T, Elbaz D, Faber SM, Lotz J, McIntosh DH, Wiklind T, Altieri B, Aussel H, Bethermin M, Bournaud F, Charmandaris V, Conselice CJ, Cooray A, Dannerbauer H, Davé R, Dunlop J, Dekel A, Ferguson HC, Grogin NA, Hwang HS, Ivison R, Kocevski D, Koekemoer A, Koo DC, Lai K, Leiton R, Lucas RA, Lutz D, Magdis G, Magnelli B, Morrison G, Mozena M, Mullaney J, Newman JA, Pope A, Popesso P, van der Wel A, Weiner B, Wuyts S (2012) GOODS-Herschel and CANDELS: The Morphologies of Ultraluminous Infrared Galaxies at z ˜ 2. Astrophys J 757:23, DOI 10.1088/0004-637X/757/1/23, 1110.4057

Kauffmann G (1996) The age of elliptical galaxies and bulges in a merger model. MNRAS 281:487–492, astro-ph/9502096

Kauffmann G, Heckman TM (2009) Feast and Famine: regulation of black hole growth in low-redshift galaxies. MNRAS 397:135–147, DOI 10.1111/j.1365-2966.2009.14960.x, 0812.1224

Kauffmann G, Heckman TM, Tremonti C, Brinchmann J, Charlot S, White SDM, Ridgway SE, Brinkmann J, Fukugita M, Hall PB, Ivezić Ž, Richards GT, Schneider DP (2003) The host galaxies of active galactic nuclei. MNRAS 346:1055–1077, DOI 10.1111/j.1365-2966.2003.07154.x, astro-ph/0304239

Kelly BC, Shen Y (2013) The Demographics of Broad-line Quasars in the Mass-Luminosity Plane. II. Black Hole Mass and Eddington Ratio Functions. Astrophys J 764:45, DOI 10.1088/0004-637X/764/1/45, 1209.0477

Kelly BC, Bechtold J, Siemiginowska A, Aldcroft T, Sobolewska M (2007) Evolution of the X-ray Emission of Radio-quiet Quasars. Astrophys J 657:116–134, astro-ph/0611120

Kelly BC, Bechtold J, Trump JR, Vestergaard M, Siemiginowska A (2008) Observational Constraints on the Dependence of Radio-Quiet Quasar X-Ray Emission on Black Hole Mass and Accretion Rate. Astrophys J Supp 176:355–373, 0801.2383

Kennicutt RC, Evans NJ (2012) Star Formation in the Milky Way and Nearby Galaxies. Ann Rev Astron Astrophys 50:531–608, DOI 10.1146/annurev-astro-081811-125610, 1204.3552

Kereš D, Katz N, Fardal M, Davé R, Weinberg DH (2009) Galaxies in a simulated ΛCDM Universe - I. Cold mode and hot cores. MNRAS 395:160–179, DOI 10.1111/j.1365-2966.2009.14541.x, 0809.1430

Kewley LJ, Maier C, Yabe K, Ohta K, Akiyama M, Dopita MA, Yuan T

(2013) The Cosmic BPT Diagram: Confronting Theory with Observations. Astrophys J Let 774:L10, DOI 10.1088/2041-8205/774/1/L10, 1307.0514

Kim M, Kim DW, Wilkes BJ, Green PJ, Kim E, Anderson CS, Barkhouse WA, Evans NR, Ivezić Ž, Karovska M, Kashyap VL, Lee MG, Maksym P, Mossman AE, Silverman JD, Tananbaum HD (2007) Chandra Multiwavelength Project X-Ray Point Source Catalog. Astrophys J Supp 169:401–429, astro-ph/0611840

Kirkpatrick A, Pope A, Alexander DM, Charmandaris V, Daddi E, Dickinson M, Elbaz D, Gabor J, Hwang HS, Ivison R, Mullaney J, Pannella M, Scott D, Altieri B, Aussel H, Bournaud F, Buat V, Coia D, Dannerbauer H, Dasyra K, Kartaltepe J, Leiton R, Lin L, Magdis G, Magnelli B, Morrison G, Popesso P, Valtchanov I (2012) GOODS-Herschel: Impact of Active Galactic Nuclei and Star Formation Activity on Infrared Spectral Energy Distributions at High Redshift. Astrophys J 759:139, DOI 10.1088/0004-637X/759/2/139, 1209.4902

Klesman AJ, Sarajedini VL (2012) A multiwavelength survey of AGN in massive clusters: AGN detection and cluster AGN fraction. MNRAS 425:1215–1238, DOI 10.1111/j.1365-2966.2012.21508.x, 1207.4830

Klesman AJ, Sarajedini VL (2014) A multi-wavelength survey of AGN in massive clusters: AGN distribution and host galaxy properties. MNRAS 442:314–326, DOI 10.1093/mnras/stu830, 1407.7318

Kocevski DD, Lubin LM, Gal R, Lemaux BC, Fassnacht CD, Squires GK (2009) Chandra Observations of the cl1604 Supercluster at z = 0.9: Evidence for an Overdensity of Active Galactic Nuclei. Astrophys J 690:295–318, DOI 10.1088/0004-637X/690/1/295, 0804.1955

Kocevski DD, Faber SM, Mozena M, Koekemoer AM, Nandra K, Rangel C, Laird ES, Brusa M, Wuyts S, Trump JR, Koo DC, Somerville RS, Bell EF, Lotz JM, Alexander DM, Bournaud F, Conselice CJ, Dahlen T, Dekel A, Donley JL, Dunlop JS, Finoguenov A, Georgakakis A, Giavalisco M, Guo Y, Grogin NA, Hathi NP, Juneau S, Kartaltepe JS, Lucas RA, McGrath EJ, McIntosh DH, Mobasher B, Robaina AR, Rosario D, Straughn AN, van der Wel A, Villforth C (2012) CANDELS: Constraining the AGN-Merger Connection with Host Morphologies at z ˜ 2. Astrophys J 744:148, DOI 10.1088/0004-637X/744/2/148, 1109.2588

Kochanek CS, Eisenstein DJ, Cool RJ, Caldwell N, Assef RJ, Jannuzi BT, Jones C, Murray SS, Forman WR, Dey A, Brown MJI, Eisenhardt P, Gonzalez AH, Green P, Stern D (2012) AGES: The AGN and Galaxy Evolution Survey. Astrophys J Supp 200:8, 1110.4371

Kormendy J, Ho LC (2013) Coevolution (Or Not) of Supermassive Black Holes and Host Galaxies. Ann Rev Astron Astrophys 51:511–653, 1304.7762

Kormendy J, Richstone D (1995) Inward Bound—The Search For Supermassive Black Holes In Galactic Nuclei. Ann Rev Astron Astrophys 33:581–+, DOI 10.1146/annurev.aa.33.090195.003053

Koshida S, Minezaki T, Yoshii Y, Kobayashi Y, Sakata Y, Sugawara S, Enya K, Suganuma M, Tomita H, Aoki T, Peterson BA (2014) Reverberation Measurements of the Inner Radius of the Dust Torus in 17 Seyfert Galaxies.

Astrophys J 788:159, 1406.2078
Koss M, Mushotzky R, Veilleux S, Winter L (2010) Merging and Clustering of the Swift BAT AGN Sample. Astrophys J Let 716:L125–L130, DOI 10.1088/2041-8205/716/2/L125, 1006.0228
Koss M, Mushotzky R, Veilleux S, Winter LM, Baumgartner W, Tueller J, Gehrels N, Valencic L (2011) Host Galaxy Properties of the Swift Bat Ultra Hard X-Ray Selected Active Galactic Nucleus. Astrophys J 739:57–+, DOI 10.1088/0004-637X/739/2/57, 1107.1237
Koulouridis E, Plionis M, Melnyk O, Elyiv A, Georgantopoulos I, Clerc N, Surdej J, Chiappetti L, Pierre M (2014) X-ray AGN in the XMM-LSS galaxy clusters: no evidence of AGN suppression. Astron Astrophys 567:A83, DOI 10.1051/0004-6361/201423601, 1402.4136
Koutoulidis L, Plionis M, Georgantopoulos I, Fanidakis N (2013) Clustering, bias and the accretion mode of X-ray-selected AGN. MNRAS 428:1382–1394, DOI 10.1093/mnras/sts119, 1209.6460
Krivonos R, Vikhlinin A, Churazov E, Lutovinov A, Molkov S, Sunyaev R (2005) Extragalactic Source Counts in the 20-50 keV Energy Band from the Deep Observation of the Coma Region by INTEGRAL IBIS. Astrophys J 625:89–94, astro-ph/0409093
Krumpe M, Miyaji T, Coil AL, Aceves H (2012) The Spatial Clustering of ROSAT All-Sky Survey Active Galactic Nuclei. III. Expanded Sample and Comparison with Optical Active Galactic Nuclei. Astrophys J 746:1, DOI 10.1088/0004-637X/746/1/1, 1110.5648
Kurucz RL (1979) Model atmospheres for G, F, A, B, and O stars. Astrophys J Supp 40:1–340, DOI 10.1086/190589
La Franca F, Fiore F, Comastri A, Perola GC, Sacchi N, Brusa M, Cocchia F, Feruglio C, Matt G, Vignali C, Carangelo N, Ciliegi P, Lamastra A, Maiolino R, Mignoli M, Molendi S, Puccetti S (2005) The HELLAS2XMM Survey. VII. The Hard X-Ray Luminosity Function of AGNs up to z = 4: More Absorbed AGNs at Low Luminosities and High Redshifts. Astrophys J 635:864–879, DOI 10.1086/497586, astro-ph/0509081
Lacy M, Storrie-Lombardi LJ, Sajina A, Appleton PN, Armus L, Chapman SC, Choi PI, Fadda D, Fang F, Frayer DT, Heinrichsen I, Helou G, Im M, Marleau FR, Masci F, Shupe DL, Soifer BT, Surace J, Teplitz HI, Wilson G, Yan L (2004) Obscured and Unobscured Active Galactic Nuclei in the Spitzer Space Telescope First Look Survey. Astrophys J Supp 154:166–169, astro-ph/0405604
Laird ES, Nandra K, Georgakakis A, Aird JA, Barmby P, Conselice CJ, Coil AL, Davis M, Faber SM, Fazio GG, Guhathakurta P, Koo DC, Sarajedini V, Willmer CNA (2009) AEGIS-X: the Chandra Deep Survey of the Extended Groth Strip. Astrophys J Supp 180:102–116, 0809.1349
Laird ES, Nandra K, Pope A, Scott D (2010) On the X-ray properties of sub-mm-selected galaxies. MNRAS 401:2763–2772, 0910.2464
LaMassa SM, Urry CM, Cappelluti N, Civano F, Ranalli P, Glikman E, Treister E, Richards G, Ballantyne D, Stern D, Comastri A, Cardamone C, Schawinski K, Böhringer H, Chon G, Murray SS, Green P, Nandra K (2013a)

Finding rare AGN: XMM-Newton and Chandra observations of SDSS Stripe 82. MNRAS 436:3581–3601, 1309.7048

LaMassa SM, Urry CM, Glikman E, Cappelluti N, Civano F, Comastri A, Treister E, Böhringer H, Cardamone C, Chon G, Kephart M, Murray SS, Richards G, Ross NP, Rozner JS, Schawinski K (2013b) Finding rare AGN: X-ray number counts of Chandra sources in Stripe 82. MNRAS 432:1351–1360, 1210.0550

Lamer G, Wagner S, Zamorani G, Mignoli M, Hasinger G, Giedke K, Staubert R (2003) Optical identifications in the Marano field XMM-Newton survey. Astronomische Nachrichten 324:16–19

Lansbury GB, Alexander DM, Del Moro A, Gandhi P, Assef RJ, Stern D, Aird J, Ballantyne DR, Baloković M, Bauer FE, Boggs SE, Brandt WN, Christensen FE, Craig WW, Elvis M, Grefenstette BW, Hailey CJ, Harrison FA, Hickox RC, Koss M, LaMassa SM, Luo B, Mullaney JR, Teng SH, Urry CM, Zhang WW (2014) NuSTAR Observations of Heavily Obscured Quasars at z ˜ 0.5. Astrophys J 785:17, DOI 10.1088/0004-637X/785/1/17, 1402.2666

Lanzuisi G, Ponti G, Salvato M, Hasinger G, Cappelluti N, Bongiorno A, Brusa M, Lusso E, Nandra PK, Merloni A, Silverman J, Trump J, Vignali C, Comastri A, Gilli R, Schramm M, Steinhardt C, Sanders D, Kartaltepe J, Rosario D, Trakhtenbrot B (2014) Active Galactic Nucleus X-Ray Variability in the XMM-COSMOS Survey. Astrophys J 781:105

Laureijs R, Amiaux J, Arduini S, Augueres J, Brinchmann J, Cole R, Cropper M, Dabin C, Duvet L, Ealet A, et al (2011) Euclid Definition Study Report. ArXiv e-prints 1110.3193

Lawrence A (1991) The relative frequency of broad-lined and narrow-lined active galactic nuclei - Implications for unified schemes. MNRAS 252:586–592

Lawrence A, Elvis M (1982) Obscuration and the various kinds of Seyfert galaxies. Astrophys J 256:410–426

Lawrence A, Elvis M (2010) Misaligned Disks as Obscurers in Active Galaxies. Astrophys J 714:561–570

Lawrence A, Warren SJ, Almaini O, Edge AC, Hambly NC, Jameson RF, Lucas P, Casali M, Adamson A, Dye S, Emerson JP, Foucaud S, Hewett P, Hirst P, Hodgkin ST, Irwin MJ, Lodieu N, McMahon RG, Simpson C, Smail I, Mortlock D, Folger M (2007) The UKIRT Infrared Deep Sky Survey (UKIDSS). MNRAS 379:1599–1617, DOI 10.1111/j.1365-2966.2007.12040.x, astro-ph/0604426

Lazio JW, Kimball A, Barger AJ, Brandt WN, Chatterjee S, Clarke TE, Condon JJ, Dickman RL, Hunyh MT, Jarvis MJ, Jurić M, Kassim NE, Myers ST, Nissanke S, Osten R, Zauderer BA (2014) Radio Astronomy in LSST Era. PASP 126:196–209, DOI 10.1086/675262

Lehmer BD, Brandt WN, Alexander DM, Bauer FE, Schneider DP, Tozzi P, Bergeron J, Garmire GP, Giacconi R, Gilli R, Hasinger G, Hornschemeier AE, Koekemoer AM, Mainieri V, Miyaji T, Nonino M, Rosati P, Silverman JD, Szokoly G, Vignali C (2005) The Extended Chandra Deep Field-

South Survey: Chandra Point-Source Catalogs. Astrophys J Supp 161:21–40, astro-ph/0506607

Lehmer BD, Brandt WN, Hornschemeier AE, Alexander DM, Bauer FE, Koekemoer AM, Schneider DP, Steffen AT (2006) The Properties and Redshift Evolution of Intermediate-Luminosity Off-Nuclear X-Ray Sources in the Chandra Deep Fields. Astron J 131:2394–2405, astro-ph/0602001

Lehmer BD, Alexander DM, Chapman SC, Smail I, Bauer FE, Brandt WN, Geach JE, Matsuda Y, Mullaney JR, Swinbank AM (2009a) The Chandra Deep Protocluster Survey: point-source catalogues for a 400-ks observation of the z = 3.09 protocluster in SSA22. MNRAS 400:299–316, 0907.4369

Lehmer BD, Alexander DM, Geach JE, Smail I, Basu-Zych A, Bauer FE, Chapman SC, Matsuda Y, Scharf CA, Volonteri M, Yamada T (2009b) The Chandra Deep Protocluster Survey: Evidence for an Enhancement of AGN Activity in the SSA22 Protocluster at z = 3.09. Astrophys J 691:687–695, DOI 10.1088/0004-637X/691/1/687, 0809.5058

Lehmer BD, Alexander DM, Bauer FE, Brandt WN, Goulding AD, Jenkins LP, Ptak A, Roberts TP (2010) A Chandra Perspective on Galaxy-wide X-ray Binary Emission and its Correlation with Star Formation Rate and Stellar Mass: New Results from Luminous Infrared Galaxies. Astrophys J 724:559–571, 1009.3943

Lehmer BD, Xue YQ, Brandt WN, Alexander DM, Bauer FE, Brusa M, Comastri A, Gilli R, Hornschemeier AE, Luo B, Paolillo M, Ptak A, Shemmer O, Schneider DP, Tozzi P, Vignali C (2012) The 4 Ms Chandra Deep Field-South Number Counts Apportioned by Source Class: Pervasive Active Galactic Nuclei and the Ascent of Normal Galaxies. Astrophys J 752:46, 1204.1977

Lehmer BD, Lucy AB, Alexander DM, Best PN, Geach JE, Harrison CM, Hornschemeier AE, Matsuda Y, Mullaney JR, Smail I, Sobral D, Swinbank AM (2013) Concurrent Supermassive Black Hole and Galaxy Growth: Linking Environment and Nuclear Activity in z = 2.23 Hα Emitters. Astrophys J 765:87, DOI 10.1088/0004-637X/765/2/87, 1301.3922

Leighly KM, Halpern JP, Jenkins EB, Grupe D, Choi J, Prescott KB (2007) The Intrinsically X-Ray Weak Quasar PHL 1811. I. X-Ray Observations and Spectral Energy Distribution. Astrophys J 663:103–117, astro-ph/0611349

Levi M, Bebek C, Beers T, Blum R, Cahn R, Eisenstein D, Flaugher B, Honscheid K, Kron R, Lahav O, McDonald P, Roe N, Schlegel D, representing the DESI collaboration (2013) The DESI Experiment, a whitepaper for Snowmass 2013. ArXiv e-prints 1308.0847

Li YR, Ho LC, Wang JM (2011) Cosmological Evolution of Supermassive Black Holes. I. Mass Function at $0 < z < 2$. Astrophys J 742:33, 1109.0089

Li YR, Wang JM, Ho LC (2012) Cosmological Evolution of Supermassive Black Holes. II. Evidence for Downsizing of Spin Evolution. Astrophys J 749:187, DOI 10.1088/0004-637X/749/2/187, 1202.3516

Loaring NS, Dwelly T, Page MJ, Mason K, McHardy I, Gunn K, Moss D, Seymour N, Newsam AM, Takata T, Sekguchi K, Sasseen T, Cordova F (2005) XMM-Newton 13^H deep field - I. X-ray sources. MNRAS 362:1371–

1395, astro-ph/0507408

Luo B, Bauer FE, Brandt WN, Alexander DM, Lehmer BD, Schneider DP, Brusa M, Comastri A, Fabian AC, Finoguenov A, Gilli R, Hasinger G, Hornschemeier AE, Koekemoer A, Mainieri V, Paolillo M, Rosati P, Shemmer O, Silverman JD, Smail I, Steffen AT, Vignali C (2008) The Chandra Deep Field-South Survey: 2 Ms Source Catalogs. Astrophys J Supp 179:19–36, DOI 10.1086/591248, 0806.3968

Luo B, Brandt WN, Xue YQ, Brusa M, Alexander DM, Bauer FE, Comastri A, Koekemoer A, Lehmer BD, Mainieri V, Rafferty DA, Schneider DP, Silverman JD, Vignali C (2010) Identifications and Photometric Redshifts of the 2 Ms Chandra Deep Field-South Sources. Astrophys J Supp 187:560–580, 1002.3154

Luo B, Brandt WN, Xue YQ, Alexander DM, Brusa M, Bauer FE, Comastri A, Fabian AC, Gilli R, Lehmer BD, Rafferty DA, Schneider DP, Vignali C (2011) Revealing a Population of Heavily Obscured Active Galactic Nuclei at $z \approx 0.5$–1 in the Chandra Deep Field-South. Astrophys J 740:37, 1107.3148

Luo B, Brandt WN, Alexander DM, Stern D, Teng SH, Arévalo P, Bauer FE, Boggs SE, Christensen FE, Comastri A, Craig WW, Farrah D, Gandhi P, Hailey CJ, Harrison FA, Koss M, Ogle P, Puccetti S, Saez C, Scott AE, Walton DJ, Zhang WW (2014) Weak Hard X-Ray Emission from Broad Absorption Line Quasars: Evidence for Intrinsic X-Ray Weakness. Astrophys J 794:70, 1408.3633

Lusso E, Comastri A, Vignali C, Zamorani G, Brusa M, Gilli R, Iwasawa K, Salvato M, Civano F, Elvis M, Merloni A, Bongiorno A, Trump JR, Koekemoer AM, Schinnerer E, Le Floc'h E, Cappelluti N, Jahnke K, Sargent M, Silverman J, Mainieri V, Fiore F, Bolzonella M, Le Fèvre O, Garilli B, Iovino A, Kneib JP, Lamareille F, Lilly S, Mignoli M, Scodeggio M, Vergani D (2010) The X-ray to optical-UV luminosity ratio of X-ray selected type 1 AGN in XMM-COSMOS. Astron Astrophys 512:A34, 0912.4166

Lusso E, Comastri A, Vignali C, Zamorani G, Treister E, Sanders D, Bolzonella M, Bongiorno A, Brusa M, Civano F, Gilli R, Mainieri V, Nair P, Aller MC, Carollo M, Koekemoer AM, Merloni A, Trump JR (2011) The bolometric output and host-galaxy properties of obscured AGN in the XMM-COSMOS survey. Astron Astrophys 534:A110, DOI 10.1051/0004-6361/201117175, 1108.4925

Lusso E, Comastri A, Simmons BD, Mignoli M, Zamorani G, Vignali C, Brusa M, Shankar F, Lutz D, Trump JR, Maiolino R, Gilli R, Bolzonella M, Puccetti S, Salvato M, Impey CD, Civano F, Elvis M, Mainieri V, Silverman JD, Koekemoer AM, Bongiorno A, Merloni A, Berta S, Le Floc'h E, Magnelli B, Pozzi F, Riguccini L (2012) Bolometric luminosities and Eddington ratios of X-ray selected active galactic nuclei in the XMM-COSMOS survey. MNRAS 425:623–640, 1206.2642

Lusso E, Hennawi JF, Comastri A, Zamorani G, Richards GT, Vignali C, Treister E, Schawinski K, Salvato M, Gilli R (2013) The Obscured Fraction of Active Galactic Nuclei in the XMM-COSMOS Survey: A Spectral Energy Distribution Perspective. Astrophys J 777:86

Lutz D (2014) Far-Infrared Surveys of Galaxy Evolution. Ann Rev Astron Astrophys 52:373–414, DOI 10.1146/annurev-astro-081913-035953, 1403.3334

Lutz D, Mainieri V, Rafferty D, Shao L, Hasinger G, Weiß A, Walter F, Smail I, Alexander DM, Brandt WN, Chapman S, Coppin K, Förster Schreiber NM, Gawiser E, Genzel R, Greve TR, Ivison RJ, Koekemoer AM, Kurczynski P, Menten KM, Nordon R, Popesso P, Schinnerer E, Silverman JD, Wardlow J, Xue YQ (2010) The LABOCA Survey of the Extended Chandra Deep Field South: Two Modes of Star Formation in Active Galactic Nucleus Hosts? Astrophys J 712:1287–1301, DOI 10.1088/0004-637X/712/2/1287, 1002.0071

Maccacaro T, Gioia IM, Wolter A, Zamorani G, Stocke JT (1988) The X-ray spectra of the extragalactic sources in the Einstein extended medium sensitivity survey. Astrophys J 326:680–690

Madau P (1992) The contribution of quasars to the ultraviolet extragalactic background. Astrophys J Let 389:L1–L4, DOI 10.1086/186334

Magnier EA, Schlafly E, Finkbeiner D, Juric M, Tonry JL, Burgett WS, Chambers KC, Flewelling HA, Kaiser N, Kudritzki RP, Morgan JS, Price PA, Sweeney WE, Stubbs CW (2013) The Pan-STARRS 1 Photometric Reference Ladder, Release 12.01. Astrophys J Supp 205:20, DOI 10.1088/0067-0049/205/2/20, 1303.3634

Magorrian J, Tremaine S, Richstone D, Bender R, Bower G, Dressler A, Faber SM, Gebhardt K, Green R, Grillmair C, Kormendy J, Lauer T (1998) The Demography of Massive Dark Objects in Galaxy Centers. Astron J 115:2285–2305, DOI 10.1086/300353, astro-ph/9708072

Mainieri V, Hasinger G, Cappelluti N, Brusa M, Brunner H, Civano F, Comastri A, Elvis M, Finoguenov A, Fiore F, Gilli R, Lehmann I, Silverman J, Tasca L, Vignali C, Zamorani G, Schinnerer E, Impey C, Trump J, Lilly S, Maier C, Griffiths RE, Miyaji T, Capak P, Koekemoer A, Scoville N, Shopbell P, Taniguchi Y (2007) The XMM-Newton Wide-Field Survey in the COSMOS Field. IV. X-Ray Spectral Properties of Active Galactic Nuclei. Astrophys J Supp 172:368–382, astro-ph/0612361

Mainieri V, Bongiorno A, Merloni A, Aller M, Carollo M, Iwasawa K, Koekemoer AM, Mignoli M, Silverman JD, Bolzonella M, Brusa M, Comastri A, Gilli R, Halliday C, Ilbert O, Lusso E, Salvato M, Vignali C, Zamorani G, Contini T, Kneib JP, Le Fèvre O, Lilly S, Renzini A, Scodeggio M, Balestra I, Bardelli S, Caputi K, Coppa G, Cucciati O, de la Torre S, de Ravel L, Franzetti P, Garilli B, Iovino A, Kampczyk P, Knobel C, Kovač K, Lamareille F, Le Borgne JF, Le Brun V, Maier C, Nair P, Pello R, Peng Y, Perez Montero E, Pozzetti L, Ricciardelli E, Tanaka M, Tasca L, Tresse L, Vergani D, Zucca E, Aussel H, Capak P, Cappelluti N, Elvis M, Fiore F, Hasinger G, Impey C, Le Floc'h E, Scoville N, Taniguchi Y, Trump J (2011) Black hole accretion and host galaxies of obscured quasars in XMM-COSMOS. Astron Astrophys 535:A80, 1105.5395

Manners JC, Johnson O, Almaini O, Willott CJ, Gonzalez-Solares E, Lawrence A, Mann RG, Perez-Fournon I, Dunlop JS, McMahon RG, Oliver SJ, Rowan-Robinson M, Serjeant S (2003) The ELAIS deep X-ray survey - I. Chandra

source catalogue and first results. MNRAS 343:293–305, astro-ph/0207622
Maoz D (2007) Low-luminosity active galactic nuclei: are they UV faint and radio loud? MNRAS 377:1696–1710, astro-ph/0702292
Marchesini D, van Dokkum PG, Förster Schreiber NM, Franx M, Labbé I, Wuyts S (2009) The Evolution of the Stellar Mass Function of Galaxies from z = 4.0 and the First Comprehensive Analysis of its Uncertainties: Evidence for Mass-Dependent Evolution. Astrophys J 701:1765–1796, DOI 10.1088/0004-637X/701/2/1765, 0811.1773
Marconi A, Risaliti G, Gilli R, Hunt LK, Maiolino R, Salvati M (2004) Local supermassive black holes, relics of active galactic nuclei and the X-ray background. MNRAS 351:169–185, astro-ph/0311619
Martin DC, Wyder TK, Schiminovich D, Barlow TA, Forster K, Friedman PG, Morrissey P, Neff SG, Seibert M, Small T, Welsh BY, Bianchi L, Donas J, Heckman TM, Lee YW, Madore BF, Milliard B, Rich RM, Szalay AS, Yi SK (2007) The UV-Optical Galaxy Color-Magnitude Diagram. III. Constraints on Evolution from the Blue to the Red Sequence. Astrophys J Supp 173:342–356, DOI 10.1086/516639, astro-ph/0703281
Martini P, Sivakoff GR, Mulchaey JS (2009) The Evolution of Active Galactic Nuclei in Clusters of Galaxies to Redshift 1.3. Astrophys J 701:66–85, DOI 10.1088/0004-637X/701/1/66, 0906.1843
Martini P, Miller ED, Brodwin M, Stanford SA, Gonzalez AH, Bautz M, Hickox RC, Stern D, Eisenhardt PR, Galametz A, Norman D, Jannuzi BT, Dey A, Murray S, Jones C, Brown MJI (2013) The Cluster and Field Galaxy Active Galactic Nucleus Fraction at z = 1-1.5: Evidence for a Reversal of the Local Anticorrelation between Environment and AGN Fraction. Astrophys J 768:1, DOI 10.1088/0004-637X/768/1/1, 1302.6253
Massardi M, Bonaldi A, Negrello M, Ricciardi S, Raccanelli A, de Zotti G (2010) A model for the cosmological evolution of low-frequency radio sources. MNRAS 404:532–544, 1001.1069
Mateos S, Alonso-Herrero A, Carrera FJ, Blain A, Severgnini P, Caccianiga A, Ruiz A (2013) Uncovering obscured luminous AGN with WISE. MNRAS 434:941–955, 1305.7237
Matsuoka K, Silverman JD, Schramm M, Steinhardt CL, Nagao T, Kartaltepe J, Sanders DB, Treister E, Hasinger G, Akiyama M, Ohta K, Ueda Y, Bongiorno A, Brandt WN, Brusa M, Capak P, Civano F, Comastri A, Elvis M, Lilly SJ, Mainieri V, Masters D, Mignoli M, Salvato M, Trump JR, Taniguchi Y, Zamorani G, Alexander DM, Schawinski K (2013) A Comparative Analysis of Virial Black Hole Mass Estimates of Moderate-luminosity Active Galactic Nuclei Using Subaru/FMOS. Astrophys J 771:64, 1301.2332
Matthews DJ, Newman JA (2010) Reconstructing Redshift Distributions with Cross-correlations: Tests and an Optimized Recipe. Astrophys J 721:456–468, 1003.0687
Mayo JH, Lawrence A (2013) The effect of partial obscuration on the luminosity dependence of the obscured fraction in active galactic nuclei. MNRAS 434:1593–1598, DOI 10.1093/mnras/stt1118, 1306.4316

McGreer ID, Jiang L, Fan X, Richards GT, Strauss MA, Ross NP, White M, Shen Y, Schneider DP, Myers AD, Brandt WN, DeGraf C, Glikman E, Ge J, Streblyanska A (2013) The z = 5 Quasar Luminosity Function from SDSS Stripe 82. Astrophys J 768:105, 1212.4493

McHardy IM, Gunn KF, Newsam AM, Mason KO, Page MJ, Takata T, Sekiguchi K, Sasseen T, Cordova F, Jones LR, Loaring N (2003) A medium-deep Chandra and Subaru survey of the 13-h XMM/ROSAT deep survey area. MNRAS 342:802–822, astro-ph/0302553

McMahon RG, Banerji M, Gonzalez E, Koposov SE, Bejar VJ, Lodieu N, Rebolo R, VHS Collaboration (2013) First Scientific Results from the VISTA Hemisphere Survey (VHS). The Messenger 154:35–37

Ménard B, Scranton R, Schmidt S, Morrison C, Jeong D, Budavari T, Rahman M (2014) Clustering-based redshift estimation: method and application to data. ArXiv e-prints 1303.4722

Menci N, Fiore F, Puccetti S, Cavaliere A (2008) The Blast Wave Model for AGN Feedback: Effects on AGN Obscuration. Astrophys J 686:219–229, 0806.4543

Menci N, Fiore F, Lamastra A (2013) The Evolution of Active Galactic Nuclei in Warm Dark Matter Cosmology. Astrophys J 766:110, 1302.2000

Merloni A, Heinz S (2013) Evolution of Active Galactic Nuclei, p 503

Merloni A, Rudnick G, Di Matteo T (2004) Tracing the cosmological assembly of stars and supermassive black holes in galaxies. MNRAS 354:L37–L42, DOI 10.1111/j.1365-2966.2004.08382.x, arXiv:astro-ph/0409187

Merloni A, Bongiorno A, Bolzonella M, Brusa M, Civano F, Comastri A, Elvis M, Fiore F, Gilli R, Hao H, Jahnke K, Koekemoer AM, Lusso E, Mainieri V, Mignoli M, Miyaji T, Renzini A, Salvato M, Silverman J, Trump J, Vignali C, Zamorani G, Capak P, Lilly SJ, Sanders D, Taniguchi Y, Bardelli S, Carollo CM, Caputi K, Contini T, Coppa G, Cucciati O, de la Torre S, de Ravel L, Franzetti P, Garilli B, Hasinger G, Impey C, Iovino A, Iwasawa K, Kampczyk P, Kneib JP, Knobel C, Kovač K, Lamareille F, Le Borgne JF, Le Brun V, Le Fèvre O, Maier C, Pello R, Peng Y, Perez Montero E, Ricciardelli E, Scodeggio M, Tanaka M, Tasca LAM, Tresse L, Vergani D, Zucca E (2010) On the Cosmic Evolution of the Scaling Relations Between Black Holes and Their Host Galaxies: Broad-Line Active Galactic Nuclei in the zCOSMOS Survey. Astrophys J 708:137–157, DOI 10.1088/0004-637X/708/1/137, 0910.4970

Merloni A, Predehl P, Becker W, Böhringer H, Boller T, Brunner H, Brusa M, Dennerl K, Freyberg M, Friedrich P, Georgakakis A, Haberl F, Hasinger G, Meidinger N, Mohr J, Nandra K, Rau A, Reiprich TH, Robrade J, Salvato M, Santangelo A, Sasaki M, Schwope A, Wilms J, German eROSITA Consortium t (2012) eROSITA Science Book: Mapping the Structure of the Energetic Universe. ArXiv e-prints 1209.3114

Merloni A, Bongiorno A, Brusa M, Iwasawa K, Mainieri V, Magnelli B, Salvato M, Berta S, Cappelluti N, Comastri A, Fiore F, Gilli R, Koekemoer A, Le Floc'h E, Lusso E, Lutz D, Miyaji T, Pozzi F, Riguccini L, Rosario DJ, Silverman J, Symeonidis M, Treister E, Vignali C, Zamorani G (2014) The

incidence of obscuration in active galactic nuclei. MNRAS 437:3550–3567, 1311.1305

Mihos JC, Hernquist L (1996) Gasdynamics and Starbursts in Major Mergers. Astrophys J 464:641, DOI 10.1086/177353, astro-ph/9512099

Miller BP, Brandt WN, Schneider DP, Gibson RR, Steffen AT, Wu J (2011) X-ray Emission from Optically Selected Radio-intermediate and Radio-loud Quasars. Astrophys J 726:20, 1010.4804

Mineo S, Gilfanov M, Lehmer BD, Morrison GE, Sunyaev R (2014) X-ray emission from star-forming galaxies - III. Calibration of the L_X-SFR relation up to redshift $z \approx 1.3$. MNRAS 437:1698–1707, 1207.2157

Miyaji T, Hasinger G, Schmidt M (2000) Soft X-ray AGN luminosity function from it ROSAT surveys. I. Cosmological evolution and contribution to the soft X-ray background. Astron Astrophys 353:25–40, astro-ph/9910410

Miyaji T, Hasinger G, Schmidt M (2001) Soft X-ray AGN luminosity function from ROSAT surveys. II. Table of the binned soft X-ray luminosity function. Astron Astrophys 369:49–56, astro-ph/0101279

Miyaji T, Griffiths RE, Lumb D, Sarajedini V, Siddiqui H (2003) XMM-Newton view of the Hubble Deep Field-North and Groth-Westphal strip regions. Astronomische Nachrichten 324:24–27, astro-ph/0211343

Miyaji T, Sarajedini V, Griffiths RE, Yamada T, Schurch M, Cristóbal-Hornillos D, Motohara K (2004) Multiwavelength Properties of the X-Ray Sources in the Groth-Westphal Strip Field. Astron J 127:3180–3191, astro-ph/0402617

Miyaji T, Krumpe M, Coil AL, Aceves H (2011) The Spatial Clustering of ROSAT All-sky Survey AGNs. II. Halo Occupation Distribution Modeling of the Cross-correlation Function. Astrophys J 726:83, DOI 10.1088/0004-637X/726/2/83, 1010.5498

Mor R, Netzer H, Elitzur M (2009) Dusty Structure Around Type-I Active Galactic Nuclei: Clumpy Torus Narrow-line Region and Near-nucleus Hot Dust. Astrophys J 705:298–313, 0907.1654

Moran EC, Filippenko AV, Chornock R (2002) "Hidden" Seyfert 2 Galaxies and the X-Ray Background. Astrophys J Let 579:L71–L74, astro-ph/0210047

Mullaney JR, Alexander DM, Huynh M, Goulding AD, Frayer D (2010) Characterizing the far-infrared properties of distant X-ray detected AGNs: evidence for evolution in the infrared-X-ray luminosity ratio. MNRAS 401:995–1012, DOI 10.1111/j.1365-2966.2009.15753.x, 0909.3842

Mullaney JR, Alexander DM, Goulding AD, Hickox RC (2011) Defining the intrinsic AGN infrared spectral energy distribution and measuring its contribution to the infrared output of composite galaxies. MNRAS 414:1082–1110, DOI 10.1111/j.1365-2966.2011.18448.x, 1102.1425

Mullaney JR, Daddi E, Béthermin M, Elbaz D, Juneau S, Pannella M, Sargent MT, Alexander DM, Hickox RC (2012a) The Hidden "AGN Main Sequence": Evidence for a Universal Black Hole Accretion to Star Formation Rate Ratio since z ˜ 2 Producing an M $_{BH}$-M $_{*}$ Relation. Astrophys J Let 753:L30, DOI 10.1088/2041-8205/753/2/L30, 1204.2824

Mullaney JR, Pannella M, Daddi E, Alexander DM, Elbaz D, Hickox RC, Bournaud F, Altieri B, Aussel H, Coia D, Dannerbauer H, Dasyra K, Dickinson M, Hwang HS, Kartaltepe J, Leiton R, Magdis G, Magnelli B, Popesso P, Valtchanov I, Bauer FE, Brandt WN, Del Moro A, Hanish DJ, Ivison RJ, Juneau S, Luo B, Lutz D, Sargent MT, Scott D, Xue YQ (2012b) GOODS-Herschel: the far-infrared view of star formation in active galactic nucleus host galaxies since $z \approx 3$. MNRAS 419:95–115, DOI 10.1111/j.1365-2966.2011.19675.x, 1106.4284

Murray N, Chiang J, Grossman SA, Voit GM (1995) Accretion Disk Winds from Active Galactic Nuclei. Astrophys J 451:498

Murray SS, Kenter A, Forman WR, Jones C, Green PJ, Kochanek CS, Vikhlinin A, Fabricant D, Fazio G, Brand K, Brown MJI, Dey A, Jannuzi BT, Najita J, McNamara B, Shields J, Rieke M (2005) XBootes: An X-Ray Survey of the NDWFS Bootes Field. I. Overview and Initial Results. Astrophys J Supp 161:1–8, astro-ph/0504084

Murray SS, Borgani S, Campana S, Citterio O, Forman W, Giacconi R, Gilli R, Paolillo M, Pareschi G, Ptak A, Rosati P, Tozzi P, Weisskopf M, the WFXT Team (2013) Wide Field X-ray Telescope (WFXT). Mem Soc Ast It 84:790

Mushotzky R (2004) How are AGN Found? In: Barger AJ (ed) Supermassive Black Holes in the Distant Universe, Astrophysics and Space Science Library, vol 308, p 53, astro-ph/0405144

Mushotzky RF, Done C, Pounds KA (1993) X-ray spectra and time variability of active galactic nuclei. Ann Rev Astron Astrophys 31:717–761

Muxlow TWB, Richards AMS, Garrington ST, Wilkinson PN, Anderson B, Richards EA, Axon DJ, Fomalont EB, Kellermann KI, Partridge RB, Windhorst RA (2005) High-resolution studies of radio sources in the Hubble Deep and Flanking Fields. MNRAS 358:1159–1194, astro-ph/0501679

Nakagawa T, Shibai H, Onaka T, Matsuhara H, Kaneda H, Kawakatsu Y, Roelfsema P (2014) The next-generation infrared astronomy mission SPICA under the new framework. In: Society of Photo-Optical Instrumentation Engineers (SPIE) Conference Series, Society of Photo-Optical Instrumentation Engineers (SPIE) Conference Series, vol 9143, p 1, DOI 10.1117/12.2055947

Nandra K, Georgakakis A, Willmer CNA, Cooper MC, Croton DJ, Davis M, Faber SM, Koo DC, Laird ES, Newman JA (2007) AEGIS: The Color-Magnitude Relation for X-Ray-selected Active Galactic Nuclei. Astrophys J Let 660:L11–L14, DOI 10.1086/517918, arXiv:astro-ph/0607270

Nandra K, Barret D, Barcons X, Fabian A, den Herder JW, Piro L, Watson M, Adami C, Aird J, Afonso JM, et al (2013) The Hot and Energetic Universe: A White Paper presenting the science theme motivating the Athena+ mission. ArXiv e-prints 1306.2307

Naylor T, Broos PS, Feigelson ED (2013) Bayesian Matching for X-Ray and Infrared Sources in the MYStIX Project. Astrophys J Supp 209:30, 1309.4491

Neistein E, Netzer H (2014) What triggers black hole growth? Insights from star formation rates. MNRAS 437:3373–3384, DOI 10.1093/mnras/stt2130,

1302.1576

Nenkova M, Sirocky MM, Nikutta R, Ivezić Ž, Elitzur M (2008) AGN Dusty Tori. II. Observational Implications of Clumpiness. Astrophys J 685:160–180, 0806.0512

Netzer H (2009) Accretion and star formation rates in low-redshift type II active galactic nuclei. MNRAS 399:1907–1920, DOI 10.1111/j.1365-2966.2009.15434.x, 0907.3575

Netzer H, Lutz D, Schweitzer M, Contursi A, Sturm E, Tacconi LJ, Veilleux S, Kim DC, Rupke D, Baker AJ, Dasyra K, Mazzarella J, Lord S (2007) Spitzer Quasar and ULIRG Evolution Study (QUEST). II. The Spectral Energy Distributions of Palomar-Green Quasars. Astrophys J 666:806–816, DOI 10.1086/520716, 0706.0818

Noble SC, Krolik JH, Hawley JF (2009) Direct Calculation of the Radiative Efficiency of an Accretion Disk Around a Black Hole. Astrophys J 692:411–421, 0808.3140

Noble SC, Krolik JH, Schnittman JD, Hawley JF (2011) Radiative Efficiency and Thermal Spectrum of Accretion onto Schwarzschild Black Holes. Astrophys J 743:115, 1105.2825

Nobuta K, Akiyama M, Ueda Y, Watson MG, Silverman J, Hiroi K, Ohta K, Iwamuro F, Yabe K, Tamura N, Moritani Y, Sumiyoshi M, Takato N, Kimura M, Maihara T, Dalton G, Lewis I, Bonfield D, Lee H, Curtis-Lake E, Macaulay E, Clarke F, Sekiguchi K, Simpson C, Croom S, Ouchi M, Hanami H, Yamada T (2012) Black Hole Mass and Eddington Ratio Distribution Functions of X-Ray-selected Broad-line AGNs at z ˜ 1.4 in the Subaru XMM-Newton Deep Field. Astrophys J 761:143, 1211.0069

Noeske KG, Weiner BJ, Faber SM, Papovich C, Koo DC, Somerville RS, Bundy K, Conselice CJ, Newman JA, Schiminovich D, Le Floc'h E, Coil AL, Rieke GH, Lotz JM, Primack JR, Barmby P, Cooper MC, Davis M, Ellis RS, Fazio GG, Guhathakurta P, Huang J, Kassin SA, Martin DC, Phillips AC, Rich RM, Small TA, Willmer CNA, Wilson G (2007) Star Formation in AEGIS Field Galaxies since z=1.1: The Dominance of Gradually Declining Star Formation, and the Main Sequence of Star-forming Galaxies. Astrophys J Let 660:L43–L46, DOI 10.1086/517926, arXiv:astro-ph/0701924

Norris RP, Hopkins AM, Afonso J, Brown S, Condon JJ, Dunne L, Feain I, Hollow R, Jarvis M, Johnston-Hollitt M, Lenc E, Middelberg E, Padovani P, Prandoni I, Rudnick L, Seymour N, Umana G, Andernach H, Alexander DM, Appleton PN, Bacon D, Banfield J, Becker W, Brown MJI, Ciliegi P, Jackson C, Eales S, Edge AC, Gaensler BM, Giovannini G, Hales CA, Hancock P, Huynh MT, Ibar E, Ivison RJ, Kennicutt R, Kimball AE, Koekemoer AM, Koribalski BS, López-Sánchez ÁR, Mao MY, Murphy T, Messias H, Pimbblet KA, Raccanelli A, Randall KE, Reiprich TH, Roseboom IG, Röttgering H, Saikia DJ, Sharp RG, Slee OB, Smail I, Thompson MA, Urquhart JS, Wall JV, Zhao GB (2011) EMU: Evolutionary Map of the Universe. PASA 28:215–248, DOI 10.1071/AS11021, 1106.3219

Norris RP, Afonso J, Bacon D, Beck R, Bell M, Beswick RJ, Best P, Bhatnagar S, Bonafede A, Brunetti G, Budavári T, Cassano R, Condon JJ,

Cress C, Dabbech A, Feain I, Fender R, Ferrari C, Gaensler BM, Giovannini G, Haverkorn M, Heald G, Van der Heyden K, Hopkins AM, Jarvis M, Johnston-Hollitt M, Kothes R, Van Langevelde H, Lazio J, Mao MY, Martínez-Sansigre A, Mary D, Mcalpine K, Middelberg E, Murphy E, Padovani P, Paragi Z, Prandoni I, Raccanelli A, Rigby E, Roseboom IG, Röttgering H, Sabater J, Salvato M, Scaife AMM, Schilizzi R, Seymour N, Smith DJB, Umana G, Zhao GB, Zinn PC (2013) Radio Continuum Surveys with Square Kilometre Array Pathfinders. PASA 30:e020, DOI 10.1017/pas.2012.020, 1210.7521

Oh S, Mulchaey JS, Woo JH, Finoguenov A, Tanaka M, Cooper MC, Ziparo F, Bauer FE, Matsuoka K (2014) The Active Galactic Nucleus Population in X-Ray-selected Galaxy Groups at $0.5 < z < 1.1$. Astrophys J 790:43, DOI 10.1088/0004-637X/790/1/43, 1406.3059

Osmer PS (2004) The Evolution of Quasars. Coevolution of Black Holes and Galaxies p 324, astro-ph/0304150

Page MJ, Mason KO, McHardy IM, Jones LR, Carrera FJ (1997) The evolution of QSOs derived from soft X-ray surveys. MNRAS 291:324–336

Page MJ, Symeonidis M, Vieira JD, Altieri B, Amblard A, Arumugam V, Aussel H, Babbedge T, Blain A, Bock J, Boselli A, Buat V, Castro-Rodríguez N, Cava A, Chanial P, Clements DL, Conley A, Conversi L, Cooray A, Dowell CD, Dubois EN, Dunlop JS, Dwek E, Dye S, Eales S, Elbaz D, Farrah D, Fox M, Franceschini A, Gear W, Glenn J, Griffin M, Halpern M, Hatziminaoglou E, Ibar E, Isaak K, Ivison RJ, Lagache G, Levenson L, Lu N, Madden S, Maffei B, Mainetti G, Marchetti L, Nguyen HT, O'Halloran B, Oliver SJ, Omont A, Panuzzo P, Papageorgiou A, Pearson CP, Pérez-Fournon I, Pohlen M, Rawlings JI, Rigopoulou D, Riguccini L, Rizzo D, Rodighiero G, Roseboom IG, Rowan-Robinson M, Portal MS, Schulz B, Scott D, Seymour N, Shupe DL, Smith AJ, Stevens JA, Trichas M, Tugwell KE, Vaccari M, Valtchanov I, Viero M, Vigroux L, Wang L, Ward R, Wright G, Xu CK, Zemcov M (2012) The suppression of star formation by powerful active galactic nuclei. Nature 485:213–216, DOI 10.1038/nature11096, 1310.4147

Palanque-Delabrouille N, Magneville C, Yèche C, Eftekharzadeh S, Myers AD, Petitjean P, Pâris I, Aubourg E, McGreer I, Fan X, Dey A, Schlegel D, Bailey S, Bizayev D, Bolton A, Dawson K, Ebelke G, Ge J, Malanushenko E, Malanushenko V, Oravetz D, Pan K, Ross NP, Schneider DP, Sheldon E, Simmons A, Tinker J, White M, Willmer C (2013) Luminosity function from dedicated SDSS-III and MMT data of quasars in $0.7 < z < 4.0$ selected with a new approach. Astron Astrophys 551:A29, 1209.3968

Pan Z, Li J, Lin W, Wang J, Kong X (2014) Quenching Depends on Morphologies: Implications from the Ultraviolet-Optical Radial Color Distributions in Green Valley Galaxies. Astrophys J Let 792:L4, DOI 10.1088/2041-8205/792/1/L4, 1407.6715

Pannella M, Carilli CL, Daddi E, McCracken HJ, Owen FN, Renzini A, Strazzullo V, Civano F, Koekemoer AM, Schinnerer E, Scoville N, Smolčić V, Taniguchi Y, Aussel H, Kneib JP, Ilbert O, Mellier Y, Salvato M, Thomp-

son D, Willott CJ (2009) Star Formation and Dust Obscuration at $z \approx 2$: Galaxies at the Dawn of Downsizing. Astrophys J Let 698:L116–L120, DOI 10.1088/0004-637X/698/2/L116, 0905.1674

Paolillo M, Schreier EJ, Giacconi R, Koekemoer AM, Grogin NA (2004) Prevalence of X-Ray Variability in the Chandra Deep Field-South. Astrophys J 611:93–106, astro-ph/0404418

Papadakis IE, Chatzopoulos E, Athanasiadis D, Markowitz A, Georgantopoulos I (2008) The long-term X-ray variability properties of AGNs in the Lockman Hole region. Astron Astrophys 487:475–483, 0805.2851

Papovich C, Moustakas LA, Dickinson M, Le Floc'h E, Rieke GH, Daddi E, Alexander DM, Bauer F, Brandt WN, Dahlen T, Egami E, Eisenhardt P, Elbaz D, Ferguson HC, Giavalisco M, Lucas RA, Mobasher B, Pérez-González PG, Stutz A, Rieke MJ, Yan H (2006) Spitzer Observations of Massive, Red Galaxies at High Redshift. Astrophys J 640:92–113, DOI 10.1086/499915, astro-ph/0511289

Park SQ, Barmby P, Willner SP, Ashby MLN, Fazio GG, Georgakakis A, Ivison RJ, Konidaris NP, Miyazaki S, Nandra K, Rosario DJ (2010) AEGIS: A Multiwavelength Study of Spitzer Power-law Galaxies. Astrophys J 717:1181–1201, 1005.3331

Pentericci L, Castellano M, Menci N, Salimbeni S, Dahlen T, Galametz A, Santini P, Grazian A, Fontana A (2013) The evolution of the AGN content in groups up to z ˜ 1. Astron Astrophys 552:A111, DOI 10.1051/0004-6361/201219759, 1302.2861

Penzias AA, Wilson RW (1965) A Measurement of Excess Antenna Temperature at 4080 Mc/s. Astrophys J 142:419–421, DOI 10.1086/148307

Persic M, Rephaeli Y (2007) Galactic star formation rates gauged by stellar end-products. Astron Astrophys 463:481–492, astro-ph/0610321

Peterson BM (2014) Measuring the Masses of Supermassive Black Holes. Space Sci. Rev. 183:253–275

Piccinotti G, Mushotzky RF, Boldt EA, Holt SS, Marshall FE, Serlemitsos PJ, Shafer RA (1982) A complete X-ray sample of the high-latitude /absolute value of B greater than 20 deg/ sky from HEAO 1 A-2 - Log N-log S and luminosity functions. Astrophys J 253:485–503, DOI 10.1086/159651

Pierce CM, Lotz JM, Laird ES, Lin L, Nandra K, Primack JR, Faber SM, Barmby P, Park SQ, Willner SP, Gwyn S, Koo DC, Coil AL, Cooper MC, Georgakakis A, Koekemoer AM, Noeske KG, Weiner BJ, Willmer CNA (2007) AEGIS: Host Galaxy Morphologies of X-Ray-selected and Infrared-selected Active Galactic Nuclei at $0.2 <= z < 1.2$. Astrophys J Let 660:L19–L22, DOI 10.1086/517922, arXiv:astro-ph/0608381

Pierce CM, Lotz JM, Primack JR, Rosario DJV, Griffith RL, Conselice CJ, Faber SM, Koo DC, Coil AL, Salim S, Koekemoer AM, Laird ES, Ivison RJ, Yan R (2010a) The effects of an active galactic nucleus on host galaxy colour and morphology measurements. MNRAS 405:718–734, DOI 10.1111/j.1365-2966.2010.16502.x, 1002.2365

Pierce CM, Lotz JM, Salim S, Laird ES, Coil AL, Bundy K, Willmer CNA, Rosario DJV, Primack JR, Faber SM (2010b) Host galaxy colour gradients

and accretion disc obscuration in AEGIS z ˜ 1 X-ray-selected active galactic nuclei. MNRAS 408:139–156, DOI 10.1111/j.1365-2966.2010.17136.x, 1006.3571

Pierre M (2012) XXL: The Ultimate XMM Extragalactic Survey. In: Science from the Next Generation Imaging and Spectroscopic Surveys

Pilbratt GL, Riedinger JR, Passvogel T, Crone G, Doyle D, Gageur U, Heras AM, Jewell C, Metcalfe L, Ott S, Schmidt M (2010) Herschel Space Observatory. An ESA facility for far-infrared and submillimetre astronomy. Astron Astrophys 518:L1, DOI 10.1051/0004-6361/201014759, 1005.5331

Pineau FX, Motch C, Carrera F, Della Ceca R, Derrière S, Michel L, Schwope A, Watson MG (2011) Cross-correlation of the 2XMMi catalogue with Data Release 7 of the Sloan Digital Sky Survey. Astron Astrophys 527:A126, 1012.1727

Plionis M, Rovilos M, Basilakos S, Georgantopoulos I, Bauer F (2008) Luminosity-dependent X-Ray Active Galactic Nucleus Clustering? Astrophys J Let 674:L5–L8, DOI 10.1086/528845

Polletta M, Tajer M, Maraschi L, Trinchieri G, Lonsdale CJ, Chiappetti L, Andreon S, Pierre M, Le Fèvre O, Zamorani G, Maccagni D, Garcet O, Surdej J, Franceschini A, Alloin D, Shupe DL, Surace JA, Fang F, Rowan-Robinson M, Smith HE, Tresse L (2007) Spectral Energy Distributions of Hard X-Ray Selected Active Galactic Nuclei in the XMM-Newton Medium Deep Survey. Astrophys J 663:81–102, DOI 10.1086/518113, arXiv:astro-ph/0703255

Polletta MdC, Wilkes BJ, Siana B, Lonsdale CJ, Kilgard R, Smith HE, Kim DW, Owen F, Efstathiou A, Jarrett T, Stacey G, Franceschini A, Rowan-Robinson M, Babbedge TSR, Berta S, Fang F, Farrah D, González-Solares E, Morrison G, Surace JA, Shupe DL (2006) Chandra and Spitzer Unveil Heavily Obscured Quasars in the Chandra/SWIRE Survey. Astrophys J 642:673–693, astro-ph/0602228

Pounds KA, Done C, Osborne JP (1995) RE 1034+39: a high-state Seyfert galaxy? MNRAS 277:L5–L10

Proga D, Stone JM, Kallman TR (2000) Dynamics of Line-driven Disk Winds in Active Galactic Nuclei. Astrophys J 543:686–696, astro-ph/0005315

Puccetti S, Fiore F, D'Elia V, Pillitteri I, Feruglio C, Grazian A, Brusa M, Ciliegi P, Comastri A, Gruppioni C, Mignoli M, Vignali C, Zamorani G, La Franca F, Sacchi N, Franceschini A, Berta S, Buttery H, Dias JE (2006) The XMM-Newton survey of the ELAIS-S1 field. I. Number counts, angular correlation function and X-ray spectral properties. Astron Astrophys 457:501–515, astro-ph/0607107

Puccetti S, Comastri A, Fiore F, Arévalo P, Risaliti G, Bauer FE, Brandt WN, Stern D, Harrison FA, Alexander DM, Boggs SE, Christensen FE, Craig WW, Gandhi P, Hailey CJ, Koss MJ, Lansbury GB, Luo B, Madejski GM, Matt G, Walton DJ, Zhang W (2014) The Variable Hard X-Ray Emission of NGC 4945 as Observed by NuSTAR. Astrophys J 793:26, 1407.3974

Rafferty DA, Brandt WN, Alexander DM, Xue YQ, Bauer FE, Lehmer BD, Luo B, Papovich C (2011) Supermassive Black Hole Growth in Starburst Galaxies over Cosmic Time: Constraints from the Deepest Chandra Fields.

Astrophys J 742:3, DOI 10.1088/0004-637X/742/1/3, 1108.3229
Raimundo SI, Fabian AC, Bauer FE, Alexander DM, Brandt WN, Luo B, Vasudevan RV, Xue YQ (2010) Radiation pressure, absorption and AGN feedback in the Chandra Deep Fields. MNRAS 408:1714–1720, DOI 10.1111/j.1365-2966.2010.17234.x, 1006.4436
Ranalli P, Comastri A, Setti G (2003) The 2-10 keV luminosity as a Star Formation Rate indicator. Astron Astrophys 399:39–50, astro-ph/0211304
Ranalli P, Comastri A, Vignali C, Carrera FJ, Cappelluti N, Gilli R, Puccetti S, Brandt WN, Brunner H, Brusa M, Georgantopoulos I, Iwasawa K, Mainieri V (2013) The XMM deep survey in the CDF-S. III. Point source catalogue and number counts in the hard X-rays. Astron Astrophys 555:A42, 1304.5717
Rau A, Meidinger N, Nandra K, Porro M, Barret D, Santangelo A, Schmid C, Struder L, Tenzer C, Wilms J, Amoros C, Andritschke R, Aschauer F, Bahr A, Gunther B, Furmetz M, Ott B, Perinati E, Rambaud D, Reiffers J, Treis J, von Kienlin A, Weidenspointner G (2013) The Hot and Energetic Universe: The Wide Field Imager (WFI) for Athena+. ArXiv e-prints 1308.6785
Reynolds CS, Nowak MA (2003) Fluorescent iron lines as a probe of astrophysical black hole systems. Phys Rep 377:389–466, DOI 10.1016/S0370-1573(02)00584-7, astro-ph/0212065
Richards GT, Lacy M, Storrie-Lombardi LJ, Hall PB, Gallagher SC, Hines DC, Fan X, Papovich C, Vanden Berk DE, Trammell GB, Schneider DP, Vestergaard M, York DG, Jester S, Anderson SF, Budavári T, Szalay AS (2006a) Spectral Energy Distributions and Multiwavelength Selection of Type 1 Quasars. Astrophys J Supp 166:470–497, DOI 10.1086/506525, astro-ph/0601558
Richards GT, Strauss MA, Fan X, Hall PB, Jester S, Schneider DP, Vanden Berk DE, Stoughton C, Anderson SF, Brunner RJ, Gray J, Gunn JE, Ivezić Ž, Kirkland MK, Knapp GR, Loveday J, Meiksin A, Pope A, Szalay AS, Thakar AR, Yanny B, York DG, Barentine JC, Brewington HJ, Brinkmann J, Fukugita M, Harvanek M, Kent SM, Kleinman SJ, Krzesiński J, Long DC, Lupton RH, Nash T, Neilsen EH Jr, Nitta A, Schlegel DJ, Snedden SA (2006b) The Sloan Digital Sky Survey Quasar Survey: Quasar Luminosity Function from Data Release 3. Astron J 131:2766–2787, astro-ph/0601434
Richardson J, Chatterjee S, Zheng Z, Myers AD, Hickox R (2013) The Halo Occupation Distribution of X-Ray-bright Active Galactic Nuclei: A Comparison with Luminous Quasars. Astrophys J 774:143, DOI 10.1088/0004-637X/774/2/143, 1303.2942
Rigby EE, Best PN, Brookes MH, Peacock JA, Dunlop JS, Röttgering HJA, Wall JV, Ker L (2011) The luminosity-dependent high-redshift turnover in the steep spectrum radio luminosity function: clear evidence for downsizing in the radio-AGN population. MNRAS 416:1900–1915, 1104.5020
Risaliti G, Young M, Elvis M (2009) The Sloan Digital Sky Survey/XMM-Newton Quasar Survey: Correlation Between X-Ray Spectral Slope and Eddington Ratio. Astrophys J Let 700:L6–L10, 0906.1983

Rodighiero G, Cimatti A, Gruppioni C, Popesso P, Andreani P, Altieri B, Aussel H, Berta S, Bongiovanni A, Brisbin D, Cava A, Cepa J, Daddi E, Dominguez-Sanchez H, Elbaz D, Fontana A, Förster Schreiber N, Franceschini A, Genzel R, Grazian A, Lutz D, Magdis G, Magliocchetti M, Magnelli B, Maiolino R, Mancini C, Nordon R, Perez Garcia AM, Poglitsch A, Santini P, Sanchez-Portal M, Pozzi F, Riguccini L, Saintonge A, Shao L, Sturm E, Tacconi L, Valtchanov I, Wetzstein M, Wieprecht E (2010) The first Herschel view of the mass-SFR link in high-z galaxies. Astron Astrophys 518:L25, DOI 10.1051/0004-6361/201014624, 1005.1089

Roelfsema P, Giard M, Najarro F, Wafelbakker K, Jellema W, Jackson B, Sibthorpe B, Audard M, Doi Y, di Giorgio A, Griffin M, Helmich F, Kamp I, Kerschbaum F, Meyer M, Naylor D, Onaka T, Poglitch A, Spinoglio L, van der Tak F, Vandenbussche B (2014) SAFARI new and improved: extending the capabilities of SPICA's imaging spectrometer. In: Society of Photo-Optical Instrumentation Engineers (SPIE) Conference Series, Society of Photo-Optical Instrumentation Engineers (SPIE) Conference Series, vol 9143, p 1, DOI 10.1117/12.2056449

Rosario DJ, Santini P, Lutz D, Shao L, Maiolino R, Alexander DM, Altieri B, Andreani P, Aussel H, Bauer FE, Berta S, Bongiovanni A, Brandt WN, Brusa M, Cepa J, Cimatti A, Cox TJ, Daddi E, Elbaz D, Fontana A, Förster Schreiber NM, Genzel R, Grazian A, Le Floch E, Magnelli B, Mainieri V, Netzer H, Nordon R, Pérez Garcia I, Poglitsch A, Popesso P, Pozzi F, Riguccini L, Rodighiero G, Salvato M, Sanchez-Portal M, Sturm E, Tacconi LJ, Valtchanov I, Wuyts S (2012) The mean star formation rate of X-ray selected active galaxies and its evolution from z ˜ 2.5: results from PEP-Herschel. Astron Astrophys 545:A45, DOI 10.1051/0004-6361/201219258, 1203.6069

Rosario DJ, Mozena M, Wuyts S, Nandra K, Koekemoer A, McGrath E, Hathi NP, Dekel A, Donley J, Dunlop JS, Faber SM, Ferguson H, Giavalisco M, Grogin N, Guo Y, Kocevski DD, Koo DC, Laird E, Newman J, Rangel C, Somerville R (2013a) X-Ray Selected AGN Host Galaxies are Similar to Inactive Galaxies out to z = 3: Results from CANDELS/CDF-S. Astrophys J 763:59, DOI 10.1088/0004-637X/763/1/59, 1110.3816

Rosario DJ, Santini P, Lutz D, Netzer H, Bauer FE, Berta S, Magnelli B, Popesso P, Alexander DM, Brandt WN, Genzel R, Maiolino R, Mullaney JR, Nordon R, Saintonge A, Tacconi L, Wuyts S (2013b) Nuclear Activity is More Prevalent in Star-forming Galaxies. Astrophys J 771:63, DOI 10.1088/0004-637X/771/1/63, 1302.1202

Rosario DJ, McIntosh DH, van der Wel A, Kartaltepe J, Lang P, Santini P, Wuyts S, Lutz D, Rafelski M, Villforth C, Alexander DM, Bauer FE, Bell EF, Berta S, Brandt WN, Conselice CJ, Dekel A, Faber SM, Ferguson HC, Genzel R, Grogin NA, Kocevski DD, Koekemoer AM, Koo DC, Lotz JM, Magnelli B, Maiolino R, Mozena M, Mullaney JR, Papovich CJ, Popesso P, Tacconi LJ, Trump JR, Avadhuta S, Bassett R, Bell A, Bernyk M, Bournaud F, Cassata P, Cheung E, Croton D, Donley J, DeGroot L, Guedes J, Hathi N, Herrington J, Hilton M, Lai K, Lani C, Martig M, McGrath E, Mutch S, Mortlock A, McPartland C, O'Leary E, Peth M, Pillepich A,

Poole G, Snyder D, Straughn A, Telford O, Tonini C, Wandro P (2014) The host galaxies of X-ray selected Active Galactic Nuclei to z=2.5: Structure, star-formation and their relationships from CANDELS and Herschel/PACS. ArXiv e-prints 1409.5122

Ross NP, Myers AD, Sheldon ES, Yèche C, Strauss MA, Bovy J, Kirkpatrick JA, Richards GT, Aubourg É, Blanton MR, Brandt WN, Carithers WC, Croft RAC, da Silva R, Dawson K, Eisenstein DJ, Hennawi JF, Ho S, Hogg DW, Lee KG, Lundgren B, McMahon RG, Miralda-Escudé J, Palanque-Delabrouille N, Pâris I, Petitjean P, Pieri MM, Rich J, Roe NA, Schiminovich D, Schlegel DJ, Schneider DP, Slosar A, Suzuki N, Tinker JL, Weinberg DH, Weyant A, White M, Wood-Vasey WM (2012) The SDSS-III Baryon Oscillation Spectroscopic Survey: Quasar Target Selection for Data Release Nine. Astrophys J Supp 199:3, 1105.0606

Ross NP, McGreer ID, White M, Richards GT, Myers AD, Palanque-Delabrouille N, Strauss MA, Anderson SF, Shen Y, Brandt WN, Yèche C, Swanson MEC, Aubourg É, Bailey S, Bizyaev D, Bovy J, Brewington H, Brinkmann J, DeGraf C, Di Matteo T, Ebelke G, Fan X, Ge J, Malanushenko E, Malanushenko V, Mandelbaum R, Maraston C, Muna D, Oravetz D, Pan K, Pâris I, Petitjean P, Schawinski K, Schlegel DJ, Schneider DP, Silverman JD, Simmons A, Snedden S, Streblyanska A, Suzuki N, Weinberg DH, York D (2013) The SDSS-III Baryon Oscillation Spectroscopic Survey: The Quasar Luminosity Function from Data Release Nine. Astrophys J 773:14, 1210.6389

Rovilos E, Georgantopoulos I (2007) Optical colours of AGN in the extended Chandra deep field South: obscured black holes in early type galaxies. Astron Astrophys 475:115–120, DOI 10.1051/0004-6361:20077651, 0708.3294

Rovilos E, Fotopoulou S, Salvato M, Burwitz V, Egami E, Hasinger G, Szokoly G (2011) Optical and infrared properties of active galactic nuclei in the Lockman Hole. Astron Astrophys 529:A135, 1102.5129

Rovilos E, Comastri A, Gilli R, Georgantopoulos I, Ranalli P, Vignali C, Lusso E, Cappelluti N, Zamorani G, Elbaz D, Dickinson M, Hwang HS, Charmandaris V, Ivison RJ, Merloni A, Daddi E, Carrera FJ, Brandt WN, Mullaney JR, Scott D, Alexander DM, Del Moro A, Morrison G, Murphy EJ, Altieri B, Aussel H, Dannerbauer H, Kartaltepe J, Leiton R, Magdis G, Magnelli B, Popesso P, Valtchanov I (2012) GOODS-Herschel: ultra-deep XMM-Newton observations reveal AGN/star-formation connection. Astron Astrophys 546:A58, DOI 10.1051/0004-6361/201218952, 1207.7129

Rutledge RE, Brunner RJ, Prince TA, Lonsdale C (2000) XID: Cross-Association of ROSAT/Bright Source Catalog X-Ray Sources with USNO A-2 Optical Point Sources. Astrophys J Supp 131:335–353, astro-ph/0004053

Salvato M, Hasinger G, Ilbert O, Zamorani G, Brusa M, Scoville NZ, Rau A, Capak P, Arnouts S, Aussel H, Bolzonella M, Buongiorno A, Cappelluti N, Caputi K, Civano F, Cook R, Elvis M, Gilli R, Jahnke K, Kartaltepe JS, Impey CD, Lamareille F, Le Floc'h E, Lilly S, Mainieri V, McCarthy P, McCracken H, Mignoli M, Mobasher B, Murayama T, Sasaki S, Sanders DB, Schiminovich D, Shioya Y, Shopbell P, Silverman J, Smolčić V, Surace

J, Taniguchi Y, Thompson D, Trump JR, Urry M, Zamojski M (2009) Photometric Redshift and Classification for the XMM-COSMOS Sources. Astrophys J 690:1250–1263, 0809.2098

Sanders DB, Soifer BT, Elias JH, Madore BF, Matthews K, Neugebauer G, Scoville NZ (1988) Ultraluminous infrared galaxies and the origin of quasars. Astrophys J 325:74–91, DOI 10.1086/165983

Santini P, Rosario DJ, Shao L, Lutz D, Maiolino R, Alexander DM, Altieri B, Andreani P, Aussel H, Bauer FE, Berta S, Bongiovanni A, Brandt WN, Brusa M, Cepa J, Cimatti A, Daddi E, Elbaz D, Fontana A, Förster Schreiber NM, Genzel R, Grazian A, Le Floc'h E, Magnelli B, Mainieri V, Nordon R, Pérez Garcia AM, Poglitsch A, Popesso P, Pozzi F, Riguccini L, Rodighiero G, Salvato M, Sanchez-Portal M, Sturm E, Tacconi LJ, Valtchanov I, Wuyts S (2012) Enhanced star formation rates in AGN hosts with respect to inactive galaxies from PEP-Herschel observations. Astron Astrophys 540:A109, DOI 10.1051/0004-6361/201118266, 1201.4394

Sarajedini VL, Koo DC, Klesman AJ, Laird ES, Perez Gonzalez PG, Mozena M (2011) Variability and Multiwavelength-detected Active Galactic Nuclei in the Goods Fields. Astrophys J 731:97, 1102.3653

Schawinski K, Virani S, Simmons B, Urry CM, Treister E, Kaviraj S, Kushkuley B (2009) Do Moderate-Luminosity Active Galactic Nuclei Suppress Star Formation? Astrophys J Let 692:L19–L23, DOI 10.1088/0004-637X/692/1/L19, 0901.1663

Schawinski K, Urry CM, Simmons BD, Fortson L, Kaviraj S, Keel WC, Lintott CJ, Masters KL, Nichol RC, Sarzi M, Skibba R, Treister E, Willett KW, Wong OI, Yi SK (2014) The green valley is a red herring: Galaxy Zoo reveals two evolutionary pathways towards quenching of star formation in early- and late-type galaxies. MNRAS 440:889–907, DOI 10.1093/mnras/stu327, 1402.4814

Schechter P (1976) An analytic expression for the luminosity function for galaxies. Astrophys J 203:297–306, DOI 10.1086/154079

Schmidt M (1968) Space Distribution and Luminosity Functions of Quasi-Stellar Radio Sources. Astrophys J 151:393

Schmidt M, Schneider DP, Gunn JE (1995) Spectrscopic CCD Surveys for Quasars at Large Redshift.IV.Evolution of the Luminosity Function from Quasars Detected by Their Lyman-Alpha Emission. Astron J 110:68

Schmidt M, Hasinger G, Gunn J, Schneider D, Burg R, Giacconi R, Lehmann I, MacKenty J, Trumper J, Zamorani G (1998) The ROSAT deep survey. II. Optical identification, photometry and spectra of X-ray sources in the Lockman field. Astron Astrophys 329:495–503, astro-ph/9709144

Schnittman JD, Krolik JH (2013) A Monte Carlo Code for Relativistic Radiation Transport around Kerr Black Holes. Astrophys J 777:11, 1302.3214

Schramm M, Silverman JD (2013) The Black Hole-Bulge Mass Relation of Active Galactic Nuclei in the Extended Chandra Deep Field-South Survey. Astrophys J 767:13, DOI 10.1088/0004-637X/767/1/13, 1212.2999

Schramm M, Silverman JD, Greene JE, Brandt WN, Luo B, Xue YQ, Capak P, Kakazu Y, Kartaltepe J, Mainieri V (2013) Unveiling a Population

of Galaxies Harboring Low-mass Black Holes with X-Rays. Astrophys J 773:150, DOI 10.1088/0004-637X/773/2/150, 1305.3826

Schulze A, Wisotzki L (2010) Low redshift AGN in the Hamburg/ESO Survey . II. The active black hole mass function and the distribution function of Eddington ratios. Astron Astrophys 516:A87, DOI 10.1051/0004-6361/201014193, 1004.2671

Scott AE, Stewart GC (2014) Do the spectral energy distributions of type 1 active galactic nuclei show diversity? MNRAS 438:2253–2266, 1312.1344

Setti G, Woltjer L (1989) Active Galactic Nuclei and the spectrum of the X-ray background. Astron Astrophys 224:L21–L23

Severgnini P, Caccianiga A, Braito V, Della Ceca R, Maccacaro T, Wolter A, Sekiguchi K, Sasaki T, Yoshida M, Akiyama M, Watson MG, Barcons X, Carrera FJ, Pietsch W, Webb NA (2003) XMM-Newton observations reveal AGN in apparently normal galaxies. Astron Astrophys 406:483–492, DOI 10.1051/0004-6361:20030625, astro-ph/0304308

Shankar F (2013) Black hole demography: from scaling relations to models. Classical and Quantum Gravity 30(24):244001, 1307.3289

Shanks T, Belokurov V, Chehade B, Croom SM, Findlay JR, Gonzalez-Solares E, Irwin MJ, Koposov S, Mann RG, Metcalfe N, Murphy DNA, Norberg PR, Read MA, Sutorius E, Worseck G (2013) VST ATLAS First Science Results. The Messenger 154:38–40

Shao L, Lutz D, Nordon R, Maiolino R, Alexander DM, Altieri B, Andreani P, Aussel H, Bauer FE, Berta S, Bongiovanni A, Brandt WN, Brusa M, Cava A, Cepa J, Cimatti A, Daddi E, Dominguez-Sanchez H, Elbaz D, Förster Schreiber NM, Geis N, Genzel R, Grazian A, Gruppioni C, Magdis G, Magnelli B, Mainieri V, Pérez García AM, Poglitsch A, Popesso P, Pozzi F, Riguccini L, Rodighiero G, Rovilos E, Saintonge A, Salvato M, Sanchez Portal M, Santini P, Sturm E, Tacconi LJ, Valtchanov I, Wetzstein M, Wieprecht E (2010) Star formation in AGN hosts in GOODS-N. Astron Astrophys 518:L26+, DOI 10.1051/0004-6361/201014606, 1005.2562

Shaver PA, Hook IM, Jackson CA, Wall JV, Kellermann KI (1999) The Redshift Cutoff and the Quasar Epoch. In: Carilli CL, Radford SJE, Menten KM, Langston GI (eds) Highly Redshifted Radio Lines, Astronomical Society of the Pacific Conference Series, vol 156, p 163, astro-ph/9801211

Shemmer O, Brandt WN, Netzer H, Maiolino R, Kaspi S (2006) The Hard X-Ray Spectral Slope as an Accretion Rate Indicator in Radio-quiet Active Galactic Nuclei. Astrophys J Let 646:L29–L32, astro-ph/0606389

Shemmer O, Brandt WN, Netzer H, Maiolino R, Kaspi S (2008) The Hard X-Ray Spectrum as a Probe for Black Hole Growth in Radio-Quiet Active Galactic Nuclei. Astrophys J 682:81–93, 0804.0803

Shen Y (2013) The mass of quasars. Bulletin of the Astronomical Society of India 41:61–115, 1302.2643

Shen Y, Kelly BC (2012) The Demographics of Broad-line Quasars in the Mass-Luminosity Plane. I. Testing FWHM-based Virial Black Hole Masses. Astrophys J 746:169, 1107.4372

Shi Y, Rieke G, Donley J, Cooper M, Willmer C, Kirby E (2008) Black Hole

Accretion in Low-Mass Galaxies since z ˜ 1. Astrophys J 688:794–806, DOI 10.1086/592192, 0807.4949

Silva L, Maiolino R, Granato GL (2004) Connecting the cosmic infrared background to the X-ray background. MNRAS 355:973–985, DOI 10.1111/j.1365-2966.2004.08380.x, astro-ph/0403381

Silverman JD, Green PJ, Barkhouse WA, Kim DW, Kim M, Wilkes BJ, Cameron RA, Hasinger G, Jannuzi BT, Smith MG, Smith PS, Tananbaum H (2008a) The Luminosity Function of X-Ray-selected Active Galactic Nuclei: Evolution of Supermassive Black Holes at High Redshift. Astrophys J 679:118–139, 0710.2461

Silverman JD, Mainieri V, Lehmer BD, Alexander DM, Bauer FE, Bergeron J, Brandt WN, Gilli R, Hasinger G, Schneider DP, Tozzi P, Vignali C, Koekemoer AM, Miyaji T, Popesso P, Rosati P, Szokoly G (2008b) The Evolution of AGN Host Galaxies: From Blue to Red and the Influence of Large-Scale Structures. Astrophys J 675:1025–1040, DOI 10.1086/527283, arXiv:0709.3455

Silverman JD, Kovač K, Knobel C, Lilly S, Bolzonella M, Lamareille F, Mainieri V, Brusa M, Cappelluti N, Peng Y, Hasinger G, Zamorani G, Scodeggio M, Contini T, Carollo CM, Jahnke K, Kneib JP, Le Fevre O, Bardelli S, Bongiorno A, Brunner H, Caputi K, Civano F, Comastri A, Coppa G, Cucciati O, de la Torre S, de Ravel L, Elvis M, Finoguenov A, Fiore F, Franzetti P, Garilli B, Gilli R, Griffiths R, Iovino A, Kampczyk P, Koekemoer A, Le Borgne JF, Le Brun V, Maier C, Mignoli M, Pello R, Perez Montero E, Ricciardelli E, Tanaka M, Tasca L, Tresse L, Vergani D, Vignali C, Zucca E, Bottini D, Cappi A, Cassata P, Marinoni C, McCracken HJ, Memeo P, Meneux B, Oesch P, Porciani C, Salvato M (2009a) The Environments of Active Galactic Nuclei within the zCOSMOS Density Field. Astrophys J 695:171–182, DOI 10.1088/0004-637X/695/1/171, 0812.3402

Silverman JD, Lamareille F, Maier C, Lilly SJ, Mainieri V, Brusa M, Cappelluti N, Hasinger G, Zamorani G, Scodeggio M, Bolzonella M, Contini T, Carollo CM, Jahnke K, Kneib JP, LeFèvre O, Merloni A, Bardelli S, Bongiorno A, Brunner H, Caputi K, Civano F, Comastri A, Coppa G, Cucciati O, de la Torre S, de Ravel L, Elvis M, Finoguenov A, Fiore F, Franzetti P, Garilli B, Gilli R, Iovino A, Kampczyk P, Knobel C, Kovač K, LeBorgne JF, LeBrun V, Mignoli M, Pello R, Peng Y, Montero EP, Ricciardelli E, Tanaka M, Tasca L, Tresse L, Vergani D, Vignali C, Zucca E, Bottini D, Cappi A, Cassata P, Fumana M, Griffiths R, Kartaltepe J, Koekemoer A, Marinoni C, McCracken HJ, Memeo P, Meneux B, Oesch P, Porciani C, Salvato M (2009b) Ongoing and Co-Evolving Star Formation in zCOSMOS Galaxies Hosting Active Galactic Nuclei. Astrophys J 696:396–410, DOI 10.1088/0004-637X/696/1/396, 0810.3653

Silverman JD, Mainieri V, Salvato M, Hasinger G, Bergeron J, Capak P, Szokoly G, Finoguenov A, Gilli R, Rosati P, Tozzi P, Vignali C, Alexander DM, Brandt WN, Lehmer BD, Luo B, Rafferty D, Xue YQ, Balestra I, Bauer FE, Brusa M, Comastri A, Kartaltepe J, Koekemoer AM, Miyaji T, Schneider DP, Treister E, Wisotski L, Schramm M (2010) The Extended Chandra

Deep Field-South Survey: Optical Spectroscopy of Faint X-ray Sources with the VLT and Keck. Astrophys J Supp 191:124–142, 1009.1923

Silverman JD, Kampczyk P, Jahnke K, Andrae R, Lilly S, Elvis M, Civano F, Mainieri V, Vignali C, Zamorani G, Nair P, Le Fevre O, de Ravel L, Bardelli S, Bongiorno A, Bolzonella M, Brusa M, Cappelluti N, Cappi A, Caputi K, Carollo CM, Contini T, Coppa G, Cucciati O, de la Torre S, Franzetti P, Garilli B, Halliday C, Hasinger G, Iovino A, Knobel C, koekemoer A, Kovac K, Lamareille F, Le Borgne J, Le Brun V, Maier C, Mignoli M, Pello R, Perez Montero E, Ricciardelli E, Peng Y, Scodeggio M, Tanaka M, Tasca L, Tresse L, Vergani D, Zucca E, Comastri A, Finoguenov A, Fu H, Gilli R, Hao H, Ho L, Salvato M (2011) The impact of galaxy interactions on AGN activity in zCOSMOS. Astrophys J in press (arXiv:11091292) 1109.1292

Simmons BD, Urry CM (2008) The Accuracy of Morphological Decomposition of Active Galactic Nucleus Host Galaxies. Astrophys J 683:644–658, DOI 10.1086/589827, 0804.1363

Simmons BD, Van Duyne J, Urry CM, Treister E, Koekemoer AM, Grogin NA, GOODS Team (2011) Obscured GOODS Active Galactic Nuclei and Their Host Galaxies at $z < 1.25$: The Slow Black Hole Growth Phase. Astrophys J 734:121, 1104.2619

Simpson C (2005) The luminosity dependence of the type 1 active galactic nucleus fraction. MNRAS 360:565–572, astro-ph/0503500

Skrutskie MF, Cutri RM, Stiening R, Weinberg MD, Schneider S, Carpenter JM, Beichman C, Capps R, Chester T, Elias J, Huchra J, Liebert J, Lonsdale C, Monet DG, Price S, Seitzer P, Jarrett T, Kirkpatrick JD, Gizis JE, Howard E, Evans T, Fowler J, Fullmer L, Hurt R, Light R, Kopan EL, Marsh KA, McCallon HL, Tam R, Van Dyk S, Wheelock S (2006) The Two Micron All Sky Survey (2MASS). Astron J 131:1163–1183, DOI 10.1086/498708

Smith RJ, Lucey JR, Hudson MJ, Allanson SP, Bridges TJ, Hornschemeier AE, Marzke RO, Miller NA (2009) A spectroscopic survey of dwarf galaxies in the Coma cluster: stellar populations, environment and downsizing. MNRAS 392:1265–1294, DOI 10.1111/j.1365-2966.2008.14180.x, 0810.5558

Sołtan A (1982) Masses of quasars. MNRAS 200:115–122

Spergel D, Gehrels N, Breckinridge J, Donahue M, Dressler A, Gaudi BS, Greene T, Guyon O, Hirata C, Kalirai J, Kasdin NJ, Moos W, Perlmutter S, Postman M, Rauscher B, Rhodes J, Wang Y, Weinberg D, Centrella J, Traub W, Baltay C, Colbert J, Bennett D, Kiessling A, Macintosh B, Merten J, Mortonson M, Penny M, Rozo E, Savransky D, Stapelfeldt K, Zu Y, Baker C, Cheng E, Content D, Dooley J, Foote M, Goullioud R, Grady K, Jackson C, Kruk J, Levine M, Melton M, Peddie C, Ruffa J, Shaklan S (2013) WFIRST-2.4: What Every Astronomer Should Know. ArXiv e-prints 1305.5425

Springel V, White SDM, Jenkins A, Frenk CS, Yoshida N, Gao L, Navarro J, Thacker R, Croton D, Helly J, Peacock JA, Cole S, Thomas P, Couchman H, Evrard A, Colberg J, Pearce F (2005) Simulations of the formation, evolution and clustering of galaxies and quasars. Nature 435:629–636, DOI 10.1038/nature03597, astro-ph/0504097

Starikova S, Cool R, Eisenstein D, Forman W, Jones C, Hickox R, Kenter A, Kochanek C, Kravtsov A, Murray SS, Vikhlinin A (2011) Constraining Halo Occupation Properties of X-Ray Active Galactic Nuclei Using Clustering of Chandra Sources in the Boötes Survey Region. Astrophys J 741:15, DOI 10.1088/0004-637X/741/1/15, 1010.1577

Steffen AT, Strateva I, Brandt WN, Alexander DM, Koekemoer AM, Lehmer BD, Schneider DP, Vignali C (2006) The X-Ray-to-Optical Properties of Optically Selected Active Galaxies over Wide Luminosity and Redshift Ranges. Astron J 131:2826–2842, astro-ph/0602407

Steidel CC, Hunt MP, Shapley AE, Adelberger KL, Pettini M, Dickinson M, Giavalisco M (2002) The Population of Faint Optically Selected Active Galactic Nuclei at z ˜ 3. Astrophys J 576:653–659, astro-ph/0205142

Stern D, Tozzi P, Stanford SA, Rosati P, Holden B, Eisenhardt P, Elston R, Wu KL, Connolly A, Spinrad H, Dawson S, Dey A, Chaffee FH (2002) SPICES II: Optical and Near-Infrared Identifications of Faint X-Ray Sources from Deep Chandra Observations of Lynx. Astron J 123:2223–2245, astro-ph/0203392

Stern D, Eisenhardt P, Gorjian V, Kochanek CS, Caldwell N, Eisenstein D, Brodwin M, Brown MJI, Cool R, Dey A, Green P, Jannuzi BT, Murray SS, Pahre MA, Willner SP (2005) Mid-Infrared Selection of Active Galaxies. Astrophys J 631:163–168, astro-ph/0410523

Stern D, Lansbury GB, Assef RJ, Brandt WN, Alexander DM, Ballantyne DR, Baloković M, Bauer FE, Benford D, Blain A, Boggs SE, Bridge C, Brightman M, Christensen FE, Comastri A, Craig WW, Del Moro A, Eisenhardt PRM, Gandhi P, Griffith RL, Hailey CJ, Harrison FA, Hickox RC, Jarrett TH, Koss M, Lake S, LaMassa SM, Luo B, Tsai CW, Urry CM, Walton DJ, Wright EL, Wu J, Yan L, Zhang WW (2014) NuSTAR and XMM-Newton Observations of Luminous, Heavily Obscured, WISE-selected Quasars at $z \sim 2$. Astrophys J 794:102, 1403.3078

Strateva I, Ivezić Ž, Knapp GR, Narayanan VK, Strauss MA, Gunn JE, Lupton RH, Schlegel D, Bahcall NA, Brinkmann J, Brunner RJ, Budavári T, Csabai I, Castander FJ, Doi M, Fukugita M, Győry Z, Hamabe M, Hennessy G, Ichikawa T, Kunszt PZ, Lamb DQ, McKay TA, Okamura S, Racusin J, Sekiguchi M, Schneider DP, Shimasaku K, York D (2001) Color Separation of Galaxy Types in the Sloan Digital Sky Survey Imaging Data. Astron J 122:1861–1874, DOI 10.1086/323301, arXiv:astro-ph/0107201

Strüder L, Briel U, Dennerl K, Hartmann R, Kendziorra E, Meidinger N, Pfeffermann E, Reppin C, Aschenbach B, Bornemann W, Bräuninger H, Burkert W, Elender M, Freyberg M, Haberl F, Hartner G, Heuschmann F, Hippmann H, Kastelic E, Kemmer S, Kettenring G, Kink W, Krause N, Müller S, Oppitz A, Pietsch W, Popp M, Predehl P, Read A, Stephan KH, Stötter D, Trümper J, Holl P, Kemmer J, Soltau H, Stötter R, Weber U, Weichert U, von Zanthier C, Carathanassis D, Lutz G, Richter RH, Solc P, Böttcher H, Kuster M, Staubert R, Abbey A, Holland A, Turner M, Balasini M, Bignami GF, La Palombara N, Villa G, Buttler W, Gianini F, Lainé R, Lumb D, Dhez P (2001) The European Photon Imaging Camera

on XMM-Newton: The pn-CCD camera. Astron Astrophys 365:L18–L26

Sugai H, Tamura N, Karoji H, Shimono A, Takato N, Kimura M, Ohyama Y, Ueda A, Aghazarian H, Vital de Arruda M, Barkhouser RH, Bennett CL, Bickerton S, Bozier A, Braun DF, Bui K, Capocasale CM, Carr MA, Castilho B, Chang YC, Chen HY, Chou RCY, Dawson OR, Dekany RG, Ek EM, Ellis RS, English RJ, Ferrand D, Ferreira D, Fisher CD, Golebiowski M, Gunn JE, Hart M, Heckman TM, Ho PTP, Hope S, Hovland LE, Hsuc SF, Hu YS, Jie Huang P, Jaquet M, Karr JE, Kempenaar JG, King ME, Le Fèvre O, Le Mignant D, Ling HH, Loomis C, Lupton RH, Madec F, Mao P, Souza Marrara L, Ménard B, Morantz C, Murayama H, Murray GJ, de Oliveira AC, Mendes de Oliveira C, Souza de Oliveira L, Orndorff JD, de Paiva Vilaça R, Partos EJ, Pascal S, Pegot-Ogier T, Reiley DJ, Riddle R, Santos L, Bispo dos Santos J, Schwochert MA, Seiffert MD, Smee SA, Smith RM, Steinkraus RE, Sodré L Jr, Spergel DN, Surace C, Tresse L, Vidal C, Vives S, Wang SY, Wen CY, Wu AC, Wyse R, Yan CH (2014) Progress with the Prime Focus Spectrograph for the Subaru Telescope: a massively multiplexed optical and near-infrared fiber spectrograph. ArXiv e-prints 1408.2825

Sutherland W, Saunders W (1992) On the likelihood ratio for source identification. MNRAS 259:413–420

Sutherland W, Emerson J, Dalton G, Atad-Ettedgui E, Beard S, Bennett R, Bezawada N, Born A, Caldwell M, Clark P, Craig S, Henry D, Jeffers P, Little B, McPherson A, Murray J, Stewart M, Stobie B, Terrett D, Ward K, Whalley M, Woodhouse G (2014) The Visible and Infrared Survey Telescope for Astronomy (VISTA): Design, Technical Overview and Performance. ArXiv e-prints 1409.4780

Symeonidis M, Rosario D, Georgakakis A, Harker J, Laird ES, Page MJ, Willmer CNA (2010) The central energy source of 70 μm-selected galaxies: starburst or AGN? MNRAS 403:1474–1490, DOI 10.1111/j.1365-2966.2009.16214.x, 0912.3038

Symeonidis M, Kartaltepe J, Salvato M, Bongiorno A, Brusa M, Page MJ, Ilbert O, Sanders D, Wel Avd (2013) AGN in dusty hosts: implications for galaxy evolution. MNRAS 433:1015–1022, DOI 10.1093/mnras/stt782, 1305.1881

Szokoly GP, Bergeron J, Hasinger G, Lehmann I, Kewley L, Mainieri V, Nonino M, Rosati P, Giacconi R, Gilli R, Gilmozzi R, Norman C, Romaniello M, Schreier E, Tozzi P, Wang JX, Zheng W, Zirm A (2004) The Chandra Deep Field-South: Optical Spectroscopy. I. Astrophys J Supp 155:271–349, astro-ph/0312324

Tacconi LJ, Neri R, Genzel R, Combes F, Bolatto A, Cooper MC, Wuyts S, Bournaud F, Burkert A, Comerford J, Cox P, Davis M, Förster Schreiber NM, García-Burillo S, Gracia-Carpio J, Lutz D, Naab T, Newman S, Omont A, Saintonge A, Shapiro Griffin K, Shapley A, Sternberg A, Weiner B (2013) Phibss: Molecular Gas Content and Scaling Relations in z ˜ 1-3 Massive, Main-sequence Star-forming Galaxies. Astrophys J 768:74, DOI 10.1088/0004-637X/768/1/74, 1211.5743

Takada M, Ellis RS, Chiba M, Greene JE, Aihara H, Arimoto N, Bundy K, Cohen J, Doré O, Graves G, Gunn JE, Heckman T, Hirata CM, Ho P, Kneib JP, Fèvre OL, Lin L, More S, Murayama H, Nagao T, Ouchi M, Seiffert M, Silverman JD, Sodré L, Spergel DN, Strauss MA, Sugai H, Suto Y, Takami H, Wyse R (2014) Extragalactic science, cosmology, and Galactic archaeology with the Subaru Prime Focus Spectrograph. PASJ 66:R1, DOI 10.1093/pasj/pst019, 1206.0737

Takahashi T, Mitsuda K, Kelley R, Aarts H, Aharonian F, Akamatsu H, Akimoto F, Allen S, Anabuki N, Angelini L, Arnaud K, Asai M, Audard M, Awaki H, Azzarello P, Baluta C, Bamba A, Bando N, Bautz M, Blandford R, Boyce K, Brown G, Cackett E, Chernyakova M, Coppi P, Costantini E, de Plaa J, den Herder JW, DiPirro M, Done C, Dotani T, Doty J, Ebisawa K, Eckart M, Enoto T, Ezoe Y, Fabian A, Ferrigno C, Foster A, Fujimoto R, Fukazawa Y, Funk S, Furuzawa A, Galeazzi M, Gallo L, Gandhi P, Gendreau K, Gilmore K, Haas D, Haba Y, Hamaguchi K, Hatsukade I, Hayashi T, Hayashida K, Hiraga J, Hirose K, Hornschemeier A, Hoshino A, Hughes J, Hwang U, Iizuka R, Inoue Y, Ishibashi K, Ishida M, Ishimura K, Ishisaki Y, Ito M, Iwata N, Iyomoto N, Kaastra J, Kallman T, Kamae T, Kataoka J, Katsuda S, Kawahara H, Kawaharada M, Kawai N, Kawasaki S, Khangaluyan D, Kilbourne C, Kimura M, Kinugasa K, Kitamoto S, Kitayama T, Kohmura T, Kokubun M, Kosaka T, Koujelev A, Koyama K, Krimm H, Kubota A, Kunieda H, LaMassa S, Laurent P, Lebrun F, Leutenegger M, Limousin O, Loewenstein M, Long K, Lumb D, Madejski G, Maeda Y, Makishima K, Marchand G, Markevitch M, Matsumoto H, Matsushita K, McCammon D, McNamara B, Miller J, Miller E, Mineshige S, Minesugi K, Mitsuishi I, Miyazawa T, Mizuno T, Mori H, Mori K, Mukai K, Murakami T, Murakami H, Mushotzky R, Nagano H, Nagino R, Nakagawa T, Nakajima H, Nakamori T, Nakazawa K, Namba Y, Natsukari C, Nishioka Y, Nobukawa M, Nomachi M, O'Dell S, Odaka H, Ogawa H, Ogawa M, Ogi K, Ohashi T, Ohno M, Ohta M, Okajima T, Okamoto A, Okazaki T, Ota N, Ozaki M, Paerels F, Paltani S, Parmar A, Petre R, Pohl M, Porter FS, Ramsey B, Reis R, Reynolds C, Russell H, Safi-Harb S, Sakai Si, Sameshima H, Sanders J, Sato G, Sato R, Sato Y, Sato K, Sawada M, Serlemitsos P, Seta H, Shibano Y, Shida M, Shimada T, Shinozaki K, Shirron P, Simionescu A, Simmons C, Smith R, Sneiderman G, Soong Y, Stawarz L, Sugawara Y, Sugita H, Sugita S, Szymkowiak A, Tajima H, Takahashi H, Takeda Si, Takei Y, Tamagawa T, Tamura T, Tamura K, Tanaka T, Tanaka Y, Tashiro M, Tawara Y, Terada Y, Terashima Y, Tombesi F, Tomida H, Tsuboi Y, Tsujimoto M, Tsunemi H, Tsuru T, Uchida H, Uchiyama Y, Uchiyama H, Ueda Y, Ueno S, Uno S, Urry M, Ursino E, de Vries C, Wada A, Watanabe S, Werner N, White N, Yamada T, Yamada S, Yamaguchi H, Yamasaki N, Yamauchi S, Yamauchi M, Yatsu Y, Yonetoku D, Yoshida A, Yuasa T (2012) The ASTRO-H X-ray Observatory. In: Society of Photo-Optical Instrumentation Engineers (SPIE) Conference Series, Society of Photo-Optical Instrumentation Engineers (SPIE) Conference Series, vol 8443, DOI 10.1117/12.926190, 1210.4378

Teng SH, Brandt WN, Harrison FA, Luo B, Alexander DM, Bauer FE, Boggs SE, Christensen FE, Comastri A, Craig WW, Fabian AC, Farrah D, Fiore F, Gandhi P, Grefenstette BW, Hailey CJ, Hickox RC, Madsen KK, Ptak AF, Rigby JR, Risaliti G, Saez C, Stern D, Veilleux S, Walton DJ, Wik DR, Zhang WW (2014) NuSTAR Reveals an Intrinsically X-Ray Weak Broad Absorption Line Quasar in the Ultraluminous Infrared Galaxy Markarian 231. Astrophys J 785:19, 1402.4811

Thacker RJ, MacMackin C, Wurster J, Hobbs A (2014) AGN feedback models: correlations with star formation and observational implications of time evolution. MNRAS 443:1125–1141, DOI 10.1093/mnras/stu1180, 1407.0685

Toba Y, Oyabu S, Matsuhara H, Malkan MA, Gandhi P, Nakagawa T, Isobe N, Shirahata M, Oi N, Ohyama Y, Takita S, Yamauchi C, Yano K (2014) Luminosity and Redshift Dependence of the Covering Factor of Active Galactic Nuclei viewed with WISE and Sloan Digital Sky Survey. Astrophys J 788:45, 1404.4937

Totani T, Yoshii Y, Iwamuro F, Maihara T, Motohara K (2001) Diffuse Extragalactic Background Light versus Deep Galaxy Counts in the Subaru Deep Field: Missing Light in the Universe? Astrophys J Let 550:L137–L141, DOI 10.1086/319646, astro-ph/0102328

Tozzi P, Gilli R, Mainieri V, Norman C, Risaliti G, Rosati P, Bergeron J, Borgani S, Giacconi R, Hasinger G, Nonino M, Streblyanska A, Szokoly G, Wang JX, Zheng W (2006) X-ray spectral properties of active galactic nuclei in the Chandra Deep Field South. Astron Astrophys 451:457–474, astro-ph/0602127

Treister E, Urry CM (2006) The Evolution of Obscuration in Active Galactic Nuclei. Astrophys J Let 652:L79–L82, astro-ph/0610525

Treister E, Urry CM (2012) The Cosmic History of Black Hole Growth from Deep Multiwavelength Surveys. Advances in Astronomy 2012:516193, 1112.0320

Treister E, Krolik JH, Dullemond C (2008) Measuring the Fraction of Obscured Quasars by the Infrared Luminosity of Unobscured Quasars. Astrophys J 679:140–148, 0801.3849

Treister E, Cardamone CN, Schawinski K, Urry CM, Gawiser E, Virani S, Lira P, Kartaltepe J, Damen M, Taylor EN, Le Floc'h E, Justham S, Koekemoer AM (2009a) Heavily Obscured AGN in Star-Forming Galaxies at z sime 2. Astrophys J 706:535–552, 0911.0003

Treister E, Urry CM, Virani S (2009b) The Space Density of Compton-Thick Active Galactic Nucleus and the X-Ray Background. Astrophys J 696:110–120, 0902.0608

Treister E, Schawinski K, Urry CM, Simmons BD (2012) Major Galaxy Mergers Only Trigger the Most Luminous Active Galactic Nuclei. Astrophys J Let 758:L39, DOI 10.1088/2041-8205/758/2/L39, 1209.5393

Treister E, Schawinski K, Volonteri M, Natarajan P (2013) New Observational Constraints on the Growth of the First Supermassive Black Holes. Astrophys J 778:130, 1310.2249

Trichas M, Georgakakis A, Rowan-Robinson M, Nandra K, Clements D, Vac-

cari M (2009) Testing the starburst/AGN connection with SWIRE X-ray/70 μm sources. MNRAS 399:663–670, DOI 10.1111/j.1365-2966.2009.15340.x, 0906.4938

Trichas M, Green PJ, Silverman JD, Aldcroft T, Barkhouse W, Cameron RA, Constantin A, Ellison SL, Foltz C, Haggard D, Jannuzi BT, Kim DW, Marshall HL, Mossman A, Pérez LM, Romero-Colmenero E, Ruiz A, Smith MG, Smith PS, Torres G, Wik DR, Wilkes BJ, Wolfgang A (2012) The Chandra Multi-wavelength Project: Optical Spectroscopy and the Broadband Spectral Energy Distributions of X-Ray-selected AGNs. Astrophys J Supp 200:17, 1204.5148

Trouille L, Barger AJ, Cowie LL, Yang Y, Mushotzky RF (2008) The OPTX Project. I. The Flux and Redshift Catalogs for the CLANS, CLASXS, and CDF-N Fields. Astrophys J Supp 179:1–18, 0811.0824

Trouille L, Barger AJ, Cowie LL, Yang Y, Mushotzky RF (2009) The OPTX Project. III. X-ray Versus Optical Spectral Type for Active Galactic Nuclei. Astrophys J 703:2160–2170, 0908.0002

Trump JR, Impey CD, Elvis M, McCarthy PJ, Huchra JP, Brusa M, Salvato M, Capak P, Cappelluti N, Civano F, Comastri A, Gabor J, Hao H, Hasinger G, Jahnke K, Kelly BC, Lilly SJ, Schinnerer E, Scoville NZ, Smolčić V (2009) The COSMOS Active Galactic Nucleus Spectroscopic Survey. I. XMM-Newton Counterparts. Astrophys J 696:1195–1212, 0811.3977

Trump JR, Impey CD, Kelly BC, Civano F, Gabor JM, Diamond-Stanic AM, Merloni A, Urry CM, Hao H, Jahnke K, Nagao T, Taniguchi Y, Koekemoer AM, Lanzuisi G, Liu C, Mainieri V, Salvato M, Scoville NZ (2011a) Accretion Rate and the Physical Nature of Unobscured Active Galaxies. Astrophys J 733:60, 1103.0276

Trump JR, Weiner BJ, Scarlata C, Kocevski DD, Bell EF, McGrath EJ, Koo DC, Faber SM, Laird ES, Mozena M, Rangel C, Yan R, Yesuf H, Atek H, Dickinson M, Donley JL, Dunlop JS, Ferguson HC, Finkelstein SL, Grogin NA, Hathi NP, Juneau S, Kartaltepe JS, Koekemoer AM, Nandra K, Newman JA, Rodney SA, Straughn AN, Teplitz HI (2011b) A CANDELS WFC3 Grism Study of Emission-line Galaxies at z ˜ 2: A Mix of Nuclear Activity and Low-metallicity Star Formation. Astrophys J 743:144, 1108.6075

Trump JR, Barro G, Juneau S, Weiner BJ, Luo B, Brammer GB, Bell EF, Brandt WN, Dekel A, Guo Y, Hopkins PF, Koo DC, Kocevski DD, McIntosh DH, Momcheva I, Faber SM, Ferguson HC, Grogin NA, Kartaltepe J, Koekemoer AM, Lotz J, Maseda M, Mozena M, Nandra K, Rosario DJ, Zeimann GR (2014) No More Active Galactic Nuclei in Clumpy Disks Than in Smooth Galaxies at z˜2 in CANDELS / 3D-HST. ArXiv e-prints 1407.7525

Tueller J, Baumgartner WH, Markwardt CB, Skinner GK, Mushotzky RF, Ajello M, Barthelmy S, Beardmore A, Brandt WN, Burrows D, Chincarini G, Campana S, Cummings J, Cusumano G, Evans P, Fenimore E, Gehrels N, Godet O, Grupe D, Holland S, Kennea J, Krimm HA, Koss M, Moretti A, Mukai K, Osborne JP, Okajima T, Pagani C, Page K, Palmer D, Parsons A, Schneider DP, Sakamoto T, Sambruna R, Sato G, Stamatikos M, Stroh M,

Ukwata T, Winter L (2010) The 22 Month Swift-BAT All-Sky Hard X-ray Survey. Astrophys J Supp 186:378–405, DOI 10.1088/0067-0049/186/2/378, 0903.3037

Turner MJL, Abbey A, Arnaud M, Balasini M, Barbera M, Belsole E, Bennie PJ, Bernard JP, Bignami GF, Boer M, Briel U, Butler I, Cara C, Chabaud C, Cole R, Collura A, Conte M, Cros A, Denby M, Dhez P, Di Coco G, Dowson J, Ferrando P, Ghizzardi S, Gianotti F, Goodall CV, Gretton L, Griffiths RG, Hainaut O, Hochedez JF, Holland AD, Jourdain E, Kendziorra E, Lagostina A, Laine R, La Palombara N, Lortholary M, Lumb D, Marty P, Molendi S, Pigot C, Poindron E, Pounds KA, Reeves JN, Reppin C, Rothenflug R, Salvetat P, Sauvageot JL, Schmitt D, Sembay S, Short ADT, Spragg J, Stephen J, Strüder L, Tiengo A, Trifoglio M, Trümper J, Vercellone S, Vigroux L, Villa G, Ward MJ, Whitehead S, Zonca E (2001) The European Photon Imaging Camera on XMM-Newton: The MOS cameras : The MOS cameras. Astron Astrophys 365:L27–L35, astro-ph/0011498

Turner TJ, Miller L (2009) X-ray absorption and reflection in active galactic nuclei. The Astron and Astrophys Rev 17:47–104, 0902.0651

Ueda Y, Takahashi T, Inoue H, Tsuru T, Sakano M, Ishisaki Y, Ogasaka Y, Makishima K, Yamada T, Ohta K, Akiyama M (1998) A population of faint galaxies that contribute to the cosmic X-ray background. Nature 391:866

Ueda Y, Watson MG, Stewart IM, Akiyama M, Schwope AD, Lamer G, Ebrero J, Carrera FJ, Sekiguchi K, Yamada T, Simpson C, Hasinger G, Mateos S (2008) The Subaru/XMM-Newton Deep Survey (SXDS). III. X-Ray Data. Astrophys J Supp 179:124–141, 0806.2846

Ueda Y, Akiyama M, Hasinger G, Miyaji T, Watson MG (2014) Toward the Standard Population Synthesis Model of the X-Ray Background: Evolution of X-Ray Luminosity and Absorption Functions of Active Galactic Nuclei Including Compton-thick Populations. Astrophys J 786:104, 1402.1836

Urry CM, Treister E (2007) Supermassive Black Holes in Deep Multiwavelength Surveys. ArXiv e-prints 0712.1041

Vagnetti F, Antonucci M, Trevese D (2013) Variability and the X-ray/UV ratio of active galactic nuclei. II. Analysis of a low-redshift Swift sample. Astron Astrophys 550:A71, 1212.3432

van Breukelen C, Simpson C, Rawlings S, Akiyama M, Bonfield D, Clewley L, Jarvis MJ, Mauch T, Readhead T, Stobbart AM, Swinbank M, Watson M (2009) Evidence of a link between the evolution of clusters and their AGN fraction. MNRAS 395:11–27, DOI 10.1111/j.1365-2966.2009.14513.x, 0901.2517

Vasudevan RV, Fabian AC (2009) Simultaneous X-ray/optical/UV snapshots of active galactic nuclei from XMM-Newton: spectral energy distributions for the reverberation mapped sample. MNRAS 392:1124–1140, 0810.3777

Veilleux S, Osterbrock DE (1987) Spectral classification of emission-line galaxies. Astrophys J Supp 63:295–310, DOI 10.1086/191166

Veilleux S, Cecil G, Bland-Hawthorn J (2005) Galactic Winds. Ann Rev Astron Astrophys 43:769–826, DOI 10.1146/annurev.astro.43.072103.150610, astro-ph/0504435

Vignali C, Brandt WN, Schneider DP, Kaspi S (2005) X-Ray Lighthouses of the High-Redshift Universe. II. Further Snapshot Observations of the Most Luminous $z \gtrsim 4$ Quasars with Chandra. Astron J 129:2519–2530, astro-ph/0503301

Vignali C, Mignoli M, Gilli R, Comastri A, Iwasawa K, Zamorani G, Mainieri V, Bongiorno A (2014) The space density of Compton-thick AGN at z˜0.8 in the zCOSMOS-Bright Survey. ArXiv e-prints 1409.6361

Vika M, Driver SP, Graham AW, Liske J (2009) The Millennium Galaxy Catalogue: the M_{bh}-$L_{spheroid}$ derived supermassive black hole mass function. MNRAS 400:1451–1460, 0908.2102

Vikhlinin A, SMARTX Collaboration (2013) SMART-X , "Square Meter, Arcsecond Resolution Telescope for X-rays". Mem Soc Ast It 84:805

Villforth C, Koekemoer AM, Grogin NA (2010) A New Extensive Catalog of Optically Variable Active Galactic Nuclei in the GOODS Fields and a New Statistical Approach to Variability Selection. Astrophys J 723:737–754, 1008.3384

Villforth C, Sarajedini V, Koekemoer A (2012) The spectral energy distributions, host galaxies and environments of variability-selected active galactic nuclei in GOODS-South. MNRAS 426:360–376, 1207.4478

Villforth C, Hamann F, Rosario DJ, Santini P, McGrath EJ, Wel Avd, Chang YY, Guo Y, Dahlen T, Bell EF, Conselice CJ, Croton D, Dekel A, Faber SM, Grogin N, Hamilton T, Hopkins PF, Juneau S, Kartaltepe J, Kocevski D, Koekemoer A, Koo DC, Lotz J, McIntosh D, Mozena M, Somerville R, Wild V (2014) Morphologies of $z \sim 0.7$ AGN host galaxies in CANDELS: no trend of merger incidence with AGN luminosity. MNRAS 439:3342–3356, DOI 10.1093/mnras/stu173, 1401.5477

Vito F, Vignali C, Gilli R, Comastri A, Iwasawa K, Brandt WN, Alexander DM, Brusa M, Lehmer B, Bauer FE, Schneider DP, Xue YQ, Luo B (2013) The high-redshift ($z > 3$) active galactic nucleus population in the 4-Ms Chandra Deep Field-South. MNRAS 428:354–369, 1209.4193

Vito F, Gilli R, Vignali C, Comastri A, Brusa M, Cappelluti N, Iwasawa K (2014a) The Hard X-Ray Luminosity Function of High-Redshift ($3 < z < 5$) Active Galactic Nuclei. ArXiv e-prints 1409.6918

Vito F, Maiolino R, Santini P, Brusa M, Comastri A, Cresci G, Farrah D, Franceschini A, Gilli R, Granato GL, Gruppioni C, Lutz D, Mannucci F, Pozzi F, Rosario DJ, Scott D, Viero M, Vignali C (2014b) Black hole accretion preferentially occurs in gas-rich galaxies*. MNRAS 441:1059–1065, DOI 10.1093/mnras/stu637, 1403.7966

Voges W, Aschenbach B, Boller T, Bräuninger H, Briel U, Burkert W, Dennerl K, Englhauser J, Gruber R, Haberl F, Hartner G, Hasinger G, Kürster M, Pfeffermann E, Pietsch W, Predehl P, Rosso C, Schmitt JHMM, Trümper J, Zimmermann HU (1999) The ROSAT all-sky survey bright source catalogue. Astron Astrophys 349:389–405, astro-ph/9909315

Volonteri M (2010) Formation of supermassive black holes. The Astron and Astrophys Rev 18:279–315, DOI 10.1007/s00159-010-0029-x, 1003.4404

Volonteri M, Natarajan P, Gültekin K (2011) How Important is the Dark

Matter Halo for Black Hole Growth? Astrophys J 737:50, DOI 10.1088/0004-637X/737/2/50, 1103.1644

Volonteri M, Sikora M, Lasota JP, Merloni A (2013) The Evolution of Active Galactic Nuclei and their Spins. Astrophys J 775:94, 1210.1025

Wall JV, Jackson CA, Shaver PA, Hook IM, Kellermann KI (2005) The Parkes quarter-Jansky flat-spectrum sample. III. Space density and evolution of QSOs. Astron Astrophys 434:133–148, astro-ph/0408122

Wang JX, Malhotra S, Rhoads JE, Brown MJI, Dey A, Heckman TM, Jannuzi BT, Norman CA, Tiede GP, Tozzi P (2004) The 172 ks Chandra Exposure of the LALA Bootes Field: X-Ray Source Catalog. Astron J 127:213–229, astro-ph/0309705

Wang JX, Zheng ZY, Malhotra S, Finkelstein SL, Rhoads JE, Norman CA, Heckman TM (2007) Chandra X-Ray Sources in the LALA Cetus Field. Astrophys J 669:765–775, 0707.3239

Wang SX, Brandt WN, Luo B, Smail I, Alexander DM, Danielson ALR, Hodge JA, Karim A, Lehmer BD, Simpson JM, Swinbank AM, Walter F, Wardlow JL, Xue YQ, Chapman SC, Coppin KEK, Dannerbauer H, De Breuck C, Menten KM, van der Werf P (2013) An ALMA Survey of Submillimeter Galaxies in the Extended Chandra Deep Field-South: The AGN Fraction and X-Ray Properties of Submillimeter Galaxies. Astrophys J 778:179, 1310.6364

Warwick RS, Saxton RD, Read AM (2012) The XMM-Newton slew survey in the 2-10 keV band. Astron Astrophys 548:A99, 1210.3992

Watson M (2012) The 3XMM Catalogue. In: Half a Century of X-ray Astronomy, Proceedings of the conference held 17-21 September, 2012 in Mykonos Island, Greece. Online at ¡A href="http://www.astro.noa.gr/xcosmo/"¿http://www.astro.noa.gr/xcosmo/¡/A¿, id.138

Watson MG, Schröder AC, Fyfe D, Page CG, Lamer G, Mateos S, Pye J, Sakano M, Rosen S, Ballet J, Barcons X, Barret D, Boller T, Brunner H, Brusa M, Caccianiga A, Carrera FJ, Ceballos M, Della Ceca R, Denby M, Denkinson G, Dupuy S, Farrell S, Fraschetti F, Freyberg MJ, Guillout P, Hambaryan V, Maccacaro T, Mathiesen B, McMahon R, Michel L, Motch C, Osborne JP, Page M, Pakull MW, Pietsch W, Saxton R, Schwope A, Severgnini P, Simpson M, Sironi G, Stewart G, Stewart IM, Stobbart AM, Tedds J, Warwick R, Webb N, West R, Worrall D, Yuan W (2009) The XMM-Newton serendipitous survey. V. The Second XMM-Newton serendipitous source catalogue. Astron Astrophys 493:339–373, 0807.1067

Webb NA, Barret D, Godet O, Servillat M, Farrell SA, Oates SR (2010) Chandra and Swift Follow-up Observations of the Intermediate-mass Black Hole in ESO 243-49. Astrophys J Let 712:L107–L110, 1002.3625

Weisskopf MC, Tananbaum HD, Van Speybroeck LP, O'Dell SL (2000) Chandra X-ray Observatory (CXO): overview. In: Truemper JE, Aschenbach B (eds) X-Ray Optics, Instruments, and Missions III, Society of Photo-Optical Instrumentation Engineers (SPIE) Conference Series, vol 4012, pp 2–16, astro-ph/0004127

Werner MW, Roellig TL, Low FJ, Rieke GH, Rieke M, Hoffmann WF, Young E, Houck JR, Brandl B, Fazio GG, Hora JL, Gehrz RD, Helou G, Soifer BT, Stauffer J, Keene J, Eisenhardt P, Gallagher D, Gautier TN, Irace W, Lawrence CR, Simmons L, Van Cleve JE, Jura M, Wright EL, Cruikshank DP (2004) The Spitzer Space Telescope Mission. Astrophys J Supp 154:1–9, astro-ph/0406223

Wilkes BJ, Tananbaum H, Worrall DM, Avni Y, Oey MS, Flanagan J (1994) The Einstein database of IPC x-ray observations of optically selected and radio-selected quasars, 1. Astrophys J Supp 92:53–109

Wilms J, Allen A, McCray R (2000) On the Absorption of X-Rays in the Interstellar Medium. Astrophys J 542:914–924, astro-ph/0008425

Winkler C, Courvoisier TJL, Di Cocco G, Gehrels N, Giménez A, Grebenev S, Hermsen W, Mas-Hesse JM, Lebrun F, Lund N, Palumbo GGC, Paul J, Roques JP, Schnopper H, Schönfelder V, Sunyaev R, Teegarden B, Ubertini P, Vedrenne G, Dean AJ (2003) The INTEGRAL mission. Astron Astrophys 411:L1–L6

Wolf C, Meisenheimer K, Kleinheinrich M, Borch A, Dye S, Gray M, Wisotzki L, Bell EF, Rix HW, Cimatti A, Hasinger G, Szokoly G (2004) A catalogue of the Chandra Deep Field South with multi-colour classification and photometric redshifts from COMBO-17. Astron Astrophys 421:913–936, astro-ph/0403666

Woody D, Padin S, Chauvin E, Clavel B, Cortes G, Kissil A, Lou J, Rasmussen P, Redding D, Zolwoker J (2012) The CCAT 25m diameter submillimeter-wave telescope. In: Society of Photo-Optical Instrumentation Engineers (SPIE) Conference Series, Society of Photo-Optical Instrumentation Engineers (SPIE) Conference Series, vol 8444, p 2, DOI 10.1117/12.925229

Wootten A, Thompson AR (2009) The Atacama Large Millimeter/Submillimeter Array. IEEE Proceedings 97:1463–1471, DOI 10.1109/JPROC.2009.2020572, 0904.3739

Worrall DM (2009) The X-ray jets of active galaxies. The Astron and Astrophys Rev 17:1–46, 0812.3401

Wright EL, Eisenhardt PRM, Mainzer AK, Ressler ME, Cutri RM, Jarrett T, Kirkpatrick JD, Padgett D, McMillan RS, Skrutskie M, Stanford SA, Cohen M, Walker RG, Mather JC, Leisawitz D, Gautier TN III, McLean I, Benford D, Lonsdale CJ, Blain A, Mendez B, Irace WR, Duval V, Liu F, Royer D, Heinrichsen I, Howard J, Shannon M, Kendall M, Walsh AL, Larsen M, Cardon JG, Schick S, Schwalm M, Abid M, Fabinsky B, Naes L, Tsai CW (2010) The Wide-field Infrared Survey Explorer (WISE): Mission Description and Initial On-orbit Performance. Astron J 140:1868, DOI 10.1088/0004-6256/140/6/1868, 1008.0031

Wu J, Brandt WN, Hall PB, Gibson RR, Richards GT, Schneider DP, Shemmer O, Just DW, Schmidt SJ (2011) A Population of X-Ray Weak Quasars: PHL 1811 Analogs at High Redshift. Astrophys J 736:28, 1104.3861

Xue YQ, Brandt WN, Luo B, Rafferty DA, Alexander DM, Bauer FE, Lehmer BD, Schneider DP, Silverman JD (2010) Color-Magnitude Relations of Active and Non-active Galaxies in the Chandra Deep Fields: High-redshift

Constraints and Stellar-mass Selection Effects. Astrophys J 720:368–391, DOI 10.1088/0004-637X/720/1/368

Xue YQ, Luo B, Brandt WN, Bauer FE, Lehmer BD, Broos PS, Schneider DP, Alexander DM, Brusa M, Comastri A, Fabian AC, Gilli R, Hasinger G, Hornschemeier AE, Koekemoer A, Liu T, Mainieri V, Paolillo M, Rafferty DA, Rosati P, Shemmer O, Silverman JD, Smail I, Tozzi P, Vignali C (2011) The Chandra Deep Field-South Survey: 4 Ms Source Catalogs. Astrophys J Supp 195:10, 1105.5643

Xue YQ, Wang SX, Brandt WN, Luo B, Alexander DM, Bauer FE, Comastri A, Fabian AC, Gilli R, Lehmer BD, Schneider DP, Vignali C, Young M (2012) Tracking down the Source Population Responsible for the Unresolved Cosmic 6-8 keV Background. Astrophys J 758:129, 1209.0467

Yencho B, Barger AJ, Trouille L, Winter LM (2009) The OPTX Project. II. Hard X-Ray Luminosity Functions of Active Galactic Nuclei for z lsim 5. Astrophys J 698:380–396, 0903.4183

York DG, Adelman J, Anderson JE Jr, Anderson SF, Annis J, Bahcall NA, Bakken JA, Barkhouser R, Bastian S, Berman E, Boroski WN, Bracker S, Briegel C, Briggs JW, Brinkmann J, Brunner R, Burles S, Carey L, Carr MA, Castander FJ, Chen B, Colestock PL, Connolly AJ, Crocker JH, Csabai I, Czarapata PC, Davis JE, Doi M, Dombeck T, Eisenstein D, Ellman N, Elms BR, Evans ML, Fan X, Federwitz GR, Fiscelli L, Friedman S, Frieman JA, Fukugita M, Gillespie B, Gunn JE, Gurbani VK, de Haas E, Haldeman M, Harris FH, Hayes J, Heckman TM, Hennessy GS, Hindsley RB, Holm S, Holmgren DJ, Huang Ch, Hull C, Husby D, Ichikawa SI, Ichikawa T, Ivezić Ž, Kent S, Kim RSJ, Kinney E, Klaene M, Kleinman AN, Kleinman S, Knapp GR, Korienek J, Kron RG, Kunszt PZ, Lamb DQ, Lee B, Leger RF, Limmongkol S, Lindenmeyer C, Long DC, Loomis C, Loveday J, Lucinio R, Lupton RH, MacKinnon B, Mannery EJ, Mantsch PM, Margon B, McGehee P, McKay TA, Meiksin A, Merelli A, Monet DG, Munn JA, Narayanan VK, Nash T, Neilsen E, Neswold R, Newberg HJ, Nichol RC, Nicinski T, Nonino M, Okada N, Okamura S, Ostriker JP, Owen R, Pauls AG, Peoples J, Peterson RL, Petravick D, Pier JR, Pope A, Pordes R, Prosapio A, Rechenmacher R, Quinn TR, Richards GT, Richmond MW, Rivetta CH, Rockosi CM, Ruthmansdorfer K, Sandford D, Schlegel DJ, Schneider DP, Sekiguchi M, Sergey G, Shimasaku K, Siegmund WA, Smee S, Smith JA, Snedden S, Stone R, Stoughton C, Strauss MA, Stubbs C, SubbaRao M, Szalay AS, Szapudi I, Szokoly GP, Thakar AR, Tremonti C, Tucker DL, Uomoto A, Vanden Berk D, Vogeley MS, Waddell P, Wang Si, Watanabe M, Weinberg DH, Yanny B, Yasuda N (2000) The Sloan Digital Sky Survey: Technical Summary. Astron J 120:1579–1587, DOI 10.1086/301513, arXiv:astro-ph/0006396

Young ET, Becklin EE, Marcum PM, Roellig TL, De Buizer JM, Herter TL, Güsten R, Dunham EW, Temi P, Andersson BG, Backman D, Burgdorf M, Caroff LJ, Casey SC, Davidson JA, Erickson EF, Gehrz RD, Harper DA, Harvey PM, Helton LA, Horner SD, Howard CD, Klein R, Krabbe A, McLean IS, Meyer AW, Miles JW, Morris MR, Reach WT, Rho J, Richter

MJ, Roeser HP, Sandell G, Sankrit R, Savage ML, Smith EC, Shuping RY, Vacca WD, Vaillancourt JE, Wolf J, Zinnecker H (2012a) Early Science with SOFIA, the Stratospheric Observatory For Infrared Astronomy. Astrophys J Let 749:L17, DOI 10.1088/2041-8205/749/2/L17, 1205.0791

Young M, Elvis M, Risaliti G (2010) The X-ray Energy Dependence of the Relation Between Optical and X-ray Emission in Quasars. Astrophys J 708:1388–1397, 0911.0474

Young M, Brandt WN, Xue YQ, Paolillo M, Alexander DM, Bauer FE, Lehmer BD, Luo B, Shemmer O, Schneider DP, Vignali C (2012b) Variability-selected Low-luminosity Active Galactic Nuclei in the 4 Ms Chandra Deep Field-South. Astrophys J 748:124, 1201.4391

Zheng Z, Berlind AA, Weinberg DH, Benson AJ, Baugh CM, Cole S, Davé R, Frenk CS, Katz N, Lacey CG (2005) Theoretical Models of the Halo Occupation Distribution: Separating Central and Satellite Galaxies. Astrophys J 633:791–809, DOI 10.1086/466510, astro-ph/0408564

Zibetti S, Charlot S, Rix HW (2009) Resolved stellar mass maps of galaxies - I. Method and implications for global mass estimates. MNRAS 400:1181–1198, DOI 10.1111/j.1365-2966.2009.15528.x, 0904.4252